Archaea

Lipid Biology of Archaea

Guest Editors: Angela Corcelli, Parkson Lee-Gau Chong, and Yosuke Koga

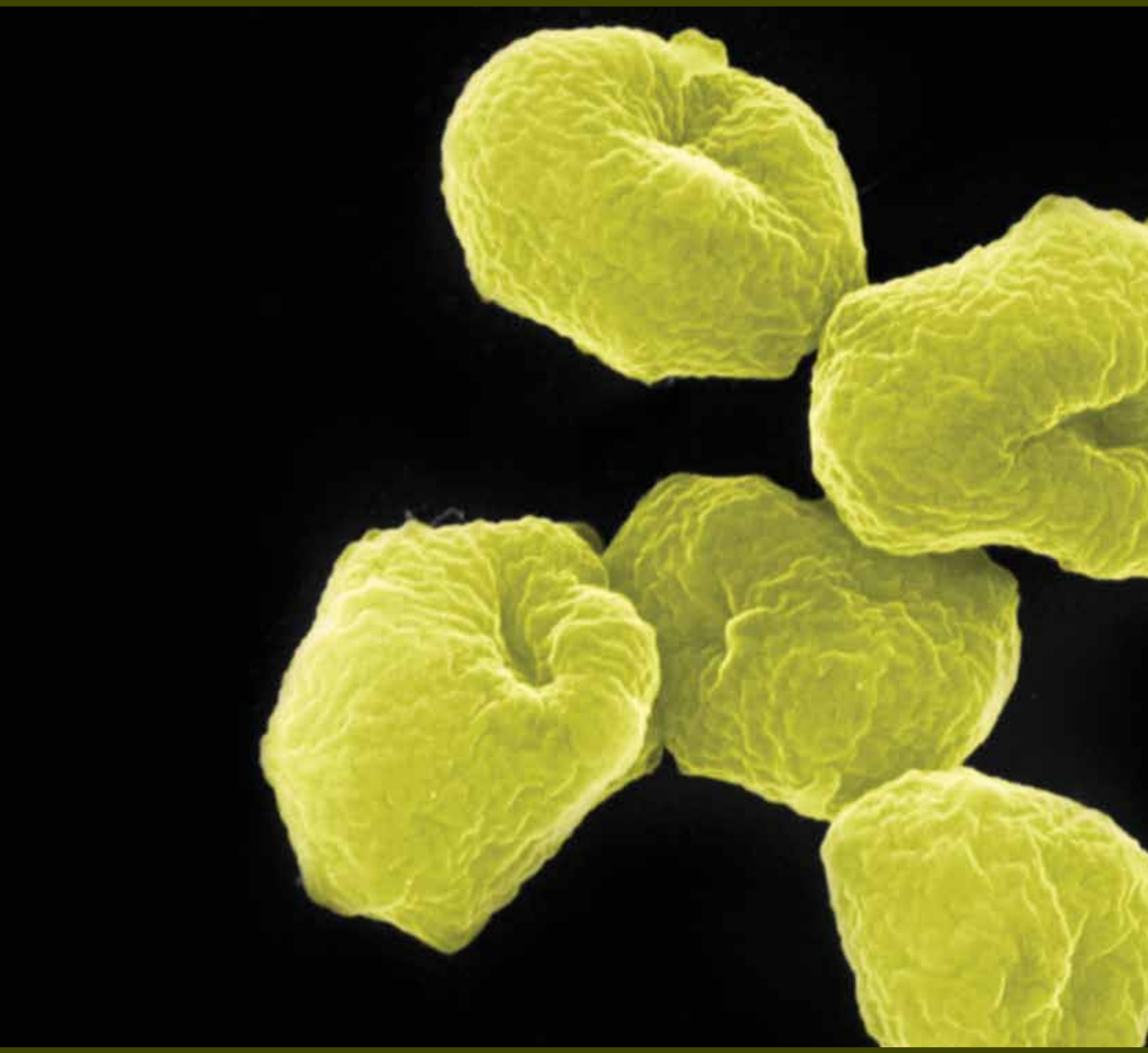

Lipid Biology of Archaea

Lipid Biology of Archaea

Guest Editors: Angela Corcelli, Parkson Lee-Gau Chong, and Yosuke Koga

Editorial Board

Contents

Hindawi Publishing Corporation
Archaea
Volume 2012, Article ID 710836, 2 pages
doi:10.1155/2012/710836

Editorial
Lipid Biology of Archaea

Angela Corcelli,[1] Parkson Lee-Gau Chong,[2] and Yosuke Koga[3]

[1] *Department of Basic Medical Sciences, University of Bari Aldo Moro, Piazza G. Cesare, 70124 Bari, Italy*
[2] *Department of Biochemistry, Temple University School of Medicine, 3420 North Broad Street, Philadelphia, PA 19140, USA*
[3] *Department of Chemistry, University of Occupational and Environmental Health, Yahatanishi-ku, Kitakyushu 807-8555, Japan*

Correspondence should be addressed to Angela Corcelli, angela.corcelli@uniba.it

Received 13 November 2012; Accepted 13 November 2012

Today, there is increasing awareness of the multiple dynamic roles of lipids in cell life.

Knowing how lipid molecular species are organized, interact with proteins, and change with environmental stress and metabolic state is crucial to understanding the membrane structure and the cellular functions.

The present view of lipid biology arises from the availability of technologies able to detect even minor lipid components with short lifetimes. In the late 1990s, the technical innovation in mass spectrometry led to the development of "lipidomics" as an evolution of lipid biochemistry. Furthermore, progress in microscopy and the availability of many types of fluorescent probes, together with genetic engineering, presently offer the possibility to move quickly towards lipid systems biology. As a consequence, besides being able to analyze major and minor lipids of all structures and sizes by mass spectrometry and nuclear magnetic resonance, we can study topology, structural organization, and dynamics of lipids by microscopy and fluorescent probes in living cells and microbes.

Lipids are among the taxonomic traits that can be used to clearly delineate the archaea from all other organisms. Archaeal phospholipids are built on glycero-1-phosphate and contain ether-linked isoprenoid chains, while bacterial and eukaryal lipids are constituted of fatty acids ester-linked to glycero-3-phosphate. The radical structural differences between lipids of archaea and bacteria or eukaryotes raise many questions about early evolution of cell membranes.

This special issue contains selected papers dealing with archaeal phospholipid biosynthetic pathways, physical chemical properties and biotechnological applications of archaeal lipids, mass spectrometry lipid analyses and lipids of the archaeal viruses.

An updated phylogenic analysis of enzymes involved in archaeal phospholipid biosynthetic pathways is presented by the group of D. Moreira. The biosynthetic pathways have also been analyzed from the experimental point of view in a study of the group of H. Hemmii, which has expressed 4 genes involved in the biosynthesis of archaeal phospholipids in *E. coli* resulting in the production of archaeal-type lipids in the bacterium; in the future such engineered *E. coli* cells may serve to test the properties of mixed membranes constituted of both archaeal and bacterial phospholipids.

Lipid components of the membranes of *Pyrococcus furiosus* have been analyzed by MALDI/TOF-MS coupled to TLC in a study of S. Lobasso et al.; while lipids of uncultured methanogens present in geological samples have been detailed characterized by ESI-MS by M. Y. Yoshinaga et al.

The ability of archaeal lipids to act as adjuvant in vaccines designed to give protection against solid tumor has been examined in a study by G. D. Sprott et al.

A review article by E. Roine and D. H. Bamford describes the specific lipid components of viral membranes of archaeal viruses, in the frame of their possible functional roles in the mechanism of infection.

The chemical physical properties of the lipid core of membranes constituted of archaeal diether lipids have been examined in a study by A. Ota et al. by using fluorescence steady-state anisotropy and electron paramagnetic resonance

measurements and in a review article of P. L. Chong et al. where the role of cyclopentane rings in the lipid chains of tetraether lipids on membrane fluidity is examined.

Finally an interesting contribution of Y. Koga comparatively examines the different mode of adaptation to high temperature of archaea and bacteria pointing out the role that differences in chemical physical properties of archaeal and bacterial lipids might have played in the differentiation of archaea and bacteria during evolution.

We hope that this issue will contribute to the understanding of the multiple roles of lipids in the cell biology of archaea and will stimulate further investigation in this field, opened by the pioneering studies of Morris Kates in the 60s.

Angela Corcelli
Parkson Lee-Gau Chong
Yosuke Koga

Hindawi Publishing Corporation
Archaea
Volume 2012, Article ID 630910, 13 pages
doi:10.1155/2012/630910

Review Article

Phylogenomic Investigation of Phospholipid Synthesis in Archaea

Jonathan Lombard, Purificación López-García, and David Moreira

Unité d'Ecologie Systématique et Evolution, CNRS UMR 8079, Université Paris-Sud, 91405 Orsay Cedex, France

Correspondence should be addressed to David Moreira, david.moreira@u-psud.fr

Received 8 August 2012; Accepted 3 September 2012

Academic Editor: Angela Corcelli

Archaea have idiosyncratic cell membranes usually based on phospholipids containing glycerol-1-phosphate linked by ether bonds to isoprenoid lateral chains. Since these phospholipids strongly differ from those of bacteria and eukaryotes, the origin of the archaeal membranes (and by extension, of all cellular membranes) was enigmatic and called for accurate evolutionary studies. In this paper we review some recent phylogenomic studies that have revealed a modified mevalonate pathway for the synthesis of isoprenoid precursors in archaea and suggested that this domain uses an atypical pathway of synthesis of fatty acids devoid of any acyl carrier protein, which is essential for this activity in bacteria and eukaryotes. In addition, we show new or updated phylogenetic analyses of enzymes likely responsible for the isoprenoid chain synthesis from their precursors and the phospholipid synthesis from glycerol phosphate, isoprenoids, and polar head groups. These results support that most of these enzymes can be traced back to the last archaeal common ancestor and, in many cases, even to the last common ancestor of all living organisms.

1. Introduction

Archaea were identified as an independent domain of life in the late 1970s thanks to the characterization of differences between their ribosomal RNA molecules and those of bacteria and eukaryotes [1]. At that time, it was already known that the so-called "archaeabacteria" held several atypical biochemical characteristics, of which the most remarkable was their unusual membrane phospholipids. Whereas all bacteria and eukaryotes were known to have membranes based on fatty acids linked by ester bonds to glycerol-phosphate, archaea appeared to have phospholipids composed of isoprenoid chains condensed with glycerol-phosphate by ether linkages [2–6]. Moreover, the archaeal glycerol ethers contained *sn*-glycerol-1-phosphate (G1P), whereas bacterial and eukaryotic ones contained *sn*-glycerol-3-phosphate (G3P) (for review, see [7, 8]). These differences, which have been at the center of an intense debate about the nature of the first cell membranes [9], have progressively been shown to be not so sharp: ether-linked lipids are common both in eukaryotes (up to 25% of the total lipids in certain animal cells, [10]) and in several thermophilic bacteria [11–13]; fatty acid phospholipids have been found in diverse archaea [14]; conversely, isoprenoids are known to be universal although they are synthesized by non-homologous pathways in the three domains of life, [15]; even the stereochemistry of the glycerol phosphate has some exceptions, as shown by the recent discovery of archaeal-like *sn*-glycerol-1-phosphate specific lipids in some bacteria [16] and in eukaryotic endosomes [17].

Today, thanks to the significant accumulation of complete genome sequence data for a wide variety of species, it is possible to study the major pathways of phospholipid synthesis and their exceptions by looking at the presence or absence of the corresponding genes in the different genomes. In addition, these data allows reconstructing the evolutionary history of each gene by combining comparative genomics and phylogenetics, namely, by using a phylogenomic approach. In this paper, we summarize the results concerning the phylogenomic studies of the biosynthesis pathways of archaeal phospholipid components and provide some new evolutionary data about the enzymes reviewed in Koga and Morii [18] and Matsumi et al. [19] as likely responsible for the assembly of archaeal lipids from these building blocks.

2. Archaea Possess an Atypical Pathway of Biosynthesis of Isoprenoid Precursors

Isoprenoids are chains of isoprene units and their derivatives and are found ubiquitously in all living beings. They are involved in very diverse functions, such as photosynthetic pigments, hormones, quinones acting in electron transport chains, plant defense compounds, and so forth [15, 20]. In archaea, isoprenoids also make up the hydrophobic lateral chains of phospholipids [7]. Isoprenoid biosynthesis requires two isoprene activated precursors, called isopentenyl pyrophosphate (IPP) and dimethylallyl diphosphate (DMAPP), which act as building parts. The first metabolic pathway responsible for the biosynthesis of isoprenoid precursors was discovered in yeasts and animals in the 1950s and named mevalonate (MVA) pathway in reference to its first committed precursor. Since its first description, the MVA pathway was thought to synthesize the isoprenoid precursors in all organisms [20], but closer scrutiny showed its absence in most bacteria [21]. An elegant series of multidisciplinary approaches allowed in the late 1990s and early 2000s describing an independent and non-homologous pathway in bacteria, the methylerythritol phosphate (MEP) pathway (see [22] for review). The MEP pathway was found to be widespread in bacteria and plastid-bearing eukaryotes, whereas the MVA pathway was assumed to operate in archaea and eukaryotes [15, 23]. In the early 2000s, archaeal isoprenoids were thought to be synthesized through the MVA pathway because the ^{14}C-labelled intermediates of this pathway were shown to be incorporated into the archaeal phospholipids [24]. However, only two of the enzymes of the eukaryotic pathway have been described in archaea [25, 26]. Moreover, the search of MVA pathway enzyme sequences in archaeal genomes revealed that from the seven enzymes acting on this pathway, most archaeal species lack the last three of them: phosphomevalonate kinase (PMK), mevalonate diphosphate decarboxylase (MDC), and isopentenyl diphosphate isomerase (IDI1), involved in the conversion of phosphomevalonate into IPP and DMAPP [27]. Attempts to characterize these missing archaeal enzymes revealed two new enzymes: the isopentenyl phosphate kinase (IPK) and an alternative isopentenyl diphosphate isomerase (IDI2) [28–30]. Although the decarboxylation reaction required to synthesize isopentenyl phosphate from phosphomevalonate has not been described yet, an alternative final MVA pathway involving IPK and IDI2 was then proposed to exist in archaea (Figure 1, [29]).

Taking advantage of the recent accumulation of genomic data, we carried out a thorough phylogenomic analysis of the pathways of isoprenoid precursor synthesis [31]. Concerning archaea, our presence-and-absence analysis extended the presence of the proposed archaeal alternative pathway to a wide archaeal diversity. The main exception to these observations was *Nanoarchaeum equitans*, which explains the dependence of this organism to obtain its lipids from its crenarchaeal host, *Ignicoccus hospitalis* [32]. Phylogenetic reconstructions of the MVA pathway enzymes present in archaea systematically revealed a clade independent from the other domains of life, representative of the archaeal diversity and generally respecting the main archaeal taxonomic groups [31]. These results are consistent with the presence of a distinctive archaeal MVA pathway in the last archaeal common ancestor (LACA) and support that different isoprenoid precursor biosynthesis pathways are characteristic of each domain of life: the classical MVA pathway in eukaryotes, the alternative MVA pathway in archaea, and the MEP pathway in bacteria.

The origin of the archaeal MVA pathway appears to be composite. The enzymes shared with the classical eukaryotic MVA pathway were also ancestral in eukaryotes and bacteria and, therefore, they can be inferred to have been present in the last common ancestor of all living organisms (the cenancestor), from which the archaeal lineage would have inherited them. The last enzymes of the eukaryotic MVA pathway were most likely present in the respective ancestors of eukaryotes and bacteria, but their distribution in archaea is scarce and complex: homologues of MDC can be detected in Haloarchaea and Thermoplasmatales and some IDI1 genes have been identified in Haloarchaea and Thaumarchaeota, although they most likely reflect recent horizontal gene transfer (HGT) events from bacterial donors, as deduced from their position well nested among bacterial sequences in phylogenetic analyses [23, 31]. In contrast, the class Sulfolobales contains PMK and MDC homologues which robustly branch in an intermediate position between the eukaryotic and the bacterial sequences, suggesting that these sequences could be ancestral versions that would have been lost in the rest of archaea [31]. If this is the case, a eukaryotic-like pathway (except for the IDI function, which remains ambiguous) can be proposed to have existed in the cenancestor. This pathway would have been replaced by the MEP pathway in the bacterial lineage, whereas in archaea only the last steps were replaced by non-homologous enzymes. We do not know the evolutionary forces that drove these changes; however, the mevalonate kinase (MVK), PMK, and MDC belong to a large family of kinases, namely the GHMP kinases [33], which is characterized by a high structural and mechanistic conservation that contrasts with the large range of substrates that they can use [34]. If we assume that ancestors of these enzymes were not very specific, this could have allowed some tolerance to recruitment of evolutionary unrelated enzymes not only in archaea but also in some eukaryotes that have replaced their ancestral PMK by a non-homologous one [35, 36]. In agreement with this idea, the archaeal IPK itself appears to be able to use different substrates [37], which could have made the replacement easier.

3. Early Evolution of Isoprenoid Chain Synthesis

Once the isoprenoid precursors, IPP and DMAPP, have been synthesized, they still have to be assembled to make isoprenoid chains. The prenyltransferases responsible for this function are the isoprenyl diphosphate synthases (IPPS). Since many more complete genome sequences are now available than at the time of previous IPPS phylogenetic

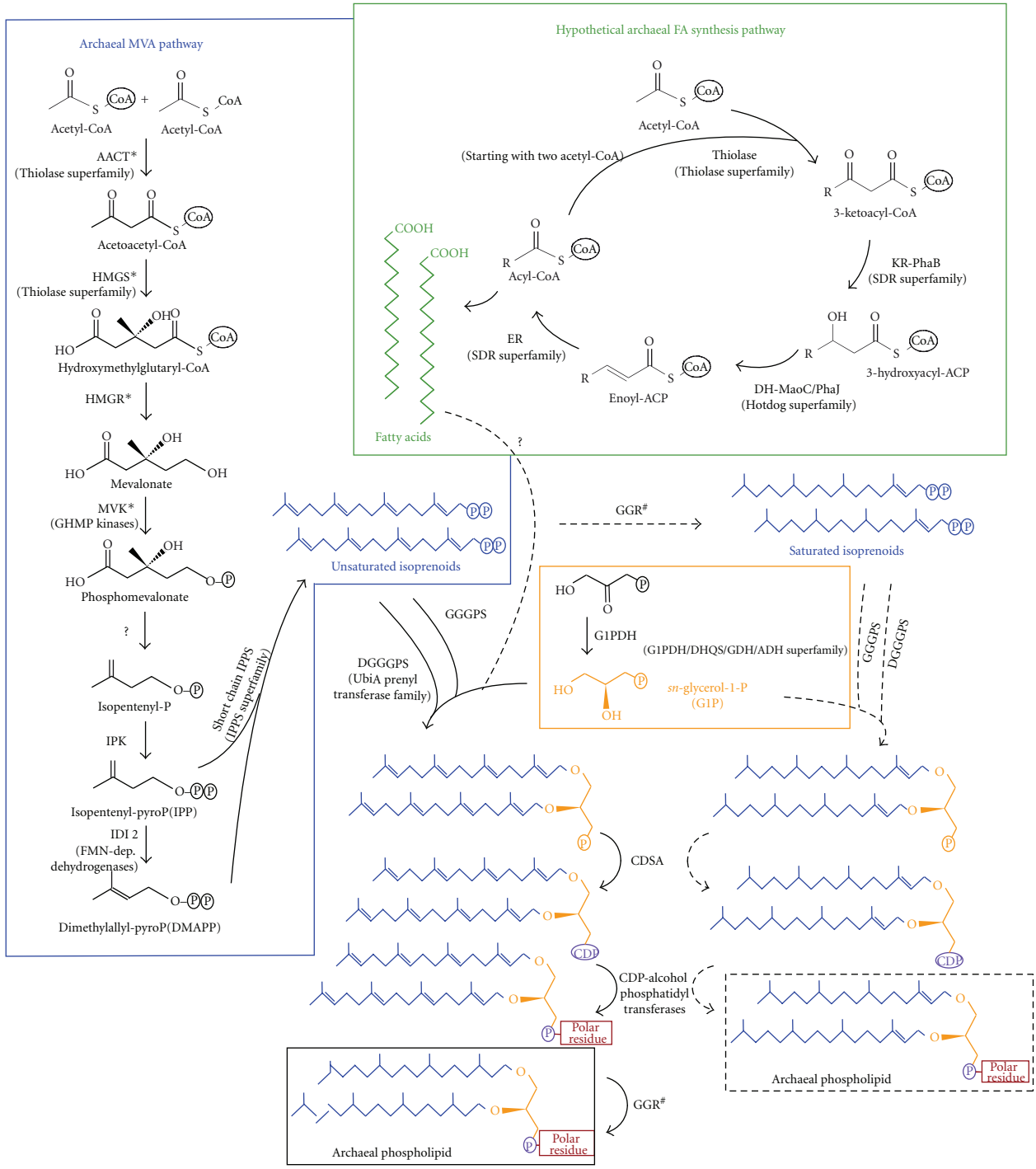

FIGURE 1: Biosynthesis pathways of phospholipid components in archaea. Abbreviations for the archaeal mevalonate (MVA) pathway: AACT, acetoacetyl-CoA thiolase; HMGS, 3-hydroxy-3-methylglutaryl-CoA synthase; HMGR, 3-hydroxy-3-methylglutaryl-CoA reductase; MVK, mevalonate kinase; IPK, isopentenyl phosphate kinase; IDI2, isopentenyl diphosphate isomerase type II. GHMP, galactokinase-homoserine kinase-mevalonate kinase-phosphomevalonate kinase; IPPS, isoprenyl diphosphate synthases (asterisks indicate enzymes shared with the eukaryotic MVA pathway). Abbreviations for the hypothetical archaeal fatty acid (FA) synthesis pathway: ACC, acetyl-CoA carboxylase; PCC, propionyl-CoA carboxylase; KR-PhaB, beta-ketoacyl reductase; DH-MaoC/PhaJ, beta-hydroxyacyl dehydratase; ER, enoyl reductase; SDR, short-chain dehydrogenases/reductases. Abbreviations for the *sn*-glycerol-1-phosphate synthesis pathway: G1PDH, glycerol-1-phosphate dehydrogenase; DHQS, 3-dehydroquinate synthase; GDH, glycerol dehydrogenase; ADH, alcohol dehydrogenase. Abbreviations for the phospholipid assembly pathway: GGGPS, (S)-3-O-geranylgeranylglyceryl phosphate synthase; DGGGPS, (S)-2,3-di-O-geranylgeranylglyceryl phosphate synthase; GGR, geranylgeranyl reductase; CDSA, CDP diglyceride synthetase. ($^{\#}$) points to the ability of GGRs to reduce isoprenoids at different steps in the biosynthesis pathway. Names between parentheses indicate the family or superfamily to which belong the archaeal enzymes postulated to carry out particular functions on the basis of phylogenomic analyses.

analyses, we present here an updated survey of the evolution of these enzymes. Although many different enzymes are required to synthesize the wide diversity of isoprenoids, the first steps are widely shared among the three domains of life [38]. They consist of the progressive addition of IPP units (5 carbons each) to an elongating allyl polyisoprenoid diphosphate molecule. Starting with DMAPP (5 carbons), consecutive condensation reactions produce geranylgeranyl diphosphate (GPP, 10 carbons), farnesyl diphosphate (FPP, 15 carbons), geranylgeranyl diphosphate (GGPP, 20 carbons), and so forth. Different IPPSs are characterized by the allylic substrate that they accept (DMAPP, GPP, FPP, ...) and by the stereochemistry of the double bonds, but the main characteristic used to classify them is the size of the products that they synthesize: they can be short-chain IPPS (~up to 25 carbons) or long-chain IPPS (>25 carbons). All IPPS are homologous and share a common reaction mechanism. Short-chain IPPS mainly differ in the size of their substrate-binding hydrophobic pocket (the smaller the pocket, the shorter the final product, [38]), but point mutations have been shown to importantly impact the size of the pocket and, thus, of their final products [39, 40]. Description of equivalent natural mutations have been reported in archaea [41], which argues against the possibility of inferring the precise product of a given IPPS only based on its phylogenetic position [41, 42].

The first published IPPS phylogenetic trees [42] only used 13 sequences (of which 12 were short-chain enzymes) and supported a split between prokaryotic and eukaryotic enzymes. At that time, archaeal IPPS were assumed to be more ancient because they were known to provide isoprenoids for several pathways while bacteria and eukaryotes were thought to have more specialized enzymes. Later phylogenetic analyses with more sequences showed two groups corresponding to the functional split between short and long-chain enzymes [41]. This was expected since the long-chain IPPS use supplementary proteins to stabilize the hydrophobic substrate [38], which would logically impact the protein structure and therefore trigger the large divergence between the short- and the long-chain enzymes. In that work, the short-chain enzymes formed three groups according to the three domains of life, which could be considered as evidence for the presence of one short-chain enzyme in the cenancestor and its subsequent inheritance in modern lineages, including archaea. Furthermore, in that phylogeny archaea did not branch as a basal lineage, disproving their previously assumed ancient character. In addition, enzymes with different product specificities branched mixed all over the tree, supporting the product plasticity of the ancestral short-chain enzyme and the subsequent evolution of particular specificities according to biological requirements in modern organisms [41]. Archaeal long-chain IPPS had not been detected in that study, but some of them were incorporated in phylogenetic studies some years later [23].

We have searched for homologues of IPPS in a representative set of 348 complete genomes from the three domains of life (including 88 archaea). A preliminary phylogenetic analysis showed that, in agreement with previous reports [23], the resulting sequences split into two clades mainly related to the short- or long-chain product specificity (data not shown). To avoid the phylogenetic artifacts that can be introduced by the high sequence divergence between short- and long-chain enzymes, we carried out independent phylogenetic analyses for each one of the two paralogues, to which we will refer as short- or long-chain IPPS with regard to dominant functions of the characterized enzymes. However, as previously mentioned [39–41], substrate specificity exchange between short and long substrates appears to be relatively common, so these partial trees must be acknowledged mainly as phylogenetic groups related to the most widespread biochemical function, but do not definitely determine the substrate specificity of all their sequences, which can only be established by biochemical studies. In preliminary short-chain IPPS phylogenies, long branches at the base of several eukaryotic paralogues evidenced for the high divergence of these sequences. Since we were here mainly interested in the archaeal sequences, we removed the divergent eukaryotic sequences from our analyses. Figure 2 and Supplementary Figure 1 (see Supplementary Material available online at doi:10.1155/2012/630910) present the phylogeny of some representative prokaryotic short-chain enzyme sequences. Most archaeal sequences branch together in a monophyletic group largely congruent with the main archaeal phyla and orders, which suggests that this enzyme was present in LACA and was vertically inherited in most archaeal lineages. Most bacterial sequences also cluster together according to the main bacterial taxonomic groups, suggesting the ancestral presence of this enzyme in the last bacterial common ancestor and, given its presence also in LACA, most likely also in the cenancestor. However, some recent HGTs can also be pointed out from this phylogeny. Concerning archaea, Thermoproteales, some Desulfurococcales, some Thermoplasmatales, *Methanocella paludicola* and *Aciduliprofundum boonei* branch within the bacterial group, so several HGTs can be invoked to explain this pattern, although in most cases the support is weak and does not allow confidently determining the identity of the bacterial donors (Figure 2).

As in the case of the short-chain enzymes, most archaeal sequences also group together in our long-chain IPPS phylogenies and, despite the weakly supported paraphyly of the euryarchaeotal sequences, the main archaeal taxonomic groups are observed (Figure 3 and Supplementary Figure 2). Bacterial sequences also group together according to main taxa, supporting that the respective common ancestors of bacteria and archaea, and thus likely also the cenancestor, had a long-chain IPPS enzyme that was inherited in modern organisms. Contrary to short-chain IPPS, eukaryotic long-chain IPPS are less divergent, so they were conserved in our analyses. Surprisingly, all the eukaryotic sequences, including those from plastid-lacking eukaryotes, branch together as the sister group of cyanobacteria, except for some algae that branch within the cyanobacterial group. In addition, some other more recent HGTs are observed, especially in the archaeal *Thermococcus* genus, which branches close to a very divergent sequence from the delta-proteobacterium *Bdellovibrio bacteriovorus*.

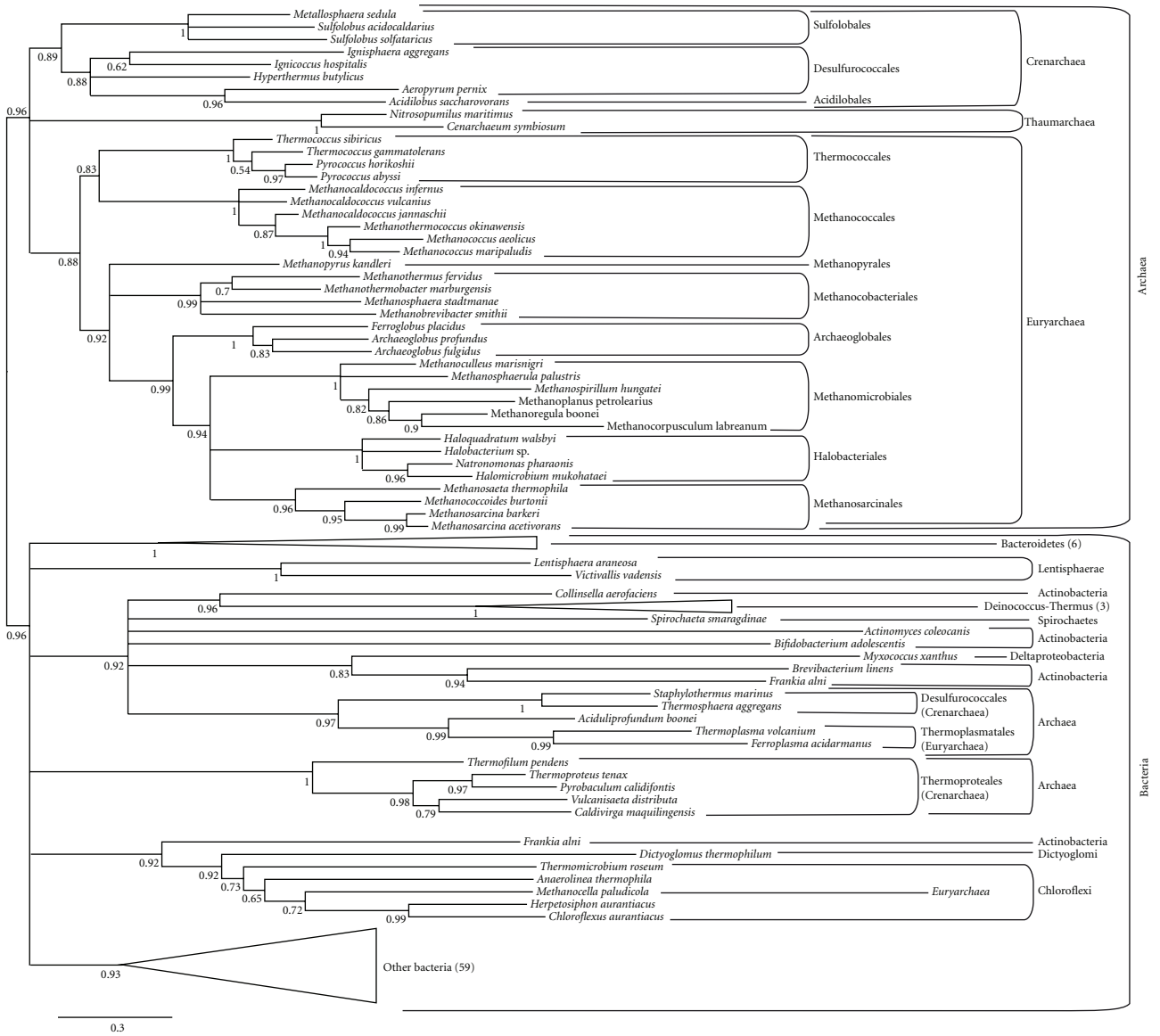

Figure 2: Short-chain IPPS phylogenetic tree reconstructed using 136 representative sequences and 244 conserved sites. Multifurcations correspond to branches with support values <0.50. Triangles correspond to well supported-bacterial clades (numbers in parentheses correspond to the number of sequences included in these clades). For the complete phylogeny, see Supplementary Figure 1.

Altogether, these results support that in spite of some recent HGTs from bacteria to archaea, most archaea have homologues of both the short- and the long-chain IPPS that were inherited from LACA and that, most likely, were already present in the cenancestor.

4. Archaea May Have an ACP-Independent Fatty Acid Biosynthesis Pathway

In bacteria and eukaryotes, fatty acids are components of membrane phospholipids, energy-storage molecules, substrates for post-translational modifications of proteins, secondary metabolites, and components of coenzymes and messenger compounds. Despite the general assumption that archaeal lipid metabolism is based on isoprenoids, a variety of experimental approaches have shown that fatty acids (FA) also exist in these organisms. Archaea show variable concentrations of free FA or their derivatives [4, 24, 43–45], which has stimulated some attempts to biochemically characterize an archaeal FA synthase [46, 47]. Archaeal FA can participate in protein structure [48–50] and acylation [47] but they have also been found as components of membrane phospholipids in very diverse euryarchaeotes [14]. Therefore, it is not surprising that homologues of several of the enzymes involved FA biosynthesis in bacteria had been detected in archaeal genomes [8, 51]. In bacteria, FA biosynthesis occurs through multiple condensations of acyl groups (malonyl-CoA) in a series of cyclical steps.

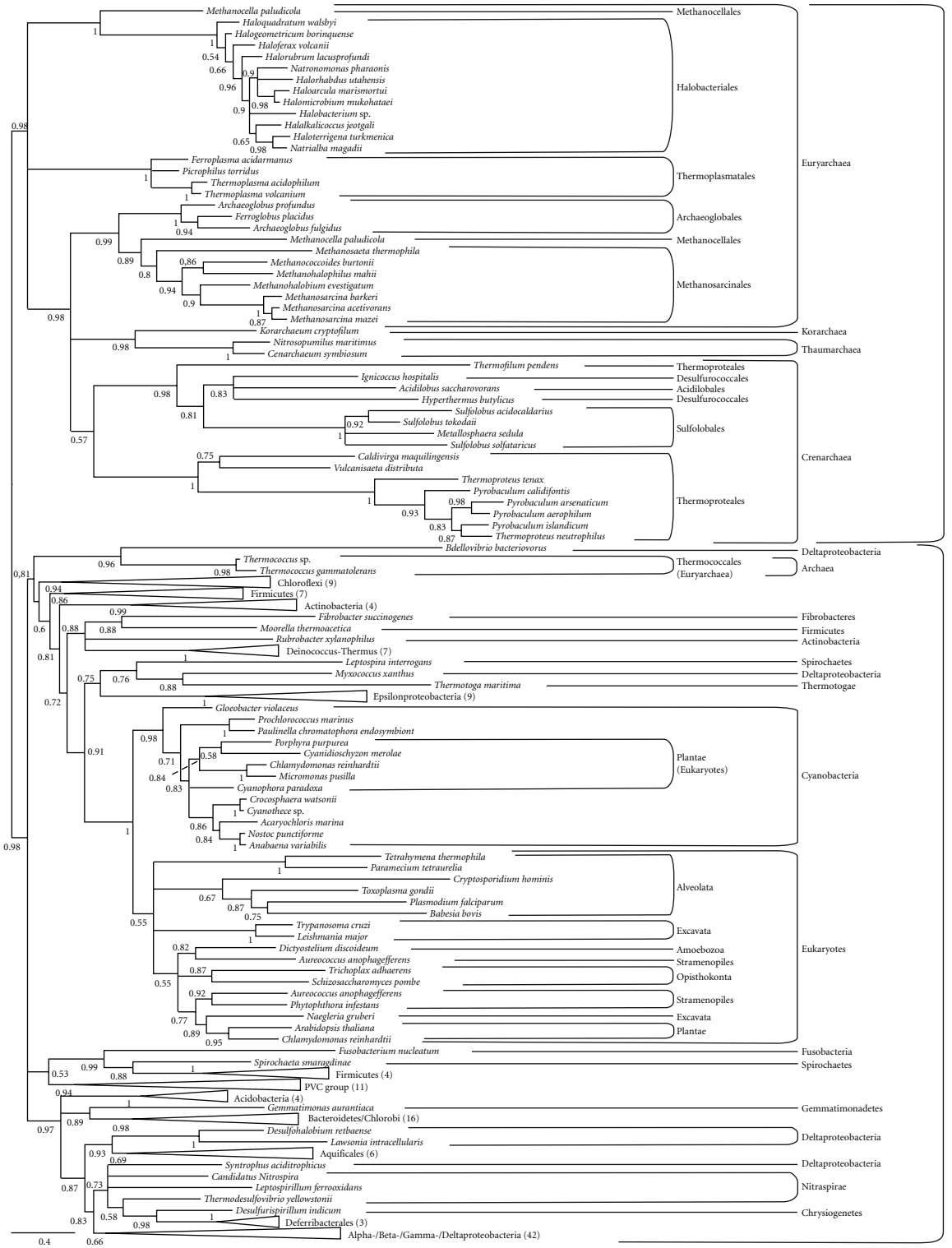

Figure 3: Long-chain IPPS phylogenetic tree reconstructed using 218 representative sequences and 241 conserved sites. Multifurcations correspond to branches with support values <0.50. Triangles correspond to well-supported clades outside Archaea (numbers in parentheses correspond to the number of sequences included in these clades). For the complete phylogeny, see Supplementary Figure 2.

The building blocks necessary to the activity of the FA synthases are provided by several reactions. First, the acetyl-CoA carboxylase (ACC) converts acetyl-coenzyme A (CoA) into malonyl-CoA. Second, the peptide cofactor acyl carrier protein (ACP), which is required to channel the elongating intermediates among the FA synthase enzymes, has to be activated through the addition of a phosphopantetheine group from CoA to the apo-ACP by an ACP synthase. Finally,

the malonyl-CoA: ACP transacylase (MCAT) charges the malonyl-CoA to holo-ACP, resulting in malonyl-ACP.

Since no archaeal FA synthase system has been described in detail yet, we recently studied the evolution of the archaeal homologues of the bacterial genes involved in FA synthesis. First, many archaea possess ACC homologues that are closely related in phylogenetic analyses, suggesting their possible monophyletic origin and, consequently, the presence of this enzyme in LACA [52, 53]. Second, only a few unrelated archaeal species have ACP and the ACP-processing machinery (ACP synthase and MCAT) and phylogenetic analysis suggests that they acquired them by HGTs from bacteria. As a result, ACP and its related enzymes are missing in most archaea and appear not to have been present in LACA [54]. For the rest of enzymes involved in the cyclic steps of FA synthesis (see Figure 1), phylogenetic analyses support that the archaeal sequences are more closely related to bacterial enzymes that are active on substrates linked to CoA than to enzymes that use substrates linked to ACP. Taking this into account, we have proposed that the ACP processing system has specifically evolved in the bacterial lineage and that archaea carry out FA synthesis using a likely ancient ACP-independent pathway [54]. Although ACC exists in archaea, the hypothetical archaeal FA synthesis pathway probably involves two acetyl-CoA instead of using malonyl and acetyl thioesters as in bacteria, since the thiolases that carry out this function are known to be decarboxylative in bacteria but non-decarboxylative in archaea [55].

Interestingly, it has been unclear for a long time if either the bacterial FA synthesis pathway specifically recognizes each acyl-ACP intermediate or if its enzymes randomly fix these intermediates, modifying the correct ones and releasing the inappropriate ones. Recent work has shown that ACP carries out its channeling function by adopting unique conformations for each enzyme of the FA elongation cycle [56]. Yet, it can be reasonably assumed that a putative ACP-independent mechanism would rather use random interactions between intermediate metabolites and enzymes, which might be assumed to be less efficient than the bacterial ACP-mediated system. Although this remains speculative and needs biochemical confirmation, the high efficiency of the ACP-mediated machinery may explain the preeminence of FA in bacterial membranes, whereas archaea would have opted by the alternative ancestral mechanism of synthesis of lateral chains for membrane phospholipids, namely, the isoprenoids [31], relegating FA to different cellular functions and, only to a small extent, to membrane synthesis [54].

5. Linking Glycerol Phosphate with the Lateral Chains

Although archaeal phospholipids were already known to use G1P instead of G3P as bacteria and eukaryotes do, the recent characterization and sequencing of the enzyme responsible for its synthesis in archaea (G1P dehydrogenase [57, 58]) was astonishing because this enzyme appeared to be totally unrelated to the canonical G3P dehydrogenase [59]. Since then, very little exceptions to this clear-cut distinction between archaea and bacteria have been described (the most remarkable is probably the description of an archaeal-like G1P dehydrogenase in the bacterium *Bacillus subtilis*, [60]), but the fact that the two dehydrogenases belong to large enzymatic superfamilies from which they were recruited has provided a model for the independent origin of these dehydrogenases from likely ancient promiscuous enzymes [8].

Geranylgeranylglyceryl diphosphate and di-O-geranylgeranylglyceryl phosphate synthases (GGGPS and DGGGPS, resp.) are the enzymes that subsequently link isoprenoids to glycerol phosphate in archaea [18]. Boucher et al. [23] found that GGGPS are widespread in archaea whereas, among bacteria, it was found only in Bacillales and in one Bacteroidetes species. They also described a very divergent homologue in halophilic archaea and in *Archaeoglobus*. Despite their divergence, these enzymes appear to carry out the same function [61]. Using an updated genome sequence database, we also retrieve the very divergent GGGPS in Methanomicrobiales, confirm that GGGPS is present in Bacillales, and extend this observation to a surprising diversity of Bacteroidetes (Supplementary Figure 3. This suggests that GGGPS plays an important role in these two bacterial groups and, indeed, it has recently been shown to participate in the synthesis of archaeal-type lipids of unknown function in these bacteria [16]. In conclusion, at least one GGGPS gene appears to have been present in LACA, whereas the divergent copy of this gene probably emerged later in a more recent group of euryarchaeota. GGGPS were probably independently transferred to the respective ancestors of Bacillales and Bacteroidetes.

Hemmi et al. [62] carried out the first phylogenetic analysis of the DGGGPS sequences and their superfamily, the UbiA prenyltransferase family (17 sequences branching in 6 different groups). Using all sequences available at present, we retrieve similar but much more diversified groups (Supplementary Figure 4. Archaeal sequences cluster together in a monophyletic assemblage, suggesting common ancestry, although crenarchaeota are paraphyletic probably as a result of reconstruction artifacts. A number of bacteroidetes sequences branch among the crenarchaeota, reflecting an HGT event to an ancestor of this bacterial group. In addition several bacterial phyla (Chlorobi, Cyanobacteria, Chloroflexi, Planctomycetales, and some proteobacterial species) possess UbiA-related homologues. However, in several of these bacterial species, these enzymes are involved in photosynthesis (they take part in the synthesis of respiratory quinones, hemes, chrolophylls, and vitamin E [62]) and it is difficult to determine if the widespread distribution in bacteria is due to the ancestral presence of a homologue of this enzyme in the last common bacterial ancestor or to several recent HGTs to these bacterial groups from archaeal donors.

The search of homologues of the bacterial glycerol phosphate acyl transferases PlsX, PlsY, PlsB, and PlsC, which carry out the addition of fatty acids to glycerol phosphate [63, 64], in the available archaeal genome sequences allowed retrieving very few homologues, all of them most likely acquired by HGT from bacterial donors (not shown).

6. Linking the Polar Head Groups

Once the two hydrocarbon chains are linked to the phospholipid backbone, two additional steps are required to add the polar head group (Figure 1). First, an enzyme replaces the phosphate linked to the glycerol moiety by a CDP group; then, this CDP is replaced by the final polar head group, which can be very diverse (glycerol, myo-inositol, serine, and so forth) [18]. The first step has been biochemically described in archaea but the enzyme that carries out this function remains unknown [65]. The bacterial counterpart is the CDP diglyceride synthetase (CdsA) [66, 67]. We looked for archaeal homologues of the bacterial enzyme and retrieved several sequences that we used as queries for exhaustive searches in archaeal genomes. This allowed us to observe that this enzyme is widespread both in bacteria and archaea. Our phylogenetic trees show two clades that correspond to archaea and bacteria and the phylogenetic relationships within each of them are congruent with the main accepted taxonomic groups (Figure 4). This supports the vertical inheritance of this gene from the cenancestor and, consequently, its presence in LACA. However, to our knowledge no archaeal CdsA has been biochemically characterized so far, which would be required to confirm that these archaeal homologues are responsible for the biochemical activity described by Morii et al. [65].

Two enzymes involved in the second step of the attachment of polar head groups have been characterized in archaea [68, 69]. These enzymes belong to the large family of the CDP alcohol phosphatidyltransferases and have homologues in bacteria [70]. The bacterial members of this enzyme family are known to have different specificities in order to add different polar head groups on phospholipids. A previous phylogenomic survey carried out by Daiyasu et al. [70] showed that the different sequences group in phylogenetic trees according to their predicted substrates. In addition, the groups of bacterial sequences were in agreement with the main bacterial taxonomic groups. Our analysis with a larger taxonomic sample confirms that homologues of these genes are widespread in archaea. All sequences group into three main categories (data not shown), one related to the addition of serine as a polar head group [68], another related to myo-inositol-phosphate transfer [69] (and maybe also glycerol in archaea, according to classification in [70]), and the last one using glycerol. Archaea are found in the first two groups but not in the last one. In order to avoid artifacts due to extreme sequence divergence, we carried out phylogenies for each of the two groups containing archaeal representatives. In the first phylogeny, archaeal sequences predicted to use serine [68] as a substrate are limited to Euryarchaeota (Supplementary Figure 5). This tree shows a poorly supported group of slow evolving bacteria together with several divergent bacterial, eukaryotic and archaeal (*Methanococcoides burtonii* and haloarchaea) sequences. Such mixed distribution dominated by strong sequence divergence and HGTs contrasts with the rest of the phylogeny, which is congruent with the main accepted taxonomic groups. Especially, one monophyletic group of euryarchaeota can be pointed out, supporting that this enzyme probably existed at least in the last euryarchaeotal common ancestor. In the second tree, a larger group of archaeal enzymes, predicted to use glycerol phosphate or myo-inositol-phosphate as substrates [69, 70], cluster in our analysis with bacterial enzymes that use myo-inositol, but these bacterial sequences are scarce and appear to have been acquired from archaea by HGT (Supplementary Figure 6). The phylogeny of archaeal sequences supports the monophyly of Crenarchaeota and a patchy distribution of several paralogues in Euryarchaeota, which makes difficult the analysis of the evolution of these enzymes in archaea without incorporating supplementary biochemical information. At any rate, the wide distribution of this enzyme family in archaea strongly suggests that at least one representative of these enzymes was already present in LACA. Whereas it was conserved in Crenarchaeota, it was subjected to several duplication and neofunctionalization events in Euryarchaeota, which would explain the complex distribution pattern observed in euryarchaeotal species.

7. Saturation of Isoprenoid Chains

So far, we have described the main synthesis and link mechanisms of archaeal phospholipid components, but a wide diversity of phospholipids actually exists in archaea [71]. A substantial characteristic of archaeal membranes is their saturation rate, since double bonds have a prominent influence on membrane stability [72]. Most archaea contain saturated phospholipids and the geranylgeranyl reductase (GGR), the enzyme responsible for the reduction of isoprenoid chains, has been recently described in the euryarchaeota *Thermoplasma acidophilum* and *Archaeoglobus fulgidus* and the crenarchaeote *Sulfolobus acidocaldarius* [73–75]. These studies show that archaeal GGR are able to use geranylgeranyl chains either isolated or attached to phospholipids as substrates. When GGPP is used as a substrate, all bonds but the one in position C2 are reduced, allowing the incorporation in phospholipids, but isoprenoids chains that are already attached to glycerol phosphate can have all their double bonds reduced by this enzyme. As a result, isoprenoid reduction can happen at different steps of the phospholipid biosynthesis pathway (Figure 1).

Archaeal GGRs are homologous to previously reported cyanobacterial and plant GGRs involved in chlorophyll synthesis [76, 77] and many different GGR paralogues have been identified in archaeal genomes that could carry out independent isoprenoid chain reductions [19]. Our phylogeny of GGRs confirms that GGRs are widespread among crenarchaeota and that at least two paralogues exist in a wide diversity of euryarchaeota, although some archaeal groups also bear supplementary GGR genes (Supplementary Figure 7). This supports the ancestral presence of at least one GGR gene in archaea, followed by a complex history of duplications and HGTs. GGRs are also present in many bacterial genomes, but several HGTs can be observed, probably related to the function of this gene in photosynthesis, making uncertain the primary origin of this gene in bacteria. Among eukaryotes, only sequences from plastid-bearing organisms were detected and these sequences clearly branched within

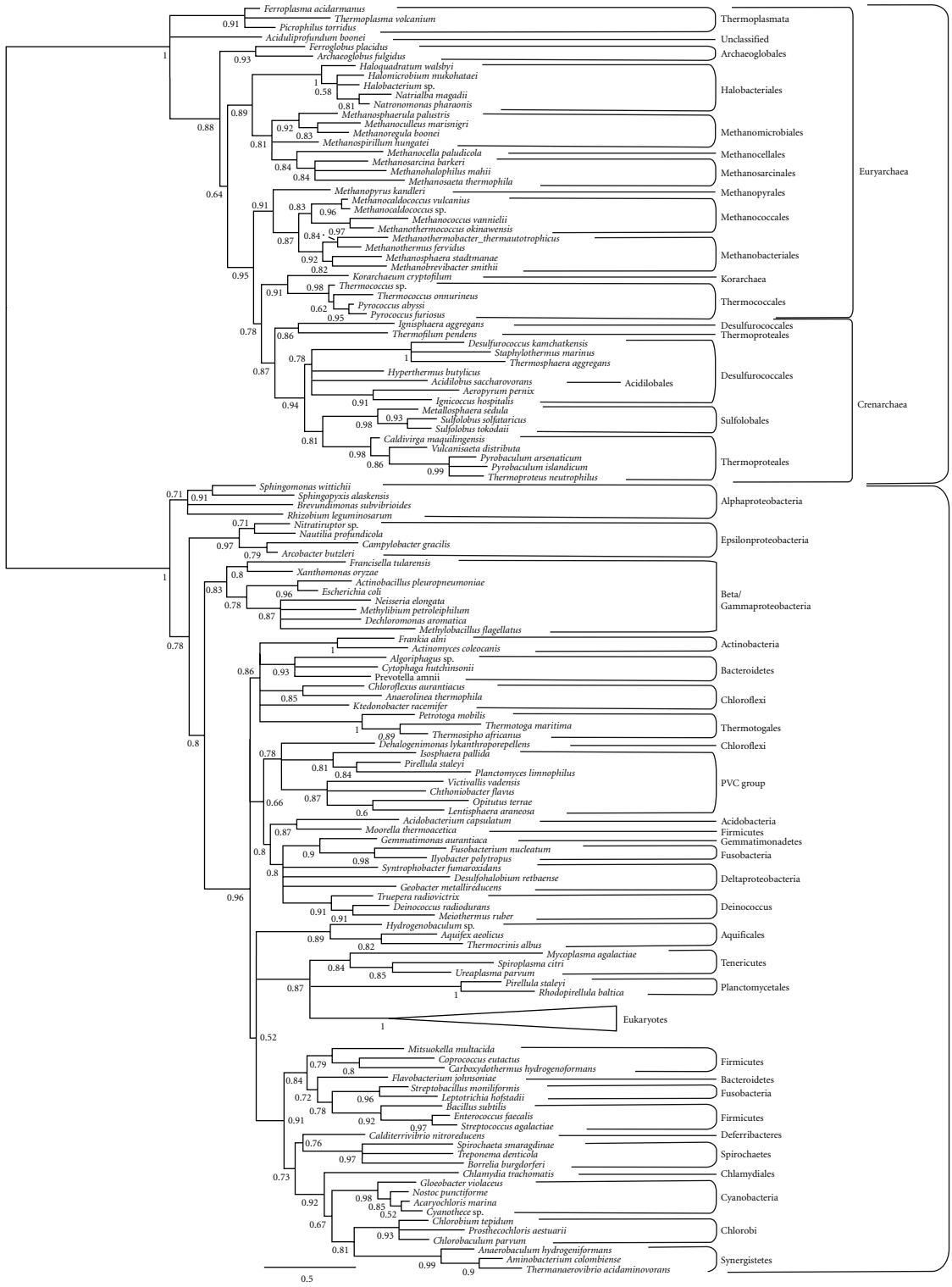

Figure 4: CdsA phylogenetic tree reconstructed using 133 representative sequences and 87 conserved sites. Branches with support values <0.50 have been collapsed. For the complete phylogeny, see Supplementary Figure 8.

one group of cyanobacterial sequences, thus supporting the plastidial origin of these genes in eukaryotes.

8. Discussion

In contrast with the rather impressive knowledge about the biochemistry and biosynthesis of bacterial cell membranes, many aspects of their archaeal counterparts remain to be elucidated. Even the synthesis of the most canonical archaeal membrane lipids, the phospholipids based on isoprenoid lateral chains, still has some unresolved points, such as the identity of the enzyme carrying out the phosphomevalonate decarboxylase activity necessary for the final steps of the synthesis of isoprenoid precursors. Moreover, it is becoming clear that archaeal membranes incorporate components that were supposed to be restricted to the other two domains of life, bacteria and eukaryotes. This is notably the case of fatty acids that, despite being relatively widespread in membrane phospholipids of euryarchaeotal species [14], are synthesized by a pathway that, most likely, has important differences with the bacterial counterpart [54].

Comparative genomics and phylogenomics provide a powerful way to address these questions, in particular by the detection of potential candidates to carry out missing enzymatic functions thanks to similarities with bacterial and eukaryotic enzymes. This has allowed us to propose, for example, the existence of an ACP-independent pathway of fatty acid synthesis in archaea [54] and allows us to propose here that archaeal CdsA homologues could carry the same function as in bacteria. This approach has also provided evidence supporting that lipid membranes were already evolved long ago, at the time of the cenancestor [9]. Thus, rather than radical inventions of new phospholipid biochemistries, bacteria and archaea appear to have specialized their cell membranes by tuning the relative importance of the different components, with isoprenoids becoming dominant in archaea and fatty acids in bacteria. Nevertheless, these bioinformatic approaches have limitations and biochemical investigation remains crucial to characterize the different missing activities (the uncharacterized MVA pathway enzymes in archaea, the hypothetical ACP-independent FA synthesis pathway, the characterization of the archaeal CdsA, and a larger diversity of CDP alcohol phosphatidyltransferases) in order to complete the puzzle of archaeal membrane synthesis.

9. Material and Methods

Sequence seeds for similarity searches were retrieved from the KEGG database (http://www.genome.jp/kegg/). Searches were carried out with BLASTp [78] against a list of completely sequenced genomes available in GenBank (Supplementary Table 1). The resulting sequences were aligned with by default parameters with Muscle 3.6 [79]. Redundant and partial sequences were removed and ambiguously aligned regions were discarded prior to phylogenetic analyses using the NET program from the MUST package [80]. Phylogenetic trees were reconstructed with the approximately maximum likelihood approach with FastTree 2.1.3 [81].

Acknowledgments

The authors thank A. Corcelli for the invitation to contribute this paper. This work was supported by the interdisciplinary programs Origine des Planètes et de la Vie and InTerrVie (Interactions Terre-Vie) of the French Centre National de la Recherche Scientifique and Institut National des Sciences de l'Univers and by French National Agency for Research (EVOLDEEP Project, contract no. ANR-08-GENM-024-002). J. Lombard is recipient of a Ph.D. fellowship of the French Research Ministry.

References

[1] C. R. Woese and G. E. Fox, "Phylogenetic structure of the prokaryotic domain: the primary kingdoms," *Proceedings of the National Academy of Sciences of the United States of America*, vol. 74, no. 11, pp. 5088–5090, 1977.

[2] M. Kates, L. S. Yengoyan, and P. S. Sastry, "A diether analog of phosphatidyl glycerophosphate in *Halobacterium cutirubrum*," *Biochimica et Biophysica Acta*, vol. 98, no. 2, pp. 252–268, 1965.

[3] T. A. Langworthy, P. F. Smith, and W. R. Mayberry, "Lipids of *Thermoplasma acidophilum*," *Journal of Bacteriology*, vol. 112, no. 3, pp. 1193–1200, 1972.

[4] T. A. Langworthy, W. R. Mayberry, and P. F. Smith, "Long chain glycerol diether and polyol dialkyl glycerol triether lipids of *Sulfolobus acidocaldarius*," *Journal of Bacteriology*, vol. 119, no. 1, pp. 106–116, 1974.

[5] C. R. Woese, L. J. Magrum, and G. E. Fox, "Archaebacteria," *Journal of Molecular Evolution*, vol. 11, no. 3, pp. 245–252, 1978.

[6] T. G. Tornabene and T. A. Langworthy, "Diphytanyl and dibiphytanyl glycerol ether lipids of methanogenic archaebacteria," *Science*, vol. 203, no. 4375, pp. 51–53, 1979.

[7] M. De Rosa, A. Gambacorta, and A. Gliozzi, "Structure, biosynthesis, and physicochemical properties of archaebacterial lipids," *Microbiological Reviews*, vol. 50, no. 1, pp. 70–80, 1986.

[8] J. Peretó, P. López-García, and D. Moreira, "Ancestral lipid biosynthesis and early membrane evolution," *Trends in Biochemical Sciences*, vol. 29, no. 9, pp. 469–477, 2004.

[9] J. Lombard, P. López-García, and D. Moreira, "The early evolution of lipid membranes and the three domains of life," *Nature Reviews Microbiology*, vol. 10, no. 7, pp. 507–515, 2012.

[10] H. K. Mangold and F. Paltauf, *Ether Lipids: Biochemical and Biomedical Aspects*, Academic Press, 1983.

[11] R. Huber, T. Wilharm, D. Huber et al., "*Aquifex pyrophilus* gen.nov. sp.nov., represents a novel group of marine hyperthermophilic hydrogen-oxidizing bacteria," *Systematic and Applied Microbiology*, vol. 15, no. 3, pp. 340–351, 1992.

[12] J. S. S. Damsté, W. I. C. Rijpstra, E. C. Hopmans, S. Schouten, M. Balk, and A. J. M. Stams, "Structural characterization of diabolic acid-based tetraester, tetraether and mixed ether/ester, membrane-spanning lipids of bacteria from the order Thermotogales," *Archives of Microbiology*, vol. 188, no. 6, pp. 629–641, 2007.

[13] T. A. Langworthy, G. Holzer, J. G. Zeikus, and T. G. Tornabene, "Iso- and anteiso-branched glycerol diethers of the thermophilic anaerobe *Thermodesulfotobacterium commune*," *Systematic and Applied Microbiology*, vol. 4, no. 1, pp. 1–17, 1983.

[14] A. Gattinger, M. Schloter, and J. C. Munch, "Phospholipid etherlipid and phospholipid fatty acid fingerprints in selected

euryarchaeotal monocultures for taxonomic profiling," *FEMS Microbiology Letters*, vol. 213, no. 1, pp. 133–139, 2002.

[15] B. M. Lange, T. Rujan, W. Martin, and R. Croteau, "Isoprenoid biosynthesis: the evolution of two ancient and distinct pathways across genomes," *Proceedings of the National Academy of Sciences of the United States of America*, vol. 97, no. 24, pp. 13172–13177, 2000.

[16] H. Guldan, F. M. Matysik, M. Bocola, R. Sterner, and P. Babinger, "Functional assignment of an enzyme that catalyzes the synthesis of an archaea-type ether lipid in bacteria," *Angewandte Chemie*, vol. 50, no. 35, pp. 8188–8191, 2011.

[17] H. H. Tan, A. Makino, K. Sudesh, P. Greimel, and T. Kobayashi, "Spectroscopic evidence for the unusual stereochemical configuration of an endosome-specific lipid," *Angewandte Chemie*, vol. 51, no. 2, pp. 533–535, 2012.

[18] Y. Koga and H. Morii, "Biosynthesis of ether-type polar lipids in archaea and evolutionary considerations," *Microbiology and Molecular Biology Reviews*, vol. 71, no. 1, pp. 97–120, 2007.

[19] R. Matsumi, H. Atomi, A. J. M. Driessen, and J. van der Oost, "Isoprenoid biosynthesis in Archaea—biochemical and evolutionary implications," *Research in Microbiology*, vol. 162, no. 1, pp. 39–52, 2011.

[20] D. J. McGarvey and R. Croteau, "Terpenoid metabolism," *The Plant Cell*, vol. 7, no. 7, pp. 1015–1026, 1995.

[21] D. Zhou and R. H. White, "Early steps of isoprenoid biosynthesis in *Escherichia coli*," *The Biochemical Journal*, vol. 273, part 3, pp. 627–634, 1991.

[22] M. Rodríguez-Concepción and A. Boronat, "Elucidation of the methylerythritol phosphate pathway for isoprenoid biosynthesis in bacteria and plastids. A metabolic milestone achieved through genomics," *Plant Physiology*, vol. 130, no. 3, pp. 1079–1089, 2002.

[23] Y. Boucher, M. Kamekura, and W. F. Doolittle, "Origins and evolution of isoprenoid lipid biosynthesis in archaea," *Molecular Microbiology*, vol. 52, no. 2, pp. 515–527, 2004.

[24] M. Kates, M. K. Wassef, and D. J. Kushner, "Radioisotopic studies on the biosynthesis of the glyceryl diether lipids of *Halobacterium cutirubrum*," *Canadian Journal of Biochemistry*, vol. 46, no. 8, pp. 971–977, 1968.

[25] W. L. Lam and W. F. Doolittle, "Mevinolin-resistant mutations identify a promoter and the gene for a eukaryote-like 3-hydroxy-3-methylglutaryl-coenzyme A reductase in the archaebacterium *Haloferax volcanii*," *The Journal of Biological Chemistry*, vol. 267, no. 9, pp. 5829–5834, 1992.

[26] D. Yang, L. W. Shipman, C. A. Roessner, A. Ian Scott, and J. C. Sacchettini, "Structure of the *Methanococcus jannaschii* mevalonate kinase, a member of the GHMP kinase superfamily," *The Journal of Biological Chemistry*, vol. 277, no. 11, pp. 9462–9467, 2002.

[27] A. Smit and A. Mushegian, "Biosynthesis of isoprenoids via mevalonate in archaea: the lost pathway," *Genome Research*, vol. 10, no. 10, pp. 1468–1484, 2000.

[28] S. J. Barkley, R. M. Cornish, and C. D. Poulter, "Identification of an Archaeal type II isopentenyl diphosphate isomerase in *Methanothermobacter thermautotrophicus*," *Journal of Bacteriology*, vol. 186, no. 6, pp. 1811–1817, 2004.

[29] L. L. Grochowski, H. Xu, and R. H. White, "*Methanocaldococcus jannaschii* uses a modified mevalonate pathway for biosynthesis of isopentenyl diphosphate," *Journal of Bacteriology*, vol. 188, no. 9, pp. 3192–3198, 2006.

[30] R. Dutoit, J. de Ruyck, V. Durisotti, C. Legrain, E. Jacobs, and J. Wouters, "Overexpression, physicochemical characterization, and modeling of a hyperthermophilic *Pyrococcus furiosus* type 2 IPP isomerase," *Proteins*, vol. 71, no. 4, pp. 1699–1707, 2008.

[31] J. Lombard and D. Moreira, "Origins and early evolution of the mevalonate pathway of isoprenoid biosynthesis in the three domains of life," *Molecular Biology and Evolution*, vol. 28, no. 1, pp. 87–99, 2011.

[32] U. Jahn, R. Summons, H. Sturt, E. Grosjean, and H. Huber, "Composition of the lipids of *Nanoarchaeum equitans* and their origin from its host *Ignicoccus* sp. strain KIN4/I," *Archives of Microbiology*, vol. 182, no. 5, pp. 404–413, 2004.

[33] P. Bork, C. Sander, and A. Valencia, "Convergent evolution of similar enzymatic function on different protein folds: the hexokinase, ribokinase, and galactokinase families of sugar kinases," *Protein Science*, vol. 2, no. 1, pp. 31–40, 1993.

[34] J. L. Andreassi II and T. S. Leyh, "Molecular functions of conserved aspects of the GHMP kinase family," *Biochemistry*, vol. 43, no. 46, pp. 14594–14601, 2004.

[35] S. M. Houten and H. R. Waterham, "Nonorthologous gene displacement of phosphomevalonate kinase," *Molecular Genetics and Metabolism*, vol. 72, no. 3, pp. 273–276, 2001.

[36] T. J. Herdendorf and H. M. Miziorko, "Phosphomevalonate kinase: functional investigation of the recombinant human enzyme," *Biochemistry*, vol. 45, no. 10, pp. 3235–3242, 2006.

[37] M. Chen and C. D. Poulter, "Characterization of thermophilic archaeal isopentenyl phosphate kinases," *Biochemistry*, vol. 49, no. 1, pp. 207–217, 2010.

[38] B. A. Kellogg and C. D. Poulter, "Chain elongation in the isoprenoid biosynthetic pathway," *Current Opinion in Chemical Biology*, vol. 1, no. 4, pp. 570–578, 1997.

[39] S. I. Ohnuma, K. Hirooka, H. Hemmi, C. Ishida, C. Ohto, and T. Nishino, "Conversion of product specificity of archaebacterial geranylgeranyl- diphosphate synthase. Identification of essential amino acid residues for chain length determination of prenyltransferase reaction," *The Journal of Biological Chemistry*, vol. 271, no. 31, pp. 18831–18837, 1996.

[40] S. I. Ohnuma, K. Hirooka, N. Tsuruoka et al., "A pathway where polyprenyl diphosphate elongates in prenyltransferase: insight into a common mechanism of chain length determination of prenyltransferases," *The Journal of Biological Chemistry*, vol. 273, no. 41, pp. 26705–26713, 1998.

[41] A. Tachibana, Y. Yano, S. Otani, N. Nomura, Y. Sako, and M. Taniguchi, "Novel prenyltransferase gene encoding farnesylgeranyl diphosphate synthase from a hyperthermophilic archaeon, *Aeropyrum pernix*. Molecular evolution with alteration in product specificity," *European Journal of Biochemistry*, vol. 267, no. 2, pp. 321–328, 2000.

[42] A. Chen, P. A. Kroon, and C. D. Poulter, "Isoprenyl diphosphate synthases: protein sequence comparisons, a phylogenetic tree, and predictions of secondary structure," *Protein Science*, vol. 3, no. 4, pp. 600–607, 1994.

[43] T. G. Tornabene, R. S. Wolfe, W. E. Balch, G. Holzer, G. E. Fox, and J. Oro, "Phytanyl-glycerol ethers and squalenes in the archaebacterium *Methanobacterium thermoautotrophicum*," *Journal of Molecular Evolution*, vol. 11, no. 3, pp. 259–266, 1978.

[44] M. Nishihara, S. Nagahama, M. Ohga, and Y. Koga, "Straight-chain fatty alcohols in the hyperthermophilic archaeon *Pyrococcus furiosus*," *Extremophiles*, vol. 4, no. 5, pp. 275–277, 2000.

[45] N. M. Carballeira, M. Reyes, A. Sostre, H. Huang, M. F. J. M. Verhagen, and M. W. W. Adams, "Unusual fatty acid compositions of the hyperthermophilic archaeon *Pyrococcus furiosus* and the bacterium *Thermotoga maritima*," *Journal of Bacteriology*, vol. 179, no. 8, pp. 2766–2768, 1997.

[46] E. L. Pugh, M. K. Wassef, and M. Kates, "Inhibition of fatty acid synthetase in Halobacterium cutirubrum and *Escherichia*

coli by high salt concentrations," *Canadian Journal of Biochemistry*, vol. 49, no. 8, pp. 953–958, 1971.

[47] E. L. Pugh and M. Kates, "Acylation of proteins of the archaebacteria *Halobacterium cutirubrum* and *Methanobacterium thermoautotraphicum*," *Biochimica et Biophysica Acta*, vol. 1196, no. 1, pp. 38–44, 1994.

[48] M. Colella, S. Lobasso, F. Babudri, and A. Corcelli, "Palmitic acid is associated with halorhodopsin as a free fatty acid radiolabeling of halorhodopsin with 3H-palmitic acid and chemical analysis of the reaction products of purified halorhodopsin with thiols and NaBH4," *Biochimica et Biophysica Acta*, vol. 1370, no. 2, pp. 273–279, 1998.

[49] A. Corcelli, S. Lobasso, M. Colella, M. Trotta, A. Guerrieri, and F. Palmisano, "Role of palmitic acid on the isolation and properties of halorhodopsin," *Biochimica et Biophysica Acta*, vol. 1281, no. 2, pp. 173–181, 1996.

[50] M. Kolbe, H. Besir, L. O. Essen, and D. Oesterhelt, "Structure of the light-driven chloride pump halorhodopsin at 1.8 Å resolution," *Science*, vol. 288, no. 5470, pp. 1390–1396, 2000.

[51] V. Iverson, R. M. Morris, C. D. Frazar, C. T. Berthiaume, R. L. Morales, and E. V. Armbrust, "Untangling genomes from metagenomes: revealing an uncultured class of marine Euryarchaeota," *Science*, vol. 335, no. 6068, pp. 587–590, 2012.

[52] J. Lombard and D. Moreira, "Early evolution of the biotin-dependent carboxylase family," *BMC Evolutionary Biology*, vol. 11, article 232, 2011.

[53] J. Lombard and D. Moreira, "Correction: early evolution of the biotin-dependent carboxylase family," *BMC Evolutionary Biology*, vol. 12, no. 1, p. 117, 2012.

[54] J. Lombard, P. López-García, and D. Moreira, "An ACP-independent fatty acid synthesis pathway in archaea: implications for the Origin of Phospholipids," *Molecular Biology and Evolution*, vol. 29, no. 11, pp. 3261–3265, 2012.

[55] C. Jiang, S. Y. Kim, and D. Y. Suh, "Divergent evolution of the thiolase superfamily and chalcone synthase family," *Molecular Phylogenetics and Evolution*, vol. 49, no. 3, pp. 691–701, 2008.

[56] E. Płoskoń, C. J. Arthur, A. L. P. Kanari et al., "Recognition of intermediate functionality by acyl carrier protein over a complete cycle of fatty acid biosynthesis," *Chemistry & Biology*, vol. 17, no. 7, pp. 776–785, 2010.

[57] M. Nishihara and Y. Koga, "Purification and properties of sn-glycerol-1-phosphate dehydrogenase from Methanobacterium thermoautotrophicum: characterization of the biosynthetic enzyme for the enantiomeric glycerophosphate backbone of ether polar lipids of archaea," *Journal of Biochemistry*, vol. 122, no. 3, pp. 572–576, 1997.

[58] Y. Koga, T. Kyuragi, M. Nishihara, and N. Sone, "Did archaeal and bacterial cells arise independently from noncellular precursors? A hypothesis stating that the advent of membrane phospholipid with enantiomeric glycerophosphate backbones caused the separation of the two lines of descent," *Journal of Molecular Evolution*, vol. 46, no. 1, pp. 54–63, 1998.

[59] H. Daiyasu, T. Hiroike, Y. Koga, and H. Toh, "Analysis of membrane stereochemistry with homology modeling of sn-glycerol-1-phosphate dehydrogenase," *Protein Engineering*, vol. 15, no. 12, pp. 987–995, 2002.

[60] H. Guldan, R. Sterner, and P. Babinger, "Identification and characterization of a bacterial glycerol-1-phosphate dehydrogenase: Ni^{2+}-dependent AraM from *Bacillus subtilis*," *Biochemistry*, vol. 47, no. 28, pp. 7376–7384, 2008.

[61] J. Payandeh, M. Fujihashi, W. Gillon, and E. F. Pai, "The crystal structure of (S)-3-O-geranylgeranylglyceryl phosphate synthase reveals an ancient fold for an ancient enzyme," *The Journal of Biological Chemistry*, vol. 281, no. 9, pp. 6070–6078, 2006.

[62] H. Hemmi, K. Shibuya, Y. Takahashi, T. Nakayama, and T. Nishino, "(S)-2,3-Di-O-geranylgeranylglyceryl phosphate synthase from the thermoacidophilic archaeon *Sulfolobus solfataricus*. Molecular cloning and characterization of a membrane-intrinsic prenyltransferase involved in the biosynthesis of archaeal ether-linked membrane lipids," *The Journal of Biological Chemistry*, vol. 279, no. 48, pp. 50197–50203, 2004.

[63] M. Yoshimura, T. Oshima, and N. Ogasawara, "Involvement of the YneS/YgiH and PlsX proteins in phospholipid biosynthesis in both *Bacillus subtilis* and *Escherichia coli*," *BMC Microbiology*, vol. 7, article 69, 2007.

[64] Y. J. Lu, Y. M. Zhang, K. D. Grimes, J. Qi, R. E. Lee, and C. O. Rock, "Acyl-phosphates initiate membrane phospholipid synthesis in Gram-positive pathogens," *Molecular Cell*, vol. 23, no. 5, pp. 765–772, 2006.

[65] H. Morii, M. Nishihara, and Y. Koga, "CTP:2,3-di-O-geranylgeranyl-sn-glycero-1-phosphate cytidyltransferase in the methanogenic archaeon *Methanothermobacter thermoautotrophicus*," *The Journal of Biological Chemistry*, vol. 275, no. 47, pp. 36568–36574, 2000.

[66] T. Icho, C. P. Sparrow, and C. R. H. Raetz, "Molecular cloning and sequencing of the gene for CDP-diglyceride synthetase of *Escherichia coli*," *The Journal of Biological Chemistry*, vol. 260, no. 22, pp. 12078–12083, 1985.

[67] C. P. Sparrow and C. R. H. Raetz, "Purification and properties of the membrane-bound CDP-diglyceride synthetase from *Escherichia coli*," *The Journal of Biological Chemistry*, vol. 260, no. 22, pp. 12084–12091, 1985.

[68] H. Morii and Y. Koga, "CDP-2,3-di-O-geranylgeranyl-sn-glycerol:L-serine O-archaetidyltransferase (archaetidylserine synthase) in the methanogenic archaeon *Methanothermobacter thermautotrophicus*," *Journal of Bacteriology*, vol. 185, no. 4, pp. 1181–1189, 2003.

[69] H. Morii, S. Kiyonari, Y. Ishino, and Y. Koga, "A novel biosynthetic pathway of archaetidyl-myo-inositol via archaetidyl-myo-inositol phosphate from CDP-archaeol and D-glucose 6-phosphate in methanoarchaeon *Methanothermobacter thermautotrophicus* cells," *The Journal of Biological Chemistry*, vol. 284, no. 45, pp. 30766–30774, 2009.

[70] H. Daiyasu, K. I. Kuma, T. Yokoi, H. Morii, Y. Koga, and H. Toh, "A study of archaeal enzymes involved in polar lipid synthesis linking amino acid sequence information, genomic contexts and lipid composition," *Archaea*, vol. 1, no. 6, pp. 399–410, 2005.

[71] Y. Koga and H. Morii, "Recent advances in structural research on ether lipids from archaea including comparative and physiological aspects," *Bioscience, Biotechnology and Biochemistry*, vol. 69, no. 11, pp. 2019–2034, 2005.

[72] O. Dannenmuller, K. Arakawa, T. Eguchi et al., "Membrane properties of archaeal macrocyclic diether phospholipids," *Chemistry*, vol. 6, no. 4, pp. 645–654, 2000.

[73] Y. Nishimura and T. Eguchi, "Biosynthesis of archaeal membrane lipids: digeranylgeranylglycerophospholipid reductase of the thermoacidophilic archaeon *Thermoplasma acidophilum*," *Journal of Biochemistry*, vol. 139, no. 6, pp. 1073–1081, 2006.

[74] M. Murakami, K. Shibuya, T. Nakayama, T. Nishino, T. Yoshimura, and H. Hemmi, "Geranylgeranyl reductase involved in the biosynthesis of archaeal membrane lipids in the hyperthermophilic archaeon *Archaeoglobus fulgidus*," *FEBS Journal*, vol. 274, no. 3, pp. 805–814, 2007.

[75] S. Sato, M. Murakami, T. Yoshimura, and H. Hemmi, "Specific partial reduction of geranylgeranyl diphosphate by an enzyme from the thermoacidophilic archaeon *Sulfolobus acidocaldarius* yields a reactive prenyl donor, not a dead-end product," *Journal of Bacteriology*, vol. 190, no. 11, pp. 3923–3929, 2008.

[76] H. A. Addlesee, L. C. D. Gibson, P. E. Jensen, and C. N. Hunter, "Cloning, sequencing and functional assignment of the chlorophyll biosynthesis gene, chlP, of Synechocystis sp. PCC 6803," *FEBS Letters*, vol. 389, no. 2, pp. 126–130, 1996.

[77] R. Tanaka, U. Oster, E. Kruse, W. Rüdiger, and B. Grimm, "Reduced activity of geranylgeranyl reductase leads to loss of chlorophyll and tocopherol and to partially geranylgeranylated chlorophyll in transgenic tobacco plants expressing antisense RNA for geranylgeranyl reductase," *Plant Physiology*, vol. 120, no. 3, pp. 695–704, 1999.

[78] S. F. Altschul, W. Gish, W. Miller, E. W. Myers, and D. J. Lipman, "Basic local alignment search tool," *Journal of Molecular Biology*, vol. 215, no. 3, pp. 403–410, 1990.

[79] R. C. Edgar, "MUSCLE: multiple sequence alignment with high accuracy and high throughput," *Nucleic Acids Research*, vol. 32, no. 5, pp. 1792–1797, 2004.

[80] H. Philippe, "MUST, a computer package of management utilities for sequences and trees," *Nucleic Acids Research*, vol. 21, no. 22, pp. 5264–5272, 1993.

[81] M. N. Price, P. S. Dehal, and A. P. Arkin, "FastTree 2—approximately maximum-likelihood trees for large alignments," *PLoS One*, vol. 5, no. 3, Article ID e9490, 2010.

Hindawi Publishing Corporation
Archaea
Volume 2012, Article ID 957852, 10 pages
doi:10.1155/2012/957852

Research Article

Coupled TLC and MALDI-TOF/MS Analyses of the Lipid Extract of the Hyperthermophilic Archaeon *Pyrococcus furiosus*

Simona Lobasso,[1] Patrizia Lopalco,[2] Roberto Angelini,[1] Rita Vitale,[2] Harald Huber,[3] Volker Müller,[4] and Angela Corcelli[1,5]

[1] *Department of Basic Medical Sciences, University of Bari Aldo Moro, Piazza G. Cesare, 70124 Bari, Italy*
[2] *Institute for Microelectronics and Microsystems, IMM-CNR, National Research Council, 73100 Lecce, Italy*
[3] *Institute for Microbiology and Archaeal Centre, University of Regensburg, 93053 Regensburg, Germany*
[4] *Molecular Microbiology and Bioenergetics, Institute of Molecular Biosciences, Goethe University of Frankfurt, 60438 Frankfurt/Main, Germany*
[5] *Institute for Chemical-Physical Processes, IPCF-CNR, National Research Council, 70126 Bari, Italy*

Correspondence should be addressed to Angela Corcelli, angela.corcelli@uniba.it

Received 16 July 2012; Accepted 27 September 2012

Academic Editor: Yosuke Koga

The lipidome of the marine hyperthermophilic archaeon *Pyrococcus furiosus* was studied by means of combined thin-layer chromatography and MALDI-TOF/MS analyses of the total lipid extract. 80–90% of the major polar lipids were represented by archaeol lipids (diethers) and the remaining part by caldarchaeol lipids (tetraethers). The direct analysis of lipids on chromatography plate showed the presence of the diphytanylglycerol analogues of phosphatidylinositol and phosphatidylglycerol, the *N*-acetylglucosamine-diphytanylglycerol phosphate plus some caldarchaeol lipids different from those previously described. In addition, evidence for the presence of the dimeric ether lipid cardiolipin is reported, suggesting that cardiolipins are ubiquitous in archaea.

1. Introduction

Pyrococcus furiosus is an aquatic anaerobic hyperthermophilic archaeon, originally isolated from geothermally heated marine sediments near Vulcano Island, Italy [1]. It can grow between 70°C and 103°C, with an optimum temperature of 100°C, and between pH 5 and pH 9 (with an optimum at pH 7). The cells appear as regular cocci of 0.8 μm to 1.5 μm diameters with monopolar polytrichous flagellation and cellular envelope composed of a glycoprotein distinguishing them from bacteria.

P. furiosus is unique among its kind in that it can use a wide range of compounds as carbon source, such as peptides and carbohydrates [2]. Unlike other hyperthermophiles, it does not need elemental sulphur for growth [3]. It is also notable that some of its enzymes are tungsten dependent, a very rare element which is to be found in biological systems [4].

P. furiosus has an unusual and intriguingly simple respiratory system, which obtains energy by reducing protons to hydrogen gas and uses this energy to create a proton gradient across its cell membrane, thereby driving ATP synthesis. The A_1A_0 ATP synthase from *P. furiosus* has been recently isolated and its three-dimensional structure was analyzed by electron microscopy [5]. The sequencing of the complete *P. furiosus* genome was completed in 2001; it is 1.91 Million *bp* long and contains approximately 2228 predicted genes [6].

One of the most peculiar features of archaea is represented by the structural properties of their membrane lipids. Archaeal membrane lipids are constituted by mostly saturated phytanyl chains in ether linkage to glycerol carbons with *sn*-2,3 configuration, forming diether (archaeol) and membrane-spanning tetraether (caldarchaeol) lipids (Figure 1) [7–9]. Furthermore, ether analogues of cardiolipins, bisphosphatidylglycerol (or BPG) and glycosyl-cardiolipins, have been found in the membranes of extremely

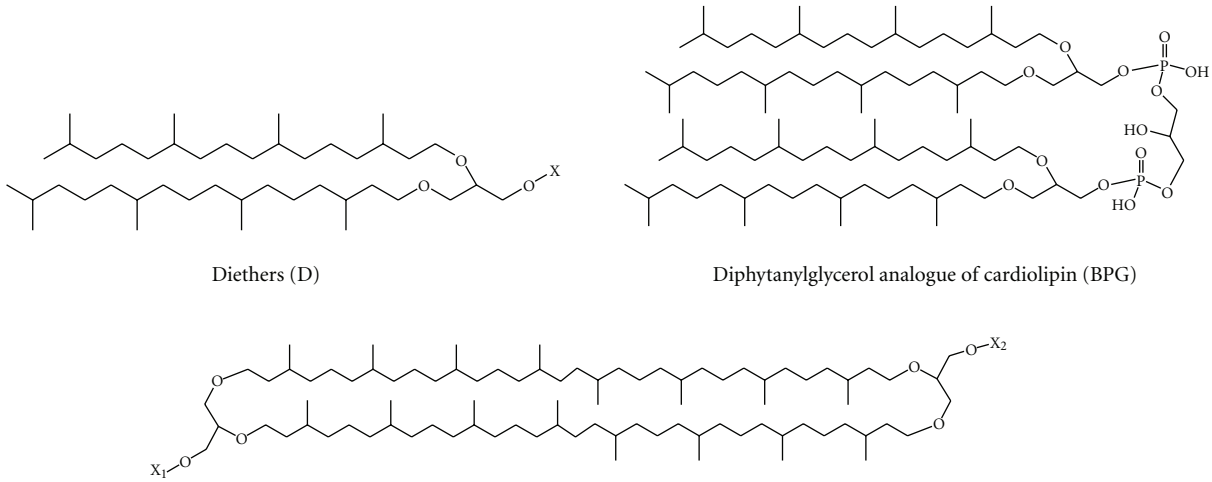

Figure 1: General structures of diphytanylglycerol-derived lipids diethers (D) and tetraethers (T). The diphytanylglycerol lipid core of membrane lipids of Archaea is also named archaeol. X, X_1, and X_2 represent the head groups of polar lipids.

halophilic archaea [10–13]. The archaeal bisphosphatidylglycerol is a dimeric phospholipid containing four identical branched C_{20} lipid chains, as it is synthesized at the expense of C_{20} C_{20} phosphatidylglycerol based on the 2,3-di-*O*-phytanyl-*sn*-glycerol diether lipid core (PG) [14, 15]. Recently ether lipid cardiolipin variants, constituted by different combinations of C_{20} and C_{25} isopranoid chains, have been found in two extremely haloalkaliphilic archaea *Natronococcus occultus* and *Natronococcus amylolyticus* [16]. Studies conducted so far have not revealed the presence of diphytanylglycerol analogues of cardiolipin in hyperthermophilic archaea.

Previous studies on lipids of hyperthermophilic archaea of the Thermococcaceae family have been reported [17–20]. Although some lipid structures of *P. furiosus* were proposed on the basis of FAB-MS studies [20], the individual lipids have not been isolated nor have complete structures to be determined.

In the present work we have reexamined the lipids of the hyperthermophilic archaeon *P. furiosus* with modern analytical methods with the aim of enriching our knowledge of the lipidome of this microorganism and in particular of checking for the possible presence of novel archaeal cardiolipins. Here we show that the dimeric phospholipid cardiolipin is present in hyperthermophilic archaea and report additional novel findings on membrane diether and tetraether lipids of this microorganism.

2. Material and Methods

2.1. Materials. 9-Aminoacridine hemihydrate was purchased from Acros Organics (Morris Plains, NJ, USA). The following commercial glycerophospholipids (used as standards): 1,1′,2,2′-tetratetradecanoyl cardiolipin, 1,1′,2,2′-tetra-(9*Z*-octadecenoyl) cardiolipin, 1,2-ditetradecanoyl-*sn*-glycero-3-phosphate, and 1,2-ditetradecanoyl-*sn*-glycero-3-phospho-(1′-*rac*-glycerol), 1,2-ditetradecanoyl-*sn*-glycero-3-phospho-L-serine, 1,2-di-(9*Z*-hexadecenoyl)-*sn*-glycero-3-phosphoethanolamine, were purchased from Avanti Polar Lipids, Inc. (Alabaster, AL, USA). In addition, the archaeal cardiolipins bisphosphatidylglycerol (BPG), isolated from *Hbt. salinarum,* and the glycosylated cardiolipin (2′-sulfo)Man*p*α1-2Glc*p*α1-1-[*sn*-2,3-di-*O*-phytanylglycerol]-6-[phospho-*sn*-2,3-di-*O*-phytanylglycerol] (S-DGD-5-PA), isolated from *Halorubrum sp.* MdS1 strain [15], were used as standard in the present study. All organic solvents used in the lipid extraction and MS analyses were commercially distilled and of the highest available purity and were purchased from Sigma Aldrich, J.T. Baker or Carlo Erba. HPTLC and TLC plates (HPTLC Silica gel 60 A, aluminium plates and TLC Silica gel 60 A glass plates), obtained from Merck, were washed twice with chloroform/methanol (1 : 1, v/v) and activated at 180°C before use.

2.2. Microorganism and Growth Conditions. P. furiosus (DSM 3638) was obtained from the Deutsche Sammlung für Mikroorganismen und Zellkulturen, Braunschweig, Germany. *P. furiosus* was grown in a 300 L fermenter at 98°C in the medium described [21]. The fermenter was pressurized to 2 bar with N_2/CO_2 (80 : 20). The gas flow through was adjusted to 1–7 L/min, depending on the growth phase. Growth was monitored by cell counts. Cells were harvested in the late exponential growth phase by centrifugation (10,000 ×g, 20 min, 4°C). The pellets were stored at −80°C.

2.3. Lipid Extraction. Total lipids were extracted using the Bligh and Dyer method [22], as modified for extreme halophiles [23]; the extracts were carefully dried under

N_2 before weighing and then dissolved in chloroform (10 mg/mL).

2.4. High-Performance Thin-Layer Chromatography (HPTLC). Total lipid extracts were analyzed by HPTLC (Merck 10 × 20 cm, aluminium back) with Solvent A (chloroform/methanol/90% acetic acid, 65 : 4 : 35, v/v). Lipid detection was carried out by spraying with 5% sulfuric acid in water, followed by charring at 180°C for 7-8 min [23], or alternatively spraying the plate with a solution of primuline [24] and detecting lipid upon excitation by UV light (336 nm). Furthermore, the following stainings were performed in order to identify the lipid classes present in the TLC bands: (a) Molybdenum-Blue Sigma spray reagent for phospholipids; (b) Azure-A/sulfuric acid for sulfatides and sulfoglycolipids; (c) ninhydrin in acetone/lutidine (9 : 1) for free amino groups [23].

2.5. Isolation and Purification of Individual Lipids from the Total Extract. The lipid components of the total lipid extract of *P. furiosus* were separated by preparative TLC (Merck 20 × 20 cm × 0.2 mm thick layer, glass plates) in Solvent A. Lipids were visualized by staining with iodine vapour and were eluted and recovered from the scraped silica, as previously described [10]. Isolated and purified phospholipids were dissolved in chloroform at the concentration of 1 mg/mL.

2.6. Preparation of Lipid Samples in Solution for MALDI-TOF/MS. Samples were prepared as previously described [25]. Briefly, the total lipid extract (10 mg/mL) and individual lipid components (1-2 mg/mL) were diluted from 20 to 200 μL with isopropanol/acetonitrile (60 : 40, v/v). Next, 10 μL of diluted sample was mixed with 10 μL of the matrix 9-aminoacridine (10 mg/mL; dissolved in isopropanol/acetonitrile (60 : 40, v/v)). Then 0.25 μL of the mixture was spotted on the MALDI target (Micro Scout Plate, MSP 96 ground steel target).

The protein pellet resulting from the lipid extraction of *P. furiosus* cells was recovered and directly analyzed by MALDI-TOF/MS avoiding the second lipid extraction, as recently described [26].

2.7. Coupling of MALDI-TOF/MS to HPTLC . The procedure was carried out according to Fuchs et al. [24], with minor modifications, cutting the HPTLC plates in pieces (about 4 × 8 cm in size) containing all the lipids present in the total extract. These pieces, which corresponded to a single lane of HPTLC, were then fixed onto the MALDI target with double-sided adhesive tape. Three small droplets of saturated matrix (9-aminoacridine) solution (in total 1.5 μL) were then deposited onto each point, obtaining a continuous deposition along the HPTLC lane. Then the matrix deposition points were numbered and each of them was assigned to HPTLC band areas of interest by comparing the retention factors resulting from staining by lipid charring. Then all the matrix deposition points were directly analyzed with MALDI-TOF/MS. Although for each TLC band a certain number of mass spectra were acquired, only the most representative spectra are shown.

2.8. MALDI-TOF Mass Spectrometry. MALDI-TOF mass spectra were acquired on a Bruker Microflex RLF mass spectrometer (Bruker Daltonics, Bremen, Germany). The system utilizes a pulsed nitrogen laser, emitting at 337 nm, the extraction voltage was 20 kV, and gated matrix suppression was applied to prevent detector saturation. 999 single laser shots (sum of 3 × 333) were averaged for each mass spectrum. The laser fluence was kept about 10% above threshold to have a good signal-to-noise ratio. In particular for the analysis of the bands on the HPTLC plates, the laser fluence was 20% more than in the analysis of the lipids in solution; in fact a major fluence is needed to desorb lipids from the silica. All spectra were acquired in reflector mode using the delayed pulsed extraction; only spectra acquired in negative ion mode are shown in this study. Spectral mass resolutions and signal-to-noise ratios were determined by the software for the instrument, "Flex Analysis 3.3.65" (Bruker Daltonics).

Post Source Decay (PSD) spectra were acquired on a Bruker Autoflex mass spectrometer (Bruker Daltonics), as previously described [27]. Briefly, the precursor ions were isolated using a time ion selector. The fragment ions were refocused onto the detector by stepping the voltage applied to the reflectron in appropriate increments. This was done automatically by using the "FAST" ("fragment analysis and structural TOF") subroutine of the Flex Analysis software.

A mix containing 1,1′,2,2′-tetratetradecanoyl cardiolipin, 1,1′2,2′-tetra-(9*Z*-octadecenoyl) cardiolipin, 1,2-ditetradecanoyl-*sn*-glycero-3-phosphate, 1,2-ditetradecanoyl-*sn*-glycero-3-phospho-(1′-rac-glycerol), 1,2-ditetradecanoyl-*sn*-glycero-3-phospho-L-serine, 1,2-di-(9*Z*-hexadecenoyl)-*sn*-glycero-3-phosphoethanolamine, and the archaeal glycosylated cardiolipin (2′-sulfo)Man*p*α1-2Glc*p*α1-1-[sn-2,3-di-*O*-phytanylglycerol]-6-[phospho-*sn*-2,3-di-*O*-phytanylglycerol] (S-DGD-5-PA) was always spotted next to the sample as external standard and an external calibration was performed before each measurement; the mass range of the authentic standards is 590–1770 a.m.u.

3. Results and Discussion

Figure 2 shows the MALDI-TOF mass spectrum of the total lipid extract of *P. furiosus* acquired in the negative ion mode, using 9-aminoacridine as matrix. Since MALDI ionization is quite soft, molecular ions of lipids are predominant in mass spectra by using the proper matrix. As MALDI-TOF/MS allows ionization and transfer of the lipid sample from the solid phase to gas phase, it is similar to FAB-MS, previously used to study the lipids of *P. furiosus* [20]. The peaks in the spectrum can be grouped in two main *m/z* ranges: signals attributable to diphytanylglycerol lipids, also named archaeol lipids, or simply diethers (D), in the range 700–1000, and those attributable to caldarchaeol lipids (i.e., tetraethers, T), typically in the range 1500–2000. The high *m/z* range is also the area of the mass spectrum where cardiolipins and

Table 1: Assignments of *m/z* values detected in the negative ion mode MALDI-TOF mass spectra and PSD analyses of the *P. furiosus* total lipid extract to various lipid components. Lipids are indicated as abbreviations.

Observed $[M–H]^-$ signals (*m/z*)	Assignments	Calculated $[M–H]^-$ (*m/z*)
1784.6	$(Hexose\text{-}P)_2$-T	1784.3
1741.5	*N*-Acetyl-hexose-hexose-P-T*cyclic*	1741.4
1701.9	$Hexose_2$-P-T *cyclic*	1702.4
1543.5	BPG plus Na^+	1542.3
1521.3	BPG	1520.3
976.2	DGD	975.8
934.8	*N*-Acetyl-hexose-P-D	934.7
922.6	*uns*-*N*-Acetyl-hexose-P-D	922.6
893.8	PI	893.7
881.6	*uns*PI	881.5
867.2	PGP minus H_2O	868.6
814.4	MGD	813.7
805.7	PG	805.7
787.5	PG minus H_2O	787.7
731.8	PA	731.6
241.3	Hexose-P minus H_2O	242.0

Abbreviations—D: diether or archaeol; T: tetraether or caldarchaeol; T*cyclic*: caldarchaeol with cyclopentane rings; P: phosphate group; *uns*: unsaturated branched-chains, 3 double bonds for chain; *N*-acetyl-hexose: *N*-acetylglucosamine; PI: diphytanylglycerol analogue of phosphatidylinositol; BPG: diphytanylglycerol analogue of bisphosphatidylglycerol (or ether lipid cardiolipin); PG: diphytanylglycerol analogue of phosphatidylglycerol; PGP: diphytanylglycerol analogue of phosphatidylglycerol-phosphate; PA: diphytanylglycerol analogue of phosphatidic acid; MGD: monoglycosyl-diphytanylglycerol; DGD: diglycosyl-diphytanylglycerol.

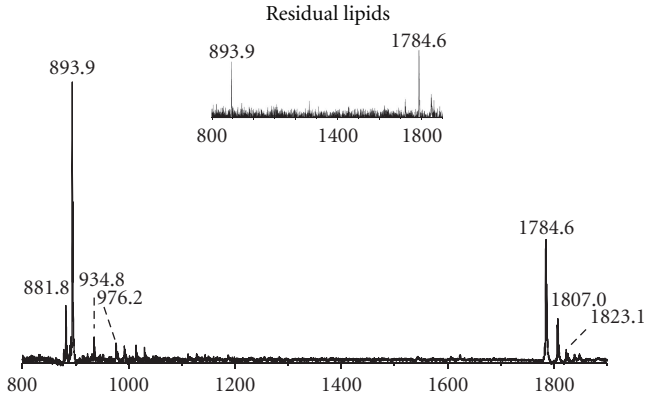

Figure 2: MALDI-TOF/MS lipid profiles of the total lipid extract of *Pyrococcus furiosus* (DSM3638) acquired in the negative ion mode using 9-aminoacridine as the matrix. The lipid components assigned to the main *m/z* ion peaks are unsaturated diphytanylglycerol analogue of phosphatidylinositol (*uns*PI), $[M\text{-}H]^-$ at *m/z* 881.8; diphytanylglycerol analogue of phosphatidylinositol (PI), $[M\text{-}H]^-$ at *m/z* 893.8; *N*-acetylglucosamine-diphytanylglycerol phosphate (*N*-acetyl-hexose-P-D) $[M\text{-}H]^-$ at *m/z* 934.8; diglycosyl-diphytanylglycerol (DGD) $[M\text{-}H]^-$ at *m/z* 976.2. The ion peak $[M\text{-}H]^-$ at *m/z* 1784.6 is attributable to a caldarchaeol lipid, with its sodium and potassium adducts at *m/z* 1807.0 and 1823.1, respectively. The detailed list of detected ion peaks is shown in Table 1. *Inset:* MALDI-TOF/MS lipid analyses in intact mode (as described in ref. [26]) of the residual pellet after the lipid extraction.

complex glycosylated-cardiolipins can be found. The main peak at *m/z* 893.9 corresponds to an inositol-diphytanylglycerol phosphate, the diphytanylglycerol analogue of phosphatidylinositol (PI), which is found in several Archaea and also previously observed in *Pyrococcus* species [18, 20]. The signal at *m/z* 881.8 can be assigned to the unsaturated inositol-diphytanylglycerol phosphate (*uns*PI), containing double bonds in its archaeol moiety, as detailed discussed in the following (Figure 4(a)). The peak at *m/z* 935.0 is likely to represent an *N*-acetylglucosamine-diphytanylglycerol phosphate (abbreviated in the following as *N*-acetyl-hexose-P-D), while that at *m/z* 976.2 represents a glycolipid derivative of diphytanylglycerol carrying two sugar units in the polar head (diglycosyl diether, DGD), both previously described in FAB mass spectrum of *P. furiosus* [20]. The peak at *m/z* 1784.6 present in the higher *m/z* range of the MALDI-TOF mass spectrum (Figure 2) is attributable to a caldarchaeol or tetraether lipid; the peaks at *m/z* 1807.0 and 1823.1

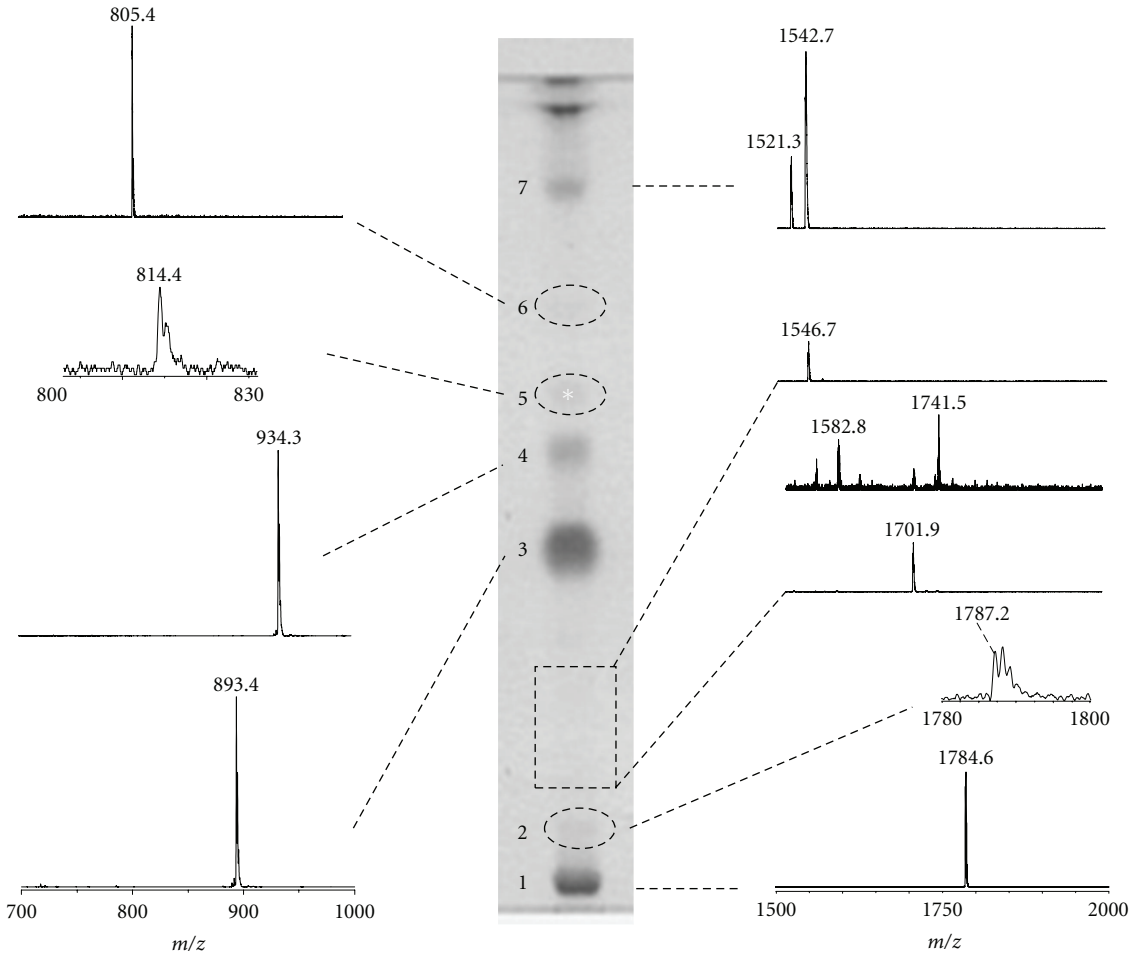

Figure 3: Coupled MALDI-TOF/MS and HPTLC analyses of the total lipid extract of *P. furiosus*. The total lipid extract was applied on the TLC plate (200 μg) in two lanes; the lipid bands in one lane were charred after spraying with 5% sulphuric acid, while 9-aminoacridine was applied manually along the other lane obtaining a continuous deposition. The main bands on the TLC plate after charring are shown in the centre of the picture, while, on the right and the left of the TLC, are shown the negative spectra obtained by MALDI scanning of the lane covered with the matrix. Dashed lines on the TLC plate were used to mark pale lipid bands.

correspond to sodium and potassium adducts, respectively. This caldarchaeol lipid has a molecular mass slightly higher than that of the diglycosyl phosphatidylglycerol tetraether (hexose$_2$-PG-T, see structure in Figure 6) giving rise to the peak at *m/z* 1778.5, previously found in FAB mass spectrum of *P. furiosus* [20].

The MALDI-TOF/MS profile of residual lipids which is still associated with the heterogeneous protein pellet left after the lipid extraction of *P. furiosus* cells is also reported in the inset of Figure 2. It can be seen that the two main peaks at *m/z* 1784.6 and 893.9 are still visible in the lipid profile of protein pellet after the lipid extraction, indicating that lipid extraction is not complete; although we have not estimated the quantity of residual lipids left behind after the first lipid extraction, as the intensity of the peak at *m/z* 1784.6, corresponding to the caldarchaeol, is higher than that of the peak at *m/z* 893.9, we conclude that it is more difficult to extract caldarchaeol lipids than diether lipids, as previously reported [28].

Furthermore MALDI-TOF mass spectrum of the total lipid extract of *P. furiosus* was also acquired in positive ion mode: only minor signals attributable to fragments of lipid branched-chains were detected in the *m/z* range 400–600, while no peaks were present in the *m/z* range of phospholipids and glycolipids (not shown). The lack of signals in the (+) MALDI-TOF mass spectrum suggests that the diether analogue of phosphatidylcholine is absent in *P. furiosus* and that most, if not all, lipid components are acidic.

In order to deeper investigate on the lipid components present in the total lipid extract of *P. furiosus*, we performed a detailed staining analysis after HPTLC and isolated some of the lipid components by preparative TLC. The TLC lipid profile of *P. furiosus* is shown in Figure 3. There are four main lipid bands (1, 3, 4, and 7), plus neutral pigments visible at the solvent front in the HPTLC plate. Individual lipid components of *P. furiosus* were identified not only by their responses to specific lipid staining, but also by MALDI-TOF/MS analysis of purified lipid components by preparative TLC; in

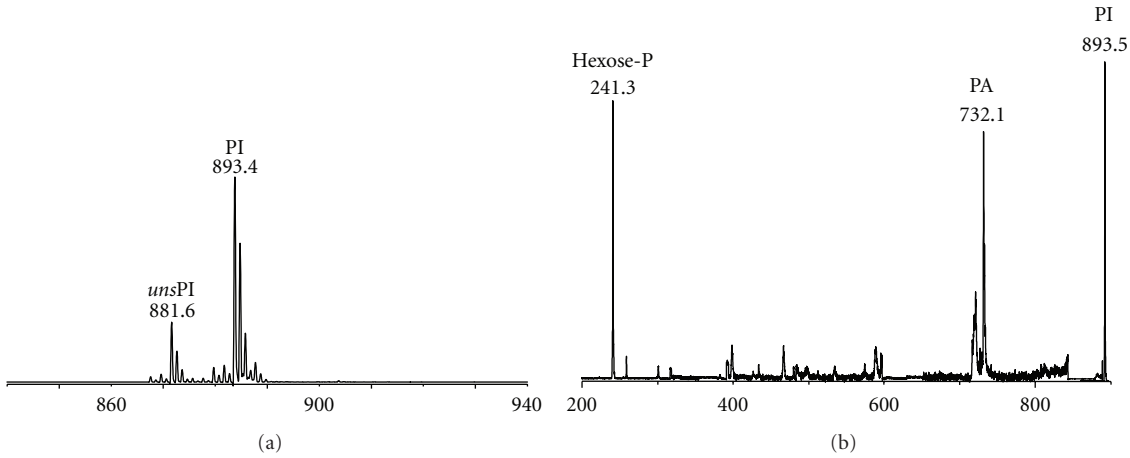

Figure 4: MALDI-TOF mass (a) and PSD fragment ion (b) spectra of band 3 of *P. furiosus*. (a): the lipid components present in band 3 (see TLC in Figure 3) were isolated and purified from the total lipid extract of the *P. furiosus* by preparative TLC. Peaks corresponding to the molecular ions of diphytanylglycerol analogue of phosphatidylinositol (PI) at *m/z* 893.4 and of the corresponding unsaturated species (*uns*PI) at *m/z* 881.6. (b): peaks corresponding to the molecular ion of PIat *m/z* 893.45 plus the ion fragments corresponding to the diphytanylglycerol analogues of PA (*m/z* 732.1) and to the sugar-phosphate residue (*m/z* 241.3).

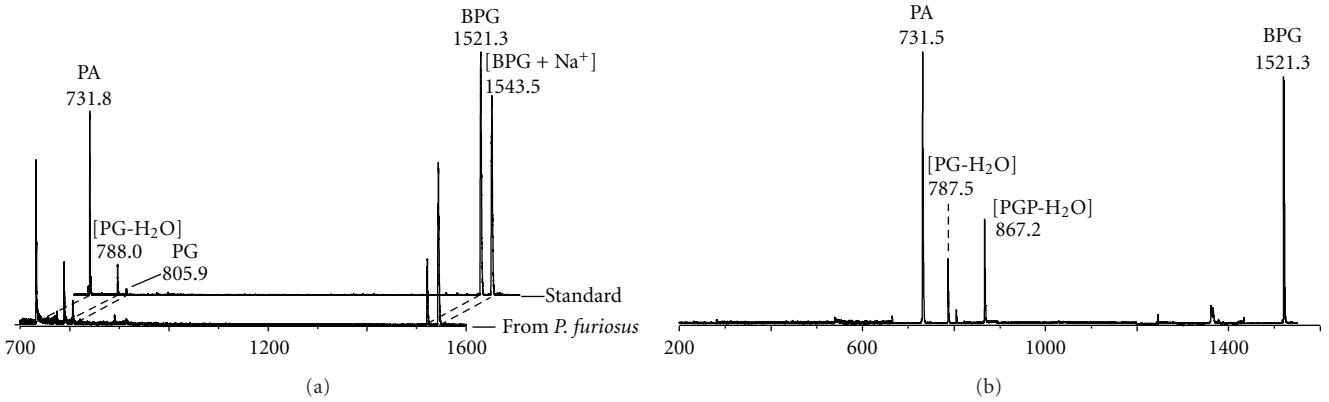

Figure 5: (a) Comparison of the MALDI-TOF mass spectra of the lipid component in band 7 of *P. furiosus* (see TLC in Figure 3) and the authentic standard BPG (i.e., diphytanylglycerol analogue of bisphosphatidylglycerol) isolated from *Halobacterium salinarum*. (b) PSD fragment ion spectrum of the diphytanylglycerol analogue of BPG of *P. furiosus*. Abbreviations: PA: diphytanylglycerol analogue of phosphatidic acid; PG: diphytanylglycerol analogue of phosphatidylglycerol; PGP: diphytanylglycerol analogue of phosphatidylglycerolphosphate.

particular the fragmentation behaviour of some polar lipids of *P. furiosus* was also investigated by using Post Source Decay (PSD) mass spectrometry analysis.

All the major lipid components were found to be positive to blue molybdenum staining (not shown). The only exception was the pale band marked by an asterisk. No lipid component was found to be positive to Azure-A or ninhydrin-staining (not shown); therefore the main lipids of *P. furiosus* are phospholipids, while do not contain sulphate or amino groups in their polar moieties.

The band 1 (in R_f order) is a tetraether phospholipid or caldarchaeol. Two diether phosphoglycolipids have been identified in bands 3 and 4, inositol-diphytanylglycerol phosphate, and *N*-acetylglucosamine-diphytanylglycerol phosphate, respectively, giving rise to MALDI-TOF/MS signals at *m/z* 893.9 and 935.0, respectively, both observed in the mass spectrum of the total lipid extract, previously shown in Figure 2. In addition, close to the solvent front, the pale band 7 corresponds to a phospholipid, having an R_f value similar to that of the authentic standard diphytanylglycerol analogue of bisphosphatidylglycerol BPG (not shown), previously described for extremely halophilic and haloalkaliphilic archaea [10–13, 16].

The individual lipid components of *P. furiosus* were also analysed directly on HPTLC plate by MALDI-TOF/MS, as described in detail in experimental procedures. Selected negative ion mass spectra, obtained during the MALDI scanning of the main bands visible on the TLC, plate are shown in Figure 3. Proceeding by R_f order, from the bottom to the top of the plate:

(1) the analysis of the first band (band 1) revealed a main signal at *m/z* 1784.6, which has been tentatively attributed to a caldarchaeol phospholipid possibly

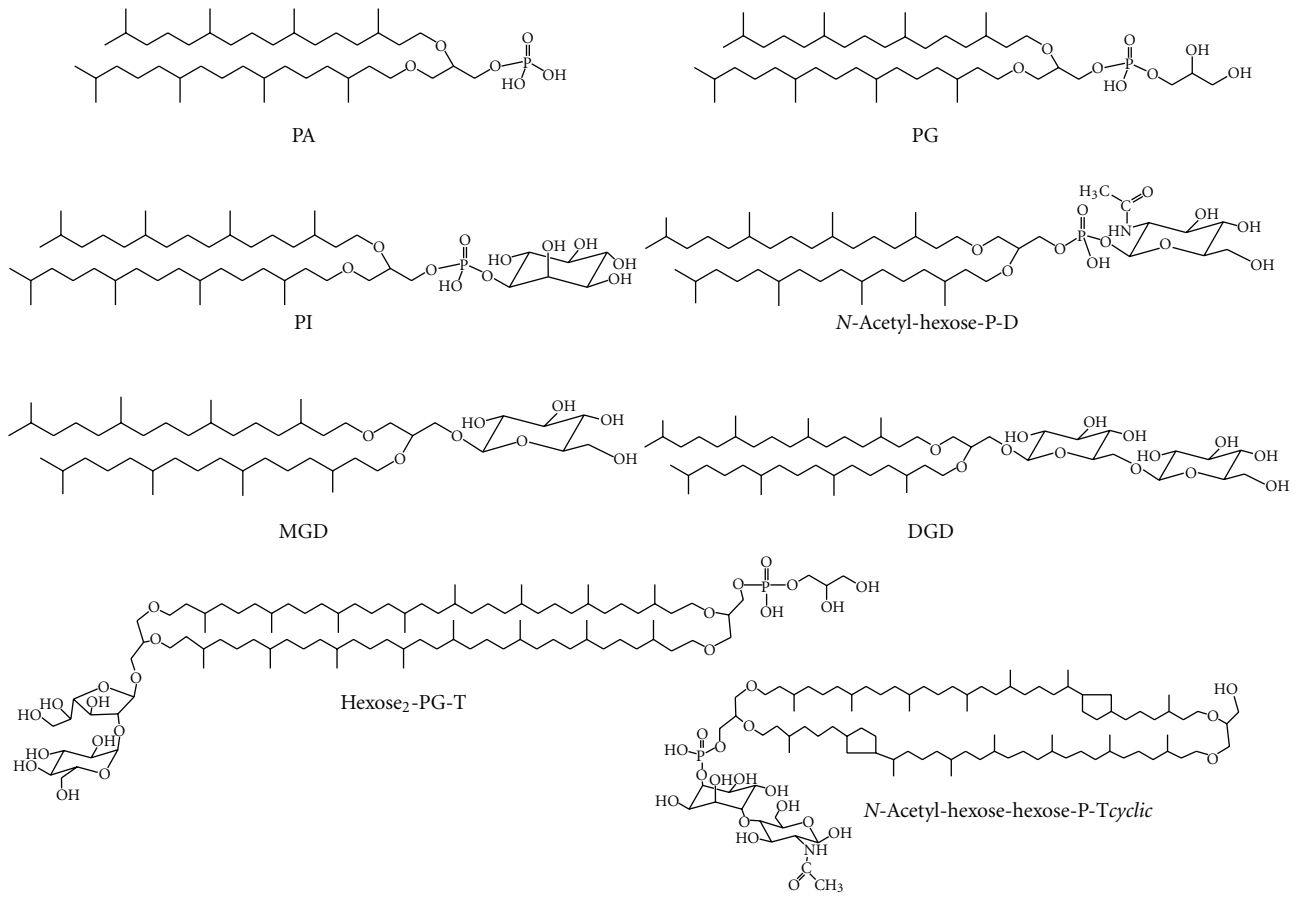

Figure 6: Polar membrane lipids of *P. furiosus*. Abbreviations used in the present study (see Table 1) to indicate phospholipids and glycolipids present in the membrane of *P. furiosus* always refer to diphytanylglycerol derived lipids. Two caldarchaeol lipids are shown: the main caldarchaeol (named *hexose$_2$-PG-T*) found in previous literature studies [20] and the structure proposed by us for the lipid component (named *N-acetyl-hexose-hexose-P-Tcyclic*) giving raise to the peak at *m/z* 1741.5 in MALDI-TOF/MS analysis.

having the general structure of (hexose-P)$_2$-T. The lipid component corresponding to band 1 has been isolated by preparative TLC and its structure was further investigated by PSD fragment ion spectra analysis (not shown). Results confirmed the presence of the caldarchaeol lipid core in the molecule, but the precise nature and location of sugar residues in the structure have not been determined;

(2) in band 2, an area of the plate located immediately upon the first band, we obtained a mass spectrum with a small signal at *m/z* 1787.2 that could correspond to a lipid compound closely related to the lipid present in band 1; furthermore, going from the bottom toward the solvent front, between the bands 2 and 3, traces of other caldarchaeol lipids, giving rise to signals at *m/z* 1701.9, 1741.5, and 1546.7 (in R_f order), have been found. These three last caldarchaeol lipids are structurally similar; the compound giving rise to the molecular ion at *m/z* 1741.5 could correspond to the acetylated form of the *m/z* 1701.9 (see proposed structure in Figure 6) lipid and it is indeed more mobile in the TLC. The lipid yielding the ion peak at *m/z* 1546.7 could correspond to a caldarchaeol bearing only one sugar unit;

(3) the MALDI-TOF/MS analysis of the major lipid band (band 3) showed a signal at *m/z* 893.4, which is assigned to the diphytanylglycerol analogue of phosphatidylinositol (PI). The mass spectrum of isolated band 3 (Figure 4(a)) showed, together with the main peak at *m/z* 893.4, a signal at *m/z* 881.6 which can be assigned to an unsaturated diphytanylglycerol analogue of phosphatidylinositol (named *uns*PI), containing six double bonds in its archaeol moiety (hexaunsaturated archaeol). Furthermore, Figure 4(b) shows the PSD fragment ion spectrum of the diphytanylglycerol analogue of phosphatidylinositol at *m/z* 893.4; as an abundant fragment at *m/z* 731.2, diagnostic for the structure of the diether analogue of phosphatidic acid (PA), was found, we can exclude the presence of another lipid having identical *m/z* (i.e., glucosyl-3-phosphate diether), previously found in *Pyrococcus* strain AN1 [18].

(4) the analysis of the band 4 showed a signal at *m/z* 934.3, which can be assigned to *N*-acetylglucosamine-diphytanylglycerol phosphate, according to previous FAB-MS analysis of *P. furiosus* [20]; as in the MALDI-TOF mass spectrum recorded at the level of band 4 the fragment at *m/z* 731.2 was not present, we conclude that the phosphate is not directly linked to the archaeol lipid core. Furthermore, the MALDI-TOF mass spectrum of the lipid component in band 4 (not shown), isolated and purified from the total lipid extract by preparative TLC, revealed the presence (at *m/z* 922.6) of minor amounts of an unsaturated analogue of the *N*-acetylglucosamine-diphytanylglycerol phosphate (abbreviated as *uns-N*-acetyl-hexose-P-D), having six double bonds in its archaeol moiety.

(5) The spectrum of the pale band 5 showed a very small signal at *m/z* 814.2, which could correspond to a monoglycosyl diphytanylglycerol (monoglycosyl diether, MGD); this compound could be the precursor of the glycolipid present in band 4;

(6) the analysis of the area corresponding to band 6 on the TLC plate revealed a small amount of the diphytanylglycerol analogue of phosphatidylglycerol (PG), having the signal of the molecular ion at *m/z* 805.4;

(7) the chromatographic behaviour coupled to information given by MALDI-TOF/MS analysis allowed an easy precise identification of lipid component in band 7. The MS analysis of the band 7, having the same R_f of diphytanylglycerol analogue of BPG, confirmed the presence of BPG in the lipid profile of *P. furiosus*, with signals at *m/z* 1521.3 and 1542.7, corresponding to $[M\text{-}H]^-$ and $[M\text{-}H+Na^+]^-$, respectively. The complete MALDI-TOF mass spectrum of the lipid component in band 7 is shown in Figure 5(a), together with the mass spectrum of the authentic BPG standard isolated from *Halobacterium salinarum*. It is concluded that the archaeal analogue of cardiolipin of *Pyrococcus* is identical to that present in *Halobacterium salinarum* and other extremely halophilic microorganisms [10–13, 16]. Furthermore, the PSD fragment ion spectrum of the lipid component in band 7 is shown in Figure 5(b): it can be seen that the ion fragments corresponding to the diphytanylglycerol analogues of PA (*m/z* 731.5), PG-H_2O (*m/z* 787.5), PG (*m/z* 805.9), and PGP-H2O (*m/z* 867.2) are present. All these peaks are diagnostic for the structure of the diphytanylglycerol analogue of bisphosphatidylglycerol, or ether lipid cardiolipin. Noteworthy, the PSD fragmentation pattern of the diphytanylglycerol analogue of cardiolipin is similar to that of mitochondrial cardiolipin [26].

In conclusion, the present study describes the presence of three different kinds of membrane lipids in the *P. furiosus*: diether lipids, dimeric diether lipids and tetraether lipids (see Figure 1). Structures of all lipids, described through the present study are illustrated in Figure 6.

Caldarchaeol lipids of *P. furiosus* found in the present study are different from those previously reported [20]. The main caldarchaeol lipid exhibits a main MALDI-TOF/MS peak at *m/z* 1784.6, tentatively assigned to an (hexose-P)$_2$-T, which do not correspond to any previous described caldarchaeol lipid of *Pyrococcus* or other hyperthermophilic archaea. We have accurately searched data in the literature and in lipid databases without finding a lipid candidate having the mass matching with that obtained in the present study. The finding of different caldarchaeols likely depends on differences in microorganism growth conditions. The precise structure of the main caldarchaeol of *P. furiosus* here found is presently under study, also with the help of analytical approaches different from mass spectrometry.

In the microorganism growth conditions of the present study diphytanylglycerol phosphoglycolipids are the most abundant lipid components of *P. furiosus*; unsaturated phosphoglycolipids have been also observed in minor proportions. The diphytanylglycerol analogue of phosphatidylglycerol is only a minor diether lipid. Altogether, diether lipids represent the majority of the lipids in the total lipid extract. This finding is in agreement with previous studies [18, 20]. Other reports have shown that the proportions between archaeol and caldarchaeol lipids can be reversed, as are profoundly influenced by the temperature and conditions of growth [29].

Only minute amounts of the diphytanylglycerol analogue of bisphosphatidylglycerol or cardiolipin have been found in the lipid extract in our experimental conditions. This is the first report describing the presence of dimeric diphytanylglycerol lipids in a hyperthermophilic archaeon. Novel cardiolipins have been recently described in uncultured methane-metabolizing archaea [30]; we also found a diphytanylglycerol analogue of bisphosphatidylglycerol in cultured *Methanocaldococcus jannaschii* (unpublished data). A number of studies report that prokaryotes contain variable amounts of cardiolipin depending on their physiologic state and experimental conditions of lipid analyses. It has been previously shown that the diether cardiolipin archaeal analogue is located in membrane domains performing bioenergetic functions, in analogy with bacteria [11, 31–34]. In consideration of the peculiarity of its respiratory system, in future studies it will be interesting to study the role of cardiolipin on the membrane enzymes involved in the bioenergetics of *P. furiosus.*

Acknowledgments

The work in the group of A. Corcelli was funded by the Laboratory Sens&Micro LAB Project (POFESR 2007–2013, code no. 15) of Apulia Region and by Ministero della Difesa Italiano (AROMA, Contract no. 1353/28.12.2010), while that of V. Müller was found by the Deutsche Forschungsgemeinschaft (SFB807).

References

[1] G. Fiala and K. O. Stetter, "*Pyrococcus furiosus* sp. nov. represents a novel genus of marine heterotrophic archaebacteria

growing optimally at 100 °C," *Archives of Microbiology*, vol. 145, no. 1, pp. 56–61, 1986.

[2] S. D. Hamilton-Brehm, G. J. Schut, and M. W. W. Adams, "Metabolic and evolutionary relationships among *Pyrococcus* species: genetic exchange within a hydrothermal vent environment," *Journal of Bacteriology*, vol. 187, no. 21, pp. 7492–7499, 2005.

[3] G. J. Schut, S. L. Bridger, and M. W. W. Adams, "Insights into the metabolism of elemental sulfur by the hyperthermophilic archaeon *Pyrococcus furiosus*: characterization of a coenzyme A-dependent NAD(P)H sulfur oxidoreductase," *Journal of Bacteriology*, vol. 189, no. 12, pp. 4431–4441, 2007.

[4] S. Mukund and M. W. W. Adams, "The novel tungsten-iron-sulfur protein of the hyperthermophilic archaebacterium, *Pyrococcus furiosus*, is an aldehyde ferredoxin oxidoreductase: evidence for its participation in a unique glycolytic pathway," *The Journal of Biological Chemistry*, vol. 266, no. 22, pp. 14208–14216, 1991.

[5] J. Vonck, K. Y. Pisa, N. Morgner, B. Brutschy, and V. Müller, "Three-dimensional structure of A1A0 ATP synthase from the hyperthermophilic archaeon *Pyrococcus furiosus* by electron microscopy," *The Journal of Biological Chemistry*, vol. 284, no. 15, pp. 10110–10119, 2009.

[6] F. T. Robb, D. L. Maeder, J. R. Brown et al., "Genomic sequence of hyperthermophile, *Pyrococcus furiosus*: implications for physiology and enzymology," *Methods in Enzymology*, vol. 330, pp. 134–157, 2001.

[7] T. A. Langworthy, "Lipids of archaebacteria," in *The Bacteria—A Treatise on Structure and Function, Volume 8: Archaebacteria*, R. S. Wolfe and C. R. Woese, Eds., pp. 459–497, Academic Press, New York, NY, USA, 1985.

[8] M. Kates, "Membrane lipids of archaea," in *The Biochemistry of Archaea (Archaebacteria)*, M. Kates, D. J. Kushner, and A. T. Matheson, Eds., pp. 261–295, Elsevier, Amsterdam, The Netherlands, 1993.

[9] Y. Koga, M. Nishihara, H. Morii, and M. Akagawa-Matsushita, "Ether polar lipids of methanogenic bacteria: structures, comparative aspects, and biosyntheses," *Microbiological Reviews*, vol. 57, no. 1, pp. 164–182, 1993.

[10] A. Corcelli, M. Colella, G. Mascolo, F. P. Fanizzi, and M. Kates, "A novel glycolipid and phospholipid in the purple membrane," *Biochemistry*, vol. 39, no. 12, pp. 3318–3326, 2000.

[11] A. Corcelli, "The cardiolipin analogues of Archaea," *Biochimica et Biophysica Acta*, vol. 1788, no. 10, pp. 2101–2106, 2009.

[12] A. Corcelli, V. M. T. Lattanzio, and A. Oren, "The archaeal cardiolipins of the extreme halophiles," in *Halophilic Microorganisms*, A. Ventosa, Ed., pp. 2101–2106, Springer, Berlin, Germany, 2004.

[13] G. D. Sprott, S. Larocque, N. Cadotte, C. J. Dicaire, M. McGee, and J. R. Brisson, "Novel polar lipids of halophilic eubacterium *Planococcus* H8 and archaeon *Haloferax volcanii*," *Biochimica et Biophysica Acta*, vol. 1633, no. 3, pp. 179–188, 2003.

[14] S. Lobasso, P. Lopalco, V. M. T. Lattanzio, and A. Corcelli, "Osmotic shock induces the presence of glycocardiolipin in the purple membrane of *Halobacterium salinarum*," *Journal of Lipid Research*, vol. 44, no. 11, pp. 2120–2126, 2003.

[15] P. Lopalco, S. Lobasso, F. Babudri, and A. Corcelli, "Osmotic shock stimulates de novo synthesis of two cardiolipins in an extreme halophilic archaeon," *Journal of Lipid Research*, vol. 45, no. 1, pp. 194–201, 2004.

[16] R. Angelini, P. Corral, P. Lopalco, A. Ventosa, and A. Corcelli, "Novel ether lipid cardiolipins in archaeal membranes of extreme haloalkaliphiles," *Biochimica et Biophysica Acta*, vol. 1818, no. 5, pp. 1365–1373, 2012.

[17] M. de Rosa, A. Gambacorta, A. Trincone, A. Basso, W. Zilig, and I. Holz, "Lipids of *Thermococcus celer*, a sulfur-reducing archaebacterium: structure and biosynthesis," *Systematic and Applied Microbiology*, vol. 9, no. 1-2, pp. 1–5, 1987.

[18] V. Lanzotti, A. Trincone, B. Nicolaus, W. Zillig, M. de Rosa, and A. Gambacorta, "Complex lipids of Pyrococcus and AN1, thermophilic members of archaebcteria belonging to *Thermococcales*," *Biochimica et Biophysica Acta*, vol. 1004, no. 1, pp. 44–48, 1989.

[19] G. Erauso, A. L. Reysenbach, A. Godfroy et al., "*Pyrococcus abyssi* sp. nov., a new hyperthermophilic archaeon isolated from a deep-sea hydrothermal vent," *Archives of Microbiology*, vol. 160, no. 5, pp. 338–349, 1993.

[20] G. D. Sprott, B. J. Agnew, and G. B. Patel, "Structural features of ether lipids in the archaeobacterial thermophiles *Pyrococcus furiosus*, *Methanopyrus kandleri*, *Methanothermus fervidus*, and *Sulfolobus acidocaldarius*," *Canadian Journal of Microbiology*, vol. 43, no. 5, pp. 467–476, 1997.

[21] G. Huber, E. Drobner, H. Huber, and K. O. Stetter, "Growth by aerobic oxidation of molecular hydrogen in Archaea—a metabolic property so far unknown for this domain," *Systematic and Applied Microbiology*, vol. 15, no. 4, pp. 502–504, 1992.

[22] E. G. Bligh and W. J. Dyer, "A rapid method of total lipid extraction and purification," *Canadian Journal of Biochemistry and Physiology*, vol. 37, no. 8, pp. 911–917, 1959.

[23] M. Kates, "Techniques of lipidology," in *Laboratory Techniques in Biochemistry and Molecular Biology*, H. Burdon and P. H. van Knippenberg, Eds., pp. 100–110, Elsevier, Amsterdam, The Netherlands, 1986.

[24] B. Fuchs, J. Schiller, R. Süß, M. Schürenberg, and D. Suckau, "A direct and simple method of coupling matrix-assisted laser desorption and ionization time-of-flight mass spectrometry (MALDI-TOF MS) to thin-layer chromatography (TLC) for the analysis of phospholipids from egg yolk," *Analytical and Bioanalytical Chemistry*, vol. 389, no. 3, pp. 827–834, 2007.

[25] G. Sun, K. Yang, Z. Zhao, S. Guan, X. Han, and R. W. Gross, "Matrix-assisted laser desorption/ionization time-of-flight mass spectrometric analysis of cellular glycerophospholipids enabled by multiplexed solvent dependent analyte-matrix interactions," *Analytical Chemistry*, vol. 80, no. 19, pp. 7576–7585, 2008.

[26] R. Angelini, R. Vitale, V. A. Patil et al., "Lipidomics of intact mitochondria by MALDI-TOF/MS," *Journal of Lipid Research*, vol. 53, no. 7, pp. 1417–1425, 2012.

[27] B. Fuchs, C. Schober, G. Richter, R. Süß, and J. Schiller, "MALDI-TOF MS of phosphatidylethanolamines: different adducts cause different post source decay (PSD) fragment ion spectra," *Journal of Biochemical and Biophysical Methods*, vol. 70, no. 4, pp. 689–692, 2007.

[28] M. Nishihara and Y. Koga, "Extraction and composition of polar lipids from the archaebacterium, *Methanobacterium thermoautotrophicum*: effective extraction of tetraether lipids by an acidified solvent," *Journal of Biochemistry*, vol. 101, no. 4, pp. 997–1005, 1987.

[29] A. Sugai, I. Uda, Y. H. Itoh, and T. Itoh, "The core lipid composition of the 17 strains of hyperthermophilic archaea, *Thermococcales*," *Journal of Oleo Science*, vol. 53, no. 1, pp. 41–44, 2004.

[30] M. Y. Yoshinaga, L. Wörmer, M. Elvert, and K.-U. Hinrichs, "Novel cardiolipins from uncultured methane-metabolizing Archaea," *Archaea*, vol. 2012, Article ID 832097, 9 pages, 2012.

[31] M. Schlame, D. Rua, and M. L. Greenberg, "The biosynthesis and functional role of cardiolipin," *Progress in Lipid Research*, vol. 39, no. 3, pp. 257–288, 2000.

[32] E. Mileykovskaya, M. Zhang, and W. Dowhan, "Cardiolipin in energy transducing membranes," *Biochemistry*, vol. 70, no. 2, pp. 154–158, 2005.

[33] A. Corcelli, S. Lobasso, L. L. Palese, M. S. Saponetti, and S. Papa, "Cardiolipin is associated with the terminal oxidase of an extremely halophilic archaeon," *Biochemical and Biophysical Research Communications*, vol. 354, no. 3, pp. 795–801, 2007.

[34] A. Corcelli, S. Lobasso, M. S. Saponetti, A. Leopold, and N. A. Dencher, "Glycocardiolipin modulates the surface interaction of the proton pumped by bacteriorhodopsin in purple membrane preparations," *Biochimica et Biophysica Acta*, vol. 1768, no. 9, pp. 2157–2163, 2007.

Hindawi Publishing Corporation
Archaea
Volume 2012, Article ID 513231, 9 pages
doi:10.1155/2012/513231

Research Article

Synthetic Archaeosome Vaccines Containing Triglycosylarchaeols Can Provide Additive and Long-Lasting Immune Responses That Are Enhanced by Archaetidylserine

G. Dennis Sprott, Angela Yeung, Chantal J. Dicaire, Siu H. Yu, and Dennis M. Whitfield

Institute for Biological Sciences, National Research Council of Canada, 100 Sussex Drive, Ottawa, ON, Canada K1A 0R6

Correspondence should be addressed to G. Dennis Sprott, dennis.sprott@nrc-cnrc.gc.ca

Received 6 July 2012; Accepted 23 August 2012

Academic Editor: Angela Corcelli

The relation between archaeal lipid structures and their activity as adjuvants may be defined and explored by synthesizing novel head groups covalently linked to archaeol (2,3-diphytanyl-sn-glycerol). Saturated archaeol, that is suitably stable as a precursor for chemical synthesis, was obtained in high yield from *Halobacterium salinarum*. Archaeosomes consisting of the various combinations of synthesized lipids, with antigen entrapped, were used to immunize mice and subsequently determine $CD8^+$ and $CD4^+$-T cell immune responses. Addition of 45 mol% of the glycolipids gentiotriosylarchaeol, mannotriosylarchaeol or maltotriosylarchaeol to an archaetidylglycerophosphate-O-methyl archaeosome, significantly enhanced the $CD8^+$ T cell response to antigen, but diminished the antibody titres in peripheral blood. Archaeosomes consisting of all three triglycosyl archaeols combined with archaetidylglycerophosphate-O-methyl (15/15/15/55 mol%) resulted in approximately additive $CD8^+$ T cell responses and also an antibody response not significantly different from the archaetidylglycerophosphate-O-methyl alone. Synthetic archaetidylserine played a role to further enhance the $CD8^+$ T cell response where the optimum content was 20–30 mol%. Vaccines giving best protection against solid tumor growth corresponded to the archaeosome adjuvant composition that gave highest immune activity in immunized mice.

1. Introduction

The total polar lipids extracted from various archaea hydrate to form liposomes (archaeosomes [1]), that were developed initially to improve the drug delivery application of conventional liposomes [2–4]. These total polar lipid archaeosomes were found subsequently to have an enhanced ability over conventional liposomes to serve as adjuvants, that promoted not only the antibody response to an entrapped protein antigen [5] but also the $CD8^+$ T cell response [6]. One mode of action could be correlated to an enhanced phagocytosis of archaeosomes compared to liposomes by various phagocytic cells [7]. This led to the observation that total polar lipids from various archaea, with their species-specific lipid structures, formed archaeosomes differing in receptor-mediated endocytosis and adjuvanticity [8].

Recently archaeol has been isolated from hydrolysed polar lipid extracts of *Halobacterium salinarum* to use as the lipid precursor to chemically synthesize various polar lipids, including glycolipids [9, 10]. The lipids so generated are described as synthetic or more precisely as semisynthetic, because the lipid moiety with specific archaeal sn-2,3 and R-methyl group stereochemistry is of biological origin, whereas a polar head group may be conjugated to the free sn-1 hydroxyl of the glycerol backbone to give a new polar lipid structure. In this way a chemically-defined, synthetic archaeosome could in theory be optimized for each application. Feasibility was demonstrated by synthesizing a series of diglycosylarchaeols and testing their interactions with antigen-presenting cells to produce immune responses *in vivo* [9].

The long-lasting $CD8^+$ T cell memory responses that are generally thought to be required for protection in intracellular pathogen and cancer vaccines are induced by certain total polar lipid archaeosomes and have been correlated to those archaeosomes having a high proportion of membrane-spanning caldarchaeol (tetraether) lipids [6, 11]. In this study we explore whether synthetic archaeosome adjuvants that are based on the archaeol lipids without caldarchaeols, can provide such long-term responses. Further, we explore if synthetic archaetidylserine, previously found to interact positively with the phosphatidylserine receptor of antigen-presenting cells [8, 12], can augment the adjuvant activity of synthetic glycolipid archaeosomes.

2. Materials and Methods

2.1. Growth of Archaea. Halobacterium salinarum (ATCC 33170) was grown aerobically at 37°C in a medium modified to be an all nonanimal origin medium consisting of: 15 g/L Phytone peptone UF (product 210931 from VWR International); 220 g/L NaCl; 6.5 g/L KCl; 10 g/L $MgSO_4 \cdot 7H_2O$; 10 mL of 0.2 g/100 mL $CaCl_2$; 10 mL of 0.2 g/100 mL $FeSO_4$. Growth of *Haloferax volcanii* (ATCC 29605) was in medium ATCC 974 at 30°C with NaCl content of 12.5% [13]. The antifoam agent used was MAZU DF 204 (BASF Canada). Biomass was grown in 20 L medium in a 28 L New Brunswick Scientific fermentor and harvested after 72 h growth. Lipids were extracted from the biomass with chloroform/methanol/water and the total polar lipids precipitated from the lipid extract with cold acetone [14].

2.2. Purification of Archaeol. Typically, 3.5 g of total polar lipid from *H. salinarum* was dissolved in 45 mL of chloroform/methanol (2 : 1, v/v) and 190 mL methanol added. This mixture was cooled to 0°C in an ice bath, and 10 mL acetyl chloride added drop-wise while being stirred magnetically. Hydrolysis was accomplished by refluxing at 62°C for 3 h. The mixture was cooled and the volume reduced by rotary evaporation to 100 mL. Upon transfer to a separatory funnel, 12 mL water and 100 mL petroleum ether was added. The mixture was mixed and allowed to separate. The top ether phase containing lipid was pooled with a second ether extraction, and evaporated.

The archaeol oil obtained above was further purified by silica gel column chromatography. The oil dissolved in chloroform/methanol (2 : 1, v/v) was loaded on a Silica gel 60 (Merck) column and archaeol eluted with pressure using hexane/t-butylmethylether/acetic acid (80/20/0.5, v/v/v). Collected fractions were tested for archaeol by mini thin-layer chromatography using the eluting solvent, and fractions containing pure archaeol pooled and dried. The yield of archaeol from total polar lipid ranged from 43 to 53%. Structural identity and purity of archaeol was confirmed by both NMR spectroscopy and electrospray ionization mass spectrometry.

2.3. Chemical Synthesis. Archaetidylethanolamine was synthesized according to [15]. Mannotriosylarchaeol, maltotriosylarchaeol, gentiobiosylarchaeol, and gentiotriosylarchaeol were synthesized according to our previous descriptions [10, 16] and structural details are shown in Figure 1. Synthesis methods for archaetidylserine can be found in Supplementary Material available online at doi:10.1155/2012/513231.

2.4. Purification of PGP. Archaetidylglycerolphosphate-O-CH_3 (PGP) was purified from the total polar lipids of *Haloferax volcanii* as described [13].

2.5. Archaeosome Vaccines. Archaeosomes were formed by hydrating 20–30 mg dried lipid at 40°C in 2 mL PBS buffer (10 mM sodium phosphate, 160 mM NaCl, pH 7.1) with ovalbumin Type VI (OVA, Sigma) as the test antigen dissolved at 10 mg/mL. Vesicle size was reduced to about 100–150 nm diameter by brief sonication in a sonic bath (Fisher Scientific), and OVA not entrapped was removed by centrifugation from 7 mL PBS followed by 2 washes (200,000 x g max for 90 min). Vesicle pellets were resuspended in 2–2.5 mL PBS and filter sterilized through 0.45 μm Millipore filters. Sterile conditions and pyrogen-free water were used throughout.

Quantification of antigen loading was conducted by separating OVA from lipids using SDS polyacrylamide gel electrophoresis and densitometry as described [14]. Loading was based on μg protein/mg salt corrected dry weight of lipid. Average diameters based on intensity were measured using a Malvern Nano Zetasizer with a He/Ne laser (Spectra Research Corp., Ontario, Canada).

2.6. Animal Trials. C57BL/6 female mice (6–8 weeks old) were immunized subcutaneously near the tail base with 0.1 mL vaccines containing the equivalent of 20 μg OVA, often entrapped in archaeosomes of various compositions. A booster consisting of the same vaccine and route was given on week 3. All protocols and SOPs were approved by the NRC Animal Care Committee and conducted within the guidelines of the Canadian Council on Animal Care.

2.7. Immune Responses. As a measure of the Th2 arm of $CD4^+$ T cell adjuvant activity, IgG antibody raised in response to the antigen in the vaccine and collected in the sera of mice (5-6 mice/group) was quantified by Elisa according to a previous description [17]. The $CD8^+$ T cell response was quantified by sacrificing duplicate mice/group to obtain their splenic cells. These splenic cells were assayed in triplicate for antigen-specific responses by standard Elispot and cytolytic T lymphocyte (CTL) methods [18].

2.8. Dendritic Cell (DC) Maturation Assay. Bone marrow was flushed from femurs and tibias of C57BL/6 mice to isolate DCs. Cells obtained were cultured in RPMI medium supplemented with 8% fetal calf serum (R8) (Thermo Scientific HyClone, UT, USA) and 5 ng/mL of granulocyte macrophage colony-stimulating factor (ID Labs, Inc., Ont., Canada) [19]. Nonadherent cells were removed on days 2 and 4 and supplied with fresh medium. Bone marrow DCs were harvested as the nonadherent cells on day 7. DC purity was greater than 90% based on flow cytometry

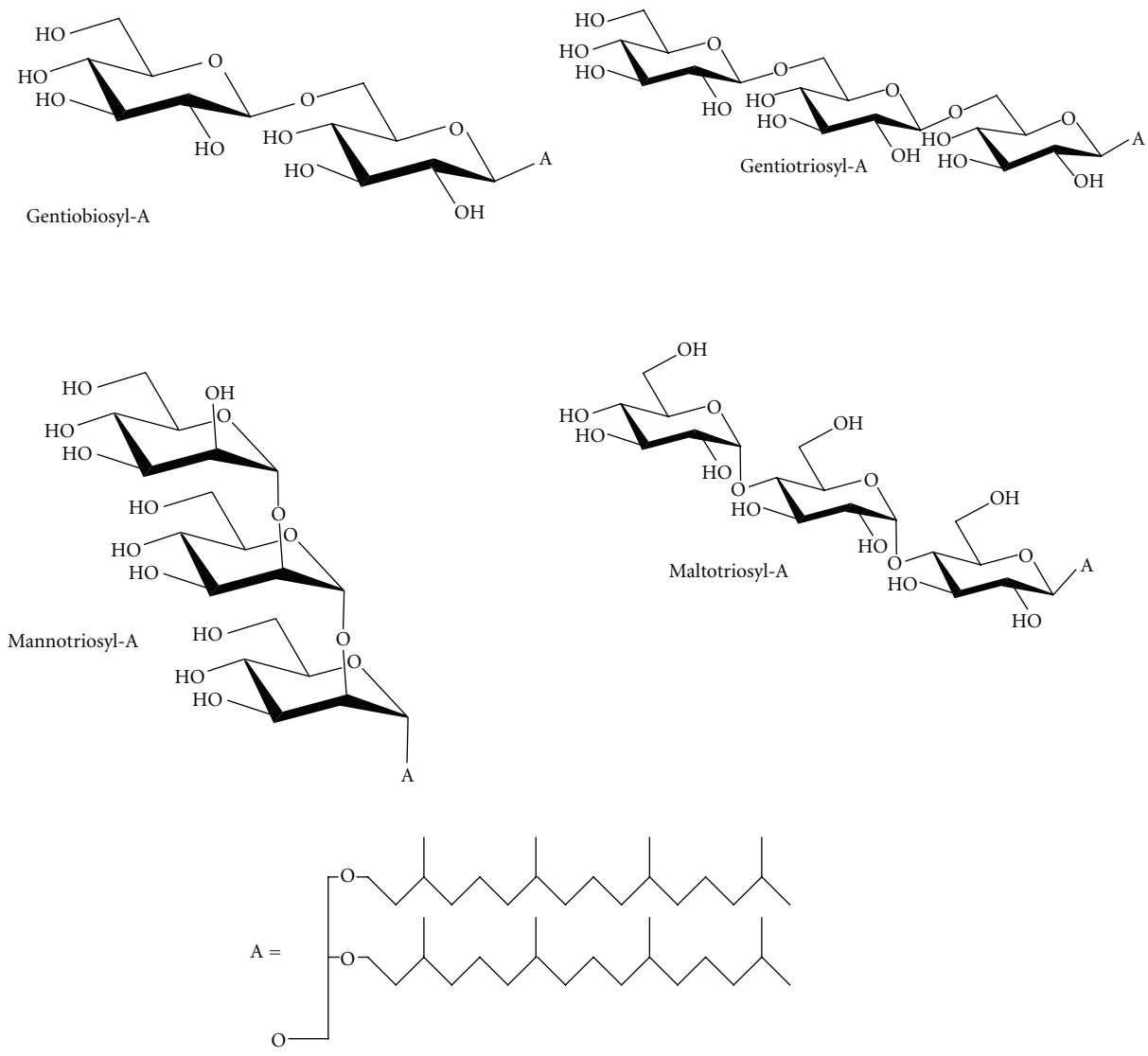

Figure 1: Semisynthetic glycoarchaeol structures showing head group details. "A" is the archaeol lipid precursor used for synthesis. gentiobiosyl-A (β-Glc$_p$-(1 → 6)-β-Glc$_p$-(1 → O)-archaeol); Gentiotriosyl-A (β-Glc$_p$-(1 → 6)-β-Glc$_p$-(1 → 6)-β-Glc$_p$-(1 → O)-archaeol); mannotriosyl-A (α-Man$_p$-(1 → 2)-α-Man$_p$-(1 → 2)-α-Man$_p$-(1 → O)-archaeol); maltotriosyl-A (α-Glc$_p$-(1 → 4)-α-Glc$_p$-(1 → 4)-β-Glc$_p$-(1 → O)-archaeol).

of cells labeled with PE-Cy7 conjugated anti-CD11c mAb (BD Biosciences, Ont., Canada). To activate, on day 7 DCs (3×10^5 cells/mL) were stimulated with 25 μg of various antigen-free archaeosomes or 1 μg *E. coli* lipopolysaccharide (LPS, Sigma-Aldrich, Ltd., Ont., Canada) per mL in 24-well plates for 24 h. Maturation was measured by the FITC-dextran (Sigma-Aldrich, Ltd., Ont., Canada) uptake assay using flow cytometry [20]. DCs were suspended in R8 medium and incubated with 1 mg/mL of FITC-dextran (Mr = 40 000) for 30 min at 4 or 37°C. After incubation, the cells were washed three times with ice cold 1% sodium azide in PBS. The quantitative uptake was calculated as the change in the Mean Fluorescence Index (MFI) between cell samples incubated at 37 and 4°C.

2.9. EG.7 Solid Tumour Model. C57BL/6 mice were immunized at 0 and 3 weeks subcutaneously with archaeosomes containing 20 μg OVA. A challenge consisting of 5×10^6 EG.7 cells was introduced subcutaneously in the shaved lower dorsal region at either 4.5 weeks, or 14 weeks from the second immunization. Tumour progression was measured in two dimensions with a digital calliper, and values multiplied to give tumour sizes. When a tumour mass of 300 mm^2 was reached the mouse was euthanized.

2.10. Statistics. A comparison of means for animal data was conducted using student's t-test to determine significance at 95% confidence, and two tailed P values calculated using GraphPad Prism 5.

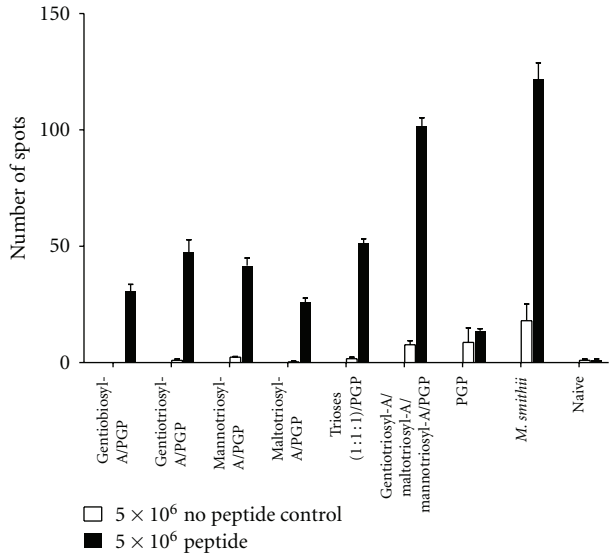

Figure 2: Antigen-specific CD8$^+$ T cell activity in splenic cells of immunized mice as assayed by Elispot. Ratios of lipids in mol% for various compositions of archaeosomes were: di or triglycosylarchaeols/PGP (45/55), and gentiotriosyl-A/maltotriosyl-A/mannotriosyl-A/PGP (15/15/15/55), where "A" refers to archaeol. Trioses (1 : 1 : 1)/PGP refers to admixed triglycosyl-A/PGP vaccines, such that each contributed equal amounts of antigen. *M. smithii* represents OVA-loaded archaeosomes consisting of total polar lipids from *M. smithii*, as positive control. Mice were immunized subcutaneously at 0 and 3 weeks with OVA-loaded archaeosome adjuvants. Nonimmunized mice (naive) were included as negative controls. Spleens from duplicate mice were collected 5.5 weeks after first injection to determine the frequency (number of spots) of interferon-gamma (IFN-γ)-secreting splenic cells (spots) by enzyme-linked immunospot assay (Elispot). Omission of the major CD8 epitope of OVA (SIINFEKL) from the assay (no peptide control) was used to test for nonspecific responses. Means significantly different ($P < 0.05$) were gentiotriosyl-A/PGP versus maltotriosyl-A/PGP ($P = 0.0204$), mannotriosyl-A/PGP versus maltotriosyl-A/PGP ($P = 0.0135$), and maltotriosyl-A/PGP versus PGP ($P = 0.0032$). Those not significantly different were gentiotriosyl-A/PGP versus mannotriosyl-A/PGP ($P = 0.4238$), gentiotriosyl-A/PGP versus gentiobiosyl-A/PGP ($P = 0.0550$), mannotriosyl-A/PGP versus gentiobiosyl-A/PGP ($P = 0.0677$), and gentiotriosyl-A/maltotriosyl-A/mannotriosyl-A/PGP versus *M. smithii* ($P = 0.0657$).

3. Results

3.1. Synthetic Glycosylarchaeols as Adjuvants. To prepare stable glycolipid archaeosome adjuvants from neutrally charged glycosylarchaeols it was necessary to include a charged lipid. This function may be served by a conventional ester-phospholipid such as phosphatidylglycerol. Although mice vaccinated with archaeosomes consisting of synthetic diglycosylarchaeols mixed with dipalmitoyl phosphatidylglycerol and antigen developed short-term CD8$^+$ T cell mediated immune responses [9], longer-term responses were lost [15]. Consequently, we avoided conventional lipids in this study designed to evaluate the potential for long-term immunity from archaeol adjuvants, and chose instead an archaeol-based anionic lipid, PGP, purified from *H. volcanii*. The combination of glycosylarchaeols with PGP resulted in stable bilayers in the 100 nm average diameter range that entrapped the OVA antigen from 12–21 μg protein/mg dry weight (Table 1).

First, we tested CD8$^+$ T cell responses in immunized mice using glycosylarchaeol/PGP adjuvants in short-term experiments assayed 2.5 weeks from the booster immunization (Figure 2). Elispot assays confirmed gentiotriosylarchaeol to be a better adjuvant than gentiobiosylarchaeol. Although not highly significant for the data shown here ($P = 0.055$), in other trials the difference in means was characteristically $P = 0.001$. Further, both gentiotriosylarchaeol and mannotriosylarchaeol were significantly better adjuvants with PGP than was maltotriosylarchaeol. When all three triosylarchaeol vaccines were admixed in equal proportion prior to immunization the CD8 response was not greatly improved. However, a strikingly improved adjuvant activity, approaching the *M. smithii* total polar lipid positive control, was observed when the triglycosylarchaeols were incorporated into the same archaeosome preparation during hydration.

CD8 responses in mice can also be measured by cytolytic T lymphocyte (CTL) assays that measure the ability of effector cells in the spleens of immunized mice to lyse an EG.7 target cell line expressing the dominant epitope (SIINFEKL) of OVA. In this assay (Figure 3) the same trends as found in Elispots occurred, although maltotriosylarchaeol/PGP was less effective as an adjuvant than pure PGP archaeosomes. The combined triosylarchaeols/PGP (45/55 mol%) again produced an adjuvant equivalent to the total polar lipid positive control. Because of these results, we omitted maltotriosylarchaeol from further studies, and continued with the combination of gentiotriosylarchaeol/mannotriosylarchaeol/PGP.

To evaluate the ability of archaeosome adjuvants to direct antigen via antigen-presenting cells through MHC class-II presentation to CD4$^+$ T cells (see Figure 1 of [9]), we assayed anti OVA antibody titres in the peripheral blood of mice (Figure 4). Best titres were found for PGP archaeosomes, indicating that these archaeosomes favour an MHC-II route of antigen presentation versus MHC-I (as measured by CD8$^+$ T cell responses). Antibody titres for PGP were significantly higher for all adjuvants except when compared to the combination of triosylarchaeols, which was not significantly different ($P = 0.056$).

3.2. Archaetidylserine (AS) and Archaetidylethanolamine (AE). The phosphatidylserine receptor is implicated in promoting phagocytosis of apoptotic cell debris [21] and archaeosomes [12]. Further, both archaetidylserine and archaetidylethanolamine are potentially fusogenic lipids, based on the assumption of similar activity to their ester analogs [22], and fusion of internalized archaeosomes with the phagolysosome membrane is the mechanism proposed to export antigen from archaeosomes to the MHC-I pathway

Table 1: Characterization of OVA-archaeosomes.

Archaeosome lipids	Average diameter (nm)	OVA content (μg/mg)
Gentiobiosyl-A/PGP	153 ± 54	19.6
Gentiotriosyl-A/PGP	90 ± 52	21.1
Mannotriosyl-A/PGP	76 ± 41	16.9
Maltotriosyl-A/PGP	97 ± 46	14.7
PGP	92 ± 54	14.2
M. smithii	88 ± 51	12.0

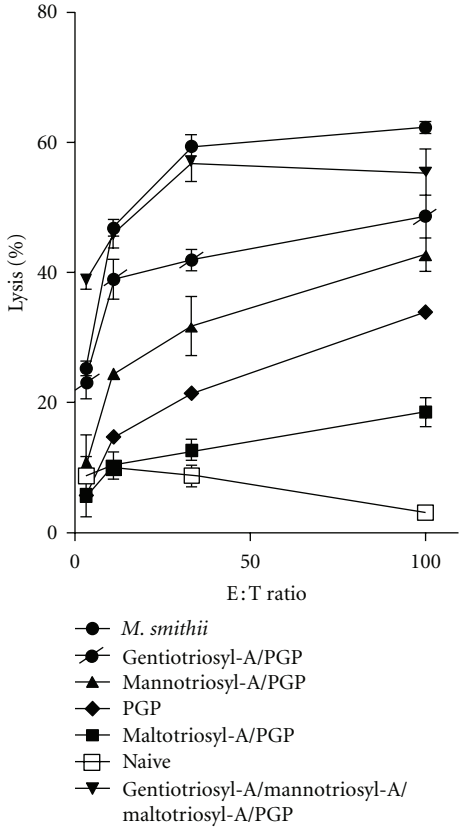

Figure 3: A cytotoxic T lymphocyte (CTL) lysis assay was used to assess the same populations of splenic cells as in Figure 1. The standard ^{51}Cr assay was conducted using specific and nonspecific target cells (EG.7 and EL-4, resp.). The ratio of effector splenic cells to target cells is shown as the E : T ratio in the graph. Results shown are for EG.7 targets. EL-4 targets produced only low nonspecific responses (not shown).

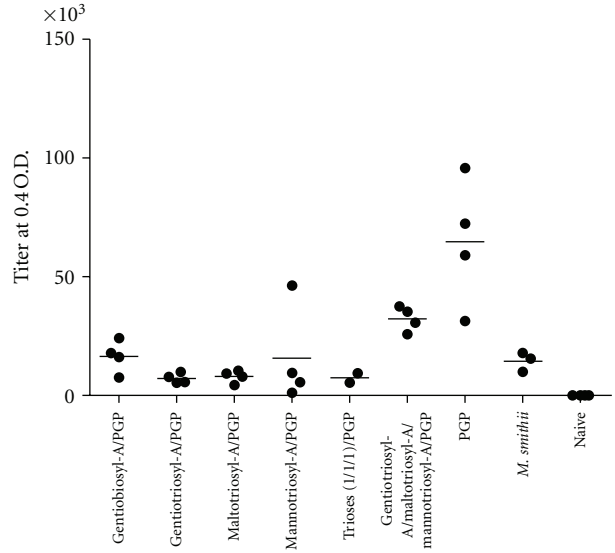

Figure 4: Antibody titres in sera of mice immunized with various archaeosome adjuvants. Peripheral blood was collected at 5.5 weeks, just prior to euthanizing mice for spleen removal (Figure 1). Each data point shown represents the titre in the serum from an individual mouse. Means were significantly higher for the OVA-PGP archaeosome vaccinated group ($P < 0.05$) compared to all groups except for Gentiotriosyl-A/Maltotriosyl-A/Mannotriosyl-A/PGP ($P = 0.0560$).

of antigen-presenting cells [12, 23]. Consequently, importance of AS or AE incorporated into the mannotriosylarchaeol/gentiotriosylarchaeol/PGP archaeosome was assessed in terms of adjuvanting CD8$^+$ T cell responses (Figure 5). Addition of 30 mol% AS to the glycotriosylarchaeol/PGP adjuvant resulted in a significantly higher CD8 response ($P = 0.0207$) that was not significantly different than the positive control (*M. smithii*). AE combined with AS had little further influence on adjuvanticity. As in other mouse trials, incorporation of glycoarchaeols to PGP archaeosomes produced a much improved CD8$^+$ T cell response. In contrast, anti OVA antibody titres in peripheral blood were not significantly higher upon inclusion of AS (data not shown).

To quantify the optimal amount of AS to adjuvant the CD8$^+$ T cell mediated response, from 0 to 30 mol% AS was incorporated into the triglycosylarchaeol/PGP archaeosome. Elispot assays (Figure 6) showed little effect of 10% AS, with an optimal effect of >20–30 mol%. Archaeosomes could not be tested with >30 mol% AS because of instability. These findings were verified by CTL assays (Figure 7), that confirmed an adjuvant activity at 30 mol% AS to be somewhat higher than the positive control. As shown in Figure 5, the addition of AE to the adjuvant mix was rarely positive.

3.3. Maturation of DCs. Loss of ability to take up dextran was used to assess the extent of activation of DCs exposed *in vitro* to the various archaeosomes (lacking antigen) (Figure 8). LPS served as a positive control. Activation was similar for LPS, *M. smithii* archaeosomes, and the combination

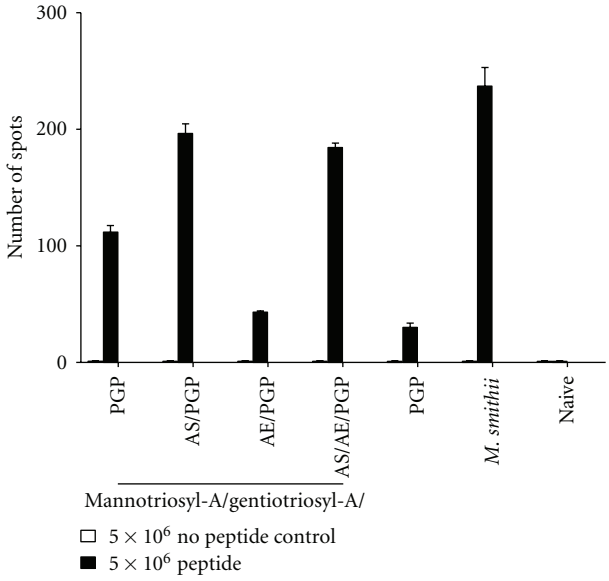

Figure 5: Elispot assay showing a relationship between adjuvant activity of glycosylarchaeol/PGP archaeosomes, archaetidylserine (AS), and archaetidylethanolamine (AE). Mol% compositions for OVA-archaeosome vaccines were mannotriosyl-A/gentiotriosyl-A/PGP (22.5/22.5/55), mannotriosyl-A/gentiotriosyl-A/AS/PGP (22.5/ 22.5/30/25), mannotriosyl-A/gentiotriosyl-A/AE/PGP (22.5/ 22.5/5/50), mannotriosyl-A/gentiotriosyl-A/AS/AE/PGP (22.5/ 22.5/30/5/20). Assays were conducted on splenic cells of mice 6 weeks post first immunization.

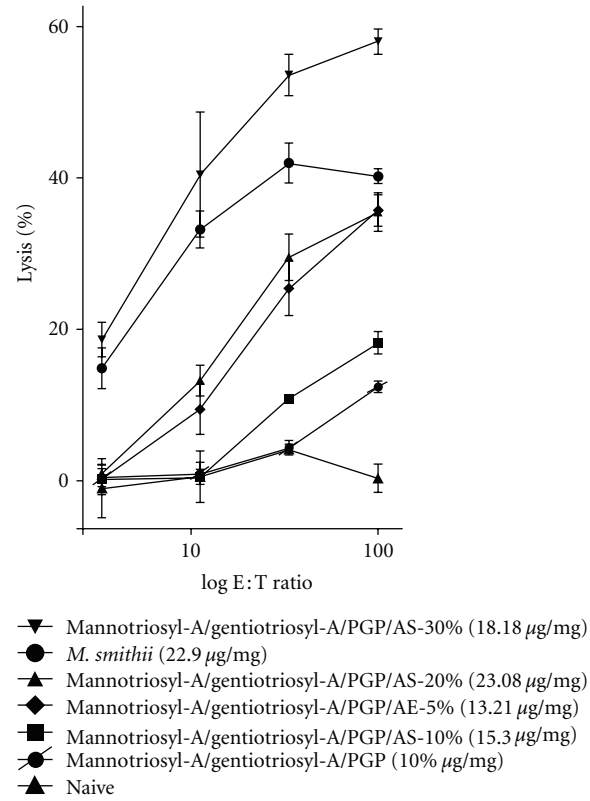

Figure 7: Cytotoxic T lymphocyte (CTL) lysis assay was used to assess the same populations of splenic cells as in Figure 6. Loadings of the OVA antigen are shown also in this figure. EL-4 control targets not expressing SIINFEKL gave <10% lysis in all cases (not shown).

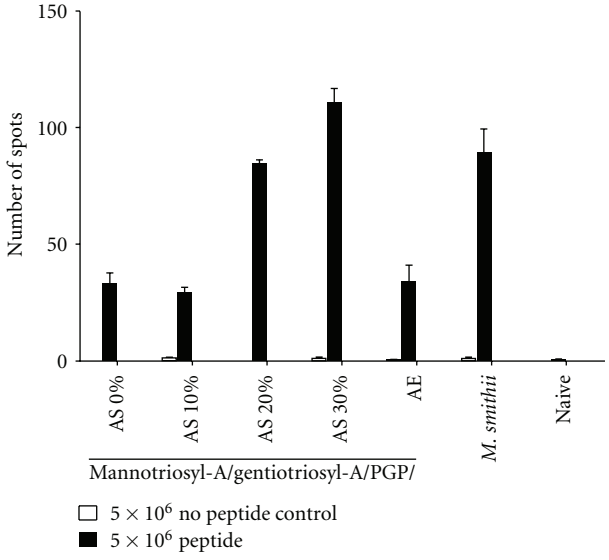

Figure 6: Elispot assay showing a relationship between mol% AS in a triglycosyl-A/PGP archaeosome and CD8 adjuvant activity. Mannotriosyl-A and gentiotriosyl-A were always 22.5 mol% each. AS was varied as shown at 0, 10, 20, and 30 mol%, with PGP making the remainder of each composition. For comparison, archaeosomes containing 5 mol% AE and *M. smithii* total polar lipid archaeosomes are included.

of gentiotriosylarchaeol/mannotriosylarchaeol/PGP with or without AS. Evidence for AS activation could be seen, however, by comparing AS/PGP (30/70 mol%) archaeosomes to either of AE/PGP (5/95 mol%), gentiotriosylarchaeol/PGP, or mannotriosylarchaeol/PGP archaeosomes.

3.4. Short and Long-Term Protective Immunity. M. smithii total polar lipid archaeosomes are capable of adjuvanting a $CD8^+$ T cell response that is long-lasting and provides protection in a solid tumour model in mice [11, 18]. Here we compare immune responses to protection in mice immunized with the various synthetic archaeosomes-OVA. Short-term immunity was assessed in animals ($n = 5$) by challenge with EG.7 tumour cells 4.5 weeks after the second immunization (Figure 9(a)). Protection could be correlated to the $CD8^+$ T cell immune responses achieved (see previous figures). Naive mice are considered unprotected and succumbed to tumour growth early. PGP-OVA archaeosomes showed only limited protection, with best protection achieved with mannotriosylarchaeol/gentiotriosylarchaeol/AS/PGP OVA-archaeosomes. Longer-term immunity was assessed by injection of EG.7 cells 14 weeks following the second immunization (Figure 9(b)). Nonimmunized naive mice and OVA immunizations (no adjuvant) showed no protection,

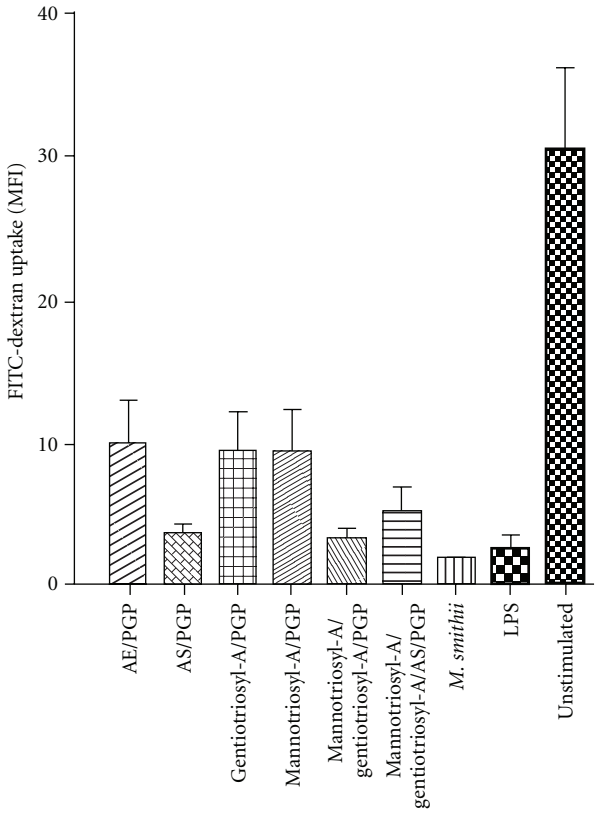

Figure 8: Maturation of dendritic cells (DCs) upon treatment with archaeosomes as measured by decrease of FITC-dextran uptake. Bone marrow DCs treated with archaeosomes *in vitro* were compared for their ability to take up FITC-dextran. The results depict the mean ΔMFI (37–4°C). Data represent means ± SD of triplicate cultures as indicated.

whereas the optimized archaeosome gave protection similar to the positive control.

4. Discussion

A goal of this study was to define an archaeosome adjuvant composition suitable for human application through use of synthetic archaeol-based lipids. Past studies on the mechanism of archaeosomes made from the total polar lipids of various archaea have shown that adjuvant activity occurs at the level of the antigen-presenting dendritic and macrophages cells [19, 24]. Glycolipids in these total polar lipid mixtures may presumably serve as effective adjuvant ingredients as they can target specific receptors on antigen-presenting cells [9, 25, 26].

As glycolipids are uncharged, a stable bilayer does not form when attempts are made to prepare pure glycolipid-liposome based vaccines. This can be achieved, as is the case for natural polar lipids consisting of both glyco and phospholipids, by including phospholipids in the glycolipid formulation [9]. Because inclusion of nonarchaeal lipids such as dipalmitoyl phosphatidylglycerol into archaeosomes results in decline in longer-term $CD8^+$ T cell mediated immune responses [15], we used the diacidic extreme halophile lipid, PGP, in our synthetic glycoarchaeol formulations.

A series of mannosylarchaeols synthesized to have from 1 to 5 sugar units, hydrated best and gave best adjuvant activity at 3 or 4 linear sugar units [16]. Similarly, we found gentiotriosylarchaeol to be a better adjuvant than gentiobiosylarchaeol. Further, the additive adjuvant effect obtained by inclusion of both gentiotriosylarchaeol and mannotriosylarchaeol suggests multiple positive interactions with receptors, to account for an observed increased activation of antigen-presenting dendritic cells (Figure 8). This additive effect of glycosylarchaeols required that the archaeosome preparation be hydrated with all lipids present, suggesting that the various head groups on the archaeosome surface were presented simultaneously to multiple receptors *in vivo*.

Archaetidylserine (AS) as a component of gentiotriosylarchaeol/mannotriosylarchaeol/PGP archaeosomes increased the $CD8^+$ T cell immune response to entrapped antigen in a concentration dependent manner, without significantly enhancing the antibody response (Figures 6–7). *M. smithii* total polar lipid archaeosomes contain AS and their endocytosis has been linked to interaction with the phosphatidylserine receptor of antigen-presenting cells [12]. The pathway of cross-presentation of antigen carried in *M. smithii* archaeosomes occurs at the late phagolysosome stage [12] when calcium is internalized [27], suggesting that AS also contributes to membrane fusion promoted by calcium in analogy to phosphatidylserine [23]. Fusion of archaeosomes with the phagolysosome membrane would contribute to export of antigen to the cytosol and provide access to the MHC class-I presentation pathway.

The longevity of $CD8^+$ T cell memory induced by total polar lipid archaeosomes of *M. smithii* and *Thermoplasma acidophilum* is generally not found in archaeosomes prepared from total polar lipids of extreme halophiles, that lack caldarchaeols [6]. For this reason, it was proposed that long-term $CD8^+$ T cell memory may require the presence of high proportions of caldarchaeol membrane-stabilizing lipids. In this study we found that protective $CD8^+$ T cell memory responses could be induced in mice immunized with antigen-archaeosomes lacking caldarchaeols. This further indicated the importance of head group in lipid composition of an all archaeol-based adjuvant [9].

5. Conclusion

The immune response to antigen may be preferentially directed to either MHC-I (CD8) or MHC-II (CD4) presentations by selection of the head group(s) of an archaeol-based adjuvant. PGP archaeosomes direct antigen primarily to an antibody pathway of response as suggested previously [10]. Additions of glycoarchaeols to PGP archaeosomes enhance greatly the MHC class I pathway of antigen presentation producing the $CD8^+$ T cell response. Combination of gentiotriosyl- and mannotriosylarchaeols in the archaeosome adjuvant enhanced the $CD8^+$ T cell response over

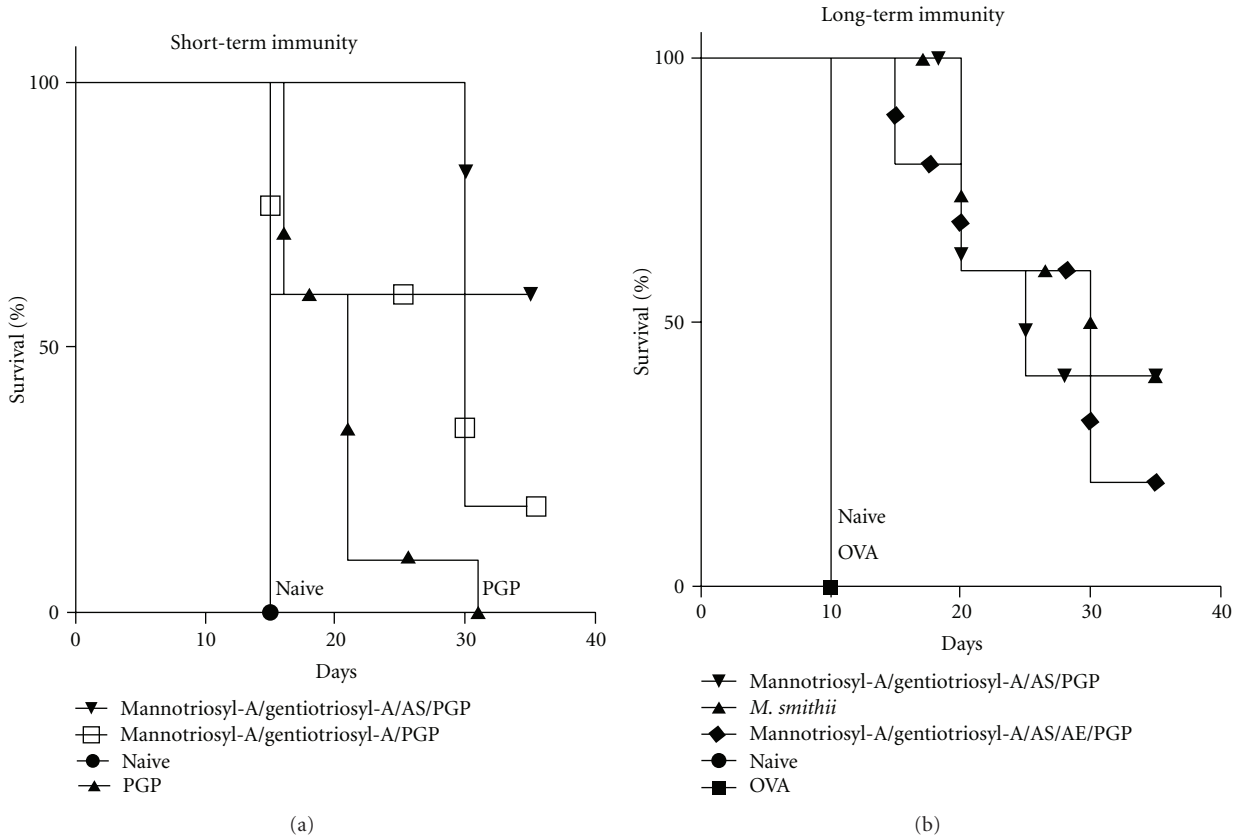

Figure 9: Protection of mice immunized with archaeosomes of various lipid compositions in a solid tumour model. Groups ($n = 5$) of unvaccinated mice (naive) or mice vaccinated with various OVA-archaeosomes were challenged with a subcutaneous injection of EG.7 cells (time zero) either 4.5 weeks (panel (a)) or 14 weeks (panel (b)) following their last vaccination.

either alone, and the additional presence of archaetidylserine was of further benefit. Finally, long-term immunity was obtained in an archaeol-based lipid archaeosome lacking caldarchaeols. We conclude that for a cancer or intracellular pathogen vaccine where a $CD8^+$ T cell response is needed, a favorable archaeosome composition is gentiotriosylarchaeol, mannotriosylarchaeol, AS, and PGP in mol% ratio 22.5/22.5/30/25.

Acknowledgments

Halobacterium salinarum biomass was produced by Mr. John Shelvey in the NRC Bacterial Culture Facility. Animal Husbandry and the bleeding of mice were conducted in the NRC Animal Facility under the guidance of Dr. Craig Bihun. The final art work for figures was done by Mr. Tom Devecseri.

References

[1] G. D. Sprott, C. J. Dicaire, L. P. Fleming, and G. B. Patel, "Stability of liposomes prepared from archaeobacterial lipids and phosphatidylcholine mixtures," *Cells and Materials*, vol. 6, no. 1–3, pp. 143–155, 1996.

[2] C. G. Choquet, G. B. Patel, T. J. Beveridge, and G. D. Sprott, "Stability of pressure-extrudes liposomes made from archaeobacterial ether lipids," *Applied Microbiology and Biotechnology*, vol. 42, no. 2-3, pp. 375–384, 1994.

[3] A. Omri, B. Makabi-Panzu, B. J. Agnew, G. D. Sprott, and G. B. Patel, "Influence of coenzyme Q10 on tissue distribution of archaeosomes, and pegylated archaeosomes, administered to mice by oral and intravenous routes," *Journal of Drug Targeting*, vol. 7, no. 5, pp. 383–392, 2000.

[4] K. Ring, B. Henkel, A. Valenteijn, and R. Gutermann, "Studies on the permeability and stability of liposomes derived from a membrane spanning bipolar archaebacterial tetraetherlipid," in *Liposomes as Drug Carriers*, K. H. Schmidt, Ed., pp. 101–123, Georg Thieme, Stuttgart, Germany, 1986.

[5] G. D. Sprott, D. L. Tolson, and G. B. Patel, "Archaeosomes as novel antigen delivery systems," *FEMS Microbiology Letters*, vol. 154, no. 1, pp. 17–22, 1997.

[6] L. Krishnan and G. D. Sprott, "Archaeosomes as self-adjuvanting delivery systems for cancer vaccines," *Journal of Drug Targeting*, vol. 11, no. 8–10, pp. 515–524, 2003.

[7] D. L. Tolson, R. K. Latta, G. B. Patel, and G. D. Sprott, "Uptake of archaeobacterial liposomes and conventional liposomes by phagocytic cells," *Journal of Liposome Research*, vol. 6, no. 4, pp. 755–776, 1996.

[8] G. D. Sprott, S. Sad, L. P. Fleming, C. J. Dicaire, G. B. Patel, and L. Krishnan, "Archaeosomes varying in lipid composition differ in receptor-mediated endocytosis and differentially adjuvant immune responses to entrapped antigen," *Archaea*, vol. 1, no. 3, pp. 151–164, 2003.

[9] D. G. Sprott, C. J. Dicaire, J. P. Côté, and D. M. Whitfield, "Adjuvant potential of archaeal synthetic glycolipid mimetics critically depends on the glyco head group structure," *Glycobiology*, vol. 18, no. 7, pp. 559–565, 2008.

[10] D. M. Whitfield, S. H. Yu, C. J. Dicaire, and G. D. Sprott, "Development of new glycosylation methodologies for the synthesis of archaeal-derived glycolipid adjuvants," *Carbohydrate Research*, vol. 345, no. 2, pp. 214–229, 2010.

[11] L. Krishnan, S. Sad, G. B. Patel, and G. D. Sprott, "Archaeosomes induce long-term $CD8^+$ cytotoxic T cell response to entrapped soluble protein by the exogenous cytosolic pathway, in the absence of $CD4^+$ T cell help," *Journal of Immunology*, vol. 165, no. 9, pp. 5177–5185, 2000.

[12] K. Gurnani, J. Kennedy, S. Sad, G. D. Sprott, and L. Krishnan, "Phosphatidylserine receptor-mediated recognition of archaeosome adjuvant promotes endocytosis and MHC class I cross-presentation of the entrapped antigen by phagosome-to-cytosol transport and classical processing," *Journal of Immunology*, vol. 173, no. 1, pp. 566–578, 2004.

[13] G. D. Sprott, S. Larocque, N. Cadotte, C. J. Dicaire, M. McGee, and J. R. Brisson, "Novel polar lipids of halophilic eubacterium Planococcus H8 and archaeon Haloferax volcanii," *Biochimica et Biophysica Acta*, vol. 1633, no. 3, pp. 179–188, 2003.

[14] G. D. Sprott, G. B. Patel, and L. Krishnan, "Archaeobacterial ether lipid liposomes as vaccine adjuvants," *Methods in Enzymology*, vol. 373, article 11, pp. 155–172, 2003.

[15] C. J. Dicaire, S. H. Yu, D. M. Whitfield, and G. D. Sprott, "Isopranoid- and dipalmitoyl-aminophospholipid adjuvants impact differently on longevity of CTL immune responses," *Journal of Liposome Research*, vol. 20, no. 4, pp. 304–314, 2010.

[16] D. M. Whitfield, E. E. Eichler, and G. D. Sprott, "Synthesis of archaeal glycolipid adjuvants-what is the optimum number of sugars?" *Carbohydrate Research*, vol. 343, no. 14, pp. 2349–2360, 2008.

[17] L. Krishnan, C. J. Dicaire, G. B. Patel, and G. D. Sprott, "Archaeosome vaccine adjuvants induce strong humoral, cell-mediated, and memory responses: comparison to conventional liposomes and alum," *Infection and Immunity*, vol. 68, no. 1, pp. 54–63, 2000.

[18] L. Krishnan, S. Sad, G. B. Patel, and G. D. Sprott, "Archaeosomes induce enhanced cytotoxic T lymphocyte responses to entrapped soluble protein in the absence of interleukin 12 and protect against tumor challenge," *Cancer Research*, vol. 63, no. 10, pp. 2526–2534, 2003.

[19] L. Krishnan, S. Sad, G. B. Patel, and G. D. Sprott, "The potent adjuvant activity of archaeosomes correlates to the recruitment and activation of macrophages and dendritic cells in vivo," *Journal of Immunology*, vol. 166, no. 3, pp. 1885–1893, 2001.

[20] M. Kato, T. K. Nell, D. B. Fearnley, A. D. McLellan, S. Vuckovic, and D. N. J. Hart, "Expression of multilectin receptors and comparative FITC-dextran uptake by human dendritic cells," *International Immunology*, vol. 12, no. 11, pp. 1511–1519, 2000.

[21] V. A. Fadok, D. L. Bratton, D. M. Rose, A. Pearson, R. A. B. Ezekewitz, and P. M. Henson, "A receptor for phosphatidylserine-specific clearance of apoptotic cells," *Nature*, vol. 405, no. 6782, pp. 85–90, 2000.

[22] S. Martens and H. T. McMahon, "Mechanisms of membrane fusion: disparate players and common principles," *Nature Reviews Molecular Cell Biology*, vol. 9, no. 7, pp. 543–556, 2008.

[23] G. D. Sprott, J. P. Côté, and H. C. Jarrell, "Glycosidase-induced fusion of isoprenoid gentiobiosyl lipid membranes at acidic pH," *Glycobiology*, vol. 19, no. 3, pp. 267–276, 2009.

[24] L. Krishnan and G. D. Sprott, "Archaeosome adjuvants: immunological capabilities and mechanism(s) of action," *Vaccine*, vol. 26, no. 17, pp. 2043–2055, 2008.

[25] R. N. Coler, S. Bertholet, M. Moutaftsi et al., "Development and characterization of synthetic glucopyranosyl lipid adjuvant system as a vaccine adjuvant," *PLoS ONE*, vol. 6, no. 1, article e16333, 2011.

[26] I. Matsunaga and D. B. Moody, "Mincle is a long sought receptor for mycobacterial cord factor," *Journal of Experimental Medicine*, vol. 206, no. 13, pp. 2865–2868, 2009.

[27] K. A. Christensen, J. T. Myers, and J. A. Swanson, "pH-dependent regulation of lysosomal calcium in macrophages," *Journal of Cell Science*, vol. 115, Part 3, pp. 599–607, 2002.

Hindawi Publishing Corporation
Archaea
Volume 2012, Article ID 384919, 8 pages
doi:10.1155/2012/384919

Review Article

Lipids of Archaeal Viruses

Elina Roine and Dennis H. Bamford

Department of Biosciences and Institute of Biotechnology, University of Helsinki, P.O. Box 56, Viikinkaari 5, 00014 Helsinki, Finland

Correspondence should be addressed to Elina Roine, elina.roine@helsinki.fi

Received 9 July 2012; Accepted 13 August 2012

Academic Editor: Angela Corcelli

Archaeal viruses represent one of the least known territory of the viral universe and even less is known about their lipids. Based on the current knowledge, however, it seems that, as in other viruses, archaeal viral lipids are mostly incorporated into membranes that reside either as outer envelopes or membranes inside an icosahedral capsid. Mechanisms for the membrane acquisition seem to be similar to those of viruses infecting other host organisms. There are indications that also some proteins of archaeal viruses are lipid modified. Further studies on the characterization of lipids in archaeal viruses as well as on their role in virion assembly and infectivity require not only highly purified viral material but also, for example, constant evaluation of the adaptability of emerging technologies for their analysis. Biological membranes contain proteins and membranes of archaeal viruses are not an exception. Archaeal viruses as relatively simple systems can be used as excellent tools for studying the lipid protein interactions in archaeal membranes.

1. Introduction

Viruses are obligate parasites. Their hallmark is the virion, an infectious particle made of proteins and encapsidating the viral genome. Many viruses, however, also contain lipids as essential components of the virion [1]. The majority of viral lipids are found in membranes, but viral proteins can also be modified with lipids [2, 3].

1.1. Membrane Containing Viruses in the Viral Universe. Membrane containing viruses can roughly be divided into two subclasses [1]. The first subclass contains viruses in which the membrane, also called an envelope, is the outermost layer of the viral particle. In the second class of viruses, the membrane is underneath the usually icosahedral protein capsid. Few viruses contain both the inner membrane as well as an envelope [1]. Lipid membranes of viruses have evolved into essential components of virions that in many cases seem to be involved in the initial stages of infection [4–6]. The majority of membrane containing viruses infect animals both vertebrate and invertebrate that do not have a cell wall surrounding the cytoplasmic membrane. For other host organisms such as plants and prokaryotes there are much fewer membrane containing viruses known [1]. Usually the cells of these organisms are covered with a cell wall. By far the majority of known viruses that infect prokaryotes, that is, bacteria (bacteriophages), and archaea (archaeal viruses) belong to the order *Caudovirales*, the tailed viruses (Figure 1) [1, 7]. These viruses are made of the icosahedrally organized head and a helical tail. Tailed viruses do not usually contain a membrane, although there are some early reports of tailed mycobacteriophages containing lipids [8, 9]. Viral proteins can also be modified with lipids [3], and there are some indications that proteins of archaeal viruses may also contain lipid modifications [10]. Since very little is known about the lipid modifications of archaeal virus proteins, this paper will concentrate mostly on the membrane lipids of archaeal viruses.

1.2. How Do Viruses Obtain Membranes? Viral-encoded genes possibly involved in lipid modifications have been found in large eukaryotic viruses such as Mimivirus [11] and *Paramecium bursaria* Chlorella virus 1 (PBCV-1) [12]. In prokaryotic viruses, however, no genes encoding components for lipid metabolism have been recognized, but the membranes of prokaryotic viruses are mostly obtained from

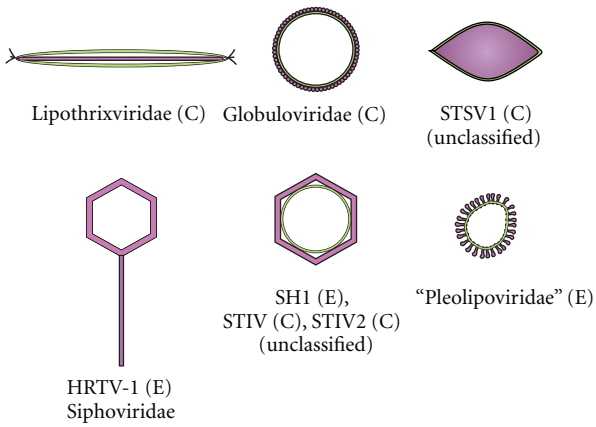

Figure 1: Schematic representation of the currently known lipid containing archaeal viruses (C = viruses infecting crenarchaeal hosts, E = viruses infecting euryarchaeal hosts). As a comparison, an archaeal virus devoid of a membrane [32] is also shown. Membrane is illustrated as a yellow layer either inside or outside of the protein capsid depicted in purple. The viral particles are not drawn in scale.

the host cytoplasmic membranes [13, 14]. Enveloped viruses obtain the membrane during budding, that is, egress of the viral particles from the cells without disturbing the cell membrane integrity [15]. The inner membrane of prokaryotic viruses is presumed to be obtained from specific patches of host cytoplasmic membrane containing viral membrane proteins and mechanistically analogous to the formation of clathrin coated pits [6, 16–18]. Consequently, enveloped viruses often exit the cells without lysis, whereas the viruses containing a membrane inside the capsid usually lyse the cells. At least one exception to this can be noted. Prokaryotic lipid containing virus $\phi 6$ contains an envelope, but its infection cycle ends in lysis of the host cells [19, 20].

As mentioned above, viral membranes are often involved in the initial stages of infection. This is especially true for the enveloped viruses where the proteins responsible for host recognition (spikes or fusion proteins) are usually incorporated in the envelope. At some point during the often multiphase entry process, the viral envelope fuses with a host membrane releasing the contents into the cell [4, 5]. Among viruses that contain the membrane inside the capsid, the involvement of the membrane in the entry has been shown for the bacteriophage PRD1. After the receptor recognition, the protein rich membrane forms a tubular structure through which the DNA enters the cell cytoplasm [21–23]. Such tubular structures, however, are not formed by all prokaryotic icosahedral viruses containing the membrane inside the capsid [24–28]. For the bacteriophage PM2 that infects the marine bacterium *Pseudoalteromonas*, fusion of the viral inner membrane with the host outer membrane was suggested [29]. Similarly, fusion of the *Sulfolobus* turreted icosahedral virus (STIV) membrane with the cytoplasmic membrane of *S. solfataricus* was suggested [30]. In addition to the function in viral entry, the inner membrane of viruses act, together with the viral membrane proteins, as the scaffold for capsid protein assembly [18, 26, 31].

2. Analysis of Viral Membranes

How do we know if a membrane is part of the viral structure? Chloroform treatment can be used as the first step in screening for viral membranes: the infectivity of the virus is usually considerably reduced if the virions contain a membrane [32–34]. Chloroform treatment can, however, also abolish the infectivity of virions that have not been reported to contain lipids [35] and therefore further studies are always required. Low buoyant density is also an indicator of the lipid membrane in the virions [6, 36]. Sudan Black B can be used to stain the polyacrylamide gel containing separated virion proteins and lipids [10, 37]. Although Sudan Black B is not entirely specific for lipids, positive staining is an indication of the presence of lipid membranes in highly purified viral material and also shows if some viral proteins are putatively lipid modified [10]. Further proof for the presence of a lipid membrane and analyses of its different components can be obtained by techniques also used for the analyses of the membrane lipids of the host cells, for example, thin layer chromatography (TLC), mass spectrometry (e.g., electrospray ionization, ESI-MS), and nuclear magnetic resonance (NMR) [38, 39]. Lipids must be obtained from highly purified viral material [10, 40, 41] or from distinct dissociation components of the virion [28, 42] as it is often difficult to separate virions from membrane vesicles of host origin.

3. Archaeal Lipids

Since the membrane lipids of archaeal viruses are derived from the host lipid pool, analysis of the host lipids is an important part of the lipid analysis of their viruses. Archaeal lipids are known to be drastically different from the ones of bacterial and eukaryotic membranes: instead of lipids based on diacylglycerol the most common core lipid of archaeal phospholipids is the diether of diphytanylglycerol [43, 44]. Archaeal lipids can be divided according to the two major kingdoms of Archaea. As a crude generalization, one can say that the haloarchaeal cell membranes consist mostly of bilayer-forming diether lipids, whereas membranes of archaeal thermophilic organisms are largely composed of tetraether lipids that form monolayer membranes [38, 45, 46]. As in other organisms, phospholipids are the major components of archaeal membranes. In halophilic Archaea, approximately 10% of total lipids are neutral lipids such as bacterioruberin [38]. The major core structure of haloarchaeal lipids consists of archaeol, a 2,3-di-*O*-phytanyl-*sn*-glycerol with C_{20} isoprenoid chains [38, 43]. One of the major lipids in extremely thermophilic archaea such as *Sulfolobus* sp. is the macrocyclic tetraether lipid caldarchaeol [46–48]. The composition of lipid membranes is modified according to the environmental conditions in all organisms, and Archaea are not an exception [38, 45, 47, 49].

Some archaeal proteins are known to be modified by isoprenoid derivatives [2, 60–62], and structural analysis revealed a diphytanylglyceryl methyl thioether lipid of one modified protein [61]. Modification of the *Haloferax volcanii*

S-layer protein with a lipid of unknown structure was shown to be crucial to the maturation of the protein [62].

4. Archaeal Membrane Containing Viruses

Our knowledge of archaeal viruses is scarce, but even less is known about their lipids. The known archaeal membrane containing viruses are listed in Table 1. Especially crenarchaeal viruses that infect thermophilic or hyperthermophilic hosts are difficult to produce in amounts high enough for closer analysis of their membrane lipids by traditional methods (e.g., [58]).

4.1. Crenarchaeal Viruses. The presence of lipid membranes have been reported for icosahedral crenarchaeal viruses STIV and *Sulfolobus* turreted icosahedral virus 2 (STIV2), for filamentous viruses *Acidianus* filamentous virus 1 (AFV-1), *Sulfolobus islandicus* filamentous virus (SIFV), and *Thermoproteus tenax* virus 1 (TTV1), for spindle-shaped *Sulfolobus tengchongensis* spindle-shaped virus 1 (STSV1), and for spherical virus *Pyrobaculum* spherical virus (PSV; Table 1). The *Acidianus* bottle-shaped virus (ABV) virions were reported to contain a 9 nm thick envelope [63]. The lipid nature of this envelope, however, has not been reported and the estimated thickness of 9 nm is more than that of usual membranes of archaea [28, 58, 64, 65].

The case of spindle-shaped viruses such as *Sulfolobus* spindle-shaped virus 1 (SSV1) of family *Fuselloviridae* is interesting, because the virions have a buoyant density that is in the same range as in those virions containing a membrane (1.24 g/cm^3 in CsCl), and the virions are sensitive to chloroform [66]. It has been reported that "10% of the SSV-1 virion envelope consists of host lipids" [67], but no further membrane studies have been conducted. This all may suggest that some other type of lipid component than a lipid membrane is present.

The situation among the members of the family *Lipothrixviridae* is also confusing, because these viruses are defined as rod-shaped viruses containing an envelope. The family is further divided into genera *Alpha-*, *Beta-*, *Gamma-*, and *Deltalipothrixvirus* according to the specific structures involved in the host attachment located in the virion ends [68]. The envelope is reported to consist of viral proteins and host derived lipids [68]. The presence of a lipid envelope has been shown for alphalipothrixvirus TTV1 [51], betalipothrixvirus SIFV, and gammalipothrixvirus AFV-1 [53]. However, no evidence for a lipid membrane in the type species of *Deltalipothrixvirus* genus, the *Acidianus* filamentous virus 2 (AFV-2), could be found [69].

Further analysis using thin layer chromatography (TLC) has been reported for AFV1 [53], SIFV [54], STSV1 [59], and PSV [50]. The lipid composition of STIV was analysed using ESI-MS [70]. In conclusion, it could be shown that in general the lipids of crenarchaeal viruses were obtained from the host lipid pool, but some lipid species were found to be quantitatively and qualitatively different from the host lipids [50, 53, 54]. Although viral lipids are considered to be derived from the host membrane lipids, it was suggested that they derived from host lipids by modification [53] and possibly by virus encoded enzyme apparatus [50]. Since no such enzyme apparatus has been described in prokaryotic let alone archaeal viruses, the more probable explanation for the differences at the moment is a strong selection for some minor lipid species of the host. Recent study on the assembly of STIV using cryo-electron tomography suggests that the viral membrane is derived *de novo* in the host cell and not as a result of a membrane invagination [31, 71]. This would, at least in theory, allow the possibility that there is viral enzymatic machinery responsible for the lipid modification. The comparative lipid analysis of STIV and its host *S. solfataricus* showed, however, that the viral lipids consisted of a subpopulation of the host lipids but in different proportions [70].

4.2. Euryarchaeal Viruses. Among euryarchaeal viruses, the icosahedral SH1 and *Haloarcula hispanica* icosahedral virus 2 (HHIV-2) virions contain an inner membrane [40, 42, 72] and the pleomorphic viruses contain a membrane envelope [10, 34, 36, 41].

SH1 was the first icosahedral virus characterized among haloarchaea [33]. Inside the rather complex protein capsid, there is a lipid membrane enclosing the approximately 31 kb linear double stranded (ds) DNA genome [28, 40, 42]. The major protein component of the membrane is the approximately 10 kDa VP12, one of the major structural proteins of the SH1 virion [42]. Although there are no detailed studies reporting the assembly steps of SH1, similarities in virion structure to PRD1 suggests a similar assembly pathway [28, 40, 42]. Therefore, it is likely that the viral capsid and the inner membrane are assembled with the help of the membrane proteins and the genome is packaged into these empty particles (procapsid) before the lysis of the cells [28, 33, 40, 42, 73]. Mass spectrometric analysis of the SH1 lipids revealed major archaeal phospholipid species of phosphatidylglycerol (PG), the methyl ester of phosphatidylglycerophosphate (PGP-Me), and phosphatidylglycerol sulfate (PGS). The proportion of PGP-Me, however, was higher in SH1 than in its host *Haloarcula hispanica* [40]. Quantitative dissociation studies of SH1 allowed the separation of the virion into fractions of soluble capsid proteins and lipid core particle (LC) which consisted of the same phospholipid classes and in the same proportions as the intact virions confirming the presence of the inner membrane [42]. Sudan Black B staining was used to show the presence of lipids in the highly purified HHIV-2 virions [72]. Cryo-electron microscopy (cryo-EM) and image reconstruction of SH1 particles show that as in PRD1 [74] and STIV [25] the inner membrane of SH1 follows the shape of the capsid and the membrane is highly curved at the fivefold vertices where there is a clear transmembrane complex probably containing VP2 protein [28].

Haloarchaeal pleomorphic viruses is a newly characterized group of viruses with relatively simple virion architecture [10, 34, 36, 41, 56, 73, 75]. The genome (single stranded or double stranded DNA) is enclosed in a membrane vesicle derived from the host membrane [10, 34, 41].

Table 1: Currently known membrane containing archaeal viruses, exit strategy, and presence of lipid envelope or inner membrane.

Family or Genus[a]	Type species/example of species/species lipids studied	Exit strategy	Lipids	References
Globuloviridae (C)	*Pyrobaculum* spherical virus, PSV	No lysis detected	Lipid envelope	[50]
Lipothrixviridae (C)				
Genus *Alphalipothrixvirus*	*Thermoproteus tenax* virus 1, TTV1	Lysis	Lipid envelope	[51, 52]
Genus *Betalipothrixvirus*	*Acidianus* filamentous virus 1, AFV1	No lysis detected	Lipid envelope	[53]
Genus *Gammalipothrixvirus*	*Sulfolobus islandicus* filamentous virus 1, SIFV1	No lysis detected	Lipid envelope	[54]
Genus *Salterprovirus* (E)	His2[b]	No lysis detected	Lipid envelope	[10, 55]
"*Pleolipoviridae*" (E)[b]	*Halorubrum* pleomorphic virus 1, HRPV-1	No lysis detected	Lipid envelope	[34, 41]
	Halorubrum pleomorphic virus 2, HRPV-2	No lysis detected	Lipid envelope	[10, 56]
	Halorubrum pleomorphic virus 3, HRPV-3	No lysis detected	Lipid envelope	[10, 56]
	Halorubrum pleomorphic virus 6, HRPV-6	No lysis detected	Lipid envelope	[10]
	Haloarcula hispanica pleomorphic virus 1, HHPV-1	No lysis detected	Lipid envelope	[36]
Unclassified	*Sulfolobus* turreted icosahedral virus, STIV (C)	Lysis	Inner membrane	[25, 57]
	Sulfolobus turreted icosahedral virus 2, STIV2 (C)	Lysis	Inner membrane	[58]
	Sulfolobus tengchongensis spindle-shaped virus 1 (C)	No lysis detected	Lipid envelope	[59]
	SH1 (E)	Lysis	Inner membrane	[33, 40, 42]

[a] Host domain: B: bacteria, C: crenarchaea, E: euryarchaea.
[b] His2 has been suggested to belong to the new family *Pleolipoviridae*. The approval of the suggested new family is pending at the ICTV.

There are two major structural proteins, the larger proteins (approximately 50 kDa in size) are mostly exposed and C-terminally anchored to the membrane [10, 41]. This larger protein is N-glycosylated in HRPV-1 [41, 76], and in HGPV-1 it stains with Sudan Black B [10] suggesting a lipid modification. The smaller structural proteins (approximately 10 to 14.5 kDa) are predicted to contain several transmembrane domains [10, 34, 41]. New progeny viruses are released from the infected cell without lysis [10, 34, 36]. Thus, the viral envelope is most probably acquired by budding from the sites of host cytoplasmic membrane containing the viral membrane proteins and the genome [10, 34, 36]. The detailed sequence of events and the viral and host proteins involved will be the subject of future studies. Currently, the group of haloarchaeal pleomorphic viruses consists of seven members: *Halorubrum* pleomorphic viruses 1, 2, 3 and 6 (HRPV-1, HRPV-2, HRPV-3, and HRPV-6), respectively [10, 34, 56], *Haloarcula hispanica* pleomorphic virus 1 (HHPV-1) [36], and *Halogeometricum* sp. pleomorphic virus 1 (HGPV-1) [56]. In addition, His2 [55], the second member of genus *Salterprovirus*, is suggested to belong to the pleomorphic viruses [10, 75]. Lipid analysis by TLC or mass spectrometry of the highly purified viral material suggests that the composition of lipids was similar to that of their hosts [10, 34, 41]. The lipids of viruses infecting *Halorubrum* sp. hosts consisted mostly of the archaeal forms of PG, PGP-Me, and PGS, whereas in *Halogeometricum* sp. the PGS was missing both in the host lipids as well as in the lipids of HGPV-1 [10, 41, 77]. Sudan Black B staining of the HGPV-1 and His2 proteins showed that some of the major structural proteins may also be lipid modified [10].

Studies on lipid containing haloarchaeal viruses of different morphotypes have also allowed the comparison of the differences in the proportions of incorporated lipids. For example, the isolation and characterization of the *Haloarcula hispanica* pleomorphic virus 1 (HHPV-1) [36] allowed to compare the differences of lipid composition between an icosahedral membrane containing virus SH1and the enveloped, pleomorphic HHPV-1 that infect the same host, *Har. hispanica* (Figure 2). The comparison showed that the lipid composition of the pleomorphic virus HHPV-1 envelope was more similar to the lipids of the host membrane than those of SH1 (Figure 2) [36]. This may be explained by the constraints that the inner membrane curvature poses on the selection of lipids in SH1 and consequently suggests that SH1 is able to selectively acquire lipids from the host membrane [36, 73]. Different lipids are known to have different shapes and therefore can be found in different positions in the curved membrane [14, 78]. It is known that different membrane proteins attract different types of lipids [79], and it would be very interesting to determine which viral proteins are involved in this process.

5. Concluding Remarks

Research on lipid containing archaeal viruses is still in its infancy. The presence of lipids and characterization of their nature has been shown for some archaeal viruses [10, 25, 34, 36, 40–42, 50, 51, 53, 54, 58, 59, 70]. Deeper understanding of their role in virus biology is largely still missing. Partly this problem can be assigned to an inability to produce enough material of high enough purity. Partly this problem is due to missing techniques comparable to those developed for lipid research of bacteria and eukaryotes. Lipid research, as many other fields of research, benefits from a thorough characterization of the systems studied. Characterization of the virus life cycle and studying its different steps using the cutting edge technologies in electron microscopy, for example, complements the information obtained using biochemical and genomic methods [25, 28, 31, 40, 42].

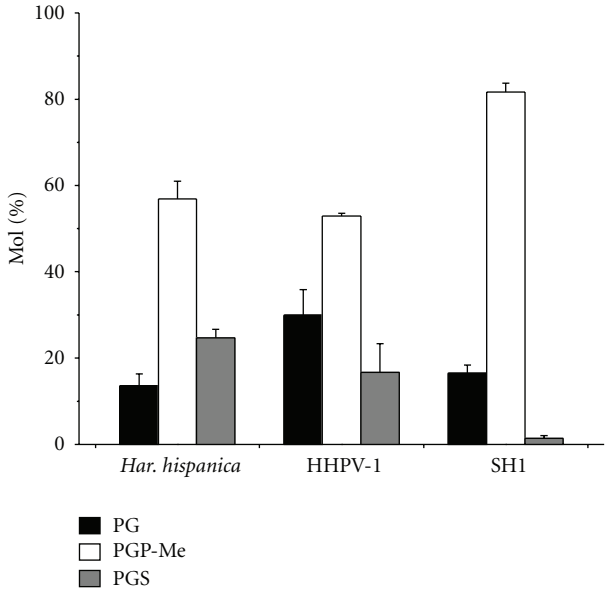

Figure 2: Comparison of the phospholipid compositions of *Har. hispanica*, HHPV-1 and SH1. Concentrations are expressed as the mol% of the total phospholipids. Only phospholipids representing more than 1% of the total are shown. Error bars represent standard deviations of data from at least three independent experiments. Copyright American Society for Microbiology, [36].

The examples set by crystallization of the whole virions of membrane containing bacteriophages PRD1 [74, 80] and PM2 [26] show how valuable different perspectives on lipid membranes can be. Studies on the finding of the proposed viral-encoded genes involved in novel lipid modifications is hampered by the fact that a high amount of predicted gene content in archaeal viruses do not have homologues in the data bases. A more systematic approach of cloning and expression analyses of genes as well as crystallization of the gene products could be used in screening for the functions of interest.

Archaeal lipids are unique in terms of their chemical, physical, structural, and biological properties. Not only can they be admired in their complexity and variability, but as material adjusted to extreme conditions, they can be considered unique for biotechnological applications designed for extreme conditions. The archaeosomes made of one of the major phospholipid of haloarchaeal membranes, the archaeal form of the methyl ester of phophatidylglycerophosphate (PGP-Me), for example, have been shown to be superior in terms of stability and low permeability in high salt conditions [81]. Similar findings were reported for the performance of archaeosomes made of thermophilic lipids in a wide range of temperatures [65]. Although the lipids of archaeal viruses are obtained from host lipids, they can be present in different proportions and the mechanisms for the selection must be driven by viral components. The simplicity of many membrane containing archaeal viruses can be exploited in studying the mechanisms of protein-lipid interplay in archaeal membranes.

Acknowledgments

This work was supported by the Helsinki University three year grant (2010–2012) to E. Roine and Academy Professor funding (Academy of Finland) grants 256197 and 256518 to D. H. Bamford.

References

[1] A. M. Q. King, M. J. Adams, E. B. Carstens, and E. J. Lefkowitz, *Virus Taxonomy, Ninth Report of the International Committee on Taxonomy of Viruses*, Elsevier, Oxford, UK, 2011.

[2] J. Eichler and M. W. W. Adams, "Posttranslational protein modification in *Archaea*," *Microbiology and Molecular Biology Reviews*, vol. 69, no. 3, pp. 393–425, 2005.

[3] D. E. Hruby and C. A. Franke, "Viral acylproteins: greasing the wheels of assembly," *Trends in Microbiology*, vol. 1, no. 1, pp. 20–25, 1993.

[4] M. M. Poranen, R. Daugelavičius, and D. H. Bamford, "Common principles in viral entry," *Annual Review of Microbiology*, vol. 56, pp. 521–538, 2002.

[5] A. E. Smith and A. Helenius, "How viruses enter animal cells," *Science*, vol. 304, no. 5668, pp. 237–242, 2004.

[6] H. M. Oksanen, M. M. Poranen, and D. H. Bamford, "Bacteriophages: lipid-containing," in *Encyclopedia of Life Sciences (ELS)*, John Wiley & Sons, Chichester, UK, 2010.

[7] H. W. Ackermann, "5500 Phages examined in the electron microscope," *Archives of Virology*, vol. 152, no. 2, pp. 227–243, 2007.

[8] B. L. Soloff, T. A. Rado, B. E. Henry II, and J. H. Bates, "Biochemical and morphological characterization of mycobacteriophage R1," *Journal of Virology*, vol. 25, no. 1, pp. 253–262, 1978.

[9] M. L. Gope and K. P. Gopinathan, "Presence of lipids in mycobacteriophage I3," *Journal of General Virology*, vol. 59, no. 1, pp. 131–138, 1982.

[10] M. K. Pietilä, N. S. Atanasova, V. Manole et al., "Virion architecture unifies globally distributed pleolipoviruses infecting halophilic *Archaea*," *Journal of Virology*, vol. 86, no. 9, pp. 5067–5079, 2012.

[11] J. M. Claverie, C. Abergel, and H. Ogata, "Mimivirus," in *Current Topics in Microbiology and Immunology*, J. L. Van Etten, Ed., vol. 328, pp. 89–121, 2009.

[12] W. H. Wilson, J. L. Van Etten, and M. J. Allen, "The *Phycodnaviridae*: the story how tiny giants rule the world," in *Current Topics in Microbiology and Immunology*, J. L. Van Etten, Ed., pp. 1–42, 2009.

[13] G. J. Brewer, "Control of membrane morphogenesis in bacteriophage," *International Review of Cytology*, vol. 68, pp. 53–96, 1980.

[14] S. Laurinavičius, *Phospholipids of lipid-containing bacteriophages and their transbilayer distribution. [Ph.D. thesis]*, University of Helsinki, Helsinki, Finland, 2008.

[15] H. Garoff, R. Hewson, and D. J. E. Opstelten, "Virus maturation by budding," *Microbiology and Molecular Biology Reviews*, vol. 62, no. 4, pp. 1171–1190, 1998.

[16] L. Mindich, D. Bamford, T. McGraw, and G. Mackenzie, "Assembly of bacteriophage PRD1: particle formation with wild-type and mutant viruses," *Journal of Virology*, vol. 44, no. 3, pp. 1021–1030, 1982.

[17] D. H. Bamford, J. Caldentey, and J. K. Bamford, "Bacteriophage PRD1: a broad host range dsDNA tectivirus with an

internal membrane," *Advances in Virus Research*, vol. 45, pp. 281–319, 1995.

[18] P. S. Rydman, J. K. H. Bamford, and D. H. Bamford, "A minor capsid protein P30 is essential for bacteriophage PRD1 capsid assembly," *Journal of Molecular Biology*, vol. 313, no. 4, pp. 785–795, 2001.

[19] A. K. Vidaver, R. K. Koski, and J. L. Van Etten, "Bacteriophage ϕ6: a lipid containing virus of *Pseudomonas phaseolicola*," *Journal of Virology*, vol. 11, no. 5, pp. 799–805, 1973.

[20] L. Mindich and J. Lehman, "Cell wall lysin as a component of the bacteriophage ϕ6 virion," *Journal of Virology*, vol. 30, no. 2, pp. 489–496, 1979.

[21] K. H. Lundström, D. H. Bamford, E. T. Palva, and K. Lounatmaa, "Lipid-containing bacteriophage PR4: structure and life cycle," *Journal of General Virology*, vol. 43, no. 3, pp. 583–592, 1979.

[22] D. Bamford and L. Mindich, "Structure of the lipid-containing bacteriophage PRD1: disruption of wild-type and nonsense mutant phage particles with guanidine hydrochloride," *Journal of Virology*, vol. 44, no. 3, pp. 1031–1038, 1982.

[23] A. M. Grahn, R. Daugelavičius, and D. H. Bamford, "Sequential model of phage PRD1 DNA delivery: active involvement of the viral membrane," *Molecular Microbiology*, vol. 46, no. 5, pp. 1199–1209, 2002.

[24] H. M. Kivelä, R. Daugelavičius, R. H. Hankkio, J. K. H. Bamford, and D. H. Bamford, "Penetration of membrane-containing double-stranded-DNA bacteriophage PM2 into *Pseudoalteromonas* hosts," *Journal of Bacteriology*, vol. 186, no. 16, pp. 5342–5354, 2004.

[25] R. Khayat, L. Tang, E. T. Larson, C. M. Lawrence, M. Young, and J. E. Johnson, "Structure of an archaeal virus capsid protein reveals a common ancestry to eukaryotic and bacterial viruses," *Proceedings of the National Academy of Sciences of the United States of America*, vol. 102, no. 52, pp. 18944–18949, 2005.

[26] N. G. Abrescia, J. M. Grimes, H. M. Kivelä et al., "Insights into virus evolution and membrane biogenesis from the structure of the marine lipid-containing bacteriophage PM2," *Molecular cell*, vol. 31, no. 5, pp. 749–761, 2008.

[27] S. T. Jaatinen, L. J. Happonen, P. Laurinmäki, S. J. Butcher, and D. H. Bamford, "Biochemical and structural characterisation of membrane-containing icosahedral dsDNA bacteriophages infecting thermophilic *Thermus thermophilus*," *Virology*, vol. 379, no. 1, pp. 10–19, 2008.

[28] H. T. Jäälinoja, E. Roine, P. Laurinmäki, H. M. Kivelä, D. H. Bamford, and S. J. Butcher, "Structure and host-cell interaction of SH1, a membrane-containing, halophilic euryarchaeal virus," *Proceedings of the National Academy of Sciences of the United States of America*, vol. 105, no. 23, pp. 8008–8013, 2008.

[29] V. Cvirkaitė-Krupovič, M. Krupovič, R. Daugelavičius, and D. H. Bamford, "Calcium ion-dependent entry of the membrane-containing bacteriophage PM2 into its *Pseudoalteromonas* host," *Virology*, vol. 405, no. 1, pp. 120–128, 2010.

[30] R. Khayat, C. Y. Fu, A. C. Ortmann, M. J. Young, and J. E. Johnson, "The architecture and chemical stability of the archaeal *Sulfolobus* turreted icosahedral virus," *Journal of Virology*, vol. 84, no. 18, pp. 9575–9583, 2010.

[31] C. Y. Fu, K. Wang, L. Gan et al., "In vivo assembly of an archaeal virus studied with whole-cell electron cryotomography," *Structure*, vol. 18, no. 12, pp. 1579–1586, 2010.

[32] P. Kukkaro and D. H. Bamford, "Virus-host interactions in environments with a wide range of ionic strengths," *Environmental Microbiology Reports*, vol. 1, no. 1, pp. 71–77, 2009.

[33] K. Porter, P. Kukkaro, J. K. H. Bamford et al., "SH1: a novel, spherical halovirus isolated from an Australian hypersaline lake," *Virology*, vol. 335, no. 1, pp. 22–33, 2005.

[34] M. K. Pietilä, E. Roine, L. Paulin, N. Kalkkinen, and D. H. Bamford, "An ssDNA virus infecting *Archaea*: a new lineage of viruses with a membrane envelope," *Molecular Microbiology*, vol. 72, no. 2, pp. 307–319, 2009.

[35] M. L. Dyall-Smith, "Genus *Salterprovirus*," in *Virus Taxonomy, Ninth Report of the International Committee on Taxonomy of Viruses*, A. M. Q. King, M. J. Adams, E. B. Carstens, and E. J. Lefkowitz, Eds., pp. 183–186, ElsevierOxford, UK, 2011.

[36] E. Roine, P. Kukkaro, L. Paulin et al., "New, closely related haloarchaeal viral elements with different nucleic acid types," *Journal of Virology*, vol. 84, no. 7, pp. 3682–3689, 2010.

[37] J. P. Prat, J. N. Lamy, and J. D. Weill, "Staining of lipoproteins after electrophoresis in polyacrylamide gel," *Bulletin de la Société de Chimie Biologique*, vol. 51, no. 9, article 1367, 1969.

[38] A. Corcelli and S. Lobasso, "Characterization of lipids of halophilic *Archaea*," in *Methods in Microbiology: Extremophiles*, F. A. Rainey and A. Oren, Eds., vol. 35, pp. 585–613, Elsevier, New York, NY, USA, 2006.

[39] M. S. da Costa, M. F. Nobre, and R. Wait, "Analysis of lipids from extremophilic bacteria," in *Methods in Microbiology: Extremophiles*, F. A. Rainey and A. Oren, Eds., vol. 35, pp. 127–159, Elsevier, New York, NY, USA, 2006.

[40] D. H. Bamford, J. J. Ravantti, G. Rönnholm et al., "Constituents of SH1, a novel lipid-containing virus infecting the halophilic euryarchaeon *Haloarcula hispanica*," *Journal of Virology*, vol. 79, no. 14, pp. 9097–9107, 2005.

[41] M. K. Pietilä, S. Laurinavičius, J. Sund, E. Roine, and D. H. Bamford, "The single-stranded DNA genome of novel archaeal virus *Halorubrum pleomorphic* virus 1 is enclosed in the envelope decorated with glycoprotein spikes," *Journal of Virology*, vol. 84, no. 2, pp. 788–798, 2010.

[42] H. M. Kivelä, E. Roine, P. Kukkaro, S. Laurinavičius, P. Somerharju, and D. H. Bamford, "Quantitative dissociation of archaeal virus SH1 reveals distinct capsid proteins and a lipid core," *Virology*, vol. 356, no. 1-2, pp. 4–11, 2006.

[43] M. Kates, "The phytanyl ether-linked polar lipids and isoprenoid neutral lipids of extremely halophilic bacteria," *Progress in the Chemistry of Fats and Other Lipids*, vol. 15, no. 4, pp. 301–342, 1977.

[44] G. D. Sprott, "Structures of archaebacterial membrane lipids," *Journal of Bioenergetics and Biomembranes*, vol. 24, no. 6, pp. 555–566, 1992.

[45] S. V. Albers, W. N. Konings, and A. J. M. Driessen, "Membranes of thermophiles and other extremophiles," in *Methods in Microbiology: Extremophiles*, F. A. Rainey and A. Oren, Eds., vol. 35, pp. 161–171, Elsevier, New York, NY, USA, 2006.

[46] Y. Boucher, "Lipids: biosynthesis, function, and evolution," in *Archaea: Molecular and Cellular Biology*, R. Cavicchioli, Ed., pp. 341–353, ASM Press, Washington, DC, USA, 2007.

[47] A. Gliozzi, R. Rolandi, M. de Rosa, and A. Gambacorta, "Monolayer black membranes from bipolar lipids of archaebacteria and their temperature-induced structural changes," *The Journal of Membrane Biology*, vol. 75, no. 1, pp. 45–56, 1983.

[48] B. Nicolaus, A. Trincone, E. Esposito, M. R. Vaccaro, A. Gambacorta, and M. de Rosa, "Calditol tetraether lipids of the

archaebacterium *Sulfolobus solfataricus*. Biosynthetic studies," *Biochemical Journal*, vol. 266, no. 3, pp. 785–791, 1990.

[49] A. Corcelli, "The cardiolipin analogues of *Archaea*," *Biochimica et Biophysica Acta*, vol. 1788, no. 10, pp. 2101–2106, 2009.

[50] M. Häring, X. Peng, K. Brügger et al., "Morphology and genome organization of the virus PSV of the hyperthermophilic archaeal genera *Pyrobaculum* and *Thermoproteus*: a novel virus family, the *Globuloviridae*," *Virology*, vol. 323, no. 2, pp. 233–242, 2004.

[51] M. Rettenberger, *Das Virus TTV1 des extreme thermophilen Schwefel-Archaebacteriums Thermoproteus tenax: Zusammensetzung und Structur [Ph.D. thesis]*, Ludwig-Maximillians-Universität, Munich, Germany, 1990.

[52] D. Janekovic, S. Wunderl, and I. Holz, "TTV1, TTV2 and TTV3, a family of viruses of the extremely thermophilic, anaerobic, sulfur reducing archaebacterium *Thermoproteus tenax*," *Molecular and General Genetics*, vol. 192, no. 1-2, pp. 39–45, 1983.

[53] M. Bettstetter, X. Peng, R. A. Garrett, and D. Prangishvili, "AFV1, a novel virus infecting hyperthermophilic *Archaea* of the genus *Acidianus*," *Virology*, vol. 315, no. 1, pp. 68–79, 2003.

[54] H. P. Arnold, W. Zillig, U. Ziese et al., "A novel lipothrixvirus, SIFV, of the extremely thermophilic crenarchaeon *Sulfolobus*," *Virology*, vol. 267, no. 2, pp. 252–266, 2000.

[55] C. Bath, T. Cukalac, K. Porter, and M. L. Dyall-Smith, "His1 and His2 are distantly related, spindle-shaped haloviruses belonging to the novel virus group, *Salterprovirus*," *Virology*, vol. 350, no. 1, pp. 228–239, 2006.

[56] N. S. Atanasova, E. Roine, A. Oren, D. H. Bamford, and H. M. Oksanen, "Global network of specific virus-host interactions in hypersaline environments," *Environmental Microbiology*, vol. 14, no. 2, pp. 426–440, 2012.

[57] G. Rice, L. Tang, K. Stedman et al., "The structure of a thermophilic archaeal virus shows a double-stranded DNA viral capsid type that spans all domains of life," *Proceedings of the National Academy of Sciences of the United States of America*, vol. 101, no. 20, pp. 7716–7720, 2004.

[58] L. J. Happonen, P. Redder, X. Peng, L. J. Reigstad, D. Prangishvili, and S. J. Butcher, "Familial relationships in hyperthermo- and acidophilic archaeal viruses," *Journal of Virology*, vol. 84, no. 9, pp. 4747–4754, 2010.

[59] X. Xiang, L. Chen, X. Huang, Y. Luo, Q. She, and L. Huang, "*Sulfolobus tengchongensis* spindle-shaped virus STSV1: virus-host interactions and genomic features," *Journal of Virology*, vol. 79, no. 14, pp. 8677–8686, 2005.

[60] H. Sagami, A. Kikuchi, K. Ogura, K. Fushihara, and T. Nishino, "Novel isoprenoid modified proteins in *Halobacteria*," *Biochemical and Biophysical Research Communications*, vol. 203, no. 2, pp. 972–978, 1994.

[61] H. Sagami, A. Kikuchi, and K. Ogura, "A novel type of protein modification by isoprenoid-derived materials. Diphytanylglycerylated proteins in *Halobacteria*," *The Journal of Biological Chemistry*, vol. 270, no. 25, pp. 14851–14854, 1995.

[62] Z. Konrad and J. Eichler, "Lipid modification of proteins in *Archaea*: attachment of a mevalonic acid-based lipid moiety to the surface-layer glycoprotein of *Haloferax volcanii* follows protein translocation," *Biochemical Journal*, vol. 366, no. 3, pp. 959–964, 2002.

[63] M. Häring, R. Rachel, X. Peng, R. A. Garrett, and D. Prangishvili, "Viral diversity in hot springs of Pozzuoli, Italy, and characterization of a unique archaeal virus, *Acidianus* bottle-shaped virus, from a new family, the *Ampullaviridae*," *Journal of Virology*, vol. 79, no. 15, pp. 9904–9911, 2005.

[64] S. Paula, A. G. Volkov, A. N. Van Hoek, T. H. Haines, and D. W. Deamer, "Permeation of protons, potassium ions, and small polar molecules through phospholipid bilayers as a function of membrane thickness," *Biophysical Journal*, vol. 70, no. 1, pp. 339–348, 1996.

[65] Y. Zhai, P. L. Chong, L. J. Taylor et al., "Physical properties of archaeal tetraether lipid membranes as revealed by differential scanning and pressure perturbation calorimetry, molecular acoustics, and neutron reflectometry: effects of pressure and cell growth temperature," *Langmuir*, vol. 28, no. 11, pp. 5211–5217, 2012.

[66] W. D. Reiter, W. Zillig, and P. Palm, "Archaebacterial viruses," *Advances in Virus Research*, vol. 34, pp. 143–188, 1988.

[67] D. Prangishvili, "Family *Fuselloviridae*," in *Virus Taxonomy, Ninth Report of the International Committee on Taxonomy of Viruses*, A. M. Q. King, M. J. Adams, E. B. Carstens, and E. J. Lefkowitz, Eds., pp. 183–186, Elsevier, Oxford, UK, 2011.

[68] D. Prangishvili, "Family *Lipothrixviridae*," in *Virus Taxonomy, Ninth Report of the International Committee on Taxonomy of Viruses*, A. M. Q. King, M. J. Adams, E. B. Carstens, and E. J. Lefkowitz, Eds., pp. 211–221, Elsevier, Oxford, UK, 2011.

[69] M. Häring, G. Vestergaard, K. Brügger, R. Rachel, R. A. Garrett, and D. Prangishvili, "Structure and genome organization of AFV2, a novel archaeal lipothrixvirus with unusual terminal and core structures," *Journal of Bacteriology*, vol. 187, no. 11, pp. 3855–3858, 2005.

[70] W. S. A. Maaty, A. C. Ortmann, M. Dlakić et al., "Characterization of the archaeal thermophile *Sulfolobus* turreted icosahedral virus validates an evolutionary link among double-stranded DNA viruses from all domains of life," *Journal of Virology*, vol. 80, no. 15, pp. 7625–7635, 2006.

[71] C. Y. Fu and J. E. Johnson, "Structure and cell biology of archaeal virus STIV," *Current Opinion in Virology*, vol. 2, no. 2, pp. 122–127, 2012.

[72] S. T. Jaakkola, R. K. Penttinen, S. T. Vilén et al., "Closely related archaeal *Haloarcula hispanica* icosahedral viruses HHIV-2 and SH1 have nonhomologous genes encoding host recognition functions," *Journal of Virology*, vol. 86, no. 9, pp. 4734–4742, 2012.

[73] E. Roine and H. M. Oksanen, "Viruses from the hypersaline environment," in *Halophiles and Hypersaline Environments: Current Research and Future Trends*, Ventosa, A. Oren, and Y. Ma, Eds., pp. 153–172, Springer, Berlin, Germany, 2011.

[74] J. J. B. Cockburn, N. G. A. Abrescia, J. M. Grimes et al., "Membrane structure and interactions with protein and DNA in bacteriophage PRD1," *Nature*, vol. 432, no. 7013, pp. 122–125, 2004.

[75] A. Senčilo, L. Paulin, S. Kellner, M. Helm, and E. Roine, "Related haloarchaeal pleomorphic viruses contain different genome types," *Nucleic Acids Research*, vol. 40, no. 12, pp. 5523–5534, 2012.

[76] L. Kandiba, O. Aitio, J. Helin et al., "Diversity in prokaryotic glycosylation: an archaeal-derived N-linked glycan contains legionaminic acid," *Molecular Microbiology*, vol. 84, no. 3, pp. 578–593, 2012.

[77] R. Montalvo-Rodríguez, R. H. Vreeland, A. Oren, M. Kessel, C. Betancourt, and J. López-Garriga, "*Halogeometricum borinquense* gen. nov., sp. nov., a novel halophilic archaeon from Puerto Rico," *International Journal of Systematic Bacteriology*, vol. 48, no. 4, pp. 1305–1312, 1998.

[78] I. R. Cooke and M. Deserno, "Coupling between lipid shape and membrane curvature," *Biophysical Journal*, vol. 91, no. 2, pp. 487–495, 2006.

[79] L. Adamian, H. Naveed, and J. Liang, "Lipid-binding surfaces of membrane proteins: evidence from evolutionary and structural analysis," *Biochimica et Biophysica Acta*, vol. 1808, no. 4, pp. 1092–1102, 2011.

[80] N. G. A. Abrescia, J. J. B. Cockburn, J. M. Grimes et al., "Insights into assembly from structural analysis of bacteriophage PRD1," *Nature*, vol. 432, no. 7013, pp. 68–74, 2004.

[81] B. Tenchov, E. M. Vescio, G. D. Sprott, M. L. Zeidel, and J. C. Mathai, "Salt tolerance of archaeal extremely halophilic lipid membranes," *The Journal of Biological Chemistry*, vol. 281, no. 15, pp. 10016–10023, 2006.

Hindawi Publishing Corporation
Archaea
Volume 2012, Article ID 138439, 11 pages
doi:10.1155/2012/138439

Review Article

On Physical Properties of Tetraether Lipid Membranes: Effects of Cyclopentane Rings

Parkson Lee-Gau Chong, Umme Ayesa, Varsha Prakash Daswani, and Ellah Chay Hur

Department of Biochemistry, Temple University School of Medicine, 3420 North Broad Street, Philadelphia, PA 19140, USA

Correspondence should be addressed to Parkson Lee-Gau Chong, pchong02@temple.edu

Received 6 July 2012; Accepted 8 August 2012

Academic Editor: Yosuke Koga

This paper reviews the recent findings related to the physical properties of tetraether lipid membranes, with special attention to the effects of the number, position, and configuration of cyclopentane rings on membrane properties. We discuss the findings obtained from liposomes and monolayers, composed of naturally occurring archaeal tetraether lipids and synthetic tetraethers as well as the results from computer simulations. It appears that the number, position, and stereochemistry of cyclopentane rings in the dibiphytanyl chains of tetraether lipids have significant influence on packing tightness, lipid conformation, membrane thickness and organization, and headgroup hydration/orientation.

1. Introduction

Archaea are subdivided into two kingdoms: euryarchaeota and crenarchaeota [1]. Euryarchaeota include methanogens and halophiles, whereas crenarchaeota are traditionally comprised of thermophilic or hyperthermophilic archaea [1]. Halophiles and some methanogens are found mostly in high salt water or hypersaline systems such as natural brines, alkaline salt lakes, and salt rocks; while thermophilic and hyperthermophilic archaea are found in very high temperature environments [2]. In recent years, crenarchaeota have also been found in nonextreme environments such as soil and pelagic areas [3, 4].

The plasma membranes of archaea are rich in tetraether lipids (TLs) and diphytanylglycerol diethers, also known as archaeols (reviewed in [11–13]). TLs are the dominating lipid species in crenarchaeota, particularly in thermoacidophilic archaea (~90–95%). They are also found in methanogens (0–50%) but are virtually absent in halophiles. Archaeal TLs contain either a caldarchaeol (GDGT) or a calditoglycerocaldarchaeol (GDNT) hydrophobic core (Figure 1) [13–17]. GDGT has two glycerols at both ends of the hydrophobic core. GDNT has a glycerol backbone at one end of the hydrophobic core and the calditol group at the other end. Typically, TLs in methanogens contain only GDGT, but TLs in thermoacidophiles, particularly in the members of the order *Sulfolobales*, have both GDGT and GDNT components. The *Metallosphaera sedula TA-2* strain from hot springs in Japan, which has only GDGT-based lipids, is an exception [18]. TLs have been thought to play an important role in the thermoacidophile's high stability against extreme growth conditions such as high temperatures (e.g., 65-90°C) and acidic environments (e.g., pH 2-3) [19]. However, more recent studies showed that GDGT-based TLs are also abundant in nonextremophilic crenarchaeota present in marine environments, lakes, soils, peat bogs, and low temperature areas [20, 21]. The functional role of tetraether lipids in crenarchaeota is not fully understood.

The hydrophobic core of archaeal TLs is made of dibiphytanyl hydrocarbon chains, which may contain up to 8 cyclopentane rings per molecule (reviewed in [13]). The number of cyclopentane rings increases as growth temperature increases [22–25], but decreases with decreasing pH in growth media [26]. The presence of cyclopentane rings is a structural feature unique for archaeal tetraether lipids. Therefore, it is of great interest to unravel its biological roles.

Various polar headgroups can be attached to the glycerol and calditol backbones and yield either monopolar or bipolar

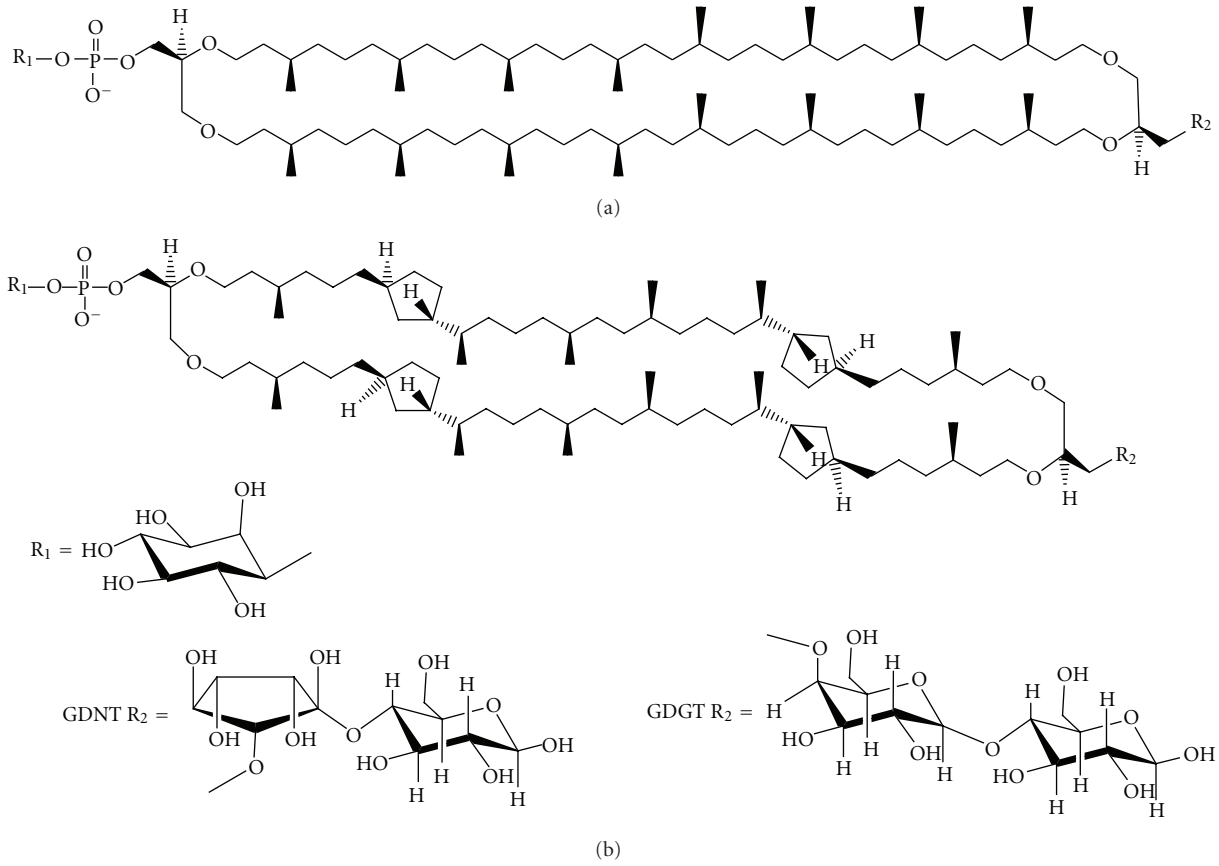

Figure 1: Illustrations of the molecular structures of the bipolar tetraether lipids in the polar lipid fraction E (PLFE) isolated from *S. acidocaldarius*. PLFE contains (a) GDGT (or caldarchaeol) and (b) GDNT (or calditolglycerocaldarchaeol). The number of cyclopentane rings in each biphytanyl chain can vary from 0 to 4. The different head groups of GDNT and GDGT are presented at the bottom. GDG(N)T-0 and GDG(N)T-4 contain 0 and 4 cyclopentane rings per molecule, respectively (taken from [5], reproduced with permission).

tetraether (BTL) lipids. Archaeal BTLs are glycolipids or phosphoglycolipids (illustrated in Figure 1). Liposomes that are made of BTLs containing two or more sugar moieties exhibit lower proton permeability than those containing only one sugar molecule [26]. It has been proposed that thermoacidophilic archaea cells adapt to low pH and high temperature by increasing the number of sugar moieties and cyclopentane rings [26, 27]. Increasing the number of cyclopentane rings tightens membrane packing (discussed later) [27]. Sugar moieties and the phosphate group in the BTL polar headgroup regions interact with each other to form a strong hydrogen bond network at the membrane surface [28].

BTLs are unique to archaea and cannot be biosynthesized by eukaryotic or bacterial cells. The ether formation from glycerol has been studied to a great extent ([29] and references cited therein). The calditol moiety of GDNTs can be synthesized via an aldol condensation between dihydroxyacetone and fructose [30]. Calditol is then reduced and alkylated to form GDNTs [30]. An *in vitro* study showed that with the aid of 1L-*myo*-inositol 1-phosphate synthase, archaetidylinositol phosphate (AIP) synthase and AIP-phosphatase, archaeal inositol phospholipid (see Figure 1 e.g.) can be formed from CDP-archaeol and D-glucose-6-phosphate via *myo*-inositol-1-phosphate and AIP [31]. It has been proposed that the cyclopentane rings in BTLs of *Sulfolobus* are synthesized from glucose by a "cyclase" enzyme of the calditol carbocycle [32].

In this paper we focus on the recent findings related to the physical properties of tetraether lipid membranes, with special attention on the effects of the number, position, and configuration of cyclopentane rings on membrane properties. We discuss the findings obtained from model membranes composed of naturally occurring archaeal tetraether lipids and synthetic tetraethers as well as the results from computer simulations.

2. Physical Properties of Model Membranes Composed of Thermoacidophilic Tetraether Lipids

2.1. Membranes Made of Total Polar Lipid Extracts. The stability and physical properties of liposomes made from

the total polar lipids (TPLs) extracted from archaea have been studied extensively (reviewed in [11, 12, 33, 34]). TPL extracts contain both diether and tetraether lipids. The general trend shows that membranes become more stable as the mole fraction of tetraether lipids increases. As an example, liposomes made of diether lipids such as *Methanosarcina mazei* TPL (0 wt% in caldarchaeols) were unstable against simulated human bile while those made of TPL from *Methanobacterium espanolae* (65% in caldarchaeols) and *Thermoplasma acidophilum* (90% in caldarchaeols) were relatively more stable [35]. Solute and water permeability also decrease as the content of tetraether lipids in membranes made with archaeal TPLs increases [36].

Sprott et al. [37] demonstrated that liposomes made with TPL from the archaeon *M. smithii AL1* can be highly fusogenic when exposed to low pH and α- and β-glucosidases. It was suggested that, at low pH (4.8), the positively charged glucosidases interact with the anionic phospholipids in *M. smithii* TPL, which in turn causes archaeosomes to rapidly aggregate [37]. Aggregation is a prerequisite for membrane fusion. This result is somewhat surprising because previous studies showed that tetraether liposomes are resistant to fusogenic compounds [38–40]. Since TPL of *M. smithii AL1* contains a significant amount of diethers, in addition to caldarchaeols (~40 wt %), it is possible that the strong fusogenic activity mentioned above comes from the diether component.

2.2. Membranes Made of Partially Purified Tetraether Lipid Fractions. Since tetraethers are the dominating lipid species in thermoacidophiles, and the presence of diethers in the total polar lipid extracts makes the data interpretation more difficult, it is of biophysical interest to study membranes made only with tetraether lipids. The physical properties of lipid membranes made of partially purified polar lipid fractions from the archaeon *Sulfolobus solfataricus* have been reviewed [11, 34]. In this section, we focus on the recent studies of membranes made of partially purified polar lipid fractions isolated from the archaeon *Sulfolobus acidocaldarius*.

2.2.1. PLFE. The polar lipid fraction E (PLFE) is one of the major bipolar tetraether lipids (BTLs) found in the thermoacidophilic archaeon *S. acidocaldarius* [41, 42]. PLFE is a mixture of GDNT and GDGT (Figure 1). The GDNT component (~90% of total PLFE) contains phospho-*myo*-inositol on the glycerol end and β-glucose on the calditol end, whereas the GDGT component (~10% of total PLFE) has phospho-*myo*-inositol attached to one glycerol and β-D-galactosyl-D-glucose to the other glycerol skeleton (Figure 1). The nonpolar regions of these lipids consist of a pair of 40-carbon biphytanyl chains, each of which may contain up to four cyclopentane rings [22].

2.2.2. PLFE Liposomes. PLFE lipids can form stable unilamellar (~60–800 nm in diameter), multilamellar, and giant unilamellar (~10–150 μm) vesicles [40, 41, 43]. The lipids in these vesicles span the entire lamellar structure, forming a monomolecular thick membrane [44], which contrasts to the bilayer structure formed by monopolar diester (or diether) phospholipids. Compared to liposomes made of diester or diether lipids, PLFE liposomes exhibit extraordinary membrane properties (reviewed in [11, 12, 34]). PLFE liposomes exhibit low proton permeability and dye leakage [45, 46], high stability against autoclaving and Ca^{2+}-induced vesicle fusion [40, 47], tight and rigid membrane packing [43], and low enthalpy and volume changes associated with the phase transitions [48, 49].

It is known that a decrease in archaeal cell growth temperature (T_g) decreases the number of cyclopentane rings in archaeal TLs [22]. In the case of *S. acidocaldarius*, the average number of cyclopentane rings per tetraether lipid molecule decreases from 4.8 to 3.4 when T_g drops from 82°C to 65°C [23]. Recent experimental work (see below) has addressed the effect of T_g, inferentially the number of cyclopentane rings, on the physical properties of tetraether lipid membranes.

2.2.3. Effect of Cyclopentane Rings on Phase Behavior of PLFE Liposomes. The phase behavior of PLFE liposomes has been characterized by small angle X-ray scattering, infrared and fluorescence spectroscopy, and differential scanning calorimetry (DSC). PLFE liposomes exhibit two thermally-induced lamellar-to-lamellar phase transitions at ~47–50°C and ~60°C [34, 43, 48, 49] and a lamellar-to-cubic phase transition at ~74–78°C [48, 49] all of which involve small or no volume changes as revealed by pressure perturbation calorimetry (PPC) [49]. The calorimetry experiments also suggested that the number of cyclopentane rings in the dibiphytanyl chains affect membrane packing in PLFE liposomes because the liposomes derived from different cell growth temperatures showed different thermodynamic properties [49]. DSC allows us to determine the enthalpy change (ΔH) of the phase transition. PPC, on the other hand, allows us to determine the relative volume change ($\Delta V/V$) at the phase transition and the thermal expansivity coefficient (α) at each temperature.

For PLFE liposomes derived from cells grown at 78°C, the DSC heating scan exhibited an endothermic transition at 46.7°C, which can be attributed to a lamellar-to-lamellar phase transition and has an unusually low ΔH (3.5 kJ/mol), when compared to that for the main phase transitions of saturated diacyl monopolar diester lipids (e.g., 1,2-dimyristoyl-*sn*-glycero-3-phosphocholine, DMPC). The PPC scan revealed that, at this same phase transition, the relative volume change ($\Delta V/V$) in the membrane is very small (~0.1%) and much lower than the $\Delta V/V$ value 2.8% for the main phase transition of DMPC. The low ΔH and $\Delta V/V$ values may arise from the restricted *transauche* conformational changes in the dibiphytanyl chain due to the presence of cyclopentane rings, branched methyl groups, and to the spanning of the lipid molecules over the whole membrane [49].

For PLFE liposomes derived from cells with growth temperature of 65°C, similar DSC and PPC profiles were obtained. However, the lower cell growth temperature

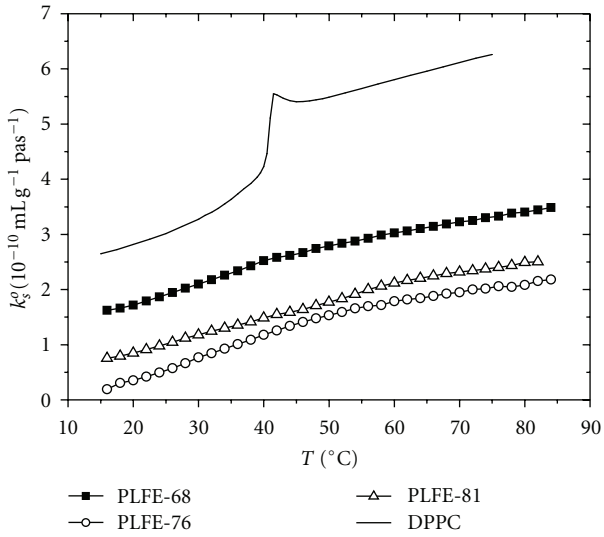

Figure 2: Adiabatic compressibilities (k_S^o) of PLFE liposomes derived from cells grown at three different temperatures: 68°C (dark squares), 76°C (open circles), and 81°C (open triangles). Solid line: DPPC liposomes for comparison (taken from [6], reproduced with permission).

yielded a higher $\Delta V/V$ (~0.25%) and ΔH (14 kJ/mol) value for the lamellar-to-lamellar phase transition measured at pH 2.1. The lower growth temperature also generated less negative temperature dependence of α. The changes in $\Delta V/V$, ΔH, and the temperature dependence of α can be attributed to the decrease in the number of cyclopentane rings in PLFE due to the lower growth temperature [49]. A decrease in the number of cyclopentane rings makes the membrane less tight and less rigid; thus, a higher $\Delta V/V$ value is shown through the phase transition.

2.2.4. Effect of Cyclopentane Rings on Compressibility and Membrane Volume Fluctuations of PLFE Liposomes. The isothermal and adiabatic compressibility and relative volume fluctuations of PLFE liposomes have been determined by using calorimetry (DSC and PPC) and molecular acoustics (ultrasound velocimetry and densimetry) [50]. The compressibility values of PLFE liposomes were low, compared to those found in a gel state of 1,2-dipalmitoyl-*sn*-glycero-3-phosphocholine (DPPC) [50]. Relative volume fluctuations of PLFE liposomes at any given temperature examined were 1.6–2.2 times more damped than those found in DPPC liposomes [50]. Volume fluctuations are closely related to solute permeation across lipid membranes [51] and lateral motion of membrane components [52]. Thus, the low values of relative volume fluctuations explain why PLFE liposomes exhibit unusually low proton permeation and dye leakage [45, 46] as well as limited lateral mobility, especially at low temperatures (e.g., <26°C) [43, 53].

Zhai et al. [6] have used the growth temperature T_g to alter the structure of PLFE lipids. They determined the compressibilities and volume fluctuations of PLFE liposomes derived from different cell growth temperatures (T_g = 68, 76, and 81°C). The compressibility and volume fluctuation values of PLFE liposomes exhibit small but significant differences with T_g. Figure 2 shows that adiabatic compressibility (k_S^o) of PLFE liposomes changes significantly with T_g: $k_S^o(T_g = 68°\mathrm{C}) > k_S^o(T_g = 81°\mathrm{C}) > k_S^o(T_g = 76°\mathrm{C})$. For isothermal compressibility (k_T^o), isothermal compressibility coefficient (β_T) and relative volume fluctuations, a similar, but somewhat different, trend is seen: (T_g = 68°C) > (T_g = 81°C) ≥ or ≈ (T_g = 76°C). These data indicate that, among the three employed growth temperatures, the growth temperature 76°C leads to the least compressible, and inferentially the most tightly packed PLFE lipid membranes. Note that 76°C is in the temperature range for optimal growth of *S. acidocaldarius* (75–80°C, [54, 55]). This finding suggests that membrane packing in PLFE liposomes may actually vary with the number of cyclopentane rings in a nonlinear manner, reaching maximal tightness when the tetraether lipids are derived from cells grown at the optimal growth temperatures [6].

2.2.5. Future Studies of Physical Properties of Tetraether Lipid Membranes. PLFE is a mixture of GDNT- and GDGT-derived BTLs with varying numbers of cyclopentane rings. Furthermore, at any given growth temperature, there is always a broad distribution of the number of cyclopentane rings. In order to gain more insight into the effect of cyclopentane rings on compressibility and membrane volume fluctuations, it will be necessary to use purified archaeal BTLs with a well-determined number and location of cyclopentane rings. It has been reported that intact polar lipids (archaeols (diethers) and caldarchaeols (GDGT)) of the archaeon *Thermoplasma acidophilum* can be separated with single cyclopentane ring resolution by high-performance liquid chromatography (HPLC) as detected by evaporative light-scattering detection [26, 56]. However, the study by Shimada et al. on *T. acidophilum* was limited to GDGT-based BTLs. To separate intact archaea BTLs at single cyclopentane ring resolution when both GDNT- and GDGT-derived BTLs are present remains a major challenge.

Hydrolyzed BTLs can also be separated with single cyclopentane ring resolution using normal phase HPLC and positive ion atmospheric pressure chemical ionization mass spectrometry [7]. Figure 3 shows the structures of the cyclopentane-containing GDGT hydrophobic cores previously identified from the archaeon *Sulfolobus solfataricus*. These structures were determined by mass spectrometry. Compounds F′ and G′ (Figure 3) were reported as minor components in *S. solfataricus* [7]. The relative distribution of these GDGT structures varies from species to species. The GDGT fraction of *S. solfataricus* is dominated by those structures with one (Structures E and G, Figure 3) or two (F) biphytanyl chains with two cyclopentane rings. The distribution of GDGTs in the extract of the archaeon *M. sedula* is somewhat different. In this case, the distribution is dominated by structures containing one or two biphytanyls with one cyclopentane ring. Physical properties of liposomes made of hydrolyzed BTLs (without sugar and phosphate

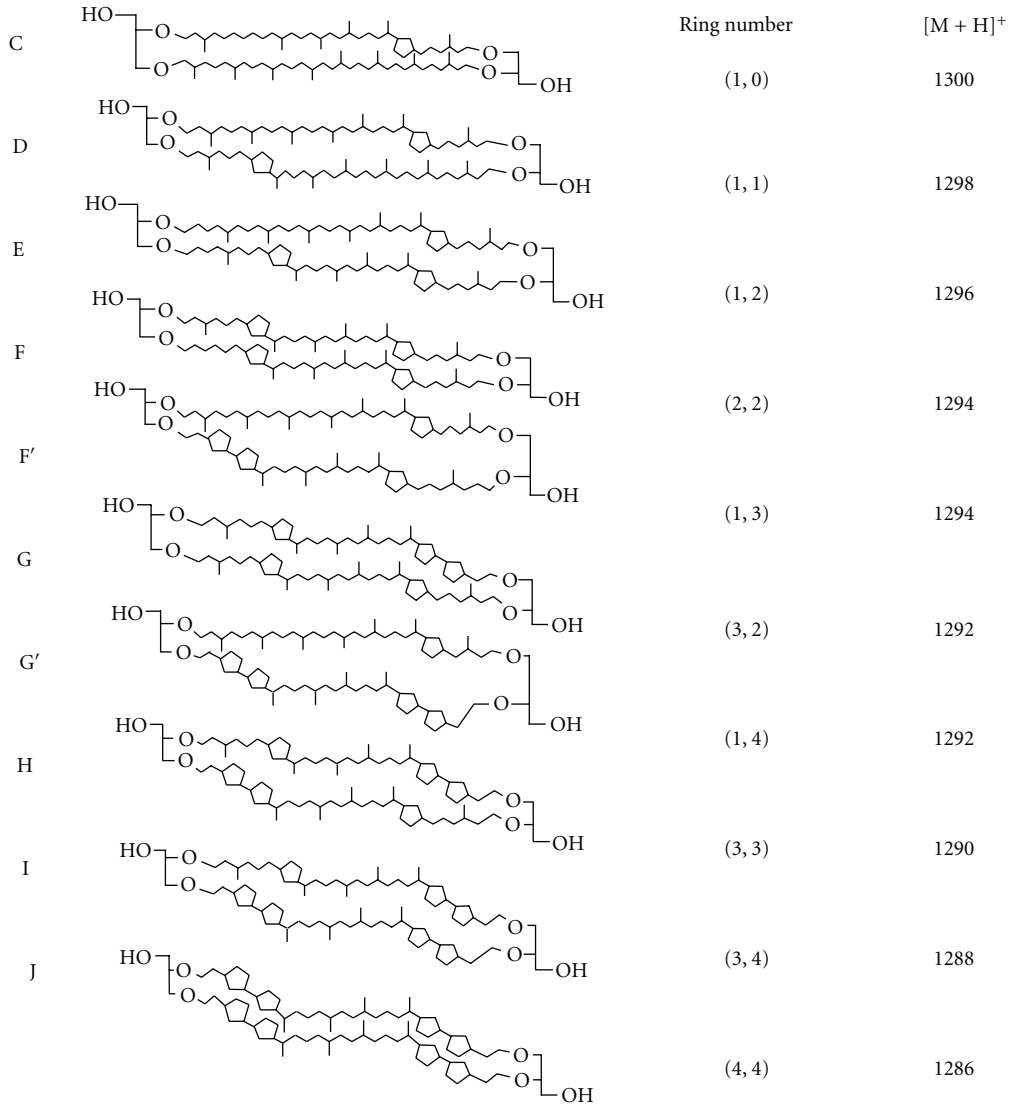

Figure 3: Structures of cyclopentane ring containing GDGTs previously reported to exist in archaea [7]. The number of cyclopentane rings in the first and second hydrocarbon chains is indicated in the parentheses. The mass-to-charge ratio (m/z) of the protonated form $[M+H]^+$ for each structure is also listed.

moieties) are not expected to be the same as those obtained from the liposomes made of intact BTLs [47].

2.2.6. Disruption of PLFE Liposome Stability. While BTL liposomes (such as PLFE liposomes) exhibit remarkable stability against a number of chemical and physical stressors as mentioned above, their stability can be attenuated or abolished under certain conditions. The most striking finding in this regard is that PLFE liposomes become excessively disrupted by the presence of two archaeal proteins, namely, CdvA and ESCRT-III (ESCRT: endosomal sorting complex required for transport) [57]. CdvA is a membrane interacting protein that forms structures at mid-cell prior to nucleoid segregation. CdvA recruits ESCRT-III to membranes in order to aid in the final steps of cell division in some species of archaea. Negative stain electron microscopy revealed extensive deformation of PLFE liposomes in the presence of both CdvA and ESCRT-III together, but not individually [57]. The molecular mechanism underlying this disruption is not clear.

PLFE liposomes are "autoclavable." However, low pH (<4) and low salt concentrations (<50 mM) are unfavorable for autoclaving PLFE-based liposomes [47]. PLFE liposomes and PLFE-based stealth liposomes (e.g., 95 mol% PLFE, 3 mol% 1,2-distearoyl-*sn*-glycerol-3-phosphoethanolamine-polyethylene glycols (2000) (DSPE-PEG(2000)) and 2 mol% DSPE-PEG(2000)-maleimide) are extraordinarily stable against autoclaving between pH 4–10 [47]. These liposomes retained their particle size and morphology against multiple autoclaving cycles. One autoclaving cycle refers to the incubation of a sample for 20 min at 121°C under a steam

pressure of ~18 psi. However, at pH 2-3, one or two autoclaving cycles appeared to disrupt these liposomal membranes, causing a significant increase in particle size [47]. PLFE liposomes were more resistant to dye leakage than the gel state of conventional diester liposomes under high salt and autoclaving conditions. As the salt concentration was decreased from 160 to 40 mM, the percent of dye molecules that leaked out from PLFE-based stealth liposomes after one autoclaving cycle increased from 10.8% to 56.3% [47].

As expected, PLFE-based liposomes can also be disrupted by surfactants. The effect of the surfactant n-tetradecyl-β-D-maltoside (TDM) on unilamellar vesicles composed of PLFE and POPC (1-palmitoyl-2-oleoyl-sn-glycero-3-phosphocholine, a monopolar diester lipid) has been examined [58]. TDM disrupts the POPC/cholesterol vesicles effectively; however, higher concentrations (~10 times) of TDM were required to disrupt PLFE/POPC vesicles.

2.2.7. Structural and Packing Properties of PLFE Monolayer Films Spread at the Interface between Air and Water. Effects of cell growth temperature, subphase temperature and pH, and lateral film pressure on PLFE lipid monolayers at the air-water interface have been examined using X-ray reflectivity (XRR) and grazing incidence X-ray diffraction (GIXD) [5]. XRR and GIXD determine the vertical and horizontal structure of the monolayers, respectively.

For PLFE derived from cells grown at 76°C, a total monolayer thickness of ~30 Å was found in the XRR measurements for all monolayers studied. This finding suggests that both head groups of a U-shaped conformation of the molecules are in contact with the subphase and that a single hydrocarbon chain region is protruded into the air. Similar U-shaped monolayer structures have been reported in other tetraether lipid membranes [59]. However, some other studies [60, 61] suggest that the U-shaped and the upright conformations may coexist in the monolayer at the same time or occur sequentially after spreading the TL lipids at the water-air interface.

At the subphase temperatures 10°C and 20°C, large, highly crystalline domains were observed by GIXD; and the thickness of the crystalline part of the monolayer is slightly larger than 30 Å, which indicates a tight packing of the whole lipid monolayer, including both the hydrocarbon chain and the head group regions. The area per hydrocarbon chain of PLFE (~19.3 Å^2) found by GIXD is significantly smaller than that of DPPC (~23.2 Å^2) or 1,2-dipalmitoyl-*sn*-glycero-3-phosphoglycerol (DPPG) (~22.6 Å^2). In fact, both the two hydrocarbon chains of a single PLFE lipid and the chains of neighbouring lipid molecules adopted an extremely tight packing.

For PLFE lipids derived from cells grown at higher temperatures, a slightly more rigid structure in the lipid dibiphytanyl chains was observed. However, the growth temperature, inferentially the number of cyclopentane rings, does not affect the parameters of the unit cell in GIXD measurements. This suggests that there exists a nearly identical crystalline packing of all the PLFE lipids examined and that, at high film pressures, membrane packing is primarily governed by the lipid headgroup region [5]. It is interesting to mention that the lack of cyclopentane rings in the bipolar tetraether lipids from *M. hungatei* has been suggested to be the cause of the U-shaped configuration adopted by these lipids in the monolayer film at the air-water interface [62]. Apparently, the presence of cyclopentane rings would hinder the dibiphytanyl hydrocarbon chains from bending to form the U-shaped configuration.

3. Physical Properties of Membranes Made of Synthetic Tetraether Lipids

The process of isolating well-defined archaeal tetraether lipids can be difficult and time consuming. In addition, archaeal tetraether lipids have several structural features distinctly different from conventional diester lipids. Therefore, it is rather difficult to elucidate the structure-activity relationship for each of the individual structural features when using native archaeal lipids. To resolve these problems to some extent, synthetic tetraether lipid analogues have been used [63–67].

3.1. Importance of the Stereochemistry of the Cyclopentane Ring. Jacquemet et al. were able to study the effect of the stereochemistry of the cyclopentane ring on BTL membrane properties by using two synthetic tetraether lipids [8, 9] (Compounds 1 and 2 in Figure 4). Both lipids have a bridging hydrocarbon chain with a single 1,3-disubstituted cyclopentane ring at the center. The substitutes on the ring are ether-linked to C3 of the two opposite glycerol moieties, while C2 of the glycerols is ether-linked to a phytanyl chain and C1 is linked to a lactosyl polar headgroup (Figure 4). The only difference between these two isomers is the configuration (*cis or trans*) of the 1,3-disubstituted cyclopentane ring [8, 9].

The *trans*-isoform showed multilamellar vesicles whereas the *cis*-counterpart led to nonspherical nanoparticles, as revealed by cryo-transmission electron microscopy [8]. Small angle X-ray scattering (SAXS) studies further showed that the *cis*-isomer exhibited L_c-L_α-Q_{II} (cystal, lamellar, and bicontinuous cubic phase (Pn3 m), resp.) phase transitions whereas the *trans*-isomer remained in L_α phase from 20 to 100°C. The electron density profiles calculated from the SAXS data were consistent with a stretched conformation of these synthetic BTLs within the L_α phase [9]. The difference in the phase behaviors was attributed to the conformation equilibrium of 1,3-disubstituted cyclopenatne rings. The dominant conformational motion in cyclopentane is pseudorotational [68]. Pseudorotation is more restricted for the *trans*-isomer whereas several more orientations of the two substituents on the ring can be created for the *cis*-1,3-dialkyl cyclopentane ring [9, 68, 69]. Even though this study shows that the stereochemistry at the cyclopentane ring has a dramatic influence on membrane properties, more work is still required in order to explain why liposomes made of PLFE, which naturally occurs and contains *trans*-1,3-disubstituted cyclopentyl rings, can undergo the L_α-to-Q_{II} phase transition [48, 49], while the synthetic *trans*

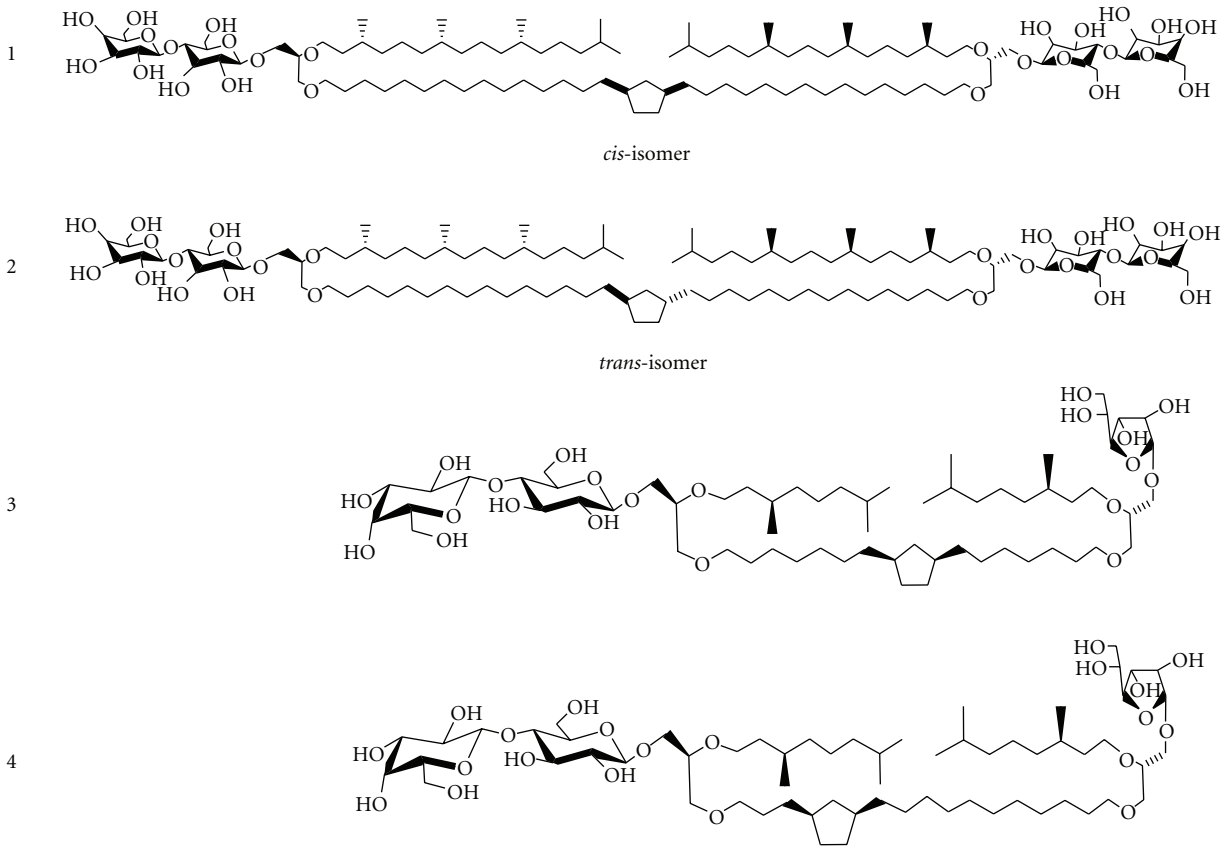

Figure 4: Synthetic tetraether lipids that have been used to study the effect of configuration (Compounds 1 and 2 [8, 9]) and position (Compounds 3 and 4 [10]) of the cyclopentane rings on membrane properties.

BTL (Figure 4) cannot [9]. Note that the placement and the number of cyclopentane rings are different between PLFE lipids (Figure 1) and the synthetic BTLs mentioned above (Figure 4). Apparently, BTLs with subtle differences in chemical structures can display distinctly different phase behaviors.

The difference in the polar headgroups between PLFE and the above-mentioned synthetic BTLs also leads to other subtle structural differences. The *d*-spacing of PLFE liposomes increases with increasing temperature [48], which is contrary to that obtained from the synthetic *trans*-isomer mentioned above (Compound 2 in Figure 4) [9]. The increased *d*-spacing with temperature is probably due to an increase in hydration at the polar headgroup of PLFE [48]. For unknown reasons, there is no change in hydration at the polar (lactosyl) headgroups in those two synthetic stereoisomers [9].

3.2. Influence of the Position of the Cyclopentane Ring. Brard et al. studied the effect of the position of the cyclopentane ring on physical properties of tetraether lipid membranes [66]. They synthesized two tetraether glycolipids, each of which contains a single *cis*-1,3-disubstituted cyclopentane ring in the bridging chain. One glycolipid contained a cyclopentane ring in the middle of the bridging chain while the other had one at three methylene units from the glycerol backbone (Compound 3 and 4 in Figure 4). This helped them determine the influences of the different positions of the cyclopentane ring.

The cyclopentane ring position appears to have a profound impact on hydration properties, lyotropic liquid crystalline behavior, and membrane organization [66]. Moreover, the synthetic BTL with the cyclopentane ring positioned at the center (Compound 3 in Figure 4) can be completely dispersed in water, and it can form sponge-like structures as revealed by electron microscopy. In contrast, the compound with the cyclopentane ring away from the center (Compound 4 in Figure 4) can only be partitially dispersed in water and it forms multilamellar vesicles. It has been suggested that the position of the cyclopentane ring in the bridging chain influences the orientation of the glycosidic polar headgroups attached to the glycerol backbone, which leads to different membrane organizations [66].

4. Membrane Properties Revealed by Computer Simulations

4.1. Effect of Cyclopentane Rings on Membrane Packing and Headgroup Orientation. An increase in growth temperature is known to increase the number of cyclopentane rings in the dibiphytanyl chains of archaeal lipids [23]. The number of cyclopentane rings may vary from 0 to 4 in each biphytanyl

chain (i.e., 0 to 8 per dibiphytanyl unit). To evaluate how the number of cyclopentane rings might affect membrane packing, Gabriel and Chong have conducted molecular modeling studies on a membrane containing 4×4 GDNT molecules (with sugar moieties, Figure 1) [27]. It was found that when 8 cyclopentane rings are contained, the headgroup of GDNT runs almost parallel to the membrane surface. However, without containing any rings, the headgroup is oriented perpendicular to the membrane surface. The molecular modeling further showed that an increase in the number of cyclopentane rings in the dibiphytanyl chains of GDNT from 0 to 8 made GDNT membrane packing tighter, more rigid, and more negative in interaction energy (-156.5 kcal/mol for 0 cyclopentane ring to -191.6 kcal/mol with 8 rings [27]). The resulting energy lowering effect is neither due to the decrease in polar headgroup separation, nor the change in the van der Waals interactions. Instead, it is due to the more favorable hydrogen bonding, and bonded interactions including harmonic bending, theta expansion bond angle bending, dihedral angle torsion, and inversion [27].

4.2. Effect of Macrocyclic Linkage on Membrane Properties. Most archaeal BTLs are macrocyclic molecules with two biphytanyl hydrocarbon chains linked to two opposite glycerol or calditol backbones (illustrated in Figure 1 for the case of PLFE). The effect of the macrocyclic linkage on membrane properties has been studied by molecular dynamics simulations [10, 70, 71]. For simplicity, coarse graining approaches were employed and BTL molecules were modeled as di-monopolar lipids such as di-DPPC [10] and diphytanyl phosphatidylcholine (DPhPC) [70]. In essence, two monopolar molecules were tethered together either at one pair of the hydrocarbon chains (acyclic di-DPPC or di-DPhPC) or at both pairs (cyclic di-DPPC or di-DPhPC). The simulations showed that in the membranes composed of macrocyclic BTL-like molecules, the upright configuration gains favor over the U-shaped configuration [70]. The macrocyclic linkage also leads to a condensing effect on the membrane surface, increases the order of the lipid hydrocarbon chains, slows lateral mobility in the membrane, and increases membrane thickness [10, 70, 71]. Furthermore, the molecular dynamics simulations made by the dissipative particle dynamics method [71] revealed the formation of two types of membrane pores. Hydrophobic pores are unstable and transient and exist at the low temperature. Hydrophilic pores are more stable with much longer lifetimes and are observed at high temperatures. The simulation data [71] suggested that hydrophilic pores can lead to the rupture of membrane vesicles. More intriguingly, it was proposed that hydrophobic pores, which occur at low temperatures, may result in the permeation of encapsulated small molecules [71]. This implies that although BTL membranes are extremely stable and tightly packed, some small leakage of entrapped molecules can still occur due to either the formation of hydrophobic pores [71] or membrane volume fluctuations [6, 50] (discussed earlier).

5. Applications of Tetraether Lipid Membranes

The extraordinary stability of tetraether lipid membranes against a variety of physical and biochemical stressors has provided the basis for using these lipids to develop technological applications. BTLs can be used as a stable lipid matrix for biosensors [72], a light harvesting device [73], and nanoparticles for targeted imaging and therapy (reviewed in [12, 74]).

It has been proposed that liposomes made of archaeal lipids (also called archaeosomes) are taken up via a phagocytosis receptor in the plasma membrane of the target cells [75]. This uptake occurs in a liposomal composition-dependent manner [75]. Total polar lipids from the archaeon, *Halobacterium salinarum CECT 396*, have been used to make archaeosomes and archaeosomal hydrogels as a possible topical delivery system for antioxidants [76]. Compared to conventional liposomes, those archaeosomes and archaeosomal hydrogels showed better stability and more sustained drug release [76]. It is of interest to extend their study from diethers (abundant in *Halobacterium salinarum CECT 396*) to tetraether lipids (e.g., PLFE lipids isolated from thermoacidophiles). BTL-based liposomes are suitable for oral delivery of therapeutic agents because BTL liposomes are stable against the harsh conditions (such as bile salts, pancreatic enzymes, and low pH) in the gastrointestinal tract [77]. Tetraether lipid membranes have also been tailored and evaluated as an intranasal peptide delivery vehicle [78]. PEGylated tetraether lipids have been synthesized and tested for their stability in test tubes and for liposomal encapsulation potential [79]. Knowledge gained from the physical studies of cyclopentane rings, sugar moieties, and macrocyclic structures should help to optimize the numerous potential applications.

Abbreviations

AIP: archaetidylinositol phosphate
BTL: bipolar tetraether lipids
DMPC: 1,2-dimyristoyl-*sn*-glycero-3-phosphocholine
DPhPC: 1,2-di-O-phytanyl-*sn*-glycero-3-phosphocholine
DPPC: 1,2-dipalmitoyl-*sn*-glycero-3-phosphocholine
DPPG: 1,2-dipalmitoyl-*sn*-glycero-3-phosphoglycerol
DSC: differential scanning calorimetry
DSPE-PEG: 1,2-distearoyl-*sn*-glycerol-3-phosphoethanolamine-polyethylene glycols
ESCRT: endosomal sorting complex required for transport
GDGT: caldarchaeol
GDNT: calditoglycerocaldarchaeol
GIXD: grazing incidence X-ray diffraction
HPLC: high-performance liquid chromatography
PLFE: polar lipid fraction E

POPC: 1-palmitoyl-2-oleoyl-*sn*-glycero-3-phosphocholine
PPC: pressure perturbation calorimetry
TDM: n-tetradecyl-β-D-maltoside
TL: tetraether lipids
TPL: total polar lipids
XRR: X-ray reflectivity.

Acknowledgment

Financial support from the NSF (DMR-1105277) is gratefully acknowledged.

References

[1] C. R. Woese, O. Kandler, and M. L. Wheelis, "Towards a natural system of organisms: proposal for the domains Archaea, Bacteria, and Eucarya," *Proceedings of the National Academy of Sciences of the United States of America*, vol. 87, no. 12, pp. 4576–4579, 1990.

[2] A. S. Andrei, H. L. Banciu, and A. Oren, "Living with salt: metabolic and phylogenetic diversity of archaea inhabiting saline ecosystems," *FEMS Microbiology Letters*, vol. 330, no. 1, pp. 1–9, 2012.

[3] L. A. Powers, J. P. Werne, T. C. Johnson, E. C. Hopmans, J. S. S. Damsté, and S. Schouten, "Crenarchaeotal membrane lipids in lake sediments: a new paleotemperature proxy continental paleoclimate reconstruction?" *Geology*, vol. 32, no. 7, pp. 613–616, 2004.

[4] M. B. Karner, E. F. Delong, and D. M. Karl, "Archaeal dominance in the mesopelagic zone of the Pacific Ocean," *Nature*, vol. 409, no. 6819, pp. 507–510, 2001.

[5] C. Jeworrek, F. Evers, M. Erlkamp et al., "Structure and phase behavior of archaeal lipid monolayers," *Langmuir*, vol. 27, no. 21, pp. 13113–13121, 2011.

[6] Y. Zhai, P. L. G. Chong, L. J. Taylor et al., "Physical properties of archaeal tetraether lipid membranes as revealed by differential scanning and pressure perturbation calorimetry, molecular acoustics, and neutron reflectometry: effects of pressure and cell growth temperature," *Langmuir*, vol. 28, no. 11, pp. 5211–5217, 2012.

[7] E. C. Hopmans, S. Schouten, R. D. Pancost, M. T. van der Meer, and J. S. Sinninghe Damste, "Analysis of intact tetraether lipids in archaeal cell material and sediments by high performance liquid chromatography/atmospheric pressure chemical ionization mass spectrometry," *Rapid Communications in Mass Spectrometry*, vol. 14, no. 7, pp. 585–589, 2000.

[8] A. Jacquemet, L. Lemiegre, O. Lambert, and T. Benvegnu, "How the stereochemistry of a central cyclopentyl ring influences the self-assembling properties of archaeal lipid analogues: synthesis and cryoTEM observations," *Journal of Organic Chemistry*, vol. 76, no. 23, pp. 9738–9747, 2011.

[9] A. Jacquemet, C. Meriadec, L. Lemiegre, F. Artzner, and T. Benvegnu, "Stereochemical effect revealed in self-assemblies based on archaeal lipid analogues bearing a central five-membered carbocycle: a SAXS study," *Langmuir*, vol. 28, no. 20, pp. 7591–7597, 2012.

[10] M. Bulacu, X. Periole, and S. J. Marrink, "In silico design of robust bolalipid membranes," *Biomacromolecules*, vol. 13, no. 1, pp. 196–205, 2012.

[11] P. L.-G. Chong, "Physical properties of membranes composed of tetraether archaeal lipids, ? In," in *Thermophiles*, F. Robb, G. Antranikian, D. Grogan, and A. Driessen, Eds., pp. 73–95, CRC Press, Boca Raton, Fla, USA, 2008.

[12] P. L.-G. Chong, "Archaebacterial bipolar tetraether lipids: physico-chemical and membrane properties," *Chemistry and Physics of Lipids*, vol. 163, no. 3, pp. 253–265, 2010.

[13] Y. Koga and H. Morii, "Recent advances in structural research on ether lipids from archaea including comparative and physiological aspects," *Bioscience, Biotechnology and Biochemistry*, vol. 69, no. 11, pp. 2019–2034, 2005.

[14] A. Sugai, R. Sakuma, I. Fukuda et al., "The structure of the core polyol of the ether lipids from Sulfolobus acidocaldarius," *Lipids*, vol. 30, no. 4, pp. 339–344, 1995.

[15] E. Untersteller, B. Fritz, Y. Blériot, and P. Sinaÿ, "The structure of calditol isolated from the thermoacidophilic archaebacterium Sulfolobus acidocaldarius," *Comptes Rendus de l'Academie des Sciences*, vol. 2, no. 7-8, pp. 429–433, 1999.

[16] A. Gambacorta, G. Caracciolo, D. Trabasso, I. Izzo, A. Spinella, and G. Sodano, "Biosynthesis of calditol, the cyclopentanoid containing moiety of the membrane lipids of the archaeon Sulfolobus solfataricus," *Tetrahedron Letters*, vol. 43, no. 3, pp. 451–453, 2002.

[17] Y. Bleriot, E. Untersteller, B. Fritz, and P. Sinay, "Total synthesis of calditol: structural clarification of this typical component of Archaea order Sulfolobales," *Chemistry*, vol. 8, no. 1, pp. 240–246, 2002.

[18] Y. H. Itoh, N. Kurosawa, I. Uda et al., "Metallosphaera sedula TA-2, a calditoglycerocaldarchaeol deletion strain of a thermoacidophilic archaeon," *Extremophiles*, vol. 5, no. 4, pp. 241–245, 2001.

[19] T. A. Langworthy and J. L. Pond, "Membranes and lipids of thermophiles," in *Thermophiles: General, Molecular, and Applied Microbiology*, T. D. Brock, Ed., pp. 107–134, John Wiley & Sons, New York, NY, USA, 1986.

[20] J. S. SinninghеDamsté, S. Schouten, E. C. Hopmans, A. C. T. Van Duin, and J. A. J. Geenevasen, "Crenarchaeol: the characteristic core glycerol dibiphytanyl glycerol tetraether membrane lipid of cosmopolitan pelagic crenarchaeota," *Journal of Lipid Research*, vol. 43, no. 10, pp. 1641–1651, 2002.

[21] J. W. H. Weijers, S. Schouten, O. C. Spaargaren, and J. S. Sinninghe Damsté, "Occurrence and distribution of tetraether membrane lipids in soils: implications for the use of the TEX86 proxy and the BIT index," *Organic Geochemistry*, vol. 37, no. 12, pp. 1680–1693, 2006.

[22] M. De Rosa, A. Gambacorta, B. Nicolaus, B. Chappe, and P. Albrecht, "Isoprenoid ethers; backbone of complex lipids of the archaebacterium Sulfolobus solfataricus," *Biochimica et Biophysica Acta (BBA)/Lipids and Lipid Metabolism*, vol. 753, no. 2, pp. 249–256, 1983.

[23] M. De Rosa, E. Esposito, A. Gambacorta, B. Nicolaus, and J. D. Bu'Lock, "Effects of temperature on ether lipid composition of Caldariella acidophila," *Phytochemistry*, vol. 19, no. 5, pp. 827–831, 1980.

[24] L. L. Yang and A. Haug, "Structure of membrane lipids and physico-biochemical properties of the plasma membrane from Thermoplasma acidophilum, adapted to growth at 37∘ C," *Biochimica et Biophysica Acta (BBA)/Lipids and Lipid Metabolism*, vol. 573, no. 2, pp. 308–320, 1979.

[25] I. Uda, A. Sugai, Y. H. Itoh, and T. Itoh, "Variation in molecular species of polar lipids from Thermoplasma acidophilum depends on growth temperature," *Lipids*, vol. 36, no. 1, pp. 103–105, 2001.

[26] H. Shimada, N. Nemoto, Y. Shida, T. Oshima, and A. Yamagishi, "Effects of pH and temperature on the composition of

polar lipids in Thermoplasma acidophilum HO-62," *Journal of Bacteriology*, vol. 190, no. 15, pp. 5404–5411, 2008.

[27] J. L. Gabriel and P. Lee Gau Chong, "Molecular modeling of archaebacterial bipolar tetraether lipid membranes," *Chemistry and Physics of Lipids*, vol. 105, no. 2, pp. 193–200, 2000.

[28] M. G. L. Elferink, J. G. de Wit, A. J. M. Driessen, and W. N. Konings, "Stability and proton-permeability of liposomes composed of archaeal tetraether lipids," *Biochimica et Biophysica Acta*, vol. 1193, no. 2, pp. 247–254, 1994.

[29] M. De Rosa, A. Gambacorta, B. Nicolaus, and S. Sodano, "Incorporation of labelled glycerols into ether lipids in Caldariella acidophila," *Phytochemistry*, vol. 21, no. 3, pp. 595–599, 1982.

[30] B. Nicolaus, A. Trincone, E. Esposito, M. R. Vaccaro, A. Gambacorta, and M. De Rosa, "Calditol tetraether lipids of the archaebacterium Sulfolobus solfataricus. Biosynthetic studies," *Biochemical Journal*, vol. 266, no. 3, pp. 785–791, 1990.

[31] H. Morii, S. Kiyonari, Y. Ishino, and Y. Koga, "A novel biosynthetic pathway of archaetidyl-myo-inositol via archaetidyl-myo-inositol phosphate from CDP-archaeol and D-glucose 6-phosphate in methanoarchaeon Methanothermobacter thermautotrophicus cells," *Journal of Biological Chemistry*, vol. 284, no. 45, pp. 30766–30774, 2009.

[32] N. Yamauchi, N. Kamada, and H. Ueoka, "The possibility of involvement of "cyclase" enzyme of the calditol carbocycle with broad substrate specificity in Sulfolobus acidcaldarius, a typical thermophilic archaea," *Chemistry Letters*, vol. 35, no. 11, pp. 1230–1231, 2006.

[33] L. Krishnan and G. D. Sprott, "Archaeosome adjuvants: immunological capabilities and mechanism(s) of action," *Vaccine*, vol. 26, no. 17, pp. 2043–2055, 2008.

[34] A. Gliozzi, A. Relini, and P. L. G. Chong, "Structure and permeability properties of biomimetic membranes of bolaform archaeal tetraether lipids," *Journal of Membrane Science*, vol. 206, no. 1-2, pp. 131–147, 2002.

[35] G. B. Patel, B. J. Agnew, L. Deschatelets, L. P. Fleming, and G. D. Sprott, "In vitro assessment of archaeosome stability for developing oral delivery systems," *International Journal of Pharmaceutics*, vol. 194, no. 1, pp. 39–49, 2000.

[36] J. C. Mathai, G. D. Sprott, and M. L. Zeidel, "Molecular Mechanisms of Water and Solute Transport across Archaebacterial Lipid Membranes," *Journal of Biological Chemistry*, vol. 276, no. 29, pp. 27266–27271, 2001.

[37] G. D. Sprott, J. P. Cote, and H. C. Jarrell, "Glycosidase-induced fusion of isoprenoid gentiobiosyl lipid membranes at acidic pH," *Glycobiology*, vol. 19, no. 3, pp. 267–276, 2009.

[38] A. Relini, D. Cassinadri, Q. Fan et al., "Effect of physical constraints on the mechanisms of membrane fusion: bolaform lipid vesicles as model systems," *Biophysical Journal*, vol. 71, no. 4, pp. 1789–1795, 1996.

[39] A. Relini, D. Cassinadri, Z. Mirghani et al., "Calcium-induced interaction and fusion of archaeobacterial lipid vesicles: a fluorescence study," *Biochimica et Biophysica Acta*, vol. 1194, no. 1, pp. 17–24, 1994.

[40] R. Kanichay, L. T. Boni, P. H. Cooke, T. K. Khan, and P. L. G. Chong, "Calcium-induced aggregation of archaeal bipolar tetraether liposomes derived from the thermoacidophilic archaeon Sulfolobus acidocaldarius," *Archaea*, vol. 1, no. 3, pp. 175–183, 2003.

[41] S. L. Lo and E. L. Chang, "Purification and characterization of a liposomal-forming tetraether lipid fraction," *Biochemical and Biophysical Research Communications*, vol. 167, no. 1, pp. 238–243, 1990.

[42] E. L. Chang and S. L. Lo, "Extraction and purification of tetraether lipids from Sulfolobus acidocaldarius," in *Protocols for Archaebacterial Research*, E. M. Fleischmann, A. R. Place, R. T. Robb, and H. J. Schreier, Eds., pp. 2.3.1–2.3.14, Maryland Biotechnology Institute, Baltimore, Md, USA, 1991.

[43] L. Bagatolli, E. Gratton, T. K. Khan, and P. L. G. Chong, "Two-photon fluorescence microscopy studies of bipolar tetraether giant liposomes from thermoacidophilic archaebacteria Sulfolobus acidocaldarius," *Biophysical Journal*, vol. 79, no. 1, pp. 416–425, 2000.

[44] M. G. L. Elferink, J. G. De Wit, R. Demel, A. J. M. Driessen, and W. N. Konings, "Functional reconstitution of membrane proteins in monolayer liposomes from bipolar lipids of Sulfolobus acidocaldarius," *Journal of Biological Chemistry*, vol. 267, no. 2, pp. 1375–1381, 1992.

[45] H. Komatsu and P. L. G. Chong, "Low permeability of liposomal membranes composed of bipolar tetraether lipids from thermoacidophilic archaebacterium Sulfolobus acidocaldarius," *Biochemistry*, vol. 37, no. 1, pp. 107–115, 1998.

[46] E. L. Chang, "Unusual thermal stability of liposomes made from bipolar tetraether lipids," *Biochemical and Biophysical Research Communications*, vol. 202, no. 2, pp. 673–679, 1994.

[47] D. A. Brown, B. Venegas, P. H. Cooke, V. English, and P. L. G. Chong, "Bipolar tetraether archaeosomes exhibit unusual stability against autoclaving as studied by dynamic light scattering and electron microscopy," *Chemistry and Physics of Lipids*, vol. 159, no. 2, pp. 95–103, 2009.

[48] P. L.-G. Chong, M. Zein, T. K. Khan, and R. Winter, "Structure and conformation of bipolar tetraether lipid membranes derived from thermoacidophilic archaeon Sulfolobus acidocaldarius as revealed by small-angle X-ray scattering and high-pressure FT-IR spectroscopy," *Journal of Physical Chemistry B*, vol. 107, no. 33, pp. 8694–8700, 2003.

[49] P. L. G. Chong, R. Ravindra, M. Khurana, V. English, and R. Winter, "Pressure perturbation and differential scanning calorimetric studies of bipolar tetraether liposomes derived from the thermoacidophilic archaeon Sulfolobus acidocaldarius," *Biophysical Journal*, vol. 89, no. 3, pp. 1841–1849, 2005.

[50] P. L.-G. Chong, M. Sulc, and R. Winter, "Compressibilities and volume fluctuations of archaeal tetraether liposomes," *Biophysical Journal*, vol. 99, no. 10, pp. 3319–3326, 2010.

[51] E. Falck, M. Patra, M. Karttunen, M. T. Hyvönen, and I. Vattulainen, "Impact of cholesterol on voids in phospholipid membranes," *Journal of Chemical Physics*, vol. 121, no. 24, pp. 12676–12689, 2004.

[52] P. F. F. Almeida, W. L. C. Vaz, and T. E. Thompson, "Lateral diffusion and percolation in two-phase, two-component lipid bilayers. topology of the solid-phase domains in-plane and across the lipid bilayer," *Biochemistry*, vol. 31, no. 31, pp. 7198–7210, 1992.

[53] Y. L. Kao, E. L. Chang, and P. L. G. Chong, "Unusual pressure dependence of the lateral motion of pyrene-labeled phosphatidylcholine in bipolar lipid vesicles," *Biochemical and Biophysical Research Communications*, vol. 188, no. 3, pp. 1241–1246, 1992.

[54] T. D. Brock, K. M. Brock, R. T. Belly, and R. L. Weiss, "Sulfolobus: a new genus of sulfur-oxidizing bacteria living at low pH and high temperature," *Archiv für Mikrobiologie*, vol. 84, no. 1, pp. 54–68, 1972.

[55] T. A. Langworthy, W. R. Mayberry, and P. F. Smith, "Long chain glycerol diether and polyol dialkyl glycerol triether lipids of Sulfolobus acidocaldarius," *Journal of Bacteriology*, vol. 119, no. 1, pp. 106–116, 1974.

[56] H. Shimada, N. Nemoto, Y. Shida, T. Oshima, and A. Yamagishi, "Complete polar lipid composition of Thermoplasma acidophilum HO-62 determined by high-performance liquid chromatography with evaporative light-scattering detection," *Journal of Bacteriology*, vol. 184, no. 2, pp. 556–563, 2002.

[57] R. Y. Samson, T. Obita, B. Hodgson et al., "Molecular and Structural Basis of ESCRT-III Recruitment to Membranes during Archaeal Cell Division," *Molecular Cell*, vol. 41, no. 2, pp. 186–196, 2011.

[58] A. Fafaj, J. Lam, L. Taylor, and P. L. G. Chong, "Unusual stability of archaeal tetraether liposomes against surfactants," *Biophysical Journal*, vol. 100, no. 3, p. 329a, 2011.

[59] M. De Rosa, "Archaeal lipids: structural features and supramolecular organization," *Thin Solid Films*, vol. 284-285, pp. 13–17, 1996.

[60] U. Bakowsky, U. Rothe, E. Antonopoulos, T. Martini, L. Henkel, and H. J. Freisleben, "Monomolecular organization of the main tetraether lipid from Thermoplasma acidophilum at the water-air interface," *Chemistry and Physics of Lipids*, vol. 105, no. 1, pp. 31–42, 2000.

[61] S. Vidawati, J. Sitterberg, U. Bakowsky, and U. Rothe, "AFM and ellipsometric studies on LB films of natural asymmetric and symmetric bolaamphiphilic archaebacterial tetraether lipids on silicon wafers," *Colloids and Surfaces B*, vol. 78, no. 2, pp. 303–309, 2010.

[62] A. Gliozzi, A. Relini, R. Rolandi, S. Dante, and A. Gambacorta, "Organization of bipolar lipids in monolayers at the air-water interface," *Thin Solid Films*, vol. 242, no. 1-2, pp. 208–212, 1994.

[63] T. Benvegnu, M. Brard, and D. Plusquellec, "Archaeabacteria bipolar lipid analogues: structure, synthesis and lyotropic properties," *Current Opinion in Colloid and Interface Science*, vol. 8, no. 6, pp. 469–479, 2004.

[64] T. Benvegnu, G. Rethore, M. Brard, W. Richter, and D. Plusquellec, "Archaeosomes based on novel synthetic tetraether-type lipids for the development of oral delivery systems," *Chemical Communications*, no. 44, pp. 5536–5538, 2005.

[65] M. Brard, C. Lainé, G. Réthoré et al., "Synthesis of archaeal bipolar lipid analogues: a way to versatile drug/gene delivery systems," *Journal of Organic Chemistry*, vol. 72, no. 22, pp. 8267–8279, 2007.

[66] M. Brard, W. Richter, T. Benvegnu, and D. Plusquellec, "Synthesis and supramolecular assemblies of bipolar archaeal glycolipid analogues containing a cis-1,3-disubstituted cyclopentane ring," *Journal of the American Chemical Society*, vol. 126, no. 32, pp. 10003–10012, 2004.

[67] G. Lecollinet, R. Auzély-Velty, M. Danel et al., "Synthetic approaches to novel archaeal tetraether glycolipid analogues," *Journal of Organic Chemistry*, vol. 64, no. 9, pp. 3139–3150, 1999.

[68] W. Cui, F. Li, and N. L. Allinger, "Simulation of conformational dynamics with the MM3 force field: the pseudorotation of cyclopentane," *Journal of the American Chemical Society*, vol. 115, no. 7, pp. 2943–2951, 1993.

[69] O. R. de Ballesteros, L. Cavallo, F. Auriemma, and G. Guerra, "Conformational analysis of poly(methylene-1,3-cyclopentane) and chain conformation in the crystalline phase," *Macromolecules*, vol. 28, no. 22, pp. 7355–7362, 1995.

[70] W. Shinoda, K. Shinoda, T. Baba, and M. Mikami, "Molecular dynamics study of bipolar tetraether lipid membranes," *Biophysical Journal*, vol. 89, no. 5, pp. 3195–3202, 2005.

[71] S. Li, F. Zheng, X. Zhang, and W. Wang, "Stability and rupture of archaebacterial cell membrane: a model study," *Journal of Physical Chemistry B*, vol. 113, no. 4, pp. 1143–1152, 2009.

[72] B. A. Cornell, V. L. B. Braach-Maksvytis, L. G. King et al., "A biosensor that uses ion-channel switches," *Nature*, vol. 387, no. 6633, pp. 580–583, 1997.

[73] K. Iida, H. Kiriyama, A. Fukai, W. N. Konings, and M. Nango, "Two-dimensional self-organization of the light-harvesting polypeptides/BChl a complex into a thermostable liposomal membrane," *Langmuir*, vol. 17, no. 9, pp. 2821–2827, 2001.

[74] T. Benvegnu, L. Lemiègre, and S. Cammas-Marion, "Archaeal lipids: innovative materials for biotechnological applications," *European Journal of Organic Chemistry*, no. 28, pp. 4725–4744, 2008.

[75] G. D. Sprott, S. Sad, L. P. Fleming, C. J. Dicaire, G. B. Patel, and L. Krishnan, "Archaeosomes varying in lipid composition differ in receptor-mediated endocytosis and differentially adjuvant immune responses to entrapped antigen," *Archaea*, vol. 1, no. 3, pp. 151–164, 2003.

[76] A. Gonzalez-Paredes, B. Clares-Naveros, M. A. Ruiz-Martinez, J. J. Durban-Fornieles, A. Ramos-Cormenzana, and M. Monteoliva-Sanchez, "Delivery systems for natural antioxidant compounds: archaeosomes and archaeosomal hydrogels characterization and release study," *International Journal of Pharmaeutics*, vol. 421, no. 2, pp. 321–331, 2011.

[77] J. Parmentier, B. Thewes, F. Gropp, and G. Fricker, "Oral peptide delivery by tetraether lipid liposomes," *International Journal of Pharmaceutics*, vol. 415, no. 1-2, pp. 150–157, 2011.

[78] G. B. Pate, H. Zhou, A. Ponce, G. Harris, and W. Chen, "Intranasal immunization with an archaeal lipid mucosal vaccine adjuvant and delivery formulation protects against a respiratory pathogen challenge," *PLoS ONE*, vol. 5, no. 12, Article ID e15574, 2010.

[79] J. Barbeau, S. Cammas-Marion, P. Auvray, and T. Benvegnu, "Preparation and characterization of stealth archaeosomes based on a synthetic PEGylated archaeal tetraether lipid," *Journal of Drug Delivery*, vol. 2011, Article ID 396068, 11 pages, 2011.

Hindawi Publishing Corporation
Archaea
Volume 2012, Article ID 789652, 6 pages
doi:10.1155/2012/789652

Review Article

Thermal Adaptation of the Archaeal and Bacterial Lipid Membranes

Yosuke Koga

Department of Chemistry, University of Occupational and Environmental Health, Yahata-nishi-Ku, Kitakyushu 807-8555, Japan

Correspondence should be addressed to Yosuke Koga, yokoga@ams.odn.ne.jp

Received 12 June 2012; Accepted 12 July 2012

Academic Editor: Angela Corcelli

The physiological characteristics that distinguish archaeal and bacterial lipids, as well as those that define thermophilic lipids, are discussed from three points of view that (1) the role of the chemical stability of lipids in the heat tolerance of thermophilic organisms: (2) the relevance of the increase in the proportion of certain lipids as the growth temperature increases: (3) the lipid bilayer membrane properties that enable membranes to function at high temperatures. It is concluded that no single, chemically stable lipid by itself was responsible for the adaptation of surviving at high temperatures. Lipid membranes that function effectively require the two properties of a high permeability barrier and a liquid crystalline state. Archaeal membranes realize these two properties throughout the whole biological temperature range by means of their isoprenoid chains. Bacterial membranes meet these requirements only at or just above the phase-transition temperature, and therefore their fatty acid composition must be elaborately regulated. A recent hypothesis sketched a scenario of the evolution of lipids in which the "lipid divide" emerged concomitantly with the differentiation of archaea and bacteria. The two modes of thermal adaptation were established concurrently with the "lipid divide."

1. Introduction

The unique structural characteristics of the archaeal polar lipids, that is, the *sn*-glycerol-1-phosphate (G-1-P) backbone, ether linkages, and isoprenoid hydrocarbon chains, are in striking contrast to the bacterial characteristics of the *sn*-glycerol-3-phosphate (G-3-P) backbone, ester linkages, and fatty acid chains. This contrast in membrane lipid structures between archaea and bacteria has been termed the "lipid divide" [1]. Because this has been repeatedly discussed [2–4], it is not discussed again here. The only thing that needs to be pointed out is that the enantiomeric difference of the lipid backbone (G-1-P and G-3-P), which is the most important feature from the evolutionary point of view, is insignificant in terms of the thermal adaptation of the membrane, because enantiomers have equivalent thermal properties.

The chemical properties and physiological roles of archaeal lipids are often discussed in terms of the presence of the chemically stable ether bonds in thermophilic archaea. However, based on the archaeal lipids analyzed thus far, as shown by lipid component parts analysis [5], the mesophilic archaea possess essentially the same core lipid composition as that of the thermophilic archaea. The ether bonds therefore do not seem to be directly related to thermophily.

What are the most crucial distinguishing physiological characteristics of the archaeal and bacterial lipids? What are the distinctive features of thermophilic lipids? These questions will be discussed in the present paper from three distinct perspectives:

(1) the relationship of the chemical stability of lipids with the heat tolerance of thermophilic organisms,

(2) the increase in proportion of certain lipids as the growth temperature rises,

(3) the lipid bilayer membrane properties that enable membranes to function at high temperatures.

Recently a hypothesis was published [1] on the differentiation of archaea and bacteria and the establishment of the "lipid divide." The present paper will discuss two fundamental aspects of the thermal adaptation of microorganisms in relation to the domain differentiation and the emergence of the "lipid divide."

A preliminary form of the present discussion was first presented as a part of our previous review paper [6]. Driessen and Albers [7] have presented similar conclusion about membrane adaptations to high temperatures in relation to the membrane mechanisms of energy metabolism. The main conclusion of these two articles almost identical, even though the papers were independently prepared and the findings discussed from originally different point of view.

2. The Chemical Stability of Lipids and the Heat Tolerance of Thermophilic Organisms

Because the ether bonds of archaeal lipids are for the most part not broken down under conditions in which ester linkages are completely methanolyzed (5% HCl/MeOH, 100°C for 3 hr), it is generally believed that the archaeal ether lipids are thermotolerant or heat resistant. This implies that thermophilic organisms are able to grow at high temperature due to the chemical stability of their membrane lipids.

Figure 1 illustrates structures of some so-called "thermophilic" lipid candidates referred to in the following text.

Ether lipids (Figure 1(a)) are always present in the archaea that reside in high-temperature environments without exceptions, but the mesophilic archaea also have ether lipids. In fact, not only archaea but also certain thermophilic bacteria contain ether lipids. The thermophilic lipid candidates, in addition to the archaeal ether lipids, are the chemically stable monobranched fatty alcohol-containing diether lipids (Figure 1(f), *Thermodesulfobacterium commune* (optimum growth temperature: 70°C [8]) and *Aquifex pyrophilus* (85°C [9]); long chain dicarboxylic fatty acids (diabolic acid, Figure 1(m)) and 15,16-dimethyl 30-glyceryloxytriacontanoic acid (Figure 1(g)) from *Thermotoga maritima* (90°C [10]) and *Fervidobacterium islandicum* (75°C [11]); a long chain 1, 2-diol (Figure 1(h), (*Long chain diol lipid: in this lipid it can be considered that the first three carbons, C1 to C3, play the role of the backbone (instead of glycerol) of the lipid. The OH at the C1 may bind a polar head group and the OH at the C2 binds the first hydrocarbon chain, and the C3 and C4 represent a C–C-bond between the "backbone" and the remainder part of the long chain.)) from *Thermomicrobium roseum* (75°C [12]); cyclohexyl fatty acid (Figure 1(n)) from *Bacillus acidocaldarius* (65°C [13]). These have been assumed to be thermophilic lipids because of their thermostability (unhydrolyzability) (diether or C–C bond in the long-chain diol or membrane-spanning nature (dicarboxylic acid) like tetraether lipids). As a matter of fact, all the thermophilic archaea possess ether lipids, but not all of the organisms possessing the so-called "thermophilic" lipids shown above are themselves thermophilic. The same structure of diabolic acid was also found in *Butyrivibrio* sp. (39°C [14]); and cyclohexyl fatty acid in *Curtobacterium pusillum* (27°C [15]). Many species of the mesophilic methanoarchaea [5] have ether core lipids. On the other hand, some of the thermophilic organisms are able to survive with ester lipids in their membranes [10–13].

Because tetraether type, membrane-spanning polar lipids (Figures 1(d) or 1(e)) were first found in thermoacidophilic archaeon [16], these lipids are considered thermophilic lipids. Tetraether lipids are extended as a result of their C40 hydrocarbon chains passing across the membrane bilayer. Thus, tetraether lipids link the leaflets of the lipid bilayer covalently and thus make the membrane rigid. This structure allows membranes to tolerate extreme conditions. However, some of the nonthermophilic methanoarchaea have the same tetraether lipids [5]. *Methanothermobacter thermautotrophicus* (65°C) has both archaeol- and caldarchaeol-based lipids, while the mesophilic species of *Methanobacterium* (37°C) has almost the same core lipid composition. Similarly, some archaea that have caldarchaeol-based (tetraether-type) polar lipids in addition to archaeol-based polar lipids grow above 85°C, and there is one that grows at 20°C. Some archaea have only archaeol-based (diether-type) polar lipids and grow below 40°C, yet there is one that grows at 90°C. The hyperthermophilic *Methanopyrus kandleri* (90°C [5]) has also only diether-type polar lipids. The distribution pattern of the archaeol- and caldarchaeol-based polar lipids make it clear that these ether lipids are not absolutely required for tolerance of high temperature.

Archaeal ether lipids are synthesized from G-1-P and geranylgeranylpyrophosphate (GGPP). The first and second ether-bonded intermediates in the archaeal phospholipid synthesis pathway are geranylgeranylglycerophosphate (GGGP) and digeranylgeranylglycerophosphate (DGGGP, Figure 1(c)) [17, 18], respectively, which are allyl ether compounds. The allyl ether compounds are just as labile as or even more labile than the ester compounds; they are broken down *in vitro* at 5% HCl/MeOH, 80°C for 1 hr. Ether bonds themselves are stable, but their biosynthetic precursors are as labile as ester compounds. Since organisms with ester lipids are heat sensitive, Archaea cannot grow well at a high temperature, because the heat-sensitive biosynthetic intermediates, which are only present in a small amount, are easily broken down, so ether lipids cannot be synthesized.

Even if the chemically stable lipids that are present in thermophiles are indeed thermophilic lipids, it has not yet been made clear how such chemical stability specifically affects the response to high temperatures by thermophilic organisms. It is not yet apparent whether the ether lipids were specifically adapted for the purpose of survival at high temperatures.

3. Increases in the Proportion of Certain Lipids as the Growth Temperature Rises

In considering thermophilic lipids, not only chemical but also biological aspects are essential to an understanding of their activity. Lipids that increase in proportion to an increase in growth temperature may thus aptly be designated "thermophilic lipids."

The fatty acid composition of a bacterium changes depending on the growth temperature. In *Escherichia coli*, unsaturated fatty acids (Figure 1(j)) increase along with a downshift in the growth temperature [19]. In *Bacillus* spp. and other bacterial species, isofatty acids (Figure 1(k)) increase along with an increase in the growth temperature, and anteiso fatty acids (Figure 1(l)) increase along with

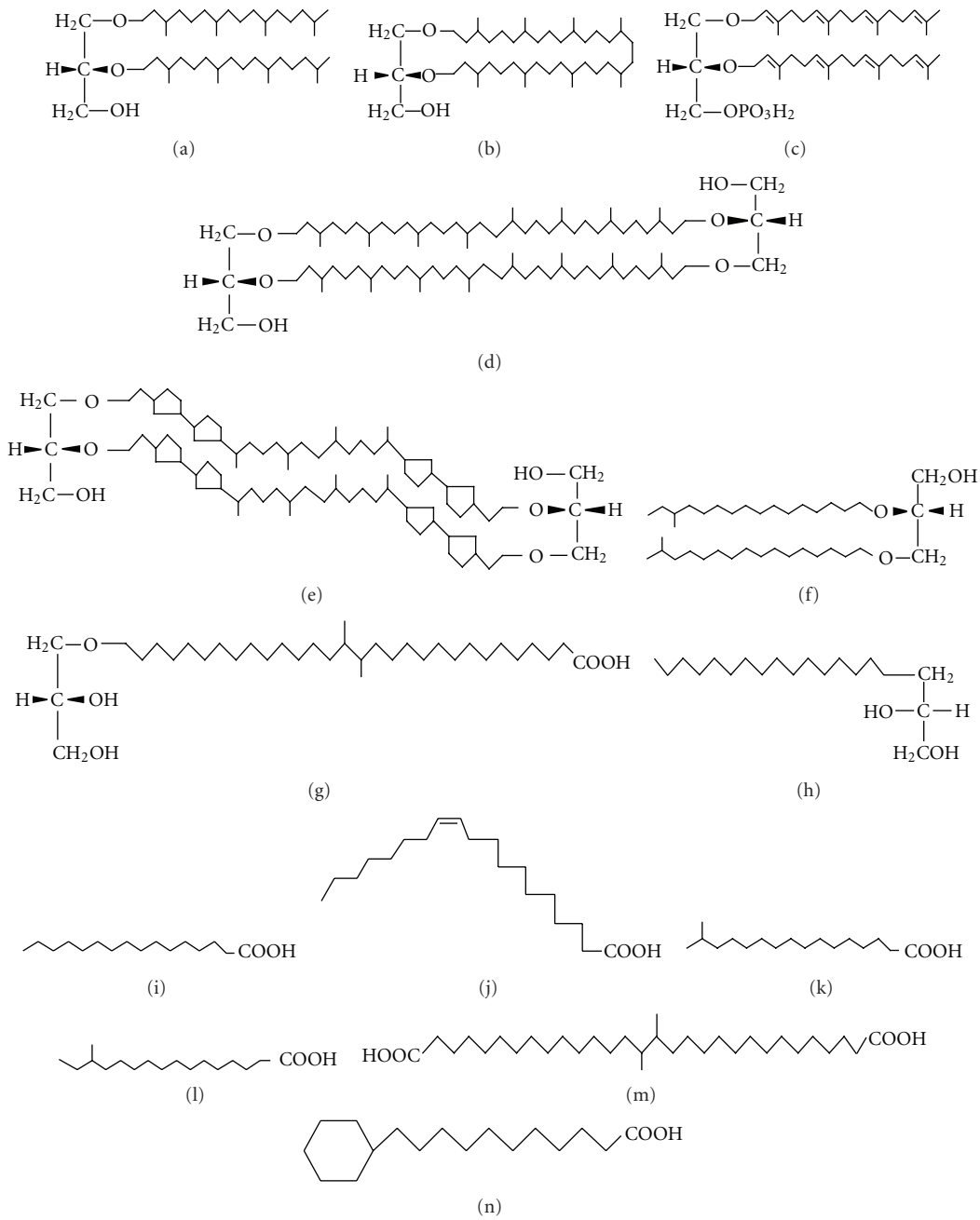

Figure 1: Structures of thermophilic lipid candidates (a) diphytanylglycerol (archaeol: archaeal diether lipid); (b) cyclic archaeol; (c) digeranylgeranylglycerophosphate (DGGGP); (d) caldarchaeol (archaeal tetraether lipid); (e) cyclopentane-containing caldarchaeol; (f) bacterial dither lipids; (g) 15,16-dimethyl-30-glyceryloxytriacontanoic acid; (h) 1,2-di-hydroxynonadecane (long-chain diol lipid); (i) palmitic acid (saturated straight chain fatty acid); (j) *cis*-vaccenic acid (monounsaturated straight chain fatty acid); (k) iso-C17 fatty acid; (l) anteiso-C17 fatty acid; (m) 15,16-dimethyltriacontandioic acid (diabolic acid); (n) 11-cyclohexylundecanoic acid. (a)–(e) Archaeal lipids; (f)–(n) bacterial lipids.

a lowering of the growth temperature [20–23]. The increasing fatty acids are often not a single fatty acid but rather a group of different fatty acids. A mesophilic strain of *Bacillus megaterium* [24] has been shown to have 25% iso-C15 and nearly 50% anteiso-C15 fatty acids at 20°C and 35% iso-C15 and 15% anteiso-C15 at 60°C. By contrast, a thermophilic strain of the organism can only grow between 45 and 70°C and the iso-C15 content (30–50%) is always higher than that of anteiso-C15 (lower than 10%). Furthermore, the growth of a psychrophilic strain of the bacterium is restricted to temperatures between 5 and 45°C, and the content of anteiso-C15 (around 50%) is always higher than that of iso-C15 (10–30%). The thermophilic or psychrophilic strains do not appear to regulate the branched chain C15 fatty acid

content. This suggests that the iso-C15 fatty acid is thermophilic and the anteiso-C15 fatty acid is psychrophilic in this bacterial species.

In the extremely thermophilic methanoarchaea *Methanocaldococcus jannaschii*, when the growth temperature increases from 45°C to 65°C, the diether lipids (archaeol-based lipids) decrease from 80% to 20%, while the standard caldarchaeol-based and cyclic archaeol-based (Figure 1(b)) lipids increase from 10% to 40%, respectively [25].

The changes in the hydrocarbon composition of membrane lipids have a nature of lawfulness, but the mode of hydrocarbon composition change is different from species to species. Therefore, the pattern of fatty acid composition found in a given species, for example, *E. coli*, should be applied to other organisms only with the greatest caution. To find the actual underlying pattern in these phenomena, another point of view would seem to be required, and this is discussed in the next section.

4. Lipids as Cell Membrane Constituents Having a Permeability Barrier and Liquid Crystalline State

The third conceptualization of thermophilic/heat-tolerant lipids is based on a rather different point of view. Because lipids do not function as single molecules but as a membrane, that is, as an enormous number of molecules acting together, which assemble into a biologically functioning organelle, thermophilic lipids should be understood as lipids that normally function as a membrane at a high temperature. This is not achieved by chemical stability alone. At the moment that a lipid membrane came to enclose the cell contents, the real cell as we know it was born. With that event, cell membranes partitioned the inner cytoplasmic compartment away from their surroundings. From this time onward, membranes effectively functioned as a permeability barrier, controlling the in-flow and out-flow of low-molecular-weight compounds. This is the most primitive and essential function of a cell membrane. When cells became enclosed by such a membrane having this sort of permeability barrier, the cells achieved a distinct "individuality" and hence began to compete with the other individual cells in order to survive within the local community, and thus natural selection came more sharply into play. Therefore, the lipid constituents that enable the membrane to function as a highly permeable barrier at high temperatures are designated thermophilic lipids.

Another essential general feature that is required for lipid membrane function is the capacity to persist in the liquid crystalline phase. The phase-transition temperature of the archaeal lipid membranes is far lower than that of fatty acyl ester lipids, reportedly being between –20 and –15°C [26]. The phase transition temperature of the normal fatty acyl ester phospholipid membrane is in a far higher temperature range (40–50°C) than the archaeal lipids, and this is dependent on their chain length, number of double bonds and the methyl branching position. Therefore, the archaeal polar lipid membrane can be presumed to be in liquid crystalline phase in the temperature range of 0 to 100°C, the range at which most archaea grow (biological temperature), while fatty acyl diester lipid membrane is in either a gel phase or liquid crystalline phase in the same temperature range, depending on their fatty acid composition.

In some archaea, the hydrocarbon chain properties are regulated by the number of cyclopentane rings (Figure 1(e), *Sulfolobus solfataricus*) [27] or the ratio of caldarchaeol/cyclic archaeol/archaeol (*Methanocaldococcus jannaschii*) [25]. The content of the transunsaturation of the isoprenoid chains was reported to decrease with a higher growth temperature in *Methanococcoides burtonii* [28]. However, the organism *Methanopyrus kandleri* has a sufficient number of double bonds in the isoprenoid chains in spite of its much higher growth temperature. Unsaturation is not related in a straightforward manner with the adaptation to low temperatures, which occurred in archaea.

One characteristic property of the archaeal lipid membrane is the extremely low permeability of solutes [29–32]. In addition, the permeability increases only slightly as the temperature goes up in the 0 to 100°C range.

In contrast to the tetraether lipid liposomes, the fatty acyl ester lipid liposomes exhibit a low permeability at a low temperature, but the permeability drastically increases as the temperature increases [29]. The experimental results suggest that highly branched isoprenoid chains are a major cause of the low permeability of liposomes, but this phenomenon does not depend on the ether or ester bonds between the glycerophosphate backbone and hydrocarbon chains.

Bacteria grow at a temperature just above the phase-transition temperature at which membrane lipids are in a liquid crystalline state and retain a minimal level of permeability. The permeability of fatty acyl ester lipid membranes is highly temperature dependent and their phase-transition temperature is dependent on the fatty acid composition, so when the growth temperature shifts, the fatty acid composition of membrane lipids is quickly regulated. The phenomena described in Section 3 (regulation of the composition of unsaturated/saturated fatty acids (Figures 1(i) and 1(j)) in *E. coli*, and iso/anteiso fatty acids in *Bacillus* spp.) are explained by this mechanism. On the other hand, the isoprenoid ether lipids in the archaeal membrane are in a low permeability liquid crystalline state throughout the possible growth temperature range (0–100°C) [33], and even if the growth temperature changes, the two requirements are met without any need of a biological regulation mechanism.

Because isoprenoid ether lipid membranes are in the liquid crystalline phase and have a low permeability at biological temperatures, archaea are found living at temperatures as low as 1°C and as high as 100°C with the same archaeol and caldarchaeol lipid composition in the membrane. This is the most fundamental characteristic of the archaeal lipid membranes. Bacterial membranes can be characterized by the highly developed regulatory mechanisms they employ to meet the two conditions. We can see actual examples in the case of the hyperthermophilic *Pyrococcus furiosus* (optimum temperature, 98°C) [34], moderately thermophilic *Methanothermobacter thermautotrophicus* (65°C) [35], mesophilic *Methanobacterium formicicum* (37°C) [5] and *Methanogenium cariaci* (23°C) [5]. They all have nearly the same core

lipid composition. Unsaturated archaeol (geranylgeranyl group-containing archaeol) is present in the psychrophilic *Methanococcoides burtonii* that can grow at 2°C [28] as well as the hyperthermophilic *Methanopyrus kandleri* (98°C) [36]. A lipid that can be utilized at both high and low temperatures because of its liquid crystalline phase and low permeability at a wide range of temperatures is aptly termed a "heat tolerant" lipid.

On the other hand, bacterial fatty acyl ester lipid membranes should only function at the lowest temperature at which both a liquid crystalline state and low permeability are retained. This condition may be met at a temperature close to and above its phase transition temperature. Therefore, many bacteria with ester lipids control their fatty acid composition so as to meet these conditions. The control mechanism varies from species to species. In *Escherichia coli*, unsaturated fatty acids are maximal at lower growth temperatures. However, unsaturation is not the only mechanism to adapt to lower temperatures. In *Bacillus* spp., temperature adaptation is regulated by changing the iso/anteiso fattyacid composition [22].

The archaeal lipid membrane does not have to regulate its hydrocarbon composition to meet the two conditions for temperature adaptation, because the two conditions are already in place at such a wide range of temperatures.

5. Evolutionary Significance of Two Modes of Thermal Adaptation

Recently, a hypothesis [1] was put forward that provides an account for the differentiation of Archaea and Bacteria from the last universal common ancestor (LUCA) by means of the enantiomeric phase separation of the glycerophosphate backbones of the membrane lipids facilitated by their different hydrocarbon chains and diastereomeric structures. In LUCA cells, at least four different kinds of core lipids (Ai, Bf, Af, and Bi) are made up of a combination of G-1-P (A) or G-3-P (B) as the phospholipid backbone and isoprenoid (i) or fatty acid (f) as the hydrocarbon chains. The archaeal Ai membranes and bacterial Bf membranes thrive differently depending on the nature of their constituent lipids. Soon after the beginning of the differentiation of LUCA, the phase separation of various core lipids was still incomplete in the membrane. As the differentiating membranes become further purified, either mode of thermal adaptation may be established. This might act as a positive selection pressure. The two different modes of thermal adaptation evolved in parallel with the emergency of the "lipid divide" and Archaea-Bacteria differentiation. The "lipid divide" was produced not only by the physicochemical phase separation of the membrane lipids but also by the different forms of thermal adaptation. Accordingly, these two different organisms have adapted to a variety of environments.

6. Conclusion

It is concluded that no single, chemically stable lipid by itself was sufficient for the adaptation to living at high temperatures. Therefore, an alternative account of the emergence of heat-tolerant lipids has been presented. This view emphasizes the functioning of organismal lipids as membranes. Vitally functioning cell membranes must have at least two characteristics: a high permeability barrier and the capacity to maintain the liquid crystalline phase. Archaeal membranes are able to meet these conditions by means of isoprenoid chains, which are functional over the entire biological temperature range and do not require a regulatory mechanism to adapt lipids to changes in the environmental temperature. Because bacterial membranes have a temperature-dependent permeability and fatty acid composition-dependent phase transition over the complete biological temperature range, they have elaborate mechanisms by which they regulate the fatty acid composition at temperatures just above the phase transition temperature. It is not unusual perhaps should not be surprising that no change in the lipid composition of archaea took place as the growth temperature changed. The presence of the transdouble bonds in isoprenoid chains does not directly entail the adaptation of organisms to low-temperature environments. Instead, the two modes of thermal adaptation are the result of the early evolution of membrane lipids that enabled the differentiation of archaea and Bacteria by means of the establishment of the "lipid divide".

References

[1] Y. Koga, "Early evolution of membrane lipids: how did the lipid divide occur?" *Journal of Molecular Evolution*, vol. 72, no. 3, pp. 274–282, 2011.

[2] Y. Koga, M. Nishihara, H. Morii, and M. Akagawa-Matsushita, "Ether polar lipids of methanogenic bacteria: structures, comparative aspects, and biosyntheses," *Microbiological Reviews*, vol. 57, no. 1, pp. 164–182, 1993.

[3] Y. Koga and H. Morii, "Special methods for the analysis of ether lipid structure and metabolism in archaea," *Analytical Biochemistry*, vol. 348, no. 1, pp. 1–14, 2006.

[4] Y. Koga and H. Morii, "Biosynthesis of ether-type polar lipids in archaea and evolutionary considerations," *Microbiology and Molecular Biology Reviews*, vol. 71, no. 1, pp. 97–120, 2007.

[5] Y. Koga and M. Nakano, "A dendrogram of archaea based on lipid component parts composition and its relationship to rRNA phylogeny," *Systematic and Applied Microbiology*, vol. 31, no. 3, pp. 169–182, 2008.

[6] Y. Koga and H. Morii, "Recent advances in structural research on ether lipids from archaea including comparative and physiological aspects," *Bioscience, Biotechnology and Biochemistry*, vol. 69, no. 11, pp. 2019–2034, 2005.

[7] A. J. M. Driessen and S. V. Albers, "Membrane adaptations of (hyper)thermophiles to high temperatures," in *Physiology and Biochemistry of Extremophiles*, C. Gerday and N. Glansdorff, Eds., pp. 104–116, ASM Press, Washington, DC, USA, 2007.

[8] T. A. Langworthy, G. Holzer, J. G. Zeikus, and T. G. Tornabene, "Iso- and anteiso-branched glycerol diethers of the thermophilic anaerobe *Thermodesulfotobacterium commune*," *Systematic and Applied Microbiology*, vol. 4, no. 1, pp. 1–17, 1983.

[9] S. Burggraf, G. J. Olsen, K. O. Stetter, and C. R. Woese, "A phylogenetic analysis of *Aquifex pyrophilus*," *Systematic and Applied Microbiology*, vol. 15, no. 3, pp. 352–356, 1992.

[10] M. De Rosa, A. Gambacorta, R. Huber et al., "A new 15,16-dimethyl-30-glyceryloxytriacontanoic acid from lipids of *Thermotoga maritima*," *Journal of the Chemical Society, Chemical Communications*, no. 19, pp. 1300–1301, 1988.

[11] R. Huber, C. R. Woese, T. A. Langworthy, J. K. Kristjansson, and K. O. Stetter, "*Fervidobacterium islandicum* sp. nov., a new extremely thermophilic eubacterium belonging to the Thermotogales," *Archives of Microbiology*, vol. 154, no. 2, pp. 105–111, 1990.

[12] J. L. Pond and T. A. Langworthy, "Effect of growth temperature on the long-chain diols and fatty acids of *Thermomicrobium roseum*," *Journal of Bacteriology*, vol. 169, no. 3, pp. 1328–1330, 1987.

[13] M. De Rosa, A. Gambacorta, and J. D. Bu'Lock, "Effects of pH and temperature on the fatty acid composition of *Bacillus acidocaldarius*," *Journal of Bacteriology*, vol. 117, no. 1, pp. 212–214, 1974.

[14] R. A. Klein, G. P. Hazlewood, P. Kemp, and R. M. C. Dawson, "A new series of long-chain dicarboxylic acids with vicinal dimethyl branching found as major components of the lipids of *Butyrivibrio* spp," *Biochemical Journal*, vol. 183, no. 3, pp. 691–700, 1979.

[15] K. Suzuki, K. Saito, and A. Kawaguchi, "Occurrence of ω-cyclohexyl fatty acids in *Curtobacterium pusillum* strains," *Journal of General and Applied Microbiology*, vol. 27, no. 3, pp. 261–266, 1981.

[16] M. de Rosa, S. de Rosa, A. Gambacorta, L. Minale, and J. D. Bu'lock, "Chemical structure of the ether lipids of thermophilic acidophilic bacteria of the *Caldariella* group," *Phytochemistry*, vol. 16, no. 12, pp. 1961–1965, 1977.

[17] D. Zhang and C. Dale Poulter, "Biosynthesis of archaebacterial lipids in *Halobacterium halobium* and *Methanobacterium thermoautotrophicum*," *Journal of Organic Chemistry*, vol. 58, no. 15, pp. 3919–3922, 1993.

[18] D. Zhang and C. Dale Poulter, "Biosynthesis of archaebacterial ether lipids. Formation of ether linkages by prenyltransferases," *Journal of the American Chemical Society*, vol. 115, no. 4, pp. 1270–1277, 1993.

[19] S. Aihara, M. Kato, M. Ishinaga, and M. Kito, "Changes in positional distribution of fatty acids in the phospholipids of *Escherichia coli* after shift-down in temperature," *Biochimica et Biophysica Acta*, vol. 270, no. 3, pp. 301–306, 1972.

[20] A. Weerkamp and W. Heinen, "Effect of temperature on the fatty acid composition of the extreme thermophiles, *Bacillus caldolyticus* and *Bacillus caldotenax*," *Journal of Bacteriology*, vol. 109, no. 1, pp. 443–446, 1972.

[21] M. Oshima and A. Miyagawa, "Comparative studies on the fatty acid composition of moderately and extremely thermophilic bacteria," *Lipids*, vol. 9, no. 7, pp. 476–480, 1974.

[22] M. C. Mansilla, L. E. Cybulski, D. Albanesi, and D. De Mendoza, "Control of membrane lipid fluidity by molecular thermosensors," *Journal of Bacteriology*, vol. 186, no. 20, pp. 6681–6688, 2004.

[23] T. Kaneda, "Positional preference of fatty acids in phospholipids of *Bacillus cereus* and its relation to growth temperature," *Biochimica et Biophysica Acta*, vol. 280, no. 2, pp. 297–305, 1972.

[24] L. Rilfors, A. Wieslander, and S. Stahl, "Lipid and protein composition of membranes of *Bacillus megaterium* variants in the temperature range 5 to 70°C," *Journal of Bacteriology*, vol. 135, no. 3, pp. 1043–1052, 1978.

[25] G. D. Sprott, M. Meloche, and J. C. Richards, "Proportions of diether, macrocyclic diether, and tetraether lipids in *Methanococcus jannaschii* grown at different temperatures," *Journal of Bacteriology*, vol. 173, no. 12, pp. 3907–3910, 1991.

[26] D. Blöcher, R. Gutermann, B. Henkel, and K. Ring, "Physicochemical characterization of tetraether lipids from *Thermoplasma acidophilum* sifferential scanning calorimetry studies on glycolipids and glycophospholipids," *Biochimica et Biophysica Acta*, vol. 778, no. 1, pp. 74–80, 1984.

[27] M. De Rosa, E. Esposito, A. Gambacorta, B. Nicolaus, and J. D. Bu'Lock, "Effects of temperature on ether lipid composition of *Caldariella acidophila*," *Phytochemistry*, vol. 19, no. 5, pp. 827–831, 1980.

[28] D. S. Nichols, M. R. Miller, N. W. Davies, A. Goodchild, M. Raftery, and R. Cavicchioli, "Cold adaptation in the Antarctic archaeon *Methanococcoides burtonii* involves membrane lipid unsaturation," *Journal of Bacteriology*, vol. 186, no. 24, pp. 8508–8515, 2004.

[29] K. Yamauchi, K. Doi, Y. Yoshida, and M. Kinoshita, "Archaebacterial lipids: highly proton-impermeable membranes from 1,2-diphytanyl-*sn*-glycero-3-phosphocholine," *Biochimica et Biophysica Acta*, vol. 1146, no. 2, pp. 178–182, 1993.

[30] K. Yamauchi, Y. Sakamoto, A. Moriya et al., "Archaebacterial lipid models. Highly thermostable membranes from 1,1′-(1,32-Dotriacontamethylene)-bis(2-phytanyl-sn-glycero-3-phosphocholine)," *Journal of the American Chemical Society*, vol. 112, no. 8, pp. 3188–3191, 1990.

[31] H. Komatsu and P. L. G. Chong, "Low permeability of liposomal membranes composed of bipolar tetraether lipids from thermoacidophilic archaebacterium *Sulfolobus acidocaldarius*," *Biochemistry*, vol. 37, no. 1, pp. 107–115, 1998.

[32] E. L. Chang, "Unusual thermal stability of liposomes made from bipolar tetraether lipids," *Biochemical and Biophysical Research Communications*, vol. 202, no. 2, pp. 673–679, 1994.

[33] G. L. Marieke, M. G. L. Elferink, J. G. de Wit, A. J. M. Driessen, and W. N. Konings, "Stability and proton-permeability of liposomes composed of archaeal tetraether lipids," *Biochimica et Biophysica Acta*, vol. 1193, no. 2, pp. 247–254, 1994.

[34] G. D. Sprott, B. J. Agnew, and G. B. Patel, "Structural features of ether lipids in the archaeobacterial thermophiles *Pyrococcus furiosus, Methanopyrus kandleri, Methanothermus fervidus*, and *Sulfolobus acidocaldarius*," *Canadian Journal of Microbiology*, vol. 43, no. 5, pp. 467–476, 1997.

[35] M. Nishihara and Y. Koga, "Extraction and composition of polar lipids from the archaebacterium, *Methanobacterium thermoautotrophicumml*: effective extraction of tetraether lipids by an acidified solvent," *Journal of Biochemistry*, vol. 101, no. 4, pp. 997–1005, 1987.

[36] M. Nishihara, H. Morii, K. Matsuno, M. Ohga, K. O. Stetter, and Y. Koga, "Structural analysis by reductive cleavage with $LiAlH_4$ of an allyl ether choline-phospholipid, archaetidylcholine, from the hyperthermophilic methanoarchaeon *Methanopyrus kandleri*," *Archaea*, vol. 1, no. 2, pp. 123–131, 2002.

Hindawi Publishing Corporation
Archaea
Volume 2012, Article ID 285152, 9 pages
doi:10.1155/2012/285152

Research Article

Effect of Growth Medium pH of *Aeropyrum pernix* on Structural Properties and Fluidity of Archaeosomes

Ajda Ota,[1] Dejan Gmajner,[1] Marjeta Šentjurc,[2] and Nataša Poklar Ulrih[1,3]

[1] *Department of Food Science and Technology, Biotechnical Faculty, University of Ljubljana, Jamnikarjeva 101, 1000 Ljubljana, Slovenia*
[2] *EPR Center, Institute Jožef Stefan, Jamova 39, 1000 Ljubljana, Slovenia*
[3] *Centre of Excellence for Integrated Approaches in Chemistry and Biology of Proteins (CipKeBiP), Jamova 39, 1000 Ljubljana, Slovenia*

Correspondence should be addressed to Nataša Poklar Ulrih, natasa.poklar@bf.uni-lj.si

Received 11 January 2012; Revised 30 March 2012; Accepted 13 April 2012

Academic Editor: Parkson Chong

The influence of pH (6.0; 7.0; 8.0) of the growth medium of *Aeropyrum pernix* K1 on the structural organization and fluidity of archaeosomes prepared from a polar-lipid methanol fraction (PLMF) was investigated using fluorescence anisotropy and electron paramagnetic resonance (EPR) spectroscopy. Fluorescence anisotropy of the lipophilic fluorofore 1,6-diphenyl-1,3,5-hexatriene and empirical correlation time of the spin probe methylester of 5-doxylpalmitate revealed gradual changes with increasing temperature for the pH. A similar effect has been observed by using the trimethylammonium-6-diphenyl-1,3,5-hexatriene, although the temperature changes were much smaller. As the fluorescence steady-state anisotropy and the empirical correlation time obtained directly from the EPR spectra alone did not provide detailed structural information, the EPR spectra were analysed by computer simulation. This analysis showed that the archaeosome membranes are heterogeneous and composed of several regions with different modes of spin-probe motion at temperatures below 70°C. At higher temperatures, these membranes become more homogeneous and can be described by only one spectral component. Both methods indicate that the pH of the growth medium of *A. pernix* does not significantly influence its average membrane fluidity. These results are in accordance with TLC analysis of isolated lipids, which show no significant differences between PLMF isolated from *A. pernix* grown in medium with different pH.

1. Introduction

Archaea are the third domain of living organisms, and they have cell structures and components that are markedly different from those of bacteria and eukaryotes. The glycerol ether lipids are the main feature that distinguishes the members of archaea from bacteria and eukarya [1]. In contrast to bacteria and eukarya, where the acyl chains of the membrane phospholipids are ester-linked to the *sn*-glycerol-3-phosphate scaffold, the backbone of archaeal lipids is composed of *sn*-glycerol-1-phosphate, with isoprenoid groups connected *via* ether linkages [2–7].

Aeropyrum pernix K1 was the first absolutely aerobic, hyperthermophilic archaeon that was isolated from a costal solfataric thermal vent in Japan [8]. The polar lipids of *A. pernix* K1 consist solely of $C_{25,25}$-archaeol (2,3-di-sesterpanyl-*sn*-glycerol), with $C_{25,25}$-archetidyl(glucosyl)inositol (AGI) accounting for 91 mol%, and $C_{25,25}$-archetidylinositol (AI) accounting for the remaining 9 mol% (Figure 1). Membranes composed of such $C_{25,25}$ diether lipids have 20% greater thickness than those composed of tetraether $C_{20,20}$ archaeal-based lipids [9].

Over the last five years, we have investigated the influence of some environmental factors on the structural properties of the membrane of *A. pernix in vivo* using electron paramagnetic resonance (EPR) and fluorescence emission spectrometry [10]. These studies included the influence of pH and temperature on the physiochemical properties of bilayer archaeosomes prepared from a polar-lipid methanol fraction (PLMF) isolated from *A. pernix* cells grown at 92°C at pH 7.0, of mixed liposomes prepared from mixtures of this PLMF and 1,2-dipalmitoyl-*sn*-glycero-3-phosphoholine

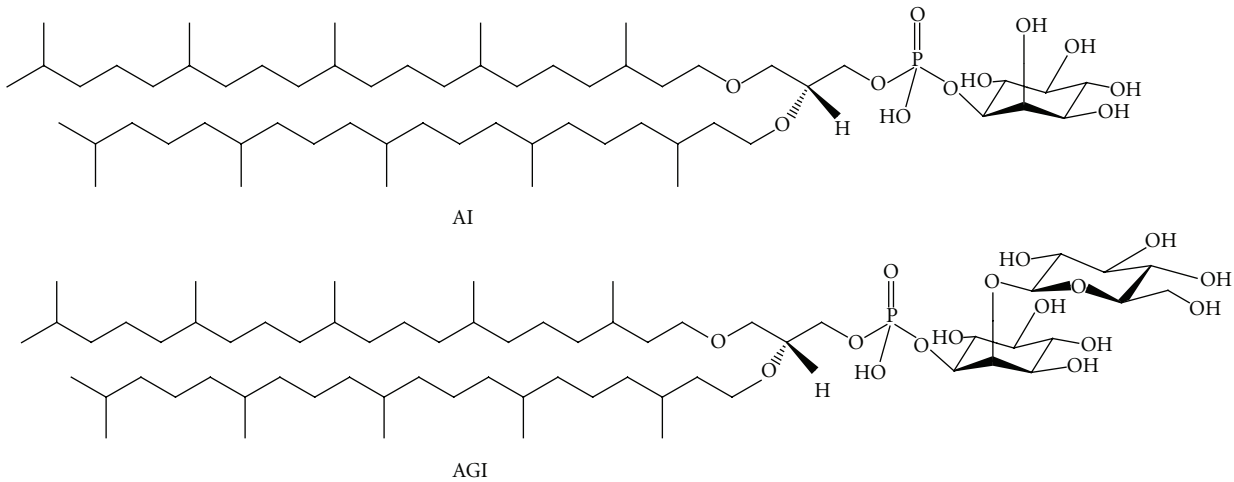

Figure 1: Structural formulas of 2,3-di-*O*-sesterpanyl-*sn*-glycerol-1-phospho-myo-inositol ($C_{25,25}$-archetidylinositol) (top: AI) and 2,3-di-*O*-sesterpanyl-*sn*-glycerol-1-phospho-1′-(2′*O*-*α*-D-glucosyl)-myo-inositol ($C_{25,25}$-archetidyl(glucosyl)inositol) (bottom: AGI).

(DPPC) at different ratios [11–13]. The major conclusion based on our differential scanning calorimetry (DSC) was that the archaeosomes do not show gel to liquid crystalline phase transition in the temperature range from 0 to 100°C [11].

Through these investigations of *A. pernix in vivo*, we have shown that the growth medium pH influences the initial growth rate and cell density [14]. A pH below 7.0 was less favourable than pH 8.0, and there was no growth of *A. pernix* at pH 5.0. Using the EPR and fluorescence emission measurements, changes in the distribution of the spin probes and their motional characteristic were monitored. These changes reflect the changes in the membrane domain structure with temperature, and they were different for *A. pernix* grown at pH 6.0 than at pH 7.0 and 8.0 [10]. Macalady and coworkers (2004) [15] suggested that there is a strong correlation between core-lipid composition and optimal pH of the growth medium.

In the present study, we have extended our EPR and fluorescence emission spectrometry to investigate the influence of growth medium pH (6.0; 7.0; 8.0) on the physiochemical properties of bilayer archaeosomes prepared from this PLMF from *A. pernix*.

2. Materials and Methods

2.1. Growth of A. pernix K1. *A. pernix* K1 was purchased from Japan Collection of Microorganisms (number 9820; Wako-shi, Japan). The culture medium comprised (per litre): 34.0 g marine broth 2216 (Difco Becton, Dickinson & Co., Franklin Lakes, NJ, USA), 5.0 g Trypticase Peptone (Becton, Dickinson and Company, Sparks, USA), 1.0 g yeast extract (Becton, Dickinson and Company, Sparks, USA) and 1.0 g $Na_2S_2O_3 \bullet 5H_2O$ (Sigma-Aldrich, St. Louis, USA). The buffer systems used were 20 mM MES [2-(N-morpholino)ethanesulfonic acid; Acros Organics, Geel, Belgium] for growth at pH 6.0, and 20 mM HEPES [4-(2-hydroxyethyl)-1-piperazineethanesulfonic acid; Sigma-Aldrich Chemie GmbH, Steinheim, Germany] for growth at pH 7.0 and pH 8.0. The *A. pernix* cells were grown in 800 mL growth medium in 1000 mL heavy-walled flasks, with a magnetic stirring hot plate and forced aeration (0.5 $L \cdot min^{-1}$) at 92°C, as described previously [14].

2.2. Isolation and Purification of Lipids. The PLMF that is composed of approximately 91% AGI and 9% AI (average molecular weight of 1181.42 $g \cdot mol^{-1}$) was prepared from the lyophilised *A. pernix* cells as described previously [11]. The lipids were fractionated using adsorption chromatography and analysed by TLC with the chloroform/methanol/acetic acid/water (85/30/15/5) solvent. Analysis was performed by 0.04 mg of PLMF isolated from *A. pernix* grown at different pH. TLC plate was developed and sprayed with 20% H_2SO_4. Lipid spots were visualized by heating at 180°C for 20 minutes [9]. TLC plates were analysed using JustTLC software (Version 3.5.3. http://www.sweday.com/), where intensity ratio of the two lipid components was compared. No differences between PLMF isolated from *A. pernix* grown in medium with different pH were observed (Figure 2).

The methanol fraction containing the polar lipids (PMLF) was used for further analysis. This lipid solution was dried by slow evaporation under a constant flow of dry nitrogen, followed by vacuum evaporation of solvent residues.

2.3. Preparation of Archaeosomes. The appropriate weights of the dried PLMF were dissolved in chloroform and transferred into glass round-bottomed flasks, where the solvent was evaporated under reduced pressure (17 mbar). The dried lipid films were then hydrated with the aqueous buffer solutions. As indicated above, the following 20 mM buffer solutions were used: MES for pH 6.0 and HEPES for pH 7.0 and 8.0. The final concentration of the lipids was 10 $mg \cdot mL^{-1}$. Multilamellar vesicles (MLVs) were prepared by vortexing the lipid suspensions for 10 min. The MLVs were further transformed into small unilamellar vesicles

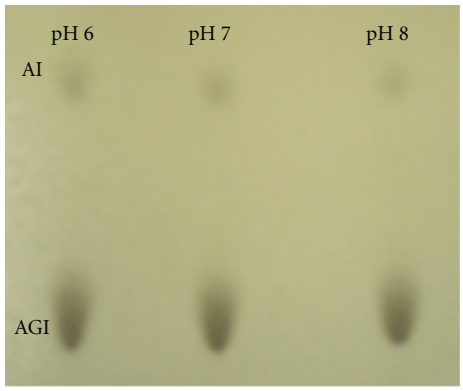

Figure 2: TLC results of PLMF from *A. pernix* grown at different pH as marked. AI and AGI stands for $C_{25,25}$-archetidylinositol and $C_{25,25}$-archetidyl(glucosyl)inositol, respectively.

(SUVs) by 30 min sonication with 10 s on-off cycles at 50% amplitude with a Vibracell Ultrasonic Disintegrator VCX 750 (Sonics and Materials, Newtown, USA). To separate the debris from SUVs after sonification, the sample was centrifuged for 10 min at 14.000 rpm (Eppendorf Centrifuge 5415C).

2.4. Fluorescence Anisotropy Measurements. Fluorescence anisotropy measurements of 1,6-diphenyl-1,3,5-hexatriene (DPH) and trimethylammonium-6-phenyl-1,3,5-hexatriene (TMA-DPH) (Figure 3) in PLMF archaeosomes were performed in a 10 mm-path-length cuvette using a Cary Eclipse fluorescence spectrophotometer (Varian, Mulgrave, Australia), in the temperature range from 20°C to 90°C, and the pH range from 6.0 to 8.0 in the relevant buffer solutions. Varian autopolarizers were used, with slit widths with a nominal band-pass of 5 nm for both excitation and emission. Here, 10 μL DPH or TMA-DPH (Sigma-Aldrich Chemie GmbH, Steinheim, Germany) in dimethyl sulphoxide (Merck KGaA, Darmstadt, Germany) was added to 2.5 mL 100 μM solutions of SUVs prepared from the PLMF from *A. pernix* in the relevant buffer, to reach a final concentration of 0.5 μM DPH and 1.0 μM TMA-DPH. DPH and TMA-DPH fluorescence anisotropy was measured at the excitation wavelength of 358 nm, with the excitation polarizer oriented in the vertical position, while the vertical and horizontal components of the polarized emission light were recorded through a monochromator at 410 nm for both probes. The emission fluorescence of DPH and TMA-DPH in aqueous solution is negligible. The anisotropy (r) was calculated using the built-in software of the instrument (1):

$$r = \frac{I_{||} - I_{\perp}}{I_{||} + 2I_{\perp}}, \tag{1}$$

where, $I_{||}$ and $I_{\perp}$ are the parallel and perpendicular emission intensities, respectively. The values of the G-factor [the ratio of the sensitivities of the detection system for vertically (I_{HV}) and horizontally polarized light (I_{HH})] were determined for each sample separately.

The lipid-order parameter S was calculated from the anisotropy using the analytical expression given in (2) [16]:

$$S = \frac{\left[1 - 2(r/r_0) + 5(r/r_0)^2\right]^{1/2} - 1 + r/r_0}{2(r/r_0)}, \tag{2}$$

where r_0 is the fluorescence anisotropy of DPH in the absence of any rotational motion of the probe. The theoretical value of r_0 of DPH is 0.4, while the experimental values of r_0 lie between 0.362 and 0.394 [16]. In our calculation, the experimental value of $r_0 = 0.370$ and $r_0 = 0.369$ for DPH and TMA-DPH in DPPC at 5°C was used, respectively.

2.5. Electron Paramagnetic Resonance Measurements. For the EPR measurements, the PLMF SUVs were spin-labelled with a methylester of 5-doxyl palmitic acid [MeFASL(10,3)] (Figure 3), and the EPR spectra recorded with a Bruker ESP 300 X-band spectrometer (Bruker Analytische Messtechnik, Rheinstein, Germany). The MeFASL(10,3) lipophilic probe was selected due to its moderate stability in the membrane and its relatively high-resolution capability for local membrane ordering and dynamics. It is dissolved in the phospholipid bilayer with nitroxide group located in the upper part of the layers.

With the MeFASL(10,3) film dried on the wall of a glass tube, 50 μL 10 mg·mL^{-1} PLMF SUVs in the relevant buffer was added, and the sample was vortexed for 15 min. This was designed for a final molar ratio of MeFASL(10,3): lipids of 1 : 250. The sample was transferred to a capillary (75 mm; Euroglas, Slovenia), and the EPR spectra were recorded using the following parameters: centre field, 332 mT; scan range, 10 mT; microwave power, 20.05 mW; microwave frequency, 9.32 GHz; modulation frequency, 100 kHz; modulation amplitude, 0.2 mT; temperature range; 5°C to 95°C. Each spectrum was the average of 10 scans, to improve the signal-to-noise ratio. From the EPR spectra, the mean empirical correlation time (τ_c) was calculated using (3) [17]:

$$\tau_c = k\Delta H_0\left[(h_0/h_{-1})^{1/2} - 1\right]. \tag{3}$$

The line width (ΔH_0; in mT) and the heights of the mid-field (h_0)and high-field (h_{-1}) lines were obtained from the EPR spectrum (Figure 6); k is a constant typical for the spin probe, which is 5.9387×10^{-11} mT^{-1} for MeFASL (10,3) [17].

2.6. Computer Simulation of the EPR Spectra. For more precise descriptions of the membrane characteristics, computer simulations of the EPR spectra line shapes were performed using the EPRSIM programme (Janez Štrancar, 1996-2003, http://www2.ijs.si/~jstrancar/software.htm). Generally, to describe the EPR spectra of spin labels, the stochastic Liouville equation is used [18–20]. However, in a membrane system labelled with fatty acid spin probes, local rotational motions are fast with respect to the EPR time scale. Modeling of the spectra taken at physiological temperature is therefore simplified by restricting the motions to the fast motional regime. Since the basic approach was already discussed elsewhere [21, 22], it is only summarized here. The model

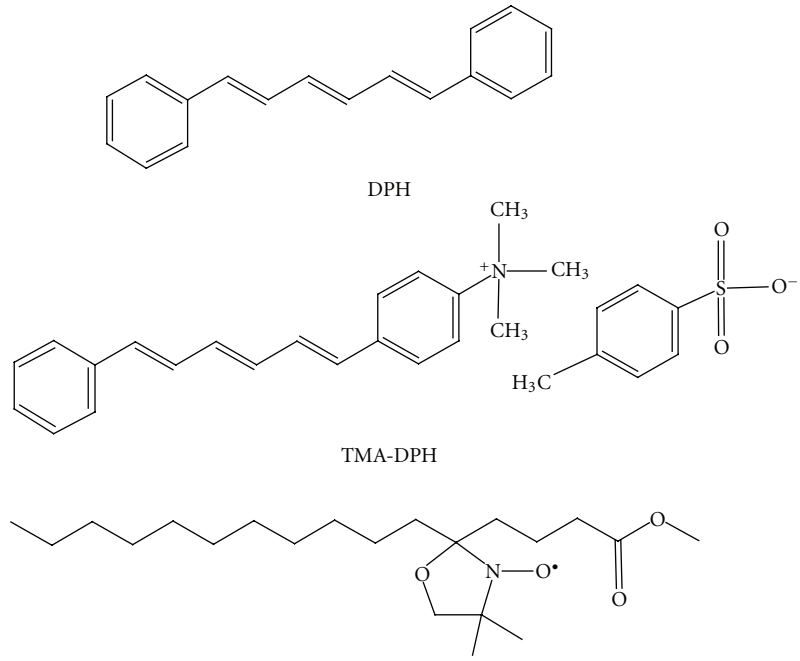

Figure 3: Structural formulas of 1,6-diphenyl-1,3,5-hexatriene (DPH), trimethylammonium-6-phenyl-1,3,5-hexatriene (TMA-DPH), and methylester of 5-doxyl palmitic acid [MeFASL (10,3)].

takes into account that the membrane is heterogeneous, and is composed of several regions that have different fluidity characteristics. Therefore, the EPR spectra are composed of several spectral components that reflect the different modes of restricted rotational motion of the spin probe molecules in the different membrane environments. Each spectral component is described by a set of spectral parameters that define the line shape. These are the order parameter (S), the rotational correlation time (τ_c), the line width correction (W), and the polarity correction factors of the magnetic tensors g and A (p_g and p_A, resp.). The S describes the orientational order of the phospholipid alkyl chains in the membrane domains, with $S = 1$ for perfectly ordered chains and $S = 0$ for isotropic alignment of the chains. Membrane domains that are more fluid are characterized by a smaller S. The τ_c describes the dynamics of the alky chain motion, with the W due to the unresolved hydrogen superhyperfine interactions, and contributions from other paramagnetic impurities (e.g., oxygen, external magnetic field inhomogeneities). The p_g and p_A polarity correction factors arise from the polarity of the environment of the spin probe nitroxide group (p_g and p_A are large in more polar environment and are below 1 in hydrophobic region). Beside these parameters, the line shape of the EPR spectra is defined by the relative proportions of each of the spectral components (d), which describes the relative amount of the spin probe with a particular motional mode, and which depends on the distribution of the spin probe between the coexisting domains with different fluidity characteristics. As the partition of the MeFASL (10,3) was found to be approximately equal between the different types of domains of phospholipid/cholesterol vesicles [23], we assumed that the same is valid also for these PLMF liposomes.

It should be stressed that the lateral motion of the spin probe is slow on the time scale of the EPR spectra [24]. Therefore, an EPR spectrum describes only the properties of the nearest surroundings of a spin probe on the nm scale. All of the regions in the membrane with similar modes of spin probe motion contribute to one and the same spectral component. Thus, each spectral component reflects the fluidity characteristics of a certain type of membrane nanodomain (with dimensions of several nm) [25].

To obtain best fit of calculated-to-experimental spectra, stochastic and population-based genetic algorithm is combined with Simplex Downhill optimization method into the evolutionary optimization method (HEO), which requires no special starting points and no user intervention [26]. In order to get a reasonable characterization one still has to define the number of spectral components before applying the optimization. To resolve this problem multirun HEO optimization is used together with a newly developed GHOST condensation procedure. According to this method, 200 independent HEO simulation runs for each EPR spectrum were applied, taking into account 4 different motional modes of spin probe (23 spectral parameters), which is around the resolution limit of EPR nitroxide experiments. From these runs only the set of parameters, which correspond to the best fits were used. All the best-fit sets of parameters obtained by 200 optimizations were evaluated according to the goodness of the fit (χ^2 filter) and according to the similarity of the parameter values of best fits (density filter). The parameters of the best fits were presented by

three two-dimensional cross-section plots using four spectral parameters: order parameter S, rotational correlation time τ_c, line broadening W, and polarity correction factor p_A (S-τ_c, S-W, and S-p_A). Groups of solutions, which represent the motional modes of spin probes in particular surrounding and which could correspond to different membrane regions, can be resolved either graphically on GHOST diagrams or numerically within GHOST condensation. Starting values of parameters of spectral components were defined using the average parameters taken from the GHOST diagrams [27]. From these plots information about the motional patterns, defined with S, τ_c, W, and p_A in different membrane regions can be obtained. In this way, the changes in the spin probe motional patterns in different membrane regions, due to the interaction of membrane with biologically active compound, due to temperature, pH, and changes in membrane composition, can be studied.

3. Results and Discussion

3.1. Fluorescence Anisotropy Measurements. Fluorescence probes have been widely used in the study of the structure and dynamic of biological membranes [28]. Their photophysical properties are affected by the physicochemical changes of the microenvironment where the probes are located. Two common probes for the study of membrane properties are DPH and its cationic derivative TMA-DPH. Since DPH is a hydrophobic probe, it is incorporated in the inner apolar core at different positions along the membrane, while the polar group region of TMA-DPH remains anchored at the lipid-water interface of the membrane with the hydrocarbon chain entering the lipid part of the membrane. Xu and London [29] showed that anisotropy values are highest in gel states, lowest in liquid-disordered states, and intermediate in liquid-ordered states. DPH and TMA-DPH r depend on the degree of molecular packing of membrane chains and can be related to the order parameter S. The fluidity may be defined as the reciprocal of the lipid order parameter S [30].

The levels of order in the SUVs composed of PLMF isolated from *A. pernix* grown at pH 6.0, pH 7.0, and pH 8.0 and measured at the same pHs or at pH 7.0 were calculated from anisotropy measurements of DPH (Figures 4(a) and 4(b)) and TMA-DPH (Figures 5(a) and 5(b)), respectively. No significant differences in the order parameters of archaeosomes were observed regardless the growth medium of the *A. pernix* cells or measured pH in the tested temperature range. The order parameter determined by applying DPH of these archaeosomes steadily decreased with increasing temperature, which indicates a gradual increase in membrane fluidity (Figures 4(a) and 4(b)). Previously, we have shown also by applying DSC that in the range from 0°C to 100°C, the archaeosomes do not undergo gel-to-liquid crystalline phase transition [11]. The initial values of the order parameter of DPH at 20°C were: pH 6.0, 0.72 ± 0.1; pH 7.0, 0.72 ± 0.1; pH 8.0, 0.73 ± 0.1. Similarly, we have not detected the significant differences in the order parameter determined by applying TMA-DPH in archaeosomes regardless

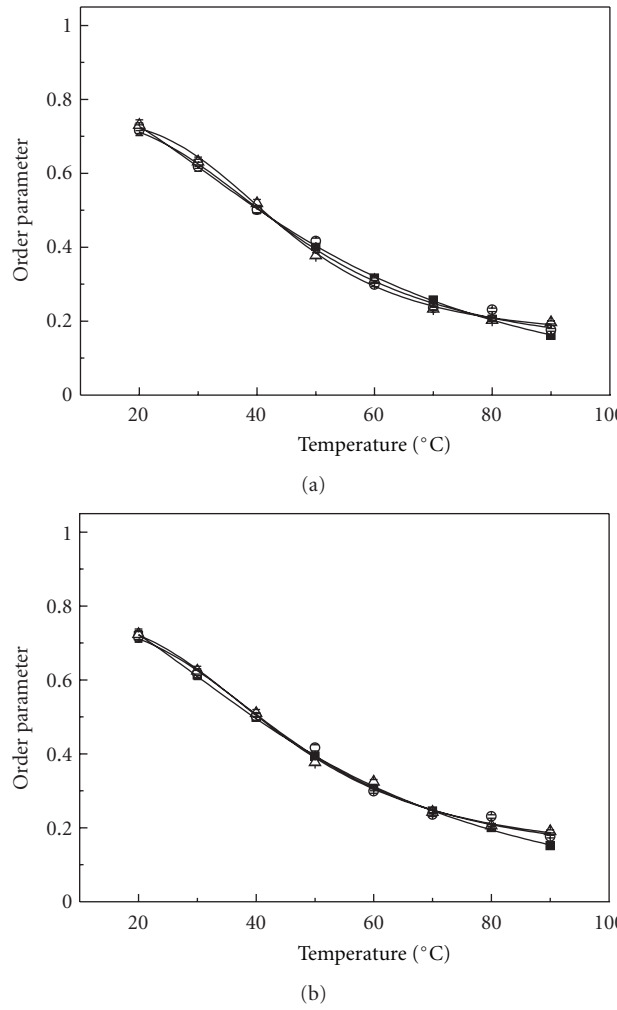

Figure 4: Temperature dependence of the lipid-order parameter of the PLMF from *A. pernix* grown in medium with different pH (■ pH 6.0; ○ pH 7.0; Δ pH 8.0) determined by measuring the anisotropy of DPH. The lines represent nonlinear curve fitting to the data points. (a) pH of measured samples was the same as the pH of growth medium; (b) experiments were performed at pH 7.0.

the growth or measured pH values. The initial value of order parameter of TMA-DPH in comparison to DPH in archaeal lipids at the same temperature and pH was higher: pH 6.0, 0.93 ± 0.1; pH 7.0, 0.91 ± 0.1; pH 8.0, 0.91 ± 0.1. Another observation, which should be stressed is that the changing in the order parameter determined by TMA-DPH is less temperature sensitive (Figures 5(a) and 5(b)). This might not be surprising since TMA-DPH is cationic probe located at the lipid-water interface of the membrane and the archaeosomes (SUV) have zeta potential of −50 mV [11]. The zeta potential of archaeosomes (LUV) was not changed with pH in the pH range from 5.0 to 10.0 [11]. It is likely that in the studied pH range from 6.0 to 8.0 the zeta potential of SUV archaeosomes is also not changing, which correlate with no observed changes in TMA-DPH anisotropy with pH.

The fact that we have not determined any significant differences in the behaviour of two fluorescence probes regardless the pH of growth medium of *A. pernix*, suggest

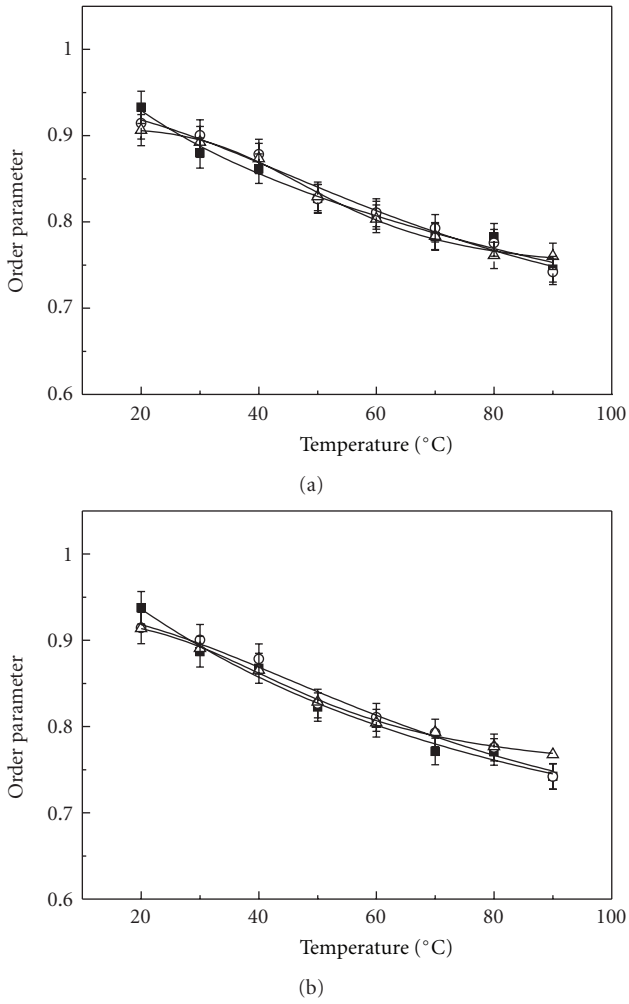

Figure 5: Temperature dependence of the lipid order parameter of the PLMF from *A. pernix* grown in medium with different pH (■ pH 6.0; ◯ pH 7.0; Δ pH 8.0) determined by measuring the anisotropy of TMA-DPH. The lines represent nonlinear curve fitting to the data points. (a) pH of measured samples was the same as the pH of growth medium; (b) experiments were performed at pH 7.0.

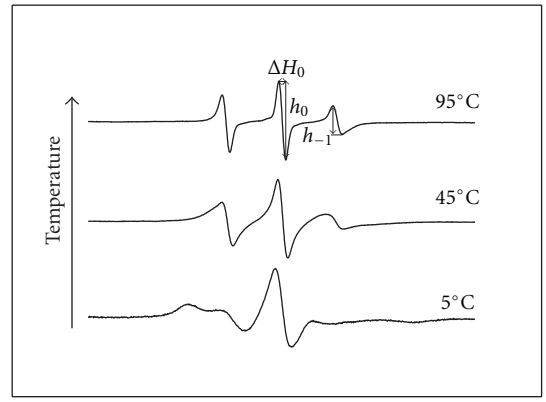

Figure 6: Representative EPR spectra of MeFASL(10,3) in the membrane of the SUV archaeosomes at pH 7.0 prepared from the PLMF isolated from *A. pernix* grown at pH 7.0.

that the lipid composition is not changing in the studied pH range of growing (from pH 6.0 to 8.0) or in the measured pH range from 6.0 to 8.0. This statement was supported by the TLC results of PLMF of *A. pernix* growth at different pHs (Figure 2). The ratio between two major lipids component in *A. pernix* membrane $C_{25,25}$-archetidylinositol (AI) and $C_{25,25}$-archetidyl(glucosyl)inositol (AGI) is at growth pH 6.0 and 7.0: 9 ± 1% of AI and 91 ± 1% of AGI and at growth pH 8.0: 8 ± 1% of AI and 92 ± 1% of AGI.

3.2. Electron Paramagnetic Resonance Measurements. The empirical correlation times of MeFASL(10,3) in these liposomes prepared from the PLMF isolated from *A. pernix* were measured directly from the EPR spectra (Figure 6). These decreased gradually with temperature and did not show significant differences with respect to the pH of the growth medium (Figure 7). The empirical correlation time reflect an average ordering and dynamics of the phospholipid alkyl chains in the spin-probe nitroxide group surrounding and is in inverse relation to membrane fluidity. The data correlate well with fluorescence anisotropy measurements of DPH incorporated into archaeosomes, which shows that the membrane fluidity increases with temperature, but on average it does not depend on the pH of the growth medium. Similar results have been reported for archaeosomes composed of bipolar tetraether lipids [31].

To obtain more detailed information about the possible influences of different growth medium pH on the membrane structural characteristics and on their changes with temperature, computer simulations of the EPR spectra were performed. At temperatures below 70°C, good fits with the experimental spectra were obtained taking into account that the spectra are composed of at least three spectral components. This indicates that the archaeosome membranes are heterogeneous and composed of several regions with different modes of spin-probe motions. All of the regions in the membranes with the same fluidity characteristics are described by a single spectral component. The corresponding EPR parameters determine motional pattern of the spin probe, irrespective to its location in the membrane. Smaller regions with the same physical characteristics could not be distinguished from few large regions. This also means that EPR does not necessarily reflect directly the macroscopic properties of the membrane or large membrane domains, but reflects also the membrane superstructure on nm scale. The three motional patterns of spin probe observed could be due to the two-component lipid composition (AI and AGI) of the membrane. Additionally, some dynamic fluctuations of phospholipids or vertical motion of spin probe within the membrane can be detected as a specific motional pattern of spin probe. These motional patterns could be altered if the membrane is influenced by some external perturbations or if the membrane composition is changed. At higher temperatures, the membranes become more homogeneous and can be described by only one spectral component. The changes in the order parameters of the different membrane

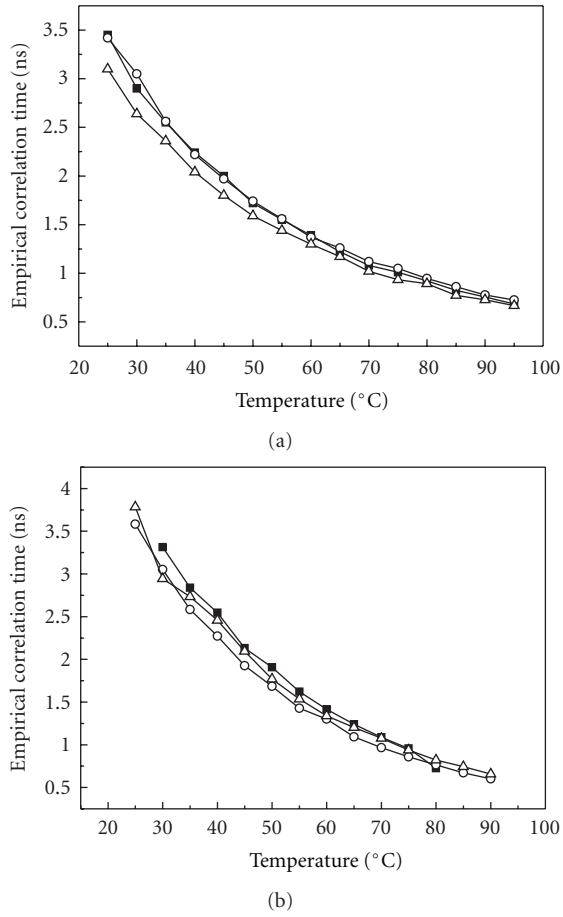

Figure 7: Temperature dependence of empirical correlation time (τ_c) of MeFASL(10,3) in SUV archaeosomes prepared from PLMF lipids isolated from *A. pernix* grown in medium with different pH (■ pH 6.0; ○ pH 7.0; Δ pH 8.0) and measured at the same pHs (a) and at pH 7.0 (b). Empirical correlation time was calculated directly from the EPR spectra according to Equation (3).

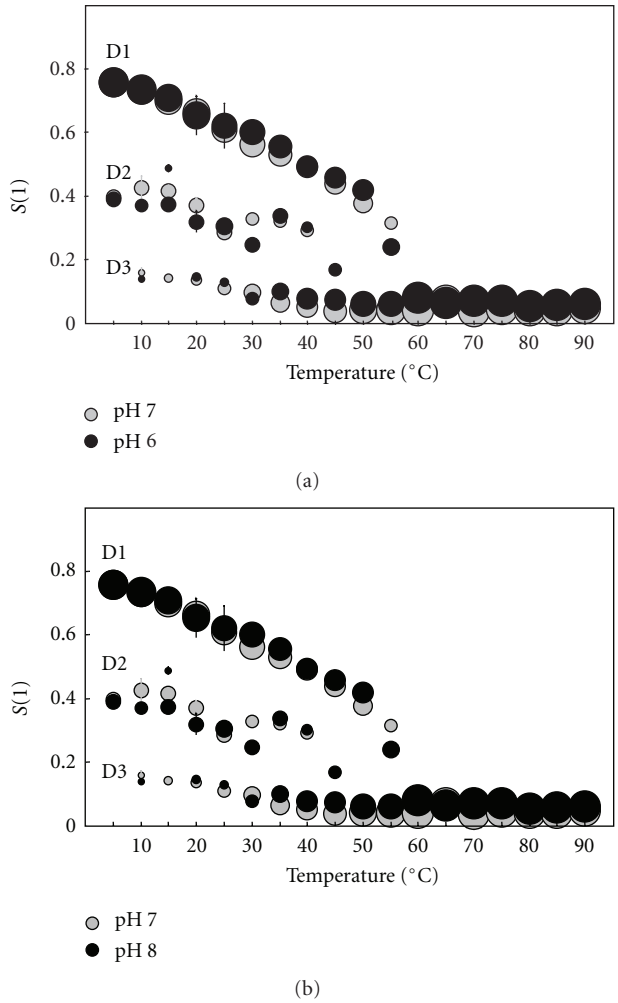

Figure 8: Temperature dependence of the order parameters (S) and proportions of MeFASL(10,3) in the membrane regions of the SUV archaeosomes prepared from the PLMF from *A. pernix* grown at pH 6.0 (black circles) and 7.0 (grey circles) (a), and at pH 7.0 (grey circles) and 8.0 (black circles) (b). The diameters of the symbols indicate the proportions of each region. D1, D2, and D3 indicate the regions with the highest, intermediate-and lowest-order parameters, respectively. Experiments were performed at pH 7.0.

regions and their proportions with temperature are shown in the form of bubble diagrams in Figure 8, where the dimensions of each symbol represent the proportions of the spin probes in the corresponding membrane regions. With increasing temperature, the order parameter of the most ordered region decreases, its proportion decreases and disappears in the temperature region between 55°C and 65°C. The proportions of the less ordered regions increase with increasing temperature, and above 70°C these remain unchanged. The calculated order parameters for the samples grown at different pH and measured at pH 7.0 are in the range uncertainty of the calculation.

Order parameters obtained by fluorescence measurement (Figures 4 and 5) and those obtained by computer simulation of EPR spectra (Figure 8) cannot be directly compared since the three probes (Figure 3), which differ appreciably in their shape and dimensions cause different perturbations in their surrounding and monitors the properties at different depth of the membrane. DPH is highly hydrophobic and reflects the properties in the inner apolar core at different positions along the membrane, TMA-DPH is anchored at water-lipid interface, while MeFASL(10,3) with nitroxide group on the 5th C atom (counting from the methyl-ester group) monitors the properties in the upper part of phospholipid layers but exhibit also some translational motion within the membrane. Besides by fluorescence polarization measurements an average order parameter in the membrane is obtained, while by computer simulation of EPR spectra order parameter is distinguished from the rotational rate and reflects differe surroundings of the spin probe at lower temperatures, which could be due to membrane heterogeneity produced by distribution between AI and AGI of the membrane but can as well be the consequence of some fluctuations or vertical motion of the spin probe within the bilayer, which seems to be influenced by temperature.

4. Conclusions

Fluorescence anisotropy measurements of DPH and TMA-DPH in addition to EPR spectrometry here showed steady decreases in the order parameter of archaeal lipids with increasing temperature, regardless the pH of growth of archaea or measuring pH. This indicates a gradual increase in the membrane fluidity in all of these samples, although no significant differences were seen for the influence of the *A. pernix* growth medium pH. TMA-DPH located close to water-lipid interface shows less temperature dependence in comparison of DPH or MeFASL(10,3). The more detailed analysis using computer simulation of the EPR spectra revealed membrane heterogeneity at temperatures below 55°C, which disappears at higher temperatures. But the EPR parameters calculated from the spectra of archaeosomes obtained from the PLMF from *A. pernix* grown at different pH and measured at pH 7.0 remains in the range of the calculation uncertainty. The results are supported by TLC analysis of isolated lipids, which show no significant differences between PLMF isolated from *A. pernix* grown in medium with different pHs.

To summarize, the present data showed that cell growth pH has no effect on membrane properties being examined. The previous *in vivo* study [14] showed that the cell growth varies with medium pH. This discrepancy is interesting since the polar lipids of *A. pernix* K1 consist solely of $C_{25,25}$-archeaol, which has not been changed by growth pH according to our data presented here. Previously, we have reported that the maximum cell density of *A. pernix* growth at pH 7.0 and 8.0 conditions were similar, while a significantly lower maximum cell density was obtained at pH 6.0 and no growth at pH 5.0 [14]. It is likely that at pHs lower than 6.0 the membranes of the neutrophilic *A. pernix* composed of $C_{25,25}$-archaeol becomes proton permeable and that the permeability is not regulated by lipid composition.

Acknowledgments

The authors would like to express their gratitude for financial support from the Slovenian Research Agency through the P4-0121 research programme and the J2-3639 project. A. Ota was partly financed by the European Social Fund of the European Union.

References

[1] C. R. Woese, O. Kandler, and M. L. Wheelis, "Towards a natural system of organisms: proposal for the domains Archaea, Bacteria, and Eucarya," *Proceedings of the National Academy of Sciences of the United States of America*, vol. 87, no. 12, pp. 4576–4579, 1990.

[2] A. A. H. Pakchung, P. J. L. Simpson, and R. Codd, "Life on earth. Extremophiles continue to move the goal posts," *Environmental Chemistry*, vol. 3, no. 2, pp. 77–93, 2006.

[3] J. Peretó, P. López-García, and D. Moreira, "Ancestral lipid biosynthesis and early membrane evolution," *Trends in Biochemical Sciences*, vol. 29, no. 9, pp. 469–477, 2004.

[4] N. P. Ulrih, D. Gmajner, and P. Raspor, "Structural and physicochemical properties of polar lipids from thermophilic archaea," *Applied Microbiology and Biotechnology*, vol. 84, no. 2, pp. 249–260, 2009.

[5] Y. Koga and H. Morii, "Recent advances in structural research on ether lipids from archaea including comparative and physiological aspects," *Bioscience, Biotechnology and Biochemistry*, vol. 69, no. 11, pp. 2019–2034, 2005.

[6] Y. Koga and H. Morii, "Biosynthesis of ether-type polar lipids in archaea and evolutionary considerations," *Microbiology and Molecular Biology Reviews*, vol. 71, no. 1, pp. 97–120, 2007.

[7] A. Cambacorta, A. Trincone, B. Nicolaus, L. Lama, and M. De Rosa, "Unique features of lipids of Archaea," *Systematic and Applied Microbiology*, vol. 16, no. 4, pp. 518–527, 1994.

[8] Y. Sako, N. Nomura, A. Uchida et al., "Aeropyrum pernix gen. nov., sp. nov., a novel aerobic hyperthermophilic archaeon growing at temperatures up to 100°C," *International Journal of Systematic Bacteriology*, vol. 46, no. 4, pp. 1070–1077, 1996.

[9] H. Morii, H. Yagi, H. Akutsu, N. Nomura, Y. Sako, and Y. Koga, "A novel phosphoglycolipid archaetidyl(glucosyl)inositol with two sesterterpanyl chains from the aerobic hyperthermophilic archaeon Aeropyrum pernix K1," *Biochimica et Biophysica Acta*, vol. 1436, no. 3, pp. 426–436, 1999.

[10] N. P. Ulrih, U. Adamlje, M. Nemec, and M. Šentjurc, "Temperature- and pH-induced structural changes in the membrane of the hyperthermophilic archaeon Aeropyrum pernix K1," *Journal of Membrane Biology*, vol. 219, no. 1–3, pp. 1–8, 2007.

[11] D. Gmajner, A. Ota, M. Šentjurc, and N. P. Ulrih, "Stability of diether C25,25 liposomes from the hyperthermophilic archaeon Aeropyrum pernix K1," *Chemistry and Physics of Lipids*, vol. 164, no. 3, pp. 236–245, 2011.

[12] D. Gmajner and N. P. Ulrih, "Thermotropic phase behaviour of mixed liposomes of archaeal diether and conventional diester lipids," *Journal of Thermal Analysis and Calorimetry*, vol. 106, no. 1, pp. 255–260, 2011.

[13] D. Gmajner, P. A. Grabnar, M. T. Žnidarič, J. Štrus, M. Šentjurc, and N. P. Ulrih, "Structural characterization of liposomes made of diether archaeal lipids and dipalmitoyl-L-α-phosphatidylcholine," *Biophysical Chemistry*, vol. 158, no. 2-3, pp. 150–156, 2011.

[14] I. Milek, B. Cigić, M. Skrt, G. Kaletunç, and N. P. Ulrih, "Optimization of growth for the hyperthermophilic archaeon Aeropyrum pernix on a small-batch scale," *Canadian Journal of Microbiology*, vol. 51, no. 9, pp. 805–809, 2005.

[15] J. L. Macalady, M. M. Vestling, D. Baumler, N. Boekelheide, C. W. Kaspar, and J. F. Banfield, "Tetraether-linked membrane monolayers in Ferroplasma spp: a key to survival in acid," *Extremophiles*, vol. 8, no. 5, pp. 411–419, 2004.

[16] H. Pottel, W. van der Meer, and W. Herreman, "Correlation between the order parameter and the steady-state fluorescence anisotropy of 1,6-diphenyl-1,3,5-hexatriene and an evaluation of membrane fluidity," *Biochimica et Biophysica Acta*, vol. 730, no. 2, pp. 181–186, 1983.

[17] L. Coderch, J. Fonollosa, M. De Pera, J. Estelrich, A. De La Maza, and J. L. Parra, "Influence of cholesterol on liposome fluidity by EPR. Relationship with percutaneous absorption," *Journal of Controlled Release*, vol. 68, no. 1, pp. 85–95, 2000.

[18] D. E. Budil, L. Sanghyuk, S. Saxena, and J. H. Freed, "Nonlinear-least-squares analysis of slow-motion EPR spectra in one and two dimensions using a modified levenberg-marquardt algorithm," *Journal of Magnetic Resonance—Series A*, vol. 120, no. 2, pp. 155–189, 1996.

[19] B. Robinson, H. Thomann, A. Beth, and L. R. Dalton, "The phenomenon of magnetic resonance: theoretical considerations," in *EPR and Advanced EPR Studies of Biological Systems*,

L. R. Dalton, Ed., pp. 11–110, CRC Press, Boca Raton, Fla, USA, 1985.

[20] D. J. Schneider and J. H. Freed, "Calculating slow motional magnetic resonance spectra: a user's guide," in *Biological Magnetic Resonance: Spin Labeling, Theory and Applications*, L. J. Berliner and J. Reuben, Eds., pp. 1–76, Plenum Press, New York, NY, USA, 1989.

[21] J. Štrancar, M. Šentjurc, and M. Schara, "Fast and accurate characterization of biological membranes by EPR spectral simulations of nitroxides," *Journal of Magnetic Resonance*, vol. 142, no. 2, pp. 254–265, 2000.

[22] H. Schindler and J. Seelig, "EPR spectra of spin labels in lipid bilayers," *Journal of Chemical Physics*, vol. 59, no. 4, pp. 1841–1850, 1973.

[23] Z. Arsov and J. Štrancar, "Determination of partition coefficient of spin probe Between different lipid membrane phases," *Journal of Chemical Information and Modeling*, vol. 45, no. 6, pp. 1662–1671, 2005.

[24] M. E. Johnson, D. A. Berk, D. Blankschtein, D. E. Golan, R. K. Jain, and R. S. Langer, "Lateral diffusion of small compounds in human stratum corneum and model lipid bilayer systems," *Biophysical Journal*, vol. 71, no. 5, pp. 2656–2668, 1996.

[25] J. Štrancar, T. Koklič, and Z. Arsov, "Soft picture of lateral heterogeneity in biomembranes," *Journal of Membrane Biology*, vol. 196, no. 2, pp. 135–146, 2003.

[26] B. Filipič and J. Štrancar, "Tuning EPR spectral parameters with a genetic algorithm," *Applied Soft Computing*, vol. 1, no. 1, pp. 83–90, 2001.

[27] J. Štrancar, T. Koklič, Z. Arsov, B. Filipič, D. Stopar, and M. A. Hemminga, "Spin label EPR-based characterization of biosystem complexity," *Journal of Chemical Information and Modeling*, vol. 45, no. 2, pp. 394–406, 2005.

[28] J. R. Lakowitz, *Principles of Fluorescence Spectroscopy*, Kluwer Academic/Plenum, New York, NY, USA, 2nd edition, 1999.

[29] X. Xu and E. London, "The effect of sterol structure on membrane lipid domains reveals how cholesterol can induce lipid domain formation," *Biochemistry*, vol. 39, no. 5, pp. 843–849, 2000.

[30] J. G. Kuhry, P. Fonteneau, G. Duportail, C. Maechling, and G. Laustriat, "TMA-DPH: a suitable fluorescence polarization probe for specific plasma membrane fluidity studies in intact living cells," *Cell Biophysics*, vol. 5, no. 2, pp. 129–140, 1983.

[31] R. Bartucci, A. Gambacorta, A. Gliozzi, D. Marsh, and L. Sportelli, "Bipolar tetraether lipids: chain flexibility and membrane polarity gradients from spin-label electron spin resonance," *Biochemistry*, vol. 44, no. 45, pp. 15017–15023, 2005.

Hindawi Publishing Corporation
Archaea
Volume 2012, Article ID 832097, 9 pages
doi:10.1155/2012/832097

Research Article

Novel Cardiolipins from Uncultured Methane-Metabolizing Archaea

Marcos Y. Yoshinaga, Lars Wörmer, Marcus Elvert, and Kai-Uwe Hinrichs

Organic Geochemistry Group, MARUM—Center for Marine Environmental Sciences & Department of Geosciences, University of Bremen, 28359 Bremen, Germany

Correspondence should be addressed to Marcos Y. Yoshinaga, marcosyukio@gmail.com

Received 23 December 2011; Accepted 28 February 2012

Academic Editor: Angela Corcelli

Novel cardiolipins from Archaea were detected by screening the intact polar lipid (IPL) composition of microbial communities associated with methane seepage in deep-sea sediments from the Pakistan margin by high-performance liquid chromatography electrospray ionization mass spectrometry. A series of tentatively identified cardiolipin analogues (dimeric phospholipids or bisphosphatidylglycerol, BPG) represented 0.5% to 5% of total archaeal IPLs. These molecules are similar to the recently described cardiolipin analogues with four phytanyl chains from extreme halophilic archaea. It is worth noting that cardiolipin analogues from the seep archaeal communities are composed of four isoprenoidal chains, which may contain differences in chain length (20 and 25 carbon atoms) and degrees of unsaturation and the presence of a hydroxyl group. Two novel diether lipids, structurally related to the BPGs, are described and interpreted as degradation products of archaeal cardiolipin analogues. Since archaeal communities in seep sediments are dominated by anaerobic methanotrophs, our observations have implications for characterizing structural components of archaeal membranes, in which BPGs are presumed to contribute to modulation of cell permeability properties. Whether BPGs facilitate interspecies interaction in syntrophic methanotrophic consortia remains to be tested.

1. Introduction

One of the most prominent aspects of archaeal biochemistry is the structure of their cellular membrane lipids [1]. Archaeal intact polar lipids (IPLs) are composed of a core lipid (isoprenoidal glycerol diethers and tetraethers) and polar headgroups (phosphoester or sugar-linked headgroups, i.e., phospholipids and glycolipids, resp.). Archaeal membrane lipids can be unequivocally differentiated from other domains of life based on the glycerol backbone stereochemistry [2, 3]. In Archaea, the isoprenoid chains are bound at *sn*-2 and *sn*-3 positions of the glycerol backbone exclusively through ether linkages and linked to a phosphate-based and/or a sugar headgroup attached to the *sn*-glycerol-1 (S configuration). Bacteria and eukaryotes contain headgroups attached to the *sn*-glycerol-3 isomer (R configuration) and core lipids (typically *n*- or methyl-branched fatty acids) bound at *sn*-1,2-diacylglycerol.

A peculiar phospholipid type found exclusively in ATP producing bacterial plasma membranes [4] and the inner membrane of mitochondria [5] is cardiolipin (or bisphosphatidylglycerol, BPG). A unique aspect of BPGs is their dimeric structure constituted by phosphatidic acid linked to phosphatidylglycerol by a phosphoester bond displaying four chains in the hydrophobic tail (Figure 1(d)). Such a structural configuration has implications for the organization of biological membranes, for example, the ability to bind to a large variety of unrelated proteins and the ability to trap protons in energy-converting membranes [6–8]. BPGs and sulfoglycosylated dimeric phospholipids attached to four phytanyl chains have previously been found in extreme halophilic Archaea from natural habitats and cultures [9–11]. In these Archaea, complex dimeric phospholipids are involved in osmoadaptation [12, 13] and cytochrome *c* oxidase activity [14].

Here, we report the structural diversity of novel BPGs and the presence of novel diether lipids in methane-metabolizing Archaea inhabiting surface sediments of methane-charged deep-ocean seeps. These sediments are

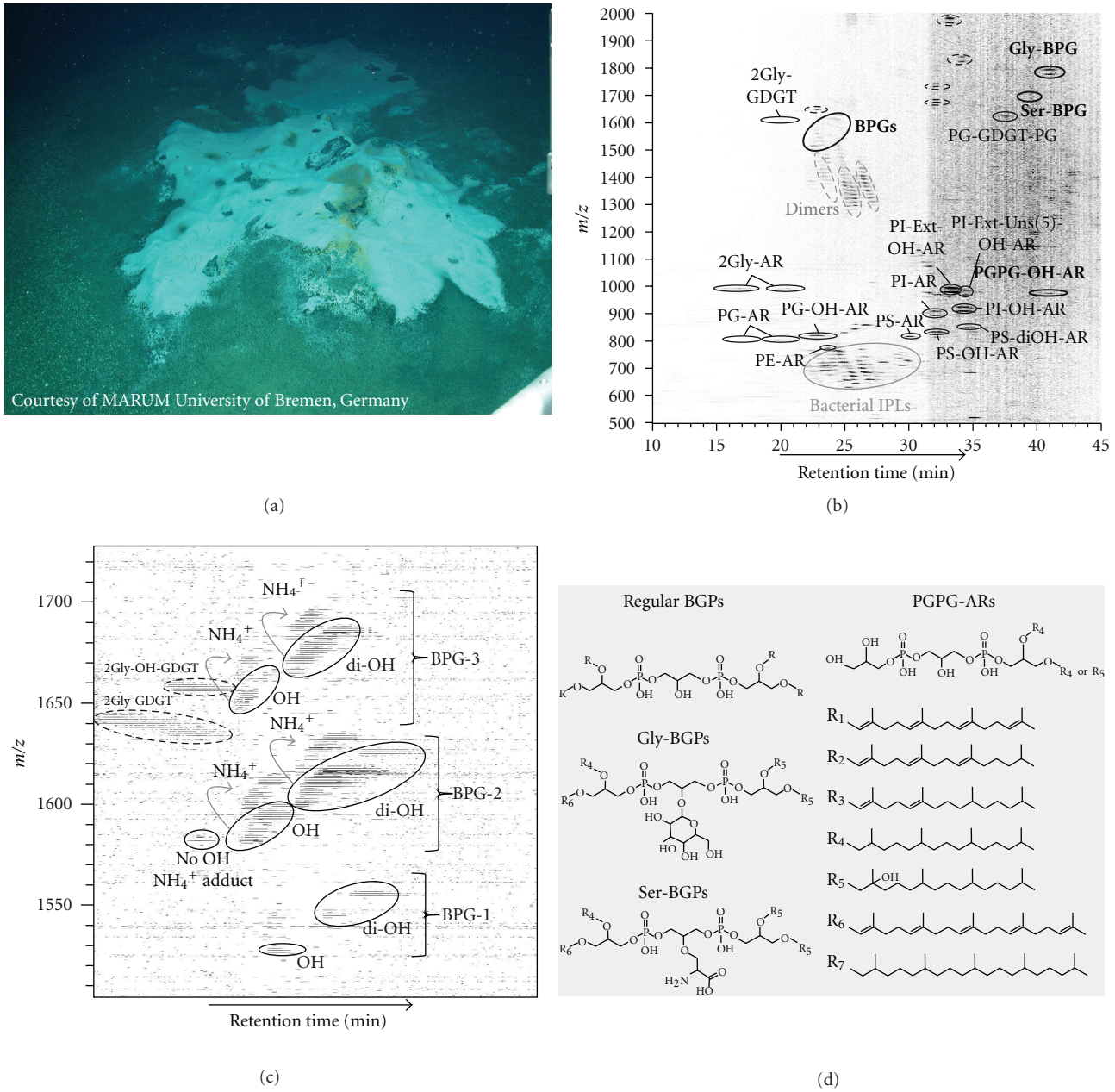

Figure 1: (a) Photography of the seafloor at site GeoB 12315 (~1000 m water depth) during expedition M74/3 taken by the remotely operated vehicle *Quest* (MARUM, University of Bremen) in the continental margin off Pakistan; (b) density map plot showing archaeal IPLs (in black), bacterial IPLs (in gray), and novel archaeal lipids (bold) analyzed in positive mode by HPLC-ESI-IT-MS; (c) zoom in the regular BPGs area of a density map generated in positive mode HPLC-ESI-ToF-MS (BPG-1 with four C_{20}, BPG-2 with three C_{20} and one C_{25}, and BPG-3 with two C_{20} and two C_{25}); (d) structure of archaeal BPGs, other archaeal cardiolipin analogues, and PGPG-ARs. R_1 to R_7 are tentatively identified isoprenoidal moieties. *Compound Abbreviations.* GDGT: glycerol dibiphytanyl glycerol tetraether (C_{40}–C_{40} isoprenoidal chains); AR: archaeol (C_{20}–C_{20} isoprenoidal chains); Ext-AR: extended archaeol (C_{20}–C_{25} isoprenoidal chains); OH-AR: monohydroxylated-archaeol (OHC_{20}–C_{20}); diOH: dihydroxylated-archaeol (OHC_{20}–OHC_{20}); Uns-AR: unsaturated-archaeol; Gly: glycosyl (hexose); PE: phosphatidylethanolamine; PG: phosphatidylglycerol; PI: phosphatidylinositol; PS: phosphatidylserine; Ser: serine.

usually dominated by the uncultured anaerobic methanotrophic (ANMEs) archaea, which are closely associated with sulfate reducing bacteria, jointly performing the anaerobic oxidation of methane (AOM) [15, 16]. This process is not only observed at seeps; AOM is ubiquitous in marine sediments and prevents large amounts of the greenhouse gas methane from escaping into the atmosphere [17]. Analyses of archaeal IPLs coupling high-performance liquid chromatography (HPLC) and ion-trap mass spectrometry (ITMS) from seeps sediments revealed a multitude of diether

lipids, including both C_{20}–C_{20} archaeol (AR) and C_{20}–C_{25} extended AR (Ext-AR) with several combinations of headgroups and presence of hydroxyl group and unsaturation at the isoprenoidal chains [18–20]. Although the diversity and chemotaxonomic relevance of archaeal IPLs from worldwide ANME seep communities have already been examined [19], to date no BPG has been detected in such systems and BPGs have only been restrictedly reported for extreme halophilic archaeal species.

2. Material and Methods

In November 2007, during expedition M74/3 onboard the research vessel *Meteor*, the remotely operated vehicle *Quest* (MARUM, University of Bremen) was launched in the continental margin off Pakistan [21]. Sediment cores (ca. 10 cm i.d. and 20 cm length) were recovered from site GeoB 12315-9 (Dive 181) at 1025 m water depth, well within the lower part of the oxygen minimum zone [21]. Surface sediments influenced by gas ebullition were associated with dense microbial mats from sulfide-oxidizing bacteria (Figure 1(a)). Detailed sediment geochemistry and gas emission potential can be found elsewhere [22, 23]. The samples were processed shipboard at 4°C with sediment sections (1-2 cm thick) and immediately placed in liquid nitrogen and later maintained at −80°C at MARUM (University of Bremen, Germany).

The total lipid extract (TLE) was obtained by extraction of 10–20 g wet sediment (0 to 15 cm core depth, 8 samples in total) after addition of 5 μg of internal standard (1-*O*-hexadecyl-2-acetoyl-*sn*-glycero-3-phosphocholine, PAF), using a modified Bligh and Dyer protocol [24]. The TLE was dissolved in a mixture of methanol and dichloromethane (5 : 1 v/v). Initial IPL analysis was performed following conditions previously described [24]. Briefly, chromatographic separation and IPLs analysis were conducted in a ThermoFinnigan Surveyor high-performance liquid chromatography (HPLC) system connected to a ThermoFinnigan LCQ Deca XP Plus ion trap (IT) multiple stage mass spectrometry (MS^n) equipped with electrospray interface (ESI). A 10 μL aliquot of the TLE (equivalent to 1% of TLE) was injected onto a LiChrospher Diol column (150 × 2.1 mm, 5 μm, Alltech, Germany) equipped with a guard column of the same material. Samples were further analyzed by high-resolution mass spectrometry for precise identification of novel lipids, which allowed mass accuracy in the ppm range. For this purpose, ESI-MS was performed on a Bruker maXis Ultra-High Resolution ToF (ToF) MS. This instrument was coupled to a Dionex Ultimate 3000 UHPLC equipped with a Waters Acquity UPLC Amide column (150 × 2.1 mm, 3.5) following a method recently developed in our lab. IPLs were measured in both positive and negative ionization modes with automated data-dependent fragmentation of base peak ions up to MS^3 (IT) or MS^2 (ToF). This method is especially suitable for rapid screening of natural, complex mixtures of membrane lipids with molecular weights in the range from 500 to 2000 Da [24]. Additionally, selected lipids were targeted for MS^2 fragmentation in multiple reaction monitoring (MRM) mode. In these cases, increasing collision energies (15–55 eV) were applied to the selected parent ion in order to better describe sequential fragmentation.

IPL quantification is semiquantitative (see [24]) and identification is based on mass spectral fragmentation. The quantification and identification of BPGs in samples ran as TLE were hampered by coelution of bacterial phospholipid dimers. To avoid these effects, we purified the analytes of interest by preparative HPLC, using a LiChrospher column (250 × 10 mm, 5 μm, Alltech, Germany) with a fraction collector, as described by [25, 26]. The purified fractions (F1 to F13) were then rerun by HPLC-MS in positive and negative modes to obtain mass spectra on the basis of which BPGs could tentatively be identified in fractions F4 and F12. Given that archaeal IPLs are better characterized by positive ionization mode using our methods [20], only the results from this mode are shown.

3. Results and Discussion

Cardiolipin analogues at the station GeoB 12315 were only detected in the upper 10 cm of the sediment column. DNA fluorescent *in situ* hybridization performed with fixed cells at the interval 1-2 cm indicated a dominance of ANME-2 over other methanotrophic archaeal taxa (M. Yoshinaga, K. Knittel, and K.-U. Hinrichs, unpublished data). The structure of BPGs (cf. [9]) and other cardiolipin analogues are described in Figure 1(d). The series of novel dimeric archaeal phospholipids identified tentatively by HPLC-ESI-MS possess masses ranging from 1526.21 to 1684.38 Da for BPGs and up to 1776.36 Da for the other cardiolipin analogues (Table 1). While the BPGs were minor components representing less than 0.5% of total archaeal IPLs, the glycosylated dimeric phospholipids represented 3–5% of total archaeal IPLs in the first 5 cm of the sediment column.

3.1. BPGs. Tentative identification of BPGs was achieved by interpretation of exact masses of both parent ions and fragments. In order to be considered for identification, the difference between calculated and measured mass ($\Delta m = (m/z_{\text{measured}} - m/z_{\text{calculated}})/m/z_{\text{calculated}}$) had to be below 3 ppm for parent ions and 5 ppm for fragments. Similarly to bacterial BPGs [24], molecular ions of BPGs occur both as protonated and as ammonium adducts in HPLC-MS ($[M + H^+]^+$ and $[M + NH_4^+]^+$, Figure 1(c)).

As illustrated in Figure 1(c), BPGs can be further divided into three major groups, containing the following combinations of isoprenoidal chains: (i) BPG-1 with four C_{20}; (ii) BPG-2 with three C_{20} and one C_{25}; (iii) BPG-3 with two C_{20} and two C_{25} (see Table 1 for detailed information). Figure 2(a) shows the fragmentation pattern for a representative BPG, precisely the $OHC_{20:0}/OHC_{20:0}/C_{20:0}/C_{25:5}$-BPG ($[M + H^+]^+$, *m/z* 1614.30). MS^2 spectra showed major fragment ions at *m/z* 1273.9, 977.6, and 681.3, matching consecutively, the loss from the molecular ion of one penta-unsaturated sesterpenyl (340.3 Da loss) and two OH phytanyl chains (296 Da loss). Other minor fragments observed in MS^2 (Figure 2(a) and Table 1) are attributed to the fragment ion of the PG headgroup attached to a glycerol

Table 1: Characterization of novel PG-based ARs and BPGs with representative fragmentation patterns observed (for abbreviations see text). Sequential losses of alkyl chains are shown together with fragmentation of the headgroup when remaining attached to the glycerol backbone containing a $C_{20:0}$ chain. Values in brackets indicate loss from the most direct precursor, not from the parent ion; (*) denotes presence of unsaturation or OH-group in isoprenoidal chains, which were not exactly determined by MS^2 spectra; **loss of OH-phytanyl chain and hexose from the headgroup; (***) loss of serine plus water from the headgroup with two chains still attached (see Figure 2). Fragments due to losses of alkyl chains are coded: underscored (fragment resulting from loss of an unsaturated chain), bold (fragment resulting from loss of C_{25} chain) and *italics* (fragment resulting from loss of a hydroxylated phytanyl chain). Additional losses of H_2O occur in hydroxylated alkyl moieties, but are not specified here. All parent ions identified show $\Delta m < 3$ ppm; all fragments identified have $\Delta m < 5$ ppm. $\Delta m = (m/z_{measured} - m/z_{calculated})/m/z_{calculated}$.

	m/z	Chain characterization				Fragmentation due to losses of chains (loss of)				Headgroup attached to glycerol containing a $C_{20:0}$ chain (loss of)				GPG fragment
						1st chain	2nd chain	3rd chain	4th chain	$C_3H_8O_3$	PO_2	$C_3H_8O_3$	PO_2	
PGPG-AR	961.687	$C_{20:0}$	$C_{20:0}$	—	—	681.374 (280.3)				589.326 (92.0)				
PGPG-OH-AR	977.682	OH–$C_{20:0}$	$C_{20:0}$	—	—	*681.374* *(296.3)*				589.326 (92.0)	527.370 (62.0)	435.324 (92.0)	355.357 (62.0)	
OH BPG-1	1538.308	OH–$C_{20:0}$	$C_{20:0}$	$C_{20:0}$	$C_{20:0}$									
	1526.214	$C_{20:3}$	$C_{20:3}$	OH–$C_{20:0}$	$C_{20:0}$	1251.948 (274.3)	977.682 (274.3)							
diOH BPG-1	1554.303	OH–$C_{20:0}$	OH–$C_{20:0}$	$C_{20:0}$	$C_{20:0}$	*1257.995* *(296.3)*	*961.687* *(296.3)*							
	1544.224	*OH–$C_{20:0}$	*OH–$C_{20:0}$	*$C_{20:3}$	*$C_{20:2}$									
BPG-2	1581.199 (NH_4^+)	*$C_{25:5}$	*$C_{20:3}$	*$C_{20:3}$	*$C_{20:3}$				**401.061** **(1180.1)**					
OH BPG-2	1598.308	$C_{25:5}$	OH–$C_{20:0}$	$C_{20:0}$	$C_{20:0}$	**1257.995** **(340.3)**	*961.687* *(296.3)*							
	1594.277	$C_{25:5}$	$C_{20:2}$	OH–$C_{20:0}$	$C_{20:0}$	**1253.963** **(340.3)**	977.682 (276.3)							
	1592.261	$C_{25:5}$	$C_{20:3}$	OH–$C_{20:0}$	$C_{20:0}$	**1251.948** **(340.3)**	977.682 (274.3)	*681.374* *(296.3)*						
	1582.183	$C_{25:5}$	$C_{20:4}$	$C_{20:4}$	OH–$C_{20:0}$			**697.369** **(884.8)**	*401.061* *(296.3)*					
diOH BPG-2	1624.381	OH–$C_{20:0}$	OH–$C_{20:0}$	$C_{25:0}$	$C_{20:0}$	*1328.073* *(296.3)*	*1031.765* *(296.3)*							
	1614.303	$C_{25:5}$	OH–$C_{20:0}$	OH–$C_{20:0}$	$C_{20:0}$	**1273.990** **(340.3)**	*977.682* *(296.3)*	*681.374* *(296.3)*	401.061 (280.3)	589.326 (92.0)	527.370 (62.0)	435.324 (92.0)		247.058
	1608.256	$C_{25:5}$	OH–$C_{20:3}$	OH–$C_{20:0}$	$C_{20:0}$	**1267.947** **(340.3)**	*977.682* *(290.3)*	*681.374* *(296.3)*		589.326 (92.0)	527.370 (62.0)	435.324 (92.0)		247.058
OH BPG-3	1668.39	*$C_{25:5}$	*$C_{25:5}$	*OH–$C_{20:0}$	*$C_{20:0}$									

Table 1: Continued.

	m/z	Chain characterization				Fragmentation due to losses of chains (loss of)				Headgroup attached to glycerol containing a $C_{20:0}$ chain (loss of)				GPG fragment
						1st chain	2nd chain	3rd chain	4th chain	$C_3H_8O_3$	PO_2	$C_3H_8O_3$	PO_2	
OH BPG-3	1652.261	$C_{25:5}$	$C_{25:5}$	$C_{20:3}$	OH–$C_{20:0}$	**1311.948 (340.3)**	1037.682 (274.3)	**697.369 (340.3)**	*401.061 (296.3)*					
diOH BPG-3	1684.381	$C_{25:5}$	OH–$C_{20:0}$	OH–$C_{20:0}$	$C_{25:0}$	**1344.068 (340.3)**	*1047.760 (296.3)*	*751.452 (296.3)*						
	1676.318	$C_{25:5}$	$C_{25:4}$	OH–$C_{20:0}$	OH–$C_{20:0}$	**1336.005 (340.3)**	**933.677 (340.3)**	*697.369 (296.3)*	*401.061 (296.3)*					
	1674.303	$C_{25:5}$	$C_{25:5}$	OH–$C_{20:0}$	OH–$C_{20:0}$	**1333.990 (340.3)**	**933.677 (340.3)**	*697.369 (296.3)*	*401.061 (296.3)*					
	1670.271	$C_{25:5}$	$C_{25:4}$	OH–$C_{20:3}$	OH–$C_{20:0}$		**987.630 (682.6)**	*697.369 (290.3)*	*401.061 (296.3)*					
Gly-BPG	1776.355	$C_{25:5}$	OH–$C_{20:0}$	OH–$C_{20:0}$	$C_{20:0}$	**1436.042 (340.3)**	*1139.734 (296.3)*	*681.373*** *(296.3 + 162.1)*						
Ser-BPG	1701.335	$C_{25:5}$	OH–$C_{20:0}$	OH–$C_{20:0}$	$C_{20:0}$	**1361.022 (340.3)**	*1064.714 (296.3)*			959.671 (105.0)***				

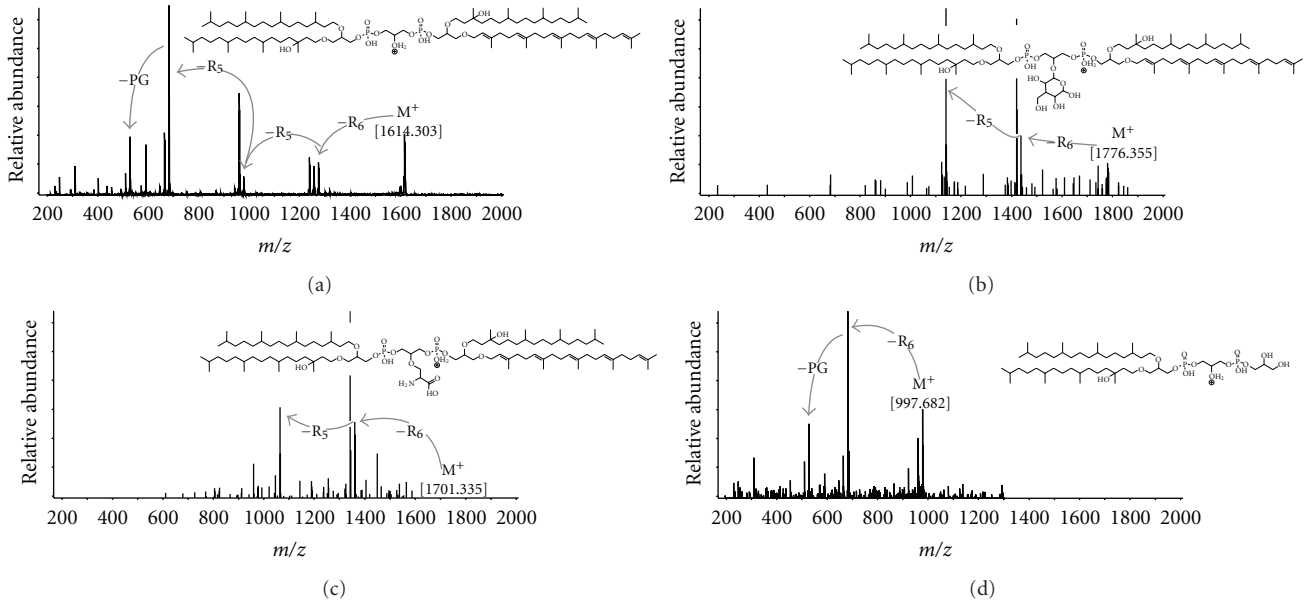

Figure 2: Positive mode MS^2 spectra of novel archaeal IPLs analyzed by HPLC-ESI-MS. (a) Representative BPG ($OHC_{20:0}/OHC_{20:0}/C_{20:0}/C_{25:5}$-BPG); (b) glycosylated BPG; (c) serine BPG; (d) PGPG-OH-AR. Losses are indicated by R_n (Figure 1(d)). Detailed information on major ions in MS^2 spectra is available in Table 1.

backbone containing a single phytanyl chain (*m/z* 527.3) and the subsequent losses of the glycerol headgroup and the phytanyl chain (*m/z* 435.3 and 247.0), which are commonly observed in PG-based AR fragmentation during ESI-MS [20]. The exact mass analysis of fragmentation patterns of this compound is thus consistent with the proposed structure and allowed to constrain the distribution of double bonds and OH moieties on the isoprenoidal chains. Similar MS^2 spectra were constructed for other BPGs and some general patterns of hydroxyl group and double bond distribution could be established (Table 1). Only phytanyl moieties were observed with one hydroxyl group per chain, while unsaturation occurred on both C_{20} and C_{25} nonhydroxylated isoprenoidal chains. These structural features of isoprenoidal chains resemble those from phosphobased ARs and Ext-ARs described earlier [20] in seep sediments.

Concerning fragmentation patterns, BPGs previously identified in halophilic archaea were analyzed by ESI-MS in negative mode [9–11], among other techniques. For example, tetra $C_{20:0}$-BPG fragmentation is characterized by the cleavage of the diphytanyl-glycerol-phosphate from the molecular ion at *m/z* 1521.3, yielding major fragment ions at *m/z* 805.6, 731.6, and 433.3, corresponding to quasi-molecular ions of PG-AR, phosphatidic acid (PA)-AR and the loss of one phytanyl chain plus water from PA-AR, respectively (e.g., [9]). Our experiments showed prominent fragmentation resulting primarily from the loss of isoprenoidal chains, with minor fragments attributed to the cleavage of the phosphatidylglycerol headgroup (Figure 2(a) and Table 1). Previously described archaeal BPGs were solely composed of four phytanyl chains [9–11]; this structural diversity has now been extended by our findings of novel derivatives (Table 1). The tentative structural assignments of archaeal BPGs by positive ion mode HPLC-ESI-MS are generally consistent with fragmentation patterns of archaeal IPLs. For example, fragmentation of phospho-ARs, such as PG-AR, is dominated by the loss of the head group, so that the MS^2 spectra display major fragment ions at *m/z* 733.6 (PA-AR). By contrast, phosphobased OH-ARs present a 296.3 Da loss corresponding to the cleavage of the hydroxylated phytanyl chain, which is favored over loss of head group or nonhydroxylated phytanyl chain [20]. Similarly, BPGs in our samples undergo primary loss of the alkyl substituent in a systematic fashion: unsaturated over hydroxylated over saturated isoprenoidal chains (Figure 2 and Table 1). These patterns are reflected in major fragment ions in MS^2 experiments. Furthermore, when isoprenoidal chains are lost, the initially formed fragment ion is accompanied by fragments resulting from additional losses of water molecules (Figure 2(a)).

3.2. Other Cardiolipin Analogues. The same combination of $OHC_{20:0}/OHC_{20:0}/C_{20:0}/C_{25:5}$ isoprenoidal chains was observed for both complex glycosylated and serine cardiolipin analogues (Gly-BPG and Ser-BPG, Figure 1(b)). The Gly-BPG is analogous to the glycosylated cardiolipin from the group B *Streptococcus* strains [27] and structurally distinct from the glycocardiolipin described in earlier studies of archaeal cardiolipin analogues [9–11]. The inclusion of a serine in the central glycerol of BPGs is similar to the D-alanyl and L-lysyl cardiolipins described, respectively, by [28, 29]. Gly-BPG and Ser-BPG showed molecular ions in MS^1 mode corresponding to the protonated and the ammonium adduct (Figure 1(b)). Fragmentation pattern in MS^2 is also similar,

with major fragment ions observed from loss of a penta-unsaturated sesterpenyl chain (340.3 Da) and a subsequent OH phytanyl (296.3 Da) loss (Figures 2(b) and 2(c)). Minor fragment ions include *m/z* 977.6 and 959.6, which can also be observed in typical BPGs (Table 1) and are consistent with the successive losses of penta-unsaturated sesterpenyl and OH phytanyl chains together with the hexose or serine.

3.3. Novel Archaeal Diether Phospholipids. In addition to cardiolipin analogues, two novel archaeal diether lipids were detected and characterized by HPLC-ESI-MS. These compounds are structurally related to the BPGs, with the difference that they contain only two isoprenoidal chains (Figure 1(d)). The fragmentation of the tentatively identified bisphosphatidylglycerol archaeol or PGPG-AR in MS^2 experiments ($[M + H^+]^+$, *m/z* 961.68) is marked by the loss of the glycerol headgroup (74.0 Da) plus water and the loss of PG (154.0 Da), resulting in major fragment ions at *m/z* 869.6 and 807.6, respectively (Table 1). Minor fragment ions at *m/z* 733.6 and 435.3 are identical to those observed for PG-AR in MS^2 positive ion mode [20]. The tentatively identified PGPG-OH-AR ($[M + H^+]^+$, *m/z* 977.68) undergoes a prominent loss of 296.3 Da and a subsequent 74.0 Da loss, yielding major fragment ions at *m/z* 681.3 and 527.3 (Figure 2(d)), which can be also observed as minor fragments during MS^2 experiments of BPGs (Table 1). These novel compounds represent less than 1% in the 1–11 cm and increase to 3% of total archaeal IPLs at the 11–15 cm horizons (data not shown).

After careful reinspection of samples dominated by ANME-2 archaea [17, 18], PGPG-OH-AR was exclusively detected in Black Sea microbial mats, Arabian Sea, and Hydrate Ridge seep sediments. Given the structural resemblance of PGPG-ARs and typical BPGs (Figure 1(d)) and their occurrence pattern restricted to seep sediments with high ANME-2 abundance, we hypothesize that these diether lipids are likely degradation products of the BPGs. However, one cannot rule out the participation of these diethers as intermediates in archaeal BPGs biosynthesis, which is still unknown.

3.4. Possible Significance of Novel Archaeal Cardiolipin Analogues in Methane-Metabolizing Archaea. Archaeal diether and tetraether IPLs generally contain saturated isoprenoidal chains (e.g., [30] and references therein). The only archaeal BPGs described so far are invariably composed of saturated phytanyl chains [9, 11]. In our samples, we observed that cardiolipin analogues are structurally more complex and attached to multiple combinations of saturated, hydroxylated, and polyunsaturated C_{20} and C_{25} isoprenoidal chains (Table 1). Unsaturated isoprenoids are found in archaeal isolates over a wide temperature range, for example, thermophilic [31, 32] and psychrophilic [33, 34], so that unsaturation of isoprenoidal chains is probably not primarily a membrane adaptation to temperature [35]. Given that the physical stability of isoprenoidal chains is the major regulating factor for low proton permeability in archaeal liposomes [36], unsaturation of isoprenoidal chains results in increased solute permeability through the cell membrane. Indeed, unsaturation appears to be widespread among halophilic archaea [33, 34, 37], the only cultivated BPG producers [38]. In addition, an increase in cardiolipin analogue content was observed in halophilic archaea when exposed to low salt conditions [12, 13]. In cold seep sediments, both core lipids (i.e., AR and OH-AR) and IPLs are relatively well characterized (e.g., [19, 39]), but thus far neither BPGs nor isoprenoidal chain unsaturation has been reported as an important feature, except for minor amounts of the recently described phosphobased unsaturated ARs [20].

The asymmetric arrangement in archaeal BPGs, that is, C_{20} and C_{25} isoprenoidal chains, including the presence of unsaturations and/or hydroxyl-group(s) (Table 1), differs from the prevalent symmetric patterns of mitochondrial cardiolipins [40]. In addition, because cardiolipins are typically minor lipids in bacterial and mitochondrial membranes, besides the fact that no clear pattern of cardiolipin unsaturation is found among different organisms, they are not believed to affect overall fluidity of the cellular membrane [7, 40]. The high diversity of typical BPGs and the relatively high abundance of the complex glycosylated and serine cardiolipin analogues in concert with the extensive presence of unsaturation in the isoprenoidal chains have implications for the bioenergetics of membrane lipids. First, an increase in proton permeability could facilitate archaeal catabolism in microbial communities mediating the anaerobic oxidation of methane, a process known to yield minimal metabolic energy [41]. Second, among the two most widespread ANME groups, ANME-2 representatives are putatively found physically associated with sulfate-reducing bacteria in cluster-like arrangements [16], whereas ANME-1 often occur as single cells (e.g., [42–44]). Under the assumption that BPGs and PGPG-ARs are affiliated with ANME-2 archaea, it is conceivable that interaction between cardiolipin analogues and membrane proteins facilitates the transport of protons, electrons, and/or metabolites (similarly to mitochondria or ATPase/synthase bound cardiolipins, e.g., [6, 8, 14]) in the cell-to-cell syntrophic surroundings.

In this study, we have tentatively identified several novel archaeal cardiolipin analogues on the basis of their fragmentation patterns during positive ion mode HPLC-ESI-MS. As methane-metabolizing archaea are yet to be isolated in culture, investigations on the function of cardiolipin analogs in Archaea should proceed with detailed lipid examination of already cultured species.

Acknowledgments

M. Y. Yoshinaga is grateful to the Alexander von Humboldt Foundation for financial support. This study was funded by the Deutsche Forschungsgemeinschaft (DFG, Germany) through the DFG-Research Center/Excellent Cluster "The Ocean in the Earth System." Additional funding has been provided by the ERC Advanced Grant DARCLIFE to Kai-Uwe Hinrichs. The crew, ROV Quest team, and participants of the expedition M74/3 aboard R/V Meteor are acknowledged. The authors are also thankful to Drs. Xiaolei Liu, Florence Schubotz, Pamela Rossel and Yu-Shih Lin for providing additional information and helpful discussions

for this manuscript. We are also in debt with Dr. Matthias Kellermann who provided the artwork on figures.

References

[1] C. R. Woese, O. Kandler, and M. L. Wheelis, "Towards a natural system of organisms: proposal for the domains Archaea, Bacteria, and Eucarya," *Proceedings of the National Academy of Sciences of the United States of America*, vol. 87, no. 12, pp. 4576–4579, 1990.

[2] M. Kates, "Membrane lipids of Archaea," in *The Biochemistry of Archaea (Archaebacteria)*, M. Kates, D. J. Kushner, and A. T. Matheson, Eds., pp. 261–295, Elsevier, Amsterdam, The Netherlands, 1995.

[3] Y. Koga, M. Nishihara, H. Morii, and M. Akagawa-Matsushita, "Ether polar lipids of methanogenic bacteria: structures, comparative aspects, and biosyntheses," *Microbiological Reviews*, vol. 57, no. 1, pp. 164–182, 1993.

[4] W. Dowhan, "Molecular basis for membrane phospholipid diversity: why are there so many lipids?" *Annual Review of Biochemistry*, vol. 66, pp. 199–232, 1997.

[5] M. Schlame, D. Rua, and M. L. Greenberg, "The biosynthesis and functional role of cardiolipin," *Progress in Lipid Research*, vol. 39, no. 3, pp. 257–288, 2000.

[6] F. L. Hoch, "Cardiolipins and biomembrane function," *Biochimica et Biophysica Acta*, vol. 1113, no. 1, pp. 71–133, 1992.

[7] M. Schlame, "Cardiolipin synthesis for the assembly of bacterial and mitochondrial membranes," *Journal of Lipid Research*, vol. 49, no. 8, pp. 1607–1620, 2008.

[8] M. Zhou, N. Morgner, N. P. Barrera et al., "Mass spectrometry of intact V-type ATPases reveals bound lipids and the effects of nucleotide binding," *Science*, vol. 334, pp. 380–385, 2011.

[9] A. Corcelli, M. Colella, G. Mascolo, F. P. Fanizzi, and M. Kates, "A novel glycolipid and phospholipid in the purple membrane," *Biochemistry*, vol. 39, no. 12, pp. 3318–3326, 2000.

[10] V. M. T. Lattanzio, A. Corcelli, G. Mascolo, and A. Oren, "Presence of two novel cardiolipins in the halophilic archaeal community in the crystallizer brines from the salterns of Margherita di Savoia (Italy) and Eilat (Israel)," *Extremophiles*, vol. 6, no. 6, pp. 437–444, 2002.

[11] G. D. Sprott, S. Larocque, N. Cadotte, C. J. Dicaire, M. McGee, and J. R. Brisson, "Novel polar lipids of halophilic eubacterium *Planococcus* H8 and archaeon *Haloferax volcanii*," *Biochimica et Biophysica Acta*, vol. 1633, no. 3, pp. 179–188, 2003.

[12] P. Lopalco, S. Lobasso, F. Babudri, and A. Corcelli, "Osmotic shock stimulates de novo synthesis of two cardiolipins in an extreme halophilic archaeon," *Journal of Lipid Research*, vol. 45, no. 1, pp. 194–201, 2004.

[13] S. Lobasso, P. Lopalco, V. M. T. Lattanzio, and A. Corcelli, "Osmotic shock induces the presence of glycocardiolipin in the purple membrane of *Halobacterium salinarum*," *Journal of Lipid Research*, vol. 44, no. 11, pp. 2120–2126, 2003.

[14] A. Corcelli, S. Lobasso, L. L. Palese, M. S. Saponetti, and S. Papa, "Cardiolipin is associated with the terminal oxidase of an extremely halophilic archaeon," *Biochemical and Biophysical Research Communications*, vol. 354, no. 3, pp. 795–801, 2007.

[15] K. U. Hinrichs, J. M. Hayes, S. P. Sylva, P. G. Brewert, and E. F. DeLong, "Methane-consuming archaebacteria in marine sediments," *Nature*, vol. 398, no. 6730, pp. 802–805, 1999.

[16] A. Boetius, K. Ravenschlag, C. J. Schubert et al., "A marine microbial consortium apparently mediating anaerobic oxidation methane," *Nature*, vol. 407, no. 6804, pp. 623–626, 2000.

[17] K.-U. Hinrichs and A. Boetius, "The anaerobic oxidation of methane: new insights in microbial ecology and biogeochemistry," in *Ocean Margin Systems*, G. Wefer, D. Billett, D. Hebbeln, B. B. Jørgensen, M. Schlüter, and T. Van Weering, Eds., pp. 457–477, Springer, Berlin, Germany, 2002.

[18] P. E. Rossel, J. S. Lipp, H. F. Fredricks et al., "Intact polar lipids of anaerobic methanotrophic archaea and associated bacteria," *Organic Geochemistry*, vol. 39, no. 8, pp. 992–999, 2008.

[19] P. E. Rossel, M. Elvert, A. Ramette, A. Boetius, and K. U. Hinrichs, "Factors controlling the distribution of anaerobic methanotrophic communities in marine environments: evidence from intact polar membrane lipids," *Geochimica et Cosmochimica Acta*, vol. 75, no. 1, pp. 164–184, 2011.

[20] M. Y. Yoshinaga, M. Y. Kellermann, P. E. Rossel, F. Schubotz, J. S. Lipp, and K.-U. Hinrichs, "Systematic fragmentation patterns of intact archaeal lipids by high-performance liquid chromatography/electrospray mass spectrometry," *Rapid Communications in Mass Spectrometry*, vol. 25, pp. 3563–3574, 2012.

[21] G. Bohrmann and Cruise participants, *Report and Preliminary Results of R/V Meteor Cruise M74/3*, Berichte, Fachbereich Geowissenschaften, Universität Bremen, Bremen, Germany, 2008.

[22] D. Fischer, H. Sahling, K. Nöthen, G. Bohrmann, M. Zabel, and S. Kasten, "Interaction between hydrocarbon seepage, chemosynthetic communities and bottom water redox at cold seeps of the Makran accretionary prism: insights from habitat-specific pore water sampling and modeling," *Biogeosciences Discussions*, vol. 8, pp. 9763–9811, 2011.

[23] M. Römer, H. Sahling, T. Pape, G. Bohrmann, and V. Spiess, "Gas bubble emission from submarine hydrocarbon seeps at the Makran continental margin (offshore Pakistan)," *Journal of Geophysical Research*. under review.

[24] H. F. Sturt, R. E. Summons, K. Smith, M. Elvert, and K. U. Hinrichs, "Intact polar membrane lipids in prokaryotes and sediments deciphered by high-performance liquid chromatography/electrospray ionization multistage mass spectrometry—new biomarkers for biogeochemistry and microbial ecology," *Rapid Communications in Mass Spectrometry*, vol. 18, no. 6, pp. 617–628, 2004.

[25] Y. S. Lin, J. S. Lipp, M. Y. Yoshinaga, S. H. Lin, M. Elvert, and K. U. Hinrichs, "Intramolecular stable carbon isotopic analysis of archaeal glycosyl tetraether lipids," *Rapid Communications in Mass Spectrometry*, vol. 24, no. 19, pp. 2817–2826, 2010.

[26] F. Schubotz, J. S. Lipp, M. Elvert, and K. U. Hinrichs, "Stable carbon isotopic compositions of intact polar lipids reveal complex carbon flow patterns among hydrocarbon degrading microbial communities at the Chapopote asphalt volcano," *Geochimica et Cosmochimica Acta*, vol. 75, no. 16, pp. 4399–4415, 2011.

[27] W. Fischer, "The polar lipids of group B *Streptococci*. I. Glucosylated diphosphatidylglycerol, a novel glycophospholipid," *Biochimica et Biophysica Acta*, vol. 487, no. 1, pp. 74–88, 1977.

[28] W. Fischer and D. Arneth-Seifert, "D-alanylcardiolipin, a major component of the unique lipid pattern of *Vagococcus fluvialis*," *Journal of Bacteriology*, vol. 180, no. 11, pp. 2950–2957, 1998.

[29] W. Fischer and K. Leopold, "Polar lipids of four listeria species containing L-lysylcardiolipin, a novel lipid structure,

and other unique phospholipids," *International Journal of Systematic Bacteriology*, vol. 49, no. 2, pp. 653–662, 1999.

[30] Y. Koga and H. Morii, "Biosynthesis of ether-type polar lipids in archaea and evolutionary considerations," *Microbiology and Molecular Biology Reviews*, vol. 71, no. 1, pp. 97–120, 2007.

[31] I. Gonthier, M. N. Rager, P. Metzger, J. Guezennec, and C. Largeau, "A di-O-dihydrogeranylgeranyl glycerol from *Thermococcus* S 557, a novel ether lipid, and likely intermediate in the biosynthesis of diethers in Archæa," *Tetrahedron Letters*, vol. 42, no. 15, pp. 2795–2797, 2001.

[32] M. Nishihara, H. Morii, K. Matsuno, M. Ohga, K. O. Stetter, and Y. Koga, "Structural analysis by reductive cleavage with $LiAlH_4$ of an allyl ether choline-phospholipid, archaetidylcholine, from the hyperthermophilic methanoarchaeon *Methanopyrus kandleri*," *Archaea*, vol. 1, no. 2, pp. 123–131, 2002.

[33] D. S. Nichols, M. R. Miller, N. W. Davies, A. Goodchild, M. Raftery, and R. Cavicchioli, "Cold adaptation in the Antarctic archaeon *Methanococcoides burtonii* involves membrane lipid unsaturation," *Journal of Bacteriology*, vol. 186, no. 24, pp. 8508–8515, 2004.

[34] J. A. E. Gibson, M. R. Miller, N. W. Davies, G. P. Neill, D. S. Nichols, and J. K. Volkman, "Unsaturated diether lipids in the psychrotrophic archaeon *Halorubrum lacusprofundi*," *Systematic and Applied Microbiology*, vol. 28, no. 1, pp. 19–26, 2005.

[35] Y. Koga and H. Morii, "Recent advances in structural research on ether lipids from archaea including comparative and physiological aspects," *Bioscience, Biotechnology and Biochemistry*, vol. 69, no. 11, pp. 2019–2034, 2005.

[36] K. Yamauchi, K. Doi, Y. Yoshida, and M. Kinoshita, "Archaebacterial lipids: highly proton-impermeable membranes from 1,2-diphytanyl-*sn*-glycero-3-phosphocholine," *Biochimica et Biophysica Acta*, vol. 1146, no. 2, pp. 178–182, 1993.

[37] T. Stiehl, J. Rullkötter, and A. Nissenbaum, "Molecular and isotopic characterization of lipids in cultured halophilic microorganisms from the Dead Sea and comparison with the sediment record of this hypersaline lake," *Organic Geochemistry*, vol. 36, no. 9, pp. 1242–1251, 2005.

[38] A. Corcelli, "The cardiolipin analogues of Archaea," *Biochimica et Biophysica Acta*, vol. 1788, no. 10, pp. 2101–2106, 2009.

[39] H. Niemann and M. Elvert, "Diagnostic lipid biomarker and stable carbon isotope signatures of microbial communities mediating the anaerobic oxidation of methane with sulphate," *Organic Geochemistry*, vol. 39, no. 12, pp. 1668–1677, 2008.

[40] M. Schlame, M. Ren, Y. Xu, M. L. Greenberg, and I. Haller, "Molecular symmetry in mitochondrial cardiolipins," *Chemistry and Physics of Lipids*, vol. 138, no. 1-2, pp. 38–49, 2005.

[41] T. M. Hoehler, M. J. Alperin, D. B. Albert, and C. S. Martens, "Field and laboratory studies of methane oxidation in an anoxic marine sediment: evidence for a methanogen-sulfate reducer consortium," *Global Biogeochemical Cycles*, vol. 8, no. 4, pp. 451–463, 1994.

[42] V. J. Orphan, C. H. House, K. U. Hinrichs, K. D. McKeegan, and E. F. DeLong, "Multiple archaeal groups mediate methane oxidation in anoxic cold seep sediments," *Proceedings of the National Academy of Sciences of the United States of America*, vol. 99, no. 11, pp. 7663–7668, 2002.

[43] K. Knittel, T. Lösekann, A. Boetius, R. Kort, and R. Amann, "Diversity and distribution of methanotrophic archaea at cold seeps," *Applied and Environmental Microbiology*, vol. 71, no. 1, pp. 467–479, 2005.

[44] K. Knittel and A. Boetius, "Anaerobic oxidation of methane: progress with an unknown process," *Annual Review of Microbiology*, vol. 63, pp. 311–334, 2009.

Hindawi Publishing Corporation
Archaea
Volume 2012, Article ID 438931, 9 pages
doi:10.1155/2012/438931

Research Article

Archaeal Phospholipid Biosynthetic Pathway Reconstructed in *Escherichia coli*

Takeru Yokoi, Keisuke Isobe, Tohru Yoshimura, and Hisashi Hemmi

Department of Applied Molecular Bioscience, Graduate School of Bioagricultural Sciences, Nagoya University, Furo-cho, Chikusa-ku, Nagoya, Aichi 460-8601, Japan

Correspondence should be addressed to Hisashi Hemmi, hhemmi@agr.nagoya-u.ac.jp

Received 19 December 2011; Accepted 23 February 2012

Academic Editor: Yosuke Koga

A part of the biosynthetic pathway of archaeal membrane lipids, comprised of 4 archaeal enzymes, was reconstructed in the cells of *Escherichia coli*. The genes of the enzymes were cloned from a mesophilic methanogen, *Methanosarcina acetivorans*, and the activity of each enzyme was confirmed using recombinant proteins. *In vitro* radioassay showed that the 4 enzymes are sufficient to synthesize an intermediate of archaeal membrane lipid biosynthesis, that is, 2,3-di-*O*-geranylgeranyl-*sn*-glycerol-1-phosphate, from precursors that can be produced endogenously in *E. coli*. Introduction of the 4 genes into *E. coli* resulted in the production of archaeal-type lipids. Detailed liquid chromatography/electron spray ionization-mass spectrometry analyses showed that they are metabolites from the expected intermediate, that is, 2,3-di-*O*-geranylgeranyl-*sn*-glycerol and 2,3-di-*O*-geranylgeranyl-*sn*-glycerol-1-phosphoglycerol. The metabolic processes, that is, dephosphorylation and glycerol modification, are likely catalyzed by endogenous enzymes of *E. coli.*

1. Introduction

Archaeal membrane lipids are very specific to the organisms in the domain Archaea and have structures that are distinct from those of bacterial/eukaryotic lipids [1–3]. Although they are, essentially, analogues of glycerolipids from bacteria or eukaryotes, they have specific structural features as follows: (1) hydrocarbon chains of archaeal lipids are multiply-branched isoprenoids typically derived from (all-*E*) geranylgeranyl diphosphate (GGPP), while linear acyl groups are general in bacterial/eukaryotic lipids; (2) the isoprenoid chains are linked with the glycerol moiety with ether bonds, while ester bonds are general in bacterial/eukaryotic lipids; (3) the glycerol moiety of archaeal lipids is derived from *sn*-glycerol-1-phosphate (G-1-P), which is the enantiomer of *sn*-glycerol-3-phosphate, the precursor for bacterial/eukaryotic glycerolipids; (4) dimerization of membrane lipids by the formation of carbon-carbon bonds between the ω-terminals of hydrocarbon chains, which generates macrocyclic structures such as caldarchaeol-type lipids with a typically 72-membered ring, is often observed in thermophilic and methanogenic archaea. These characteristics affect the properties of membranes formed with the lipids. In general, the permeability of membranes composed of archaeal lipids is lower than that of membranes that consist of bacterial/eukaryotic lipids [4, 5]. Moreover, the structural differences between archaeal and bacterial/eukaryotic lipids are believed to cause their black-and-white distribution between these domains without exception (the "lipid divide") [6, 7]. This hypothesis is based on the idea that a membrane composed of both archaeal- and bacterial/eukaryotic-type lipids is disadvantageous to the organism, compared with membranes composed of one type. Although this hypothesis is attractive, no proof of it has been reported so far. To obtain proof of this hypothesis, two lines of experiments can be designed. One is to compare the physical properties of artificial membranes prepared with the archaeal- and/or bacterial/eukaryotic-type lipids. A few studies of this type have been done [8, 9]. Shimada and Yamagishi [9] recently reported that hybrid liposomes constructed from both archaeal- and bacterial-type lipids were generally more stable (impermeable) than they had expected. Based on these results, they concluded that the common ancestor of life (and the origin of eukaryotes

supposedly formed by the fusion of archaea- and bacteria-like cells) might have had such hybrid lipid membranes, but they did not explain how the lipid divide occurred. The other, more straightforward line of experiments is to generate an organism that synthesizes both archaeal- and bacterial/eukaryotic-type membrane lipids and therefore has hybrid membranes. If the hybrid membranes are disadvantageous for the organism because of properties such as stability, permeability, and fluidity, the organism may lower viability or become susceptible to stresses such as heat and osmotic shock. Lai et al. recently reported the construction of such an organism, although they did not determine its phenotypes [10]. In their study, phospholipid biosynthetic genes from a hyperthermophilic archaeon *Archaeoglobus fulgidus* were introduced into *Escherichia coli*. The authors demonstrated the synthesis of precursors for archaeal membrane lipids, that is, 3-*O*-geranylgeranyl-*sn*-glycerol-1-phosphate (GGGP) and 2,3-di-*O*-geranylgeranyl-*sn*-glycerol-1-phosphate (DGGGP), in the recombinant *E. coli*, based on the detection of corresponding alcohols from the lipid extract from the cells after phosphatase treatment. However, it was still unclear whether the archaeal-type lipids produced in the cells actually acted as the structural components of a membrane bilayer, because the authors did not show the intact structures of the lipids. Moreover, they did not describe the level of production of the archaeal-type lipids, which is also important to the evaluation of their effects on the membranes of *E. coli*.

In the present study, we reconstructed a part of the biosynthetic pathway of an archaeal phospholipid (Figure 1), which consisted of G-1-P dehydrogenase, GGPP synthase, GGGP synthase, and DGGGP synthase from a mesophilic methanogenic archaeon, *Methanosarcina acetivorans*, in *E. coli*. These enzymes can synthesize DGGGP from the endogenous precursors of isoprenoid in *E. coli*, that is, (all-*E*) farnesyl diphosphate (FPP), isopentenyl diphosphate (IPP), and dihydroxyacetone phosphate (DHAP). In addition, the enzymes from the mesophile were expected to have optimal activities at the growth temperature of *E. coli*, which would lead to high-level production of the archaeal phospholipid precursor and its derivatives. We evaluated the total amount and intact structures of the archaeal-type lipids extracted from the cells by liquid chromatography/electron spray ionization-mass spectrometry (LC/ESI-MS) analysis and showed that DGGGP was metabolized by enzymes endogenous to *E. coli*.

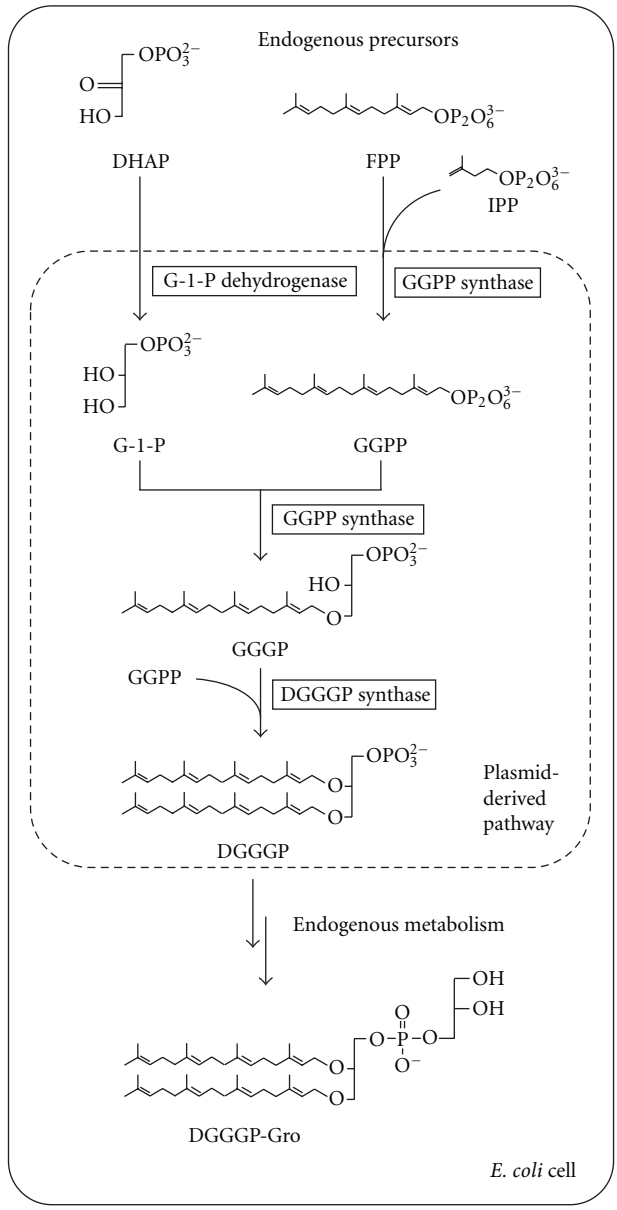

Figure 1: Biosynthetic pathway of archaeal-type lipids reconstructed in *E. coli*.

2. Materials and Methods

2.1. Materials. LKC-18F precoated, reversed-phase, thin-layer chromatography plates were purchased from Whatman, UK. FPP was donated by Drs. Kyozo Ogura and Tanetoshi Koyama, Tohoku University. [1-^{14}C]IPP was purchased from American Radiolabeled Chemicals, USA. All other chemicals were of analytical grade.

2.2. General Procedures. Restriction enzyme digestions, transformations, and other standard molecular biological techniques were carried out as described by Sambrook et al. [11].

2.3. Cultivation of M. acetivorans. The *M. acetivorans* C2A (JCM 12185) strain was provided by the Japan Collection of Microorganisms (JCM), RIKEN BRC, through the Natural Bio-Resource Project of the MEXT, Japan. The mesophilic methanogenic archaeon was cultivated in a JCM 385 *Methanosarcina acetivorans* medium at 37°C and harvested at the log phase.

2.4. Construction of Plasmids Containing Phospholipid Biosynthetic Genes from M. acetivorans. The genome of *M. acetivorans* was extracted from the cells using a DNA extraction kit,

Table 1: Primers used for plasmid construction.

Primers	Sequences (restriction enzymes that recognize the underlined sites)
For the construction of pBAD-MA0606	
ma0606fw	GTAAAGAATTCAGATATAAGGAAATAGATGTGATGCTTATGATGCTTAT (*Eco*RI)
ma0606rv	GGTATTTCTAGATTGTATCCTTATTTTTCAGTATTCCCTTGCAATCA (*Xba*I)
For the construction of pBAD-MA3969	
ma3969fw	TTATATAGCTAGCTATTAAAAATAAGGATAATTAATGCAGGTGGAAGCACACCT (*Nhe*I)
ma3969rv	GAAATGTCGACGATATATCTCCTTTTATTTTTAGCTTTTTATAGCTGATA (*Sal*I)
For the construction of pBAD-MA0961	
ma0961fw	ATAGAATTCAAGAAGATTATAATGTCTGCCGGAATAC (*Eco*RI)
ma0961rv	GATTCTAGATCATACACCGGCAATGAAAG (*Xba*I)
For the construction of pBAD-MA3686	
ma3686fw	CTATTGAGCTCAAATAAAAGGAGATATATCATGAAATTGACCATCAATA (*Sac*I)
ma3686rv	ATATTGGTACCATCTATTTCCTTATATCTTCAACTTATGACCTTTGTGA (*Kpn*I)
For the construction of pBAD-ALB2 by amplification of *ma0961*	
alb2fw	ACAATCTAGAGTCGAAGGAAGATTATAATGTCTGCCGGAATAC
alb2rv	ATGCCTGCAGGTCGACTCATACACCGGCAATGAAAG (*Sal*I)
For the construction of pBAD-ALB3 by amplification of *ma3969*	
alb3fw	CGGTGTATGAGTCGAAAGGAGTAATTAATGCAGGTGGAAGCACACCT
alb3rv	ATGCCTGCAGGTCGACTTAGCTTTTTATAGCTGATA (*Sal*I)
For the construction of pBAD-ALB4 by amplification of *ma3686*	
alb4fw	AAAAAGCTAAGTCGAAAGGAGATATATCATGAAATTGACCATCAATA
alb4rv	ATGCCTGCAGGTCGACTCAACTTATGACCTTTGTGA (*Sal*I)

ISOPLANT II (Nippon Gene). Each of the hypothetical genes for archaeal phospholipid biosynthesis, that is, *MA3686*, *MA0606*, *MA3969*, and *MA0961*, was amplified using the primers shown in Table 1, using the genome of *M. acetivorans* as a template, and using KOD DNA polymerase (Toyobo, Japan). The amplified DNA fragment was digested by restriction enzymes that recognize the sites in the primers and then inserted into the pBAD18 vector cut with the same restriction enzymes to construct the plasmid for expression of each archaeal enzyme, that is, pBAD-MA3686, pBAD-MA0606, pBAD-MA3969, and pBAD-MA0961.

For the construction of plasmids for expression of multiple archaeal genes, an In-Fusion Advantage PCR cloning kit (Takara, Japan) was used according to the manufacturer's instructions. The *MA0961* gene was amplified using the primers shown in Table 1 and pBAD-MA0961 as a template. By the action of the In-Fusion enzyme, the amplified fragment was inserted into the plasmid pBAD-MA0606, which had been digested with *Sal*I, to construct the plasmid pBAD-ALB2. Next, the *MA3969* gene, which was amplified using the primers in Table 1 and pBAD-MA3969 as a template, was inserted into pBAD-ALB2 digested with *Sal*I to construct pBAD-ALB3. The plasmid was then digested with *Sal*I, and the *MA3686* gene, amplified using the primers in Table 1 and pBAD-MA3686 as a template, was inserted to construct pBAD-ALB4.

2.5. Recombinant Expression of the Archaeal Enzymes. *E. coli* Top10, transformed with each plasmid containing a homologous gene for archaeal phospholipid biosynthesis, that is, pBAD-MA0606, pBAD-MA3969, pBAD-MA0961, pBAD-MA3686, or pBAD-ALB4, was cultivated at 37°C in 250 mL LB medium supplemented with 100 mg/L ampicillin. When the optical density at 660 nm of the culture reached 0.5, then 0.02% of L-arabinose was added for induction. After an additional 16 h incubation, the cells were harvested and disrupted by sonication in 5 mL of 100 mM 3-(*N*-morpholino)propanesulfonic acid (MOPS)-NaOH buffer, pH 7.0. The homogenates were centrifuged at 24,000 g for 30 min to recover the supernatants as a crude extract, which was used for enzyme assay.

2.6. In Vitro Assay for the Biosynthesis of Phospholipid Precursors. The assay mixture for prenyltransferases contained, in a final volume of 200 μL 0.2 nmol of [1-^{14}C]IPP (2.04 GBq/mmol), 1 nmol of FPP, 2.0 μmol of $MgCl_2$, 20 μmol of MOPS-NaOH, pH 7.0, and suitable volumes of the crude extracts from *E. coli* containing pBAD-MA0606, pBAD-MA3969, or pBAD-MA0961. α-Glycerophosphate (racemic mixture) was added only to the mixtures containing MA3969.

The assay mixture for G-1-P dehydrogenase contained, in a final volume of 200 μL, 0.2 nmol of [1-^{14}C]IPP (2.04 GBq/mmol), 1 nmol of FPP, 2.0 μmol of $MgCl_2$, 20 μmol of MOPS-NaOH, pH 7.0, and suitable volumes of the crude extracts from *E. coli* containing pBAD-MA0606, pBAD-MA3969, or pBAD-MA3686. If needed, 200 nmol of α-glycerophosphate or DHAP was added to the mixture.

In a final volume of 200 μL, the assay mixture for the 4 archaeal enzymes simultaneously expressed in *E. coli* contained, 0.2 nmol of [1-^{14}C]IPP (2.04 GBq/mmol), 1 nmol of FPP, 200 nmol of DHAP, 2.0 μmol of $MgCl_2$, 20 μmol of MOPS-NaOH, pH 7.0, and a suitable volume of the crude extract from *E. coli* containing pBAD-ALB4.

After incubation at 37°C for 30 min, the reaction was stopped by chilling in an ice bath. 200 μL of water saturated with NaCl was added to the mixture, and then the products were extracted with 600 μL of 1-butanol saturated with NaCl-saturated water. They were treated with acid phosphatase according to the method of Fujii et al. [12], and the hydrolysates were extracted with *n*-pentane and analyzed by reversed-phase, thin-layer chromatography (TLC) using a precoated plate LKC-18F developed with acetone/H_2O (9 : 1). The distribution of radioactivity was detected using a BAS2000 bioimaging analyzer (Fujifilm, Japan). The authentic samples were prepared as described in our previous reports, using the enzymes from *Sufolobus acidocaldarius* and *S. solfataricus* [13].

2.7. Lipid Isolation from E. coli Harboring pBAD-ALB4. Lipid was extracted from 2 g of wet cells of *E. coli* harboring pBAD-ALB4, cultured as described above, except that induction with l-arabinose was performed for 18 h. The cells were dissolved with 15 mL of 1-butanol/75 mM ammonium water/ethanol (4 : 5 : 11). The mixture was heated to 70°C and shaken vigorously for 1 min. It was heated again at 70°C for 20 min and shaken vigorously again for 1 min. After cooling to room temperature, the mixture was centrifuged at 1,000 *g* for 10 min. The supernatant was recovered and dried under a stream of nitrogen at 55°C. The dried residue was then dissolved with 7.2 mL of 1-butanol/methanol/0.5 M acetate buffer, pH 4.6 (3 : 10 : 5). Lipids in the mixture were extracted with 3 mL *n*-pentane and dried under a stream of nitrogen at 55°C. The dried residue was then redissolved in 1 mL of methanol/2-propanol (1 : 1).

2.8. LC/ESI-MS Analysis. ESI-MS was performed with an Esquire 3000 ion trap system (Bruker Daltonics, USA). MS-parameters used were as follows: sheath gas, N_2 of 30 psi; dry gas, N_2 of 7.0 L·min^{-1} at 320°C; scanning range, 50–1,000 *m/z*; scan speed, 13,000 *m/z*·sec^{-1}; ion charge control target, 50,000 or 20,000; maximum accumulation time, 100 ms; averages, 10; rolling averaging, 2. The system was equipped with an Agilent 1100 Series HPLC system (Agilent Technologies, USA) using UV detection at 210 nm and COSMOSIL Packed Column 5C_{18}-AR-II (2.0 × 150 mm, Nacalai, Japan). The mobile phase consisted of methanol/100 mg·L^{-1} sodium acetate (9 : 1) or methanol/120 mg·L^{-1} potassium acetate (9 : 1). The flow rate was 0.2 mL·min^{-1}.

2.9. Sodium Periodate Treatment. For sodium periodate treatment of 2,3-di-*O*-geranylgeranyl-*sn*-glycero-1-phosphoglycerol (DGGGP-Gro), the peak fraction from HPLC contained about 1 nmol of the mixture of DGGGP-Gro and 2,3-di-*O*-geranylgeranyl-*sn*-glycerol (DGGGOH), and 1 μmol sodium periodate was added to 1 mL of 1-butanol/75 mM ammonium water/ethanol (4 : 5 : 11). The mixture was reacted at 25°C for 1 h in the dark. The reaction was stopped by adding 1.5 μmol of glycerol. After 15 min, the product was extracted by 1 mL of *n*-pentane and dried with N_2. The dried residue was dissolved with 100 μL of methanol/2-propanol (1 : 1) and analyzed by LC/ESI-MS.

3. Results and Discussion

We first searched for and cloned the genes from a mesophilic, methanogenic archaeon, *M. acetivorans,* which encoded the closest homologues of the enzymes involved in the biosynthesis of archaeal membrane lipids. The homologue of G-1-P dehydrogenase, which shows 59% sequential identity with G-1-P dehydrogenase from *Methanothermobacter thermautotrophicus* [14], is encoded in the gene *MA3686*. The closest homologue of GGPP synthase, with 39% identity with the enzyme from *S. acidocaldarius* [15], is encoded in *MA0606*. The GGGP synthase homologue with 57% identity with the enzyme from *M. thermautotrophicus* [16] is encoded in *MA3969*. The closest homologue of DGGGP synthase, with 31% identity with the enzyme from *S. solfataricus* [13], is encoded in *MA0961*. Each of the genes, *MA3686*, *MA0606*, *MA3969*, and *MA0961*, was recombinantly expressed in *E. coli*. The cells of *E. coli* were disrupted and centrifuged to recover the supernatant as the crude extract. Then the enzyme activity in the crude extract was confirmed by radio-TLC assay. As shown in Figure 2(a), incubation of the crude extract from *E. coli* expressing *MA0606* with FPP and [^{14}C]IPP yielded a radiolabeled hydrophobic product, and treatment of the product with acid phosphatase produced a compound that comigrated with authentic (all-*E*) geranylgeraniol on a reversed-phase TLC plate (R_f = 0.60). Addition of the crude extract from *E. coli* expressing *MA3969* and α-glycerophosphate to the reaction mixture resulted in the movement of the radiolabeled spot on TLC. The new spot (R_f = 0.68) comigrated with authentic 3-*O*-geranylgeranyl-*sn*-glycerol (GGGOH). The movement did not occur in the absence of α-glycerophosphate (data not shown). When the crude extract from *E. coli* expressing *MA0961* was additionally mixed, new radiolabeled spots (R_f = 0.34 and 0.12) emerged on TLC, accompanied by diminishing radioactivity of the other spot. The spot with an R_f of 0.34 comigrated with authentic DGGGOH. These results indicate that *MA0606*, *MA3969*, and *MA0961* encode, as expected from their homologies, GGPP synthase, GGGP synthase, and DGGGP synthase, respectively. The spot with an R_f of 0.12 was considered to have originated from an unknown modification of DGGGP catalyzed by enzymes contained in the crude extracts. To confirm G-1-P dehydrogenase activity in the crude extract of *E. coli* expressing *MA3686*, the extract was incubated with the crude extracts containing

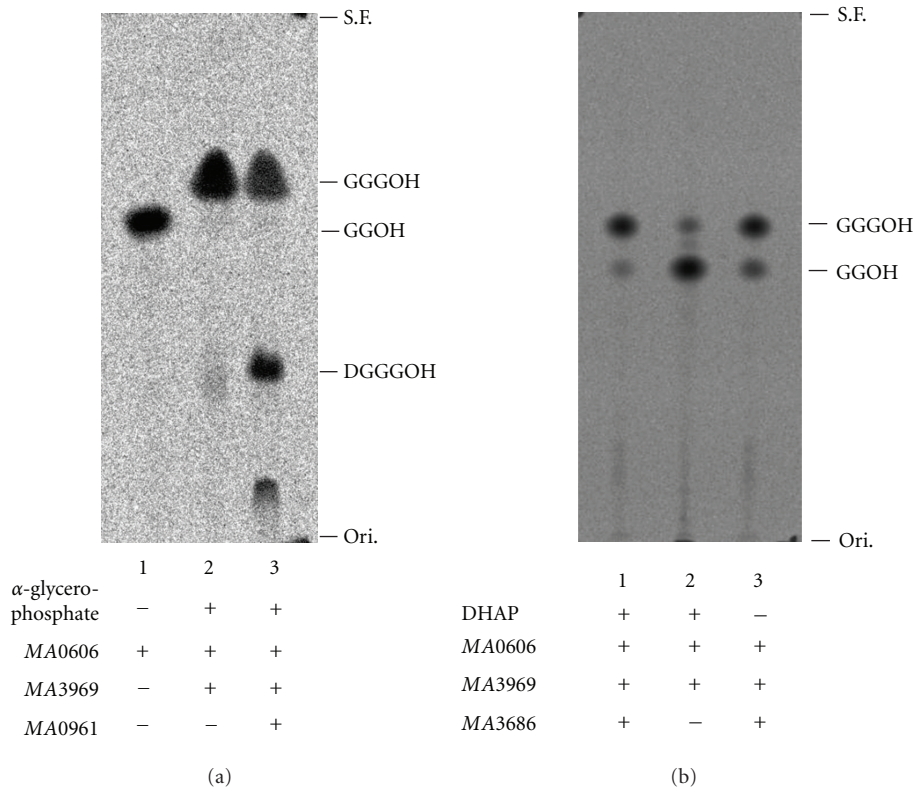

Figure 2: *In vitro* assay of the archaeal enzymes for phospholipid biosynthesis. (a) Thin-layer radiochromatogram of the dephosphorylated products from the reactions with recombinant *M. acetivorans* GGPP synthase, GGGP synthase, and/or DGGGP synthase. The enzyme assays were performed using FPP, [^{14}C]IPP, and α-glycerophosphate as the substrates. (b) Thin-layer radiochromatogram of the products from the reaction with recombinant *M. acetivorans* G-1-P dehydrogenase, coupled with GGPP synthase and GGGP synthase. FPP, [^{14}C]IPP, and DHAP were used as the substrates. S.F., solvent front; Ori., origin.

M. acetivorans GGPP synthase and GGGP synthase, DHAP, FPP, and [^{14}C]IPP. The hydrophobic product was extracted, treated with phosphatase, and analyzed by TLC, giving a main spot that comigrated with GGGOH (Figure 2(b)). After removal of the crude extract of *E. coli* expressing *MA3686* from the reaction mixture, the GGGOH spot became thinner, and a spot that comigrated with geranylgeraniol became the major spot. This result shows that *MA3686* encodes G-1-P dehydrogenase. In contrast, removal of DHAP from the mixture did not change the TLC profile of the products, suggesting that a sufficient amount of DHAP existed in the reaction mixture, which contained cell extracts from *E. coli*. It is noteworthy that a small amount of GGGOH appears to be synthesized even in the absence of *M. acetivorans* G-1-P dehydrogenase. It is possible that the enzyme has only low affinity for *sn*-glycerol-3-phosphate, as has been reported with G-1-P-specific archaeal homologues [17–19].

We next constructed a plasmid vector containing the 4 archaeal genes, which formed an artificial operon in the order *MA0606-MA0961-MA3969-MA3686*, to reconstruct the biosynthetic pathway of archaeal phospholipid in *E. coli*. The activities of the enzymes were confirmed by *in vitro* radio-TLC assay. The cell extract from recombinant *E. coli* expressing the 4 archaeal genes showed activities related to the formation of DGGGP from DHAP, IPP, and FPP *in vitro* (Figure 3(a)), which indicated that the enzymes from *M. acetivorans*, that is, G-1-P dehydrogenase, GGPP synthase, GGGP synthase, and DGGGP synthase, were all expressed in the cells. In addition, a radioactive spot with a lower R_f value (~0.1) was observed. This spot probably corresponded with the one with an R_f of 0.12 observed in Figure 2(a). Because these spots accompanied the formation of DGGGP and because reaction mixtures for these assays contained cell extracts from *E. coli*, they were considered to arise from an unknown derivative of DGGGP, which might be formed through endogenous metabolic pathways in *E. coli*.

Thus, we extracted lipids from the recombinant *E. coli* cells to confirm *in vivo* synthesis of the archaeal phospholipid precursors or their derivatives. The results of LC/ESI-MS analysis of the extract from *E. coli* containing pBAD-ALB4 showed a relatively broad LC peak of A_{210}, which eluted from the column at ~22 min (Figure 3(b)). This peak was absent in the analysis of the extract from *E. coli* containing the parent plasmid pBAD18. Specific ion peaks with *m/z* of 659.6 and 835.6 were detected through MS analysis of the peak in the positive ion mode (Figure 3(c)). These ions had similar but slightly different peak retention times, so the smaller ion was unlikely derived from fragmentation of the larger one. The smaller ion with *m/z* of 659.6 corresponded with [DGGGOH+Na]$^+$. As shown in Figure 3(d), MS/MS

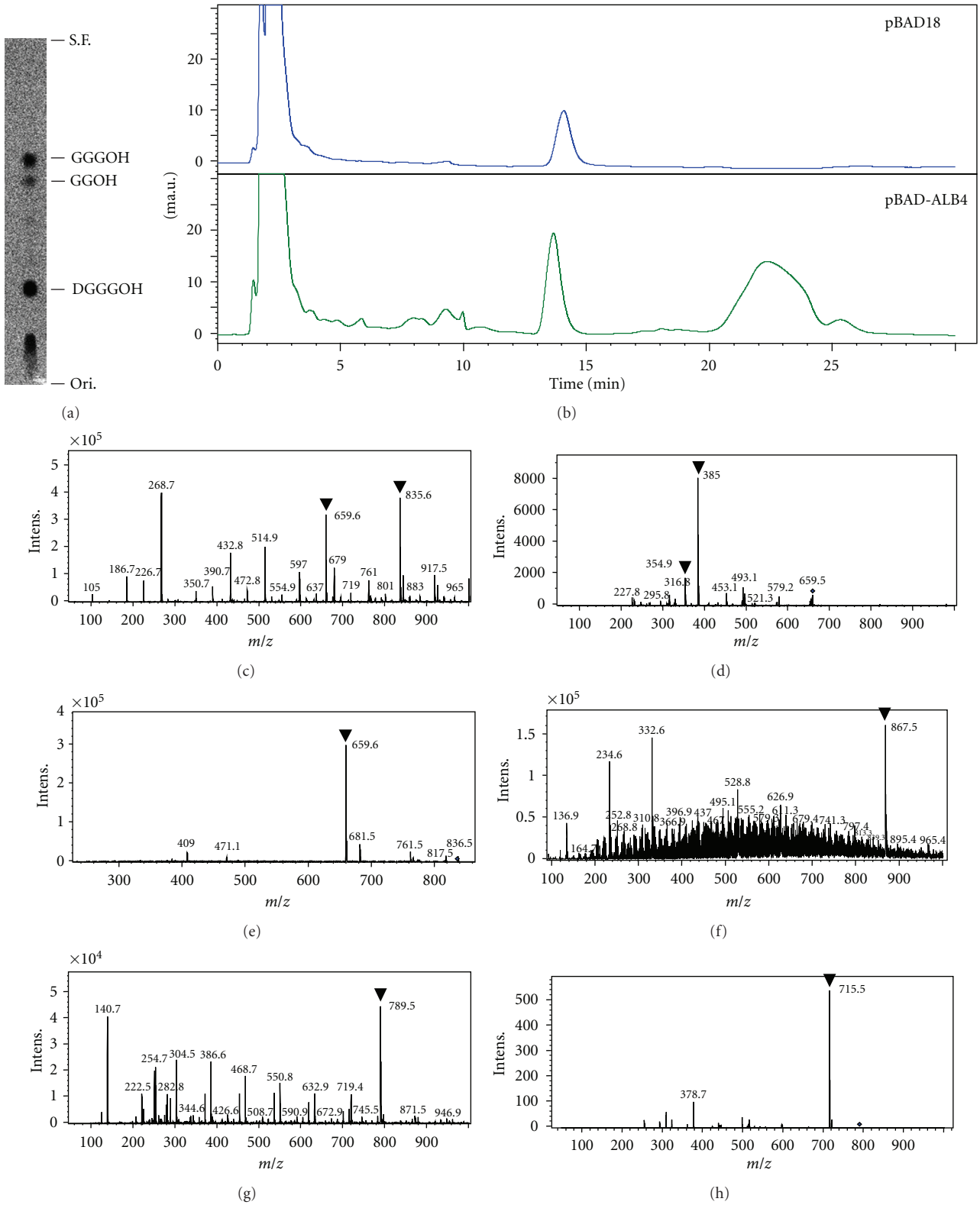

FIGURE 3: Radio-TLC and LC/ESI-MS analyses of the archaeal-type lipids synthesized in *E. coli*. (a) Crude extract from *E. coli* harboring pBAD-ALB4 was incubated with FPP, [^{14}C]IPP, and DHAP. Reversed-phase radio-TLC analysis of the products was performed after dephosphorylation. S.F., solvent front; Ori., origin. (b) LC profiles of lipids extracted from *E. coli* harboring pBAD-ALB4 (lower) or its parent plasmid, pBAD18 (upper). (c) Positive ESI-MS ion spectrum of a peak in (b) around 22 min. (d) and (e) MS/MS analyses of the ions in (c), with *m/z* of 659.6 and 835.6, respectively. (f) Positive ESI-MS ion spectrum of the LC peak corresponding with that analyzed in (c). Exclusively for this analysis, the elution buffer was changed from sodium based to potassium based. (g) Negative ESI-MS ion spectrum of a peak in (b) around 22 min. (h) MS/MS analysis of the ion in (g), with an *m/z* of 789.5.

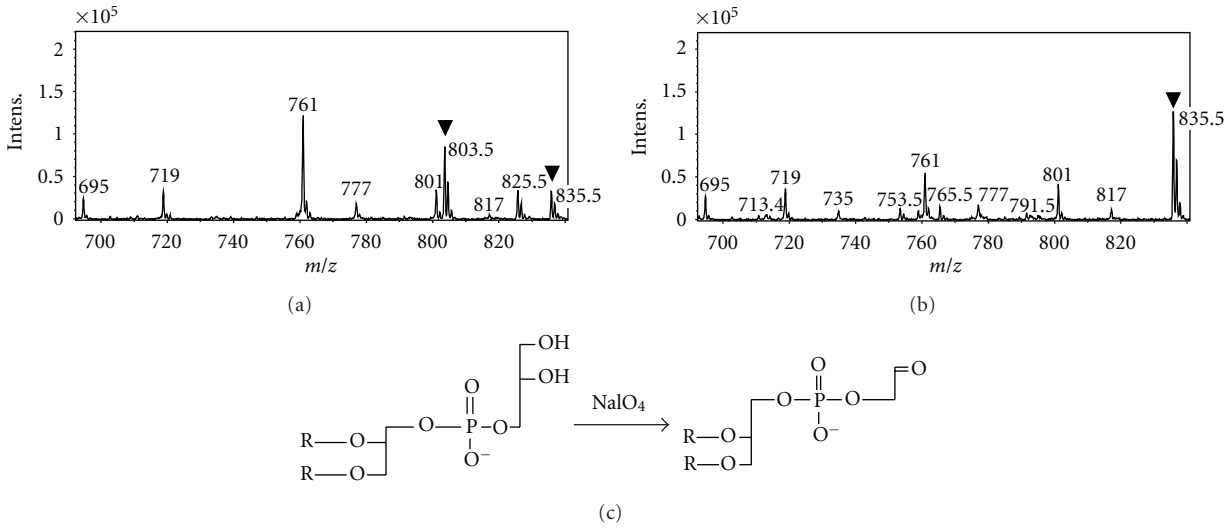

Figure 4: Sodium periodate treatment of DGGGP-Gro. (a) Positive ion spectrum from LC/ESI-MS analysis of the archaeal-type phospholipid postperiodate treatment and (b) preperiodate treatment. (c) The scheme of periodate treatment of DGGGP-Gro. R represents a geranylgeranyl group.

analysis of the ion gave a fragment ion with an *m/z* of 385.0, which corresponded with $[GGGOH+Na\text{-}2H]^+$. In addition, a smaller fragment ion with an *m/z* of 354.9, which corresponded with $[GGGOH+Na\text{-}CH_2O]^+$, was detected. The fragmentation pattern supported the idea that the peak in Figure 3(b) contained DGGGOH, which probably synthesized by the action of the exogenous archaeal enzymes and endogenous phosphatases in *E. coli*. On the other hand, the MS/MS analysis of the larger ion with *m/z* of 835.6 found a fragment ion with an *m/z* of 659.6, suggesting that the parent ion contained the DGGGOH structure (Figure 3(e)). The MS/MS/MS analysis of the fragment ion with an *m/z* of 659.6 yielded fragment ions similar to those observed in Figure 3(d) (data not shown). We therefore presumed that the ion peak with an *m/z* of 835.6 was derived from the cationic bisodium salt of the phosphatidylglycerol-type derivative of DGGGP (DGGGP-Gro). To confirm this idea, the elution buffer for LC/ESI-MS was changed from one containing sodium acetate to one containing potassium acetate, and the same lipid extract was analyzed. As a result, an ion with *m/z* of 867.5, which corresponded well with that expected for the cationic bis-potassium salt of DGGGP-Gro, was detected instead (Figure 3(f)). In addition, MS analysis of the ion shown in Figure 3(b), in the negative ion mode, yielded an ion with *m/z* of 789.5, which corresponded with $[DGGGP\text{-}Gro]^-$ (Figure 3(g)). MS/MS analysis of the ion showed a fragmentation ion with an *m/z* of 715.5, which is consistent with $[DGGGP]^-$ (Figure 3(h)).

Moreover, we recovered the LC peak in Figure 3(b), which probably contained DGGGP-Gro, and treated the phospholipid with sodium periodate to confirm the structure of the polar head group. LC/ESI-MS analysis of the treated lipid with the elution buffer containing sodium acetate gave a positive ion with an *m/z* of 803.5 (Figure 4(a)), which was absent in the analysis of the untreated sample (Figure 4(b)). The emergence of this ion seemed to accompany the decline of the ion with an *m/z* of 835.5. The *m/z* of 803.5 corresponded well with the cationic bisodium salt of DGGGP modified with glycoaldehyde (2,3-di-*O*-geranylgeranyl-*sn*-glycero-1-phosphoglycoaldehyde), which had been expected as the product of the sodium periodate treatment of DGGGP-Gro (Figure 4(c)).

These results show that DGGGP, which should be synthesized from the precursors in *E. coli* cells by the action of the 4 exogenous archaeal enzymes, has been metabolized by endogenous *E. coli* enzymes to yield DGGGP-Gro. It is unclear whether the radioactive TLC spots with of ~0.1, observed in Figures 2(a) and 3(a), are derived from DGGGP-Gro. The archaeal-type phospholipid probably acts as a component of membranes in *E. coli*. Modification of phospholipids with glycerol is usual in *E. coli*, which produces phosphatidylglycerol as a major component of membrane phospholipids [20]. However, the most common phospholipid in the bacterium is phosphatidylethanolamine. The biosynthesis of these phospholipids starts from the cytidylation of phosphatidic acid, which yields CDP-diacylglycerol [21]. *sn*-Glycerol-3-phosphate or L-serine is then transferred to form phosphatidyl-*sn*-glycero-3-phosphate or phosphatidyl-L-serine, respectively. Dephosphorylation of the former intermediate yields phosphatidylglycerol, while decarboxylation of the latter yields phosphatidylethanolamine. If the formation of DGGGP-Gro proceeds through this pathway, the cytidyltransferase, *sn*-glycerol-3-phosphate transferase, and phosphatase of *E. coli* must accept the archaeal-type phospholipid as the substrate. However, the addition of CTP to the reaction mixture of the *in vitro* radio-TLC assay did not intensify the spot with an R_f of ~0.1 (data not shown). In contrast, the fact that DGGGP modified with ethanolamine (or serine) was not detected in the LC/ESI-MS analyses suggested that the L-serine transferase did not accept the

archaeal-type substrate. In fact, *E. coli* phosphatidylserine synthase, which belongs to an enzyme superfamily different from that which includes archaeal phosphatidylserine synthases, reportedly does not accept CDP-activated DGGGOH [22]. If the cytidylation-dependent pathway does not work, which seems more likely, the inner membrane-periplasmic phosphoglyceroltransferase system [23, 24] may transfer the *sn*-1-phosphoglycerol group from the 6-(glycerophospho)-D-glucose moiety of osmoregulated periplasmic glucans "membrane derived oligosaccharides", or their lipid-linked precursors, to DGGGOH to yield DGGGP-Gro directly.

It should be noted that the growth rate of *E. coli* harboring pBAD-ALB4 was almost identical to that of *E. coli* harboring pBAD18 (data not shown). This fact suggests that the production of archaeal-type glycerolipids, which differ from endogenous bacterial ones in hydrocarbon structures and in chirality of the glycerol moiety, does not strongly affect the viability of *E. coli*. The total amount of archaeal-type lipids extracted from *E. coli* cells, which was estimated by comparing the area of the LC peak at A_{210} with that of known amounts of GGPP, was only ~60 μg/g of wet cells. In addition, the archaeal-type lipids detected in this work, that is, DGGGP-Gro and DGGGOH, still retained double bonds in their hydrocarbon chains, which are rarely found in mature archaeal lipids. Therefore, it appears to be too early to conclude that the coexistence of archaeal and bacterial lipids is not disadvantageous for the organisms.

Acknowledgments

This work was supported by grants-in-aid for scientific research from the Asahi Glass Foundation (for H. H.) and from MEXT, Japan (No. 23108531, for H. Hemmi). The authors thank Dr. Susumu Asakawa, Nagoya University, for his help with the cultivation of *M. acetivorans*. They thank Mr. Shigeyuki Kitamura, Nagoya University, for his help with LC/ESI-MS analyses.

References

[1] M. De Rosa and A. Gambacorta, "The lipids of archaebacteria," *Progress in Lipid Research*, vol. 27, no. 3, pp. 153–175, 1988.

[2] A. Gambacorta, A. Trincone, B. Nicolaus, L. Lama, and M. De Rosa, "Unique features of lipids of Archaea," *Systematic and Applied Microbiology*, vol. 16, no. 4, pp. 518–527, 1994.

[3] Y. Koga and H. Morii, "Biosynthesis of ether-type polar lipids in archaea and evolutionary considerations," *Microbiology and Molecular Biology Reviews*, vol. 71, no. 1, pp. 97–120, 2007.

[4] J. C. Mathai, G. D. Sprott, and M. L. Zeidel, "Molecular mechanisms of water and solute transport across archaebacterial lipid membranes," *Journal of Biological Chemistry*, vol. 276, no. 29, pp. 27266–27271, 2001.

[5] J. L. C. M. van de Vossenberg, A. J. M. Driessen, and W. N. Konings, "The essence of being extremophilic: the role of the unique archaeal membrane lipids," *Extremophiles*, vol. 2, no. 3, pp. 163–170, 1998.

[6] Y. Koga, "Early evolution of membrane lipids: how did the lipid divide occur?" *Journal of Molecular Evolution*, vol. 72, no. 3, pp. 274–282, 2011.

[7] G. Wächtershäuser, "From pre-cells to Eukarya—a tale of two lipids," *Molecular Microbiology*, vol. 47, no. 1, pp. 13–22, 2003.

[8] Q. Fan, A. Relini, D. Cassinadri, A. Gambacorta, and A. Gliozzi, "Stability against temperature and external agents of vesicles composed of archaeal bolaform lipids and egg PC," *Biochimica et Biophysica Acta*, vol. 1240, no. 1, pp. 83–88, 1995.

[9] H. Shimada and A. Yamagishi, "Stability of heterochiral hybrid membrane made of bacterial *sn*-G3P lipids and archaeal *sn*-G1P lipids," *Biochemistry*, vol. 50, no. 19, pp. 4114–4120, 2011.

[10] D. Lai, B. Lluncor, I. Schröder, R. P. Gunsalus, J. C. Liao, and H. G. Monbouquette, "Reconstruction of the archaeal isoprenoid ether lipid biosynthesis pathway in *Escherichia coli* through digeranylgeranylglyceryl phosphate," *Metabolic Engineering*, vol. 11, no. 3, pp. 184–191, 2009.

[11] J. Sambrook, *Molecular Cloning, A Laboratory Manual*, 2nd edition, 1989.

[12] H. Fujii, T. Koyama, and K. Ogura, "Efficient enzymatic hydrolysis of polyprenyl pyrophosphates," *Biochimica et Biophysica Acta*, vol. 712, no. 3, pp. 716–718, 1982.

[13] H. Hemmi, K. Shibuya, Y. Takahashi, T. Nakayama, and T. Nishino, "(*S*)-2,3-Di-*O*-geranylgeranylglyceryl phosphate synthase from the thermoacidophilic archaeon *Sulfolobus solfataricus*: molecular cloning and characterization of a membrane-intrinsic prenyltransferase involved in the biosynthesis of archaeal ether-linked membrane lipids," *Journal of Biological Chemistry*, vol. 279, no. 48, pp. 50197–50203, 2004.

[14] Y. Koga, T. Kyuragi, M. Nishihara, and N. Sone, "Did archaeal and bacterial cells arise independently from noncellular precursors? A hypothesis stating that the advent of membrane phospholipid with enantiomeric glycerophosphate backbones caused the separation of the two lines of descent," *Journal of Molecular Evolution*, vol. 46, no. 1, pp. 54–63, 1998.

[15] S. I. Ohnuma, M. Suzuki, and T. Nishino, "Archaebacterial ether-linked lipid biosynthetic gene. Expression cloning, sequencing, and characterization of geranylgeranyldiphosphate synthase," *Journal of Biological Chemistry*, vol. 269, no. 20, pp. 14792–14797, 1994.

[16] T. Soderberg, A. Chen, and C. D. Poulter, "Geranylgeranylglyceryl phosphate synthase. Characterization of the recombinant enzyme from *Methanobacterium thermoautotrophicum*," *Biochemistry*, vol. 40, no. 49, pp. 14847–14854, 2001.

[17] A. Chen, D. Zhang, and C. D. Poulter, "(*S*)-geranylgeranylglyceryl phosphate synthase. Purification and characterization of the first pathway-specific enzyme in archaebacterial membrane lipid biosynthesis," *Journal of Biological Chemistry*, vol. 268, no. 29, pp. 21701–21705, 1993.

[18] N. Nemoto, T. Oshima, and A. Yamagishi, "Purification and characterization of geranylgeranylglyceryl phosphate synthase from a thermoacidophilic archaeon, *Thermoplasma acidophilum*," *Journal of Biochemistry*, vol. 133, no. 5, pp. 651–657, 2003.

[19] D. Zhang and C. Dale Poulter, "Biosynthesis of archaebacterial ether lipids. Formation of ether linkages by prenyltransferases," *Journal of the American Chemical Society*, vol. 115, no. 4, pp. 1270–1277, 1993.

[20] C. Miyazaki, M. Kuroda, A. Ohta, and I. Shibuya, "Genetic manipulation of membrane phospholipid composition in *Escherichia coli*: pgsA mutants defective in phosphatidylglycerol synthesis," *Proceedings of the National Academy of Sciences of the United States of America*, vol. 82, no. 22, pp. 7530–7534, 1985.

[21] J. E. Cronan and P. R. Vagelos, "Metabolism and function of the membrane phospholipids of *Escherichia coli*," *Biochimica et Biophysica Acta*, vol. 265, no. 1, pp. 25–60, 1972.

[22] H. Morii and Y. Koga, "CDP-2,3-di-*O*-geranylgeranyl-*sn*-glycerol:L-serine *O*-archaetidyltransferase (archaetidylserine synthase) in the methanogenic archaeon *Methanothermobacter thermautotrophicus*," *Journal of Bacteriology*, vol. 185, no. 4, pp. 1181–1189, 2003.

[23] B. J. Jackson, J. P. Bohin, and E. P. Kennedy, "Biosynthesis of membrane-derived oligosaccharides: characterization of *mdoB* mutants defective in phosphoglycerol transferase I activity," *Journal of Bacteriology*, vol. 160, no. 3, pp. 976–981, 1984.

[24] B. J. Jackson and E. P. Kennedy, "The biosynthesis of membrane-derived oligosaccharides. A membrane-bound phosphoglycerol transferase," *Journal of Biological Chemistry*, vol. 258, no. 4, pp. 2394–2398, 1983.